

THE SELECTIVE POISONING OF  
METAL CATALYSTS  
FOR HYDROGENATION REACTIONS.

THESIS

submitted for the degree of

DOCTOR OF PHILOSOPHY

of the

UNIVERSITY OF GLASGOW

by

J. IAN MACNAB, B.Sc.

October, 1968.

ProQuest Number: 11011861

All rights reserved

INFORMATION TO ALL USERS

The quality of this reproduction is dependent upon the quality of the copy submitted.

In the unlikely event that the author did not send a complete manuscript and there are missing pages, these will be noted. Also, if material had to be removed, a note will indicate the deletion.



ProQuest 11011861

Published by ProQuest LLC (2018). Copyright of the Dissertation is held by the Author.

All rights reserved.

This work is protected against unauthorized copying under Title 17, United States Code  
Microform Edition © ProQuest LLC.

ProQuest LLC.  
789 East Eisenhower Parkway  
P.O. Box 1346  
Ann Arbor, MI 48106 – 1346

## ABSTRACT

The interaction of 1-butene and 1,3-butadiene with hydrogen has been investigated on supported rhodium catalysts. The poisoning effects of adsorbed mercury upon these reactions have also been studied with the use of radiochemical techniques.

The hydroisomerisation of 1-butene has been studied on alumina- and silica-supported rhodium catalysts at temperatures between  $-20^{\circ}$  and  $153^{\circ}\text{C}$ ; activation energies and kinetic orders in each reaction have been determined for both hydrogenation and isomerisation. The temperature dependence of the activity of each catalyst for isomerisation arises from the difference between the activation energies of hydrogenation and isomerisation; this is rather less with  $\text{Rh}/\text{SiO}_2$  than  $\text{Rh}/\text{Al}_2\text{O}_3$ . Preferential formation of the cis isomer is observed with both catalysts. The effect of adsorbed mercury is to inhibit the hydrogenation reaction to a much greater extent than the isomerisation, apparently by a direct reduction of the coverages of both 1-butene and hydrogen; there is evidence to suggest that clustering of mercury atoms on the surface may occur during reactions.

It was not possible to determine whether the mercury exerted any effects other than the physical blocking of surface sites.

The 1-butene exchange reaction is shown to be rapid,

but independent of isomerisation, while the rate of hydrogen exchange is relatively slow. The activation energy of 1-butene exchange is apparently intermediate between those of hydrogenation and isomerisation. The presence of adsorbed mercury decreases the overall exchange reaction, but slightly increases the rate of hydrogen exchange.

It is concluded that hydrogenation involves the successive addition of two hydrogen atoms to adsorbed 1-butene, and that isomerisation occurs via a  $\pi$ -allylic- $C_4H_7$  intermediate. It is postulated that 1-butene exchange occurs mainly by the reversible formation of a 1-butyl intermediate.

The supports were shown to be virtually inactive for the reactions studied; it was apparent, however, that hydrogen adsorbed on the support may play a significant role in the supported metal-catalysed reactions.

In the hydrogenation of 1,3-butadiene the Rh/SiO<sub>2</sub> - catalyst exhibits very high selectivity for butene formation; the 1-butene/2-butene product ratio is independent of conversion and temperature, while the trans/cis ratio falls with increasing temperature, but is independent of conversion. The exchange of adsorbed 1,3-butadiene is shown to be fast, but the rate of hydrogen exchange is very slow. The effect of mercury was to increase the selectivity even

higher, and to decrease the trans/cis ratio; the rates of addition and to a lesser extent of both the exchange reactions were reduced. It is concluded that the 1- and 2-butenes are formed by separate 1,2- and 1,4-addition processes, while the trans/cis ratio is apparently determined by the relative stabilities of the corresponding adsorbed intermediates.

## ACKNOWLEDGMENTS

I would like to express my gratitude to Dr. G. Webb for suggesting this problem and for his interest, advice, and encouragement throughout the work.

I would also like to thank Dr. S.J. Thomson and Dr. K.C. Campbell for helpful discussions and suggestions.

I acknowledge also the assistance given by members of the technical staff of the Department. In particular, I would like to thank Messrs. J. Connelly and T. Pitt for assistance with glass-blowing; Mr. J. Hardy for designing and constructing the electronic integrator; and Miss Frances Green and Messrs. A. McQuarrie and A. Ritchie for general assistance in the laboratory.

Special thanks are due to Mr. Andrew McKendrick for writing the computer programmes; the use of the Computing Department's KDF9 computer is also acknowledged.

I also have to thank my typist, Miss J. Reid for her patience and skill in typing this thesis.

Finally, I gratefully acknowledge a Science Research Council award for the duration of this work.

J. Ian Macnab.

## ABSTRACT

The interaction of 1-butene and 1,3-butadiene with hydrogen has been investigated on supported rhodium catalysts. The poisoning effects of adsorbed mercury upon these reactions have also been studied with the use of radiochemical techniques.

The hydroisomerisation of 1-butene has been studied on alumina- and silica-supported rhodium catalysts at temperatures between  $-20^{\circ}$  and  $153^{\circ}\text{C}$ ; activation energies and kinetic orders in each reaction have been determined for both hydrogenation and isomerisation. The temperature dependence of the activity of each catalyst for isomerisation arises from the difference between the activation energies of hydrogenation and isomerisation; this is rather less with  $\text{Rh}/\text{SiO}_2$  than  $\text{Rh}/\text{Al}_2\text{O}_3$ . Preferential formation of the cis isomer is observed with both catalysts. The effect of adsorbed mercury is to inhibit the hydrogenation reaction to a much greater extent than the isomerisation, apparently by a direct reduction of the coverages of both 1-butene and hydrogen; there is evidence to suggest that clustering of mercury atoms on the surface may occur during reactions. It was not possible to determine whether the mercury exerted any effects other than the physical blocking of surface sites.

The 1-butene exchange reaction is shown to be rapid, but independent of isomerisation, while the rate of hydrogen exchange is relatively slow. The activation energy of 1-butene exchange is apparently intermediate between those of hydrogenation and isomerisation. The presence of adsorbed mercury decreases the overall exchange reaction, but slightly increases the rate of hydrogen exchange.

It is concluded that hydrogenation involves the successive addition of two hydrogen atoms, to adsorbed 1-butene, and that isomerisation occurs via a  $\pi$ -allylic- $C_4H_7$  intermediate. It is postulated that 1-butene exchange occurs mainly by the reversible formation of a 1-butyl intermediate.

The supports were shown to be virtually inactive for the reactions studied; it was apparent, however, that hydrogen adsorbed on the support may play a significant role in the supported metal-catalysed reactions.

In the hydrogenation of 1,3-butadiene, the Rh/SiO<sub>2</sub>-catalyst exhibits very high selectivity for butene formation; the 1-butene/2-butene product ratio is independent of conversion and temperature, while the trans/cis ratio falls with increasing temperature, but is independent of conversion. The exchange of adsorbed 1,3-butadiene is shown to be fast, but the rate of hydrogen exchange is very slow. The effect of mercury was to increase the



selectivity even higher, and to decrease the trans/cis ratio; the rates of addition and to a lesser extent of both the exchange reactions were reduced. It is concluded that the 1- and 2-butenes are formed by separate 1,2- and 1,4-addition processes, while the trans/cis ratio is apparently determined by the relative stabilities of the corresponding adsorbed intermediates.

## CONTENTS

	page
Acknowledgments	
Abstract	
<u>Chapter 1</u> Introduction	1
1.1 Introduction	1
1.2 Adsorption on Metals	2
1 The Thermodynamics of Adsorption	2
2 The Nature of Surface Sites	6
1.3 The Role of the Metal in Catalysis	9
1 The Nature of the Catalyst	9
2 Geometric & Electronic Factors in Catalysis	10
1.4 Catalytic Reactions of Unsaturated Hydrocarbons	13
1 Introduction	13
2 Nature of the Chemisorbed Species	15
3 The Hydrogenation of Olefins	18
4 The Isomerisation & Exchange of Olefins on Metals	21
5 Isomerisation of n-Butenes on Acid Catalysts	29
6 The Hydrogenation of Diolefins	31
1.5 The Poisoning of Metal Catalysts	39
1 Introduction	39
2 Group Vb and VIb Poisons	41
3 Poisoning by Heavy Metals	45

	page
1.5.4 Poisons Containing Multiple-bonds	49
5 Further Features of Catalyst Poisoning	49
6 Conclusion	50
<u>Chapter 2</u> Objects of Present Work	51
<u>Chapter 3</u> Experimental	53
3.1 Materials	53
3.2 Apparatus	54
1 The Vacuum System	54
2 The Reaction Vessel	55
3.3 Experimental Procedure	56
3.4 The Analysis of Reaction Products	57
1 The Gas Chromatography System	57
2 Mass Spectrometric Analysis	61
3.5 Apparatus & Procedure for Poisoning of Catalysts	62
1 Preparation of Mercury	62
2 Modifications to the Reaction Vessel	62
3 The Counting Problem	63
4 Procedure	65
5 Total Mercury Determination	66
<u>Chapter 4</u> Treatment of Experimental Data	68
4.1 The Hydrogenation Reaction	68
4.2 The Butene Distribution	68
1 Interpretation of Gas Chromatography Traces	68

	page	
4.2.2	The Initial Rate of Isomerisation	69
4.3	Determination of Reaction Kinetics	70
4.4	Determination of Activation Energies	70
4.5	Interpretation of Mass Spectra	71
1	Analysis of Hydrocarbons	71
2	Analysis of Hydrogen/Deuterium	73
	<u>Results - Section A</u>	
<u>Chapter 5</u>	Reactions of 1-Butene on Unpoisoned Catalysts	74
5.1	Reaction of 1-Butene with Hydrogen on Rh/Al <sub>2</sub> O <sub>3</sub>	74
5.2	Reaction of 1-Butene with Hydrogen on Rh/SiO <sub>2</sub>	79
5.3	Kinetics & Activation Energies of 1-Butene Hydrogenation & Isomerisation	83
1	Kinetics on Rh/Al <sub>2</sub> O <sub>3</sub>	83
2	Kinetics on Rh/SiO <sub>2</sub>	89
3	Effect of Temperature on Reactions on Rh/Al <sub>2</sub> O <sub>3</sub>	95
4	Effect of Temperature on Reactions on Rh/SiO <sub>2</sub>	99
5.4	Reaction of 1-Butene in Absence of Molecular Hydrogen	104
1	Reactions on Rh/Al <sub>2</sub> O <sub>3</sub>	104
2	Reactions on Rh/SiO <sub>2</sub>	106
<u>Chapter 6</u>	Investigation of Support Effect	109
6.1	Introduction	109

	page
6.2	Reactions on $\text{Al}_2\text{O}_3$ 110
6.3	Reactions on $\text{SiO}_2$ 111
6.4	Reactions on Mixed Catalysts 112
6.5	Conclusions 113
<u>Results - Section B</u>	
<u>Chapter 7</u>	The Reaction of 1-Butene with Deuterium on Mercury Poisoned Rh/ $\text{SiO}_2$ Catalysts 114
7.1.1	The Adsorption of Mercury on Rh/ $\text{SiO}_2$ 114
2	Determination of Gas-Phase Count 115
3	Effect of Temperature on Adsorbed Mercury 117
7.2	Reaction of 1-Butene with Deuterium on Poisoned & Unpoisoned Catalysts 121
7.3.1	Hydrogenation & Isomerisation at $0^\circ\text{C}$ 121
2	Deuterium Exchange Reactions at $0^\circ\text{C}$ 125
3	The Hydrogen Exchange Reaction at $0^\circ\text{C}$ 130
7.4.1	Hydrogenation & Isomerisation at $21^\circ\text{C}$ 130
2	Deuterium Exchange at $21^\circ\text{C}$ 132
7.5.1	Hydrogenation & Isomerisation at $69^\circ\text{C}$ 138
2	Deuterium Exchange at $69^\circ\text{C}$ 140
3	Hydrogen Exchange at $69^\circ\text{C}$ 146
7.6	The Mass Balance 147
<u>Chapter 8</u>	The Poisoning of the Reaction of 1,3-Butadiene with Deuterium on Rh/ $\text{SiO}_2$ 149
8.1	Introduction 149
8.2	Reactions of 1,3-Butadiene at $25^\circ\text{C}$ 150

		page
8.3	Reactions of 1,3-Butadiene at 48°C	160
8.4	Reactions of 1,3-Butadiene at 83°C	168
8.5	The Mass Balance	178
<u>Chapter 9</u>	Discussion of the Hydroisomerisation of 1-Butene	180
9.1	The Hydrogenation of 1-Butene	181
9.2	The Isomerisation of 1-Butene	183
9.3	Deactivation of the Catalysts	191
9.4	The Support Effect	193
9.5	Conclusions	195
<u>Chapter 10</u>	Discussion of Mercury Adsorption	197
10.1	Characteristics of Mercury Adsorption	197
10.2	Conclusion	200
<u>Chapter 11</u>	Discussion of the Reaction of 1-Butene with Deuterium in the Presence & Absence of Mercury	202
11.1	Poisoning of the Catalyst for Hydrogenation	202
11.2	Poisoning of the Catalyst for Isomerisation	205
1	The Rate of Isomerisation	205
2	The Trans/Cis Ratio	206
11.3	The Exchange Reactions	207
1	Butene Exchange on Unpoisoned Catalysts	207
2	Butene Exchange on Poisoned Catalysts	212
11.4	Conclusion	213

	page
<u>Chapter 12</u> Discussion of 1,3-Butadiene Reactions	215
12.1 The Hydrogenation Reaction	215
1 The Selectivity Ratio	216
2 The Butene Distribution	219
12.2 The Exchange Reactions	224
12.3 The Effect of Mercury Poisoning	230
1 The Poisoning of the Catalyst for Hydrogenation	230
2 The Poisoning of the Catalyst for Exchange Reactions	235
3 Conclusion	237
Appendix A	238
References	241

CHAPTER 1I N T R O D U C T I O N .1.1 Introduction.

A catalyst may be defined as a substance which increases the rate of approach to equilibrium of a given chemical change with only a slight modification of the free energy change of the process. Heterogeneous catalysis is the study of reactions which occur at the phase boundary between gases or liquids and solids. Reactions at the gas-solid interface are by far the more important, and many such reactions are now of considerable industrial importance. Parallel with their rise in importance, has been the increase in the understanding of the mode of operation of catalysts, although there are still many problems which remain unsolved.

The foundation of modern theories of catalysis was laid by Langmuir's work around 1915, when the concept of a metal surface as a geometric array of atoms on which gaseous atoms or molecules could adsorb at random with specific, short range bonds, was advanced. The separate concepts of physical adsorption and chemisorption were developed by several workers, and were explained in a semi-quantitative manner by Lennard-Jones<sup>1</sup> in 1932 in terms of potential energy diagrams. Taylor<sup>2</sup> suggested around 1930 that chemisorption was an activated process, although this was later disputed



by a number of workers.<sup>3</sup>

By the law of mass action the rate of a chemical reaction on a metal surface is dependent on the surface concentrations of the reactants. Any study of catalysis must therefore presume an intimate knowledge of adsorption phenomena, in terms of bond energies, concentrations, and types of species adsorbed.

## 1.2. Adsorption on Metals.

### 1.2.1 The Thermodynamics of Adsorption.

Physical adsorption is caused by weak van der Waals forces between the adsorbent and adsorbate, and the bond lengths are consequently the sum of the van der Waals radii. The heat of adsorption,  $-\Delta H_p$ , is generally similar to the heat of liquefaction, due to the similarity in the nature of the bonds, the values usually being in the range 1 - 5 kcal. mole<sup>-1</sup>. There is no potential barrier to physical adsorption, as shown in the potential energy diagram in Fig. 1.1, and hence it may occur at very low temperatures. As the adsorbate electron distributions are only slightly affected, the molecules are not activated.

Chemisorption is characterised by the formation of chemical bonds to specific metal atoms. The chemisorbed molecules are therefore not mobile on the surface, at least at low temperatures, and the heat of chemisorption,  $-\Delta H_c$ ,

is generally 10 — 100 kcal. mole<sup>-1</sup>. Nearly all chemisorption processes are exothermic, as may be predicted from the thermodynamic equation relating the enthalpy to free energy and entropy, i.e.  $\Delta H = \Delta G + T\Delta S$ . As  $\Delta G$  is negative for a spontaneous reaction, and  $\Delta S$  is negative for chemisorption except in a few cases involving dissociation of the adsorbate, it follows that  $\Delta H$  must be negative. The bond lengths are of the order of 1.5 to 3Å, comparable that is to bond lengths in chemical compounds. Chemisorption may involve a small activation energy, according to the position of the point of intersection, X, of the curves (a) and (b) in Fig. 1.1. which illustrates the physical adsorption (a) and chemisorption (b) potential energy curves for a diatomic molecule. If, as shown, X is above the standard zero energy, then  $E_a > 0$ , as a physically adsorbed molecule must be activated by the amount  $E_a$  in order to dissociate and become chemisorbed, releasing heat  $-\Delta H_a$ . If, however, the shapes of the curves and the lengths of the adsorption bonds are such that the point of intersection lies below the zero energy level, a molecule  $A_2$  may dissociate without acquiring any further energy, so that the separate atoms chemisorb. Physical adsorption may thus be a transient intermediate to chemisorption. Diatomic molecules are generally dissociated

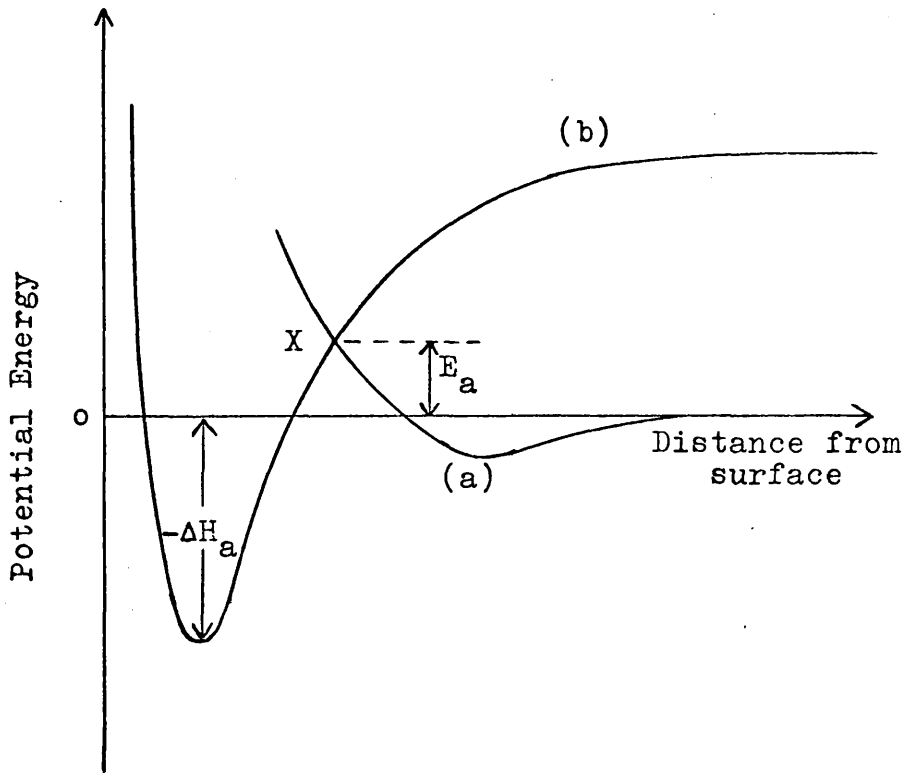


Fig. 1.1 Potential energy curves for (a) physical adsorption and (b) chemisorption.

when chemisorbed, but molecules such as CO or  $C_2H_4$  may undergo associative chemisorption. The general curve (b) is still valid, however, as it represents an excited molecular state capable of bonding to the surface. The energy D is thus the heat of dissociation or excitation. The majority of chemisorption processes, at least on metal films, have no activation energy, and are very fast, but there are also many known examples of activated adsorption, e.g. saturated hydrocarbons on Group VIII metals, and ammonia on tungsten and nickel films.

A further factor which may influence the nature of chemisorbed species and which is of considerable importance to catalysis is the heterogeneity of the surface. The concept of "active sites" was first advanced by Taylor<sup>4</sup> in 1925 to account for the observed fall in the heat of adsorption with increasing coverage, the "active sites" being those most active for adsorption, and characterised by a high heat of adsorption and strong adsorption bonds. This explanation may be understood in terms of the potential energy diagram as it can be seen that if  $-\Delta H_a$  has a high value, the point of intersection of (b) with (a) will be at a low or zero activation energy, and as  $-\Delta H_a$  falls, the value of  $E_a$  will rise. It thus becomes apparent that the active sites are those on which adsorption requires

least activation; there is more recent evidence that the catalytically most active sites are those on which activated adsorption occurs.<sup>5</sup>

Desorption is always an activated process, according to the equation  $E_d = E_a - \Delta H_a$ , and must of necessity reach equilibrium with adsorption process.

Quantitative studies of the adsorption of gases on metal surfaces have been carried out by many workers, and a number of different isotherms derived on the basis of different theoretical surface models. The most frequently used is the Langmuir isotherm, for which three assumptions must be made: (i) each site may adsorb only one molecule; (ii) the adsorbed molecules are in a monolayer; and (iii) the surface energy, and hence the adsorption energy, of all sites is identical and remains so during adsorption on neighbouring sites. This third assumption is of very doubtful validity, but despite this the isotherm is of considerable general value. At equilibrium between adsorption and desorption, the isotherm may be derived kinetically as  $\theta = \frac{bp}{1+bp}$ . In the case of competitive adsorption of gases A and B, the equation is  $\theta_A = \frac{b_A p_A}{1+b_A p_A + b_B p_B}$ . The main features of the isotherm are that  $\theta$  is initially proportional to pressure, and at higher pressures a saturation value ( $\theta = 1$ ) is predicted.

Various attempts have been made to take account of the surface heterogeneity, but the mathematical difficulties are formidable. A Boltzman distribution of sites of different energies leads to an equation of the form  $\theta = C_p \frac{RT}{q}$ , where  $q$  = heat of adsorption. This has the same form as the empirical Freundlich isotherm,  $\theta = kp^{1/n}$ , where  $k$  and  $n$  are constants for a given system. Its main weakness, however, is that it does not predict a saturation limit as pressure increases, though it is valid at low coverages. The Temkin isotherm is based on the assumption that the heat of adsorption falls linearly with increasing coverage, i.e.  $-\Delta H_a = -\Delta H_0 (1-\alpha\theta)$ , where  $-\Delta H_0$  is the heat of adsorption when  $\theta$  is zero, and  $\alpha$  is a constant. This produces the equation  $\theta = \frac{RT}{-\Delta H_0} \ln Bp$ , which is operative in the range  $0.2 < \theta < 0.8$ .

### 1.2.2 The Nature of Surface Sites.

The simplest model of the surface of a metal is of regular array of metal atoms, each being a potential adsorption site. The coordination number of the surface atoms must necessarily be less than that of the bulk atoms, and hence there must be a surface free energy due to the orbitals unused for metal - metal bonding. This simple model is, however, inadequate for the explanation of all aspects of chemisorption and catalysis.

The concept of the heterogeneity has been established from studies of the fall of the heat of adsorption, and certain desorption patterns. The heterogeneity may be inherent or induced by the adsorption itself. Intrinsic heterogeneity is due to various surface defects or dislocations, and these probably give rise to a continuous distribution of site energies. The rapid initial fall in the heat of adsorption in some curves may be caused by this factor, as it is generally found that evaporated metal films have higher initial heats of adsorption than have other forms, such as metal powder and supported metal catalysts.<sup>6</sup> Studies of chemisorption on single crystals and oriented metal films show also that many adsorption parameters vary on different crystal faces.<sup>7</sup> The mutual van der Waals interaction of adsorbed molecules increases with coverage, though this factor alone is insufficient to explain the observed effects of increasing coverage. The simple surface model assumes that adsorption will not affect adjacent sites, but there is, however, evidence that the work function increases with coverage,<sup>8</sup> this being interpreted in terms of the Band Theory of Metals as requiring an increasing energy to excite an electron from the Fermi surface to the covalent adsorbate - metal molecular orbital energy.<sup>9</sup>

Adsorption will thus occur preferentially on the sites

which are energetically most favourable - these are generally termed "active sites" (for adsorption). As the heat of adsorption falls, the activation energy rises correspondingly (Fig. 1.1) and the latter stages of the adsorption may be a slow activated process. The activation energy of desorption from these sites decreases, and accordingly the reaction becomes more easily reversible. These sites are hence frequently the most "catalytically active", but it is significant that sites active for one reaction may be inactive for another.<sup>10</sup>

The migration of an adsorbed molecule from one site to another may be regarded as a partial desorption process. Thus, the smaller is the heat of adsorption ( $-\Delta H_a$ ), the lower is the activation energy for desorption and the easier it is for a molecule to undergo surface migration. This mobility will increase with temperature and coverage and cause the most active (adsorption) sites to become saturated.

The concept of an adsorbed monolayer is important in catalysis. It implies that all available sites are occupied but as the sites which are active for adsorption vary according to the gas, the ratio of adsorbate to metal will also vary. As there is also evidence for more than one type of chemisorption, some possibly being



molecular in nature, the concept may be of very doubtful physical interpretation, but when defined for particular circumstances it may nevertheless still be a useful concept.

### 1.3 The Role of the Metal in Catalysis.

#### 1.3.1 The Nature of the Catalyst.

The catalytic properties of a particular substance are dependent upon its chemical nature, and its ability to adsorb the reactants or products. The principal types of heterogeneous catalysts may be briefly classified according to the types of reaction which they catalyse, as follows:

- (i) Metals - hydrogenation, dehydrogenation, and isomerisation;
- (ii) Metal oxides and sulphides - oxidation, reduction, isomerisation, (hydrogenation);
- (iii) Salts and acids - polymerisation, isomerisation, and hydrocarbon cracking.

Although metals may be used in the massive state as catalysts, they are more commonly employed in one of a variety of microscopic forms, either with or without some other component. The three main types of metal catalyst are evaporated films, powders, and metals supported on an "inert" carrier. These microscopic forms consist of a large number of microcrystals exposing a wide variety of

crystal planes and having many simple disorders. In comparison with metal powders and supported catalysts, evaporated films frequently suffer from the disadvantage of becoming poisoned by virtue of the strength of adsorption of the reactants or products. Supported metals have other distinct advantages, as they are more stable, readily prepared, and easily handled. As a result of these factors they are widely used for industrial purposes. The exact role of the support is as yet unknown, but it is becoming increasingly apparent there is some kind of interaction between metal and support.

Supported metals are therefore the most convenient for studying activity patterns on a number of catalysts, whereas evaporated films would be more suitable for low temperature and specific activity investigations.

### 1.3.2 Geometric and Electronic Factors in Catalysis.

One of the earliest correlations of catalytic activity with the surface geometry was Balandin's Multiplet Theory. This was based on the reactions of cyclo-hexane and aromatics on metals having hexagonal symmetry, but was shown to be inadequate by reactions such as the dehydrogenation of decahydroazulene on palladium. While the hexagonal symmetry may have some relevance to the reactions of  $C_6$  ring compounds, it is clear that other more fundamental

issues are involved.

It has been shown by investigations on oriented films and single crystals that both physical adsorption and chemisorption occur preferentially on certain crystal planes.<sup>7,11</sup> It was similarly found by Beeck, Gwathmey and others<sup>11,12,13</sup> that the activity of a catalyst for a particular reaction varies considerably from one face to another. This is interpreted with regard to the metal - metal bond lengths, which are determined by two factors, (i) the atomic radius, and (ii) the crystal plane. Acetylene, for example will adsorb most readily on interatomic spacings which allow it to be strainfree - assuming it to be associatively adsorbed - and calculations show that on f.c.c. metals adsorption is expected to occur only on the 100 and 110 faces, and not on the 111 face, which has a shorter spacing.<sup>14</sup> Further developments such as the concept of  $\pi$ -bonded intermediates, however, cast some doubt on the validity of these calculations, and it is now largely accepted that electronic rather than geometric considerations are the more significant.

It is significant that the catalytically active metals are mainly in the Transition Series and Group Ib and it is therefore concluded that d-orbitals must play an important part. Theoretical approaches based on both the Band Theory

of metals<sup>15</sup> and Pauling's Valence Bond Theory<sup>16</sup> have attempted to correlate the electronic structures of metals with their catalytic activity. Eley and Dowden<sup>17</sup> have assumed the bonds are essentially similar to bulk metal - metal bonds, while Trapnell<sup>18</sup> suggested that normal covalent bonds were formed.

Pauling<sup>19</sup> has calculated the extent of d-orbital contribution to dsp hybrids, and Beeck<sup>20</sup> showed there was a good correlation between this and catalytic activity. As the lattice spacing is largely dependent on the electronic structure, Pauling<sup>19</sup> also pointed out that apparent geometric effects may in reality be electronic in origin.

Practical investigations of these ideas have employed as catalysts Hume-Rothery alloys to produce a continuous change in % d-character without affecting the lattice type. Schwab<sup>21</sup> found that addition of antimony, lead, and bismuth to silver doubled the activation energy of 17.6 kcal. mole<sup>-1</sup> for the decomposition of formic acid on silver alone. In Band Theory terms, empty levels in the Brillouin zone favour adsorption and catalysis. The more saturated this zone is, the higher is the activation energy required to promote electrons to it. Similar results have been obtained on Transition metal alloys. The classical example of this is the work of Couper and Eley<sup>22</sup> on the activity of palladium/

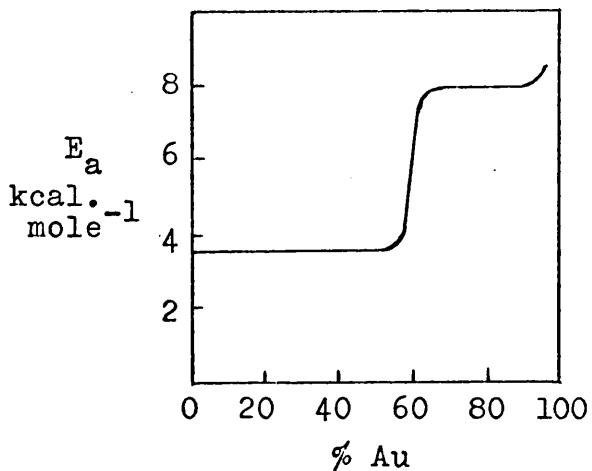


Fig. 1.2(a) Activation energy of p-H<sub>2</sub> conversion on Pd-Au alloys.

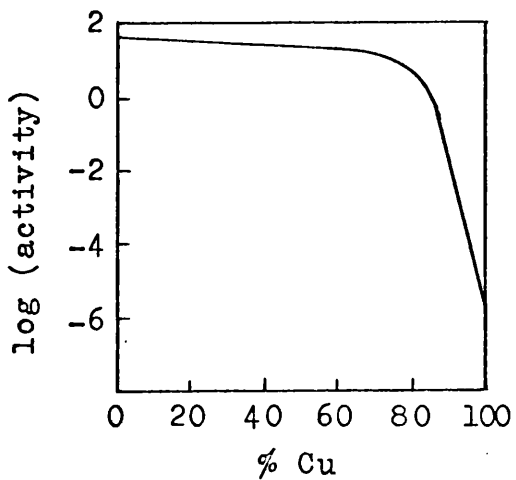


Fig. 1.2(b) Activity of Pt-Cu alloys for ethylene hydrogenation as a function of composition.

/gold alloys for p-H<sub>2</sub> conversion. It has been calculated that at 60% gold, the palladium d-band holes should just be filled, and a decrease in catalytic activity would hence be predicted at this point. The plot of the activation energy against % gold is shown in Fig. 1.2(a) and is in striking agreement with predictions. Similar results have been obtained for the hydrogenation of ethylene on platinum/copper and palladium/copper alloys,<sup>23</sup> as shown in the plot of activity vs. composition in Fig. 1.2(b). The inactivity of platinum and palladium containing dissolved hydrogen may also be explained by this theory.

The strength of the chemisorption bond is considerably dependent on the availability of adsorbate electrons. This may be seen from the order of adsorption strengths of hydrocarbons, for example, acetylene > ethylene > ethane, although this will be discussed later, and it does not follow that the activity sequence is the same.

#### 1.4 Catalytic Reactions of Unsaturated Hydrocarbons.

##### 1.4.1 Introduction.

One of the most frequently investigated reaction systems in the study of catalysis by metals is that between unsaturated hydrocarbons and hydrogen, as they provide many parameters which are of use in the elucidation of the mechan-

-isms of surface reactions. The relative abundance of variables is a consequence of the possibility that the hydrocarbon may undergo a number of separate reactions simultaneously. Which particular parameters may be measured in a reaction system depends upon the size and degree of unsaturation of the hydrocarbon. Olefins, for example, may undergo any or all of the following reactions simultaneously.

- (1) Hydrogenation. This is the simple addition of hydrogen across a double bond to form alkane.
- (2) Isomerisation. In the case of  $C_4$  or larger hydrocarbons, double bond migration may occur, together with cis-trans isomerisation.
- (3) Exchange. If deuterium is used, two separate exchange processes may occur, with the incorporation of deuterium in the olefin and hydrogen in the deuterium. These reactions are termed "olefin exchange" and "hydrogen exchange" respectively.
- (4) Cracking. Under certain conditions large molecules may break down into smaller fragments.

### 1.4.2 Nature of the Chemisorbed Species.

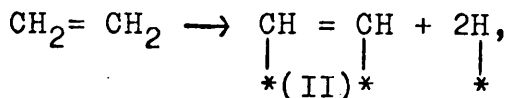
As it is generally accepted that one or more of the reactants must be chemisorbed before reacting, it is apparent that the nature of the chemisorbed molecule will play an important role in determining the course of the reaction. The structure of adsorbed hydrocarbons has therefore been studied using both direct techniques, e.g. infra red spectroscopy and indirect techniques, e.g. deuterium exchange studies.

Farkas, Farkas and Rideal<sup>24</sup> suggested in 1934 that ethylene underwent "dissociative adsorption" on nickel, viz.

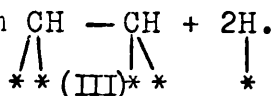
$$\text{CH}_2=\text{CH}_2 \rightarrow \text{CH}_2=\underset{\substack{| \\ \text{(I)*}}}{\text{CH}} + \underset{\substack{| \\ *}}{\text{H}}.$$

Olefin exchange was thereby explained by the incorporation of deuterium in the reverse step, while hydrogenation was assumed to proceed by the simultaneous addition of two hydrogen atoms to the adsorbed molecule.

Beeck et al.<sup>11,25</sup> postulated a form of dissociative adsorption for ethylene on nickel films requiring four surface sites;



where a surface "acetylenic complex" is formed. It has also been suggested that at 100°C ethylene may be dissociatively adsorbed in the form



Evidence



has been obtained by Taylor and co-workers<sup>26,27</sup> for dissociative adsorption of ethylene on a number of different catalysts.

Eley,<sup>28</sup> however, found that para-hydrogen conversion was inhibited by the presence of ethylene, while Conn and Twigg<sup>29</sup> found that no exchange occurred between ethylene and d<sub>4</sub>-ethylene. The latter accordingly proposed an associative mechanism.

Conclusive evidence for the dissociative adsorption of saturated hydrocarbons has been given by a number of workers. H.S. Taylor<sup>26</sup> showed that exchange occurred between methanes at 140°C on nickel, while T.l. Taylor<sup>30</sup> obtained similar results with platinum at temperatures above 20°C. He also found evidence of preferential exchange at the secondary position; this result was later confirmed by Kemball.<sup>31</sup>

An alternative mechanism whereby olefins may chemisorb on a metal surface is by associative adsorption. This involves the rupture of the double bond and the formation of an adsorbed alkane:-

$$\text{CH}_2=\text{CH}_2 \rightarrow \begin{array}{c} \text{CH}_2-\text{CH}_2 \\ | \qquad | \\ \text{*(IV)*} \end{array}$$

This was first postulated for ethylene in 1934 by Horiuti and Polanyi et al.<sup>32,33</sup> and has since been favoured by a number of workers.<sup>29,34</sup> Eley calculated the heats of adsorption on nickel of each type of adsorbed ethylene molecule, and

found that the figure for associative adsorption was closest to the experimental value, while Greenhalgh and Polanyi<sup>35</sup> made a complete survey of the existing data in 1939 and concluded that associative adsorption was the principal process for unsaturated hydrocarbons.

The concept of the diadsorbed intermediate (IV) bonded to two metal atoms was generally accepted and received relatively little modification until around 1960. It then became necessary to reconsider certain features which could not be adequately explained by this concept. Bond<sup>14</sup> showed that acetylene and ethylene would not be expected to adsorb on the same interatomic spacings, and concluded that the relative activity of different metals for the hydrogenation of each should vary considerably. In fact, acetylene generally inhibits the reaction of ethylene, implying that the same sites may adsorb both acetylene and ethylene. The results of certain exchange reactions of cycloalkanes<sup>36</sup> were also inexplicable in the conventional terms, and on the basis of evidence such as this, Rooney and Webb<sup>36,37,38</sup> postulated a modified form of associative adsorption. They suggested that an olefin-metal complex was formed in which a  $\sigma$ -bond was formed by donation of the olefin  $\pi$ -electrons to an unfilled metal d-orbital together with a  $\pi$ -bond resulting from donation of charge from filled metal d-orbitals to the

anti-bonding  $\pi$ -orbital of the olefin. The effect of this  $\pi$ -bonding was to strengthen the metal-olefin bond, but to weaken the carbon - carbon bond. Such a complex would require only a single metal atom for adsorption. Initially, it was suggested that interconversion between the olefinic  $\pi$ - complex (V) and  $\sigma$ - adsorbed complex (IV) was relatively unimportant, and that  $\pi$ -allyl complexes (VI), formed by the loss of an allylic hydrogen atom, were more significant catalytically.<sup>36</sup>

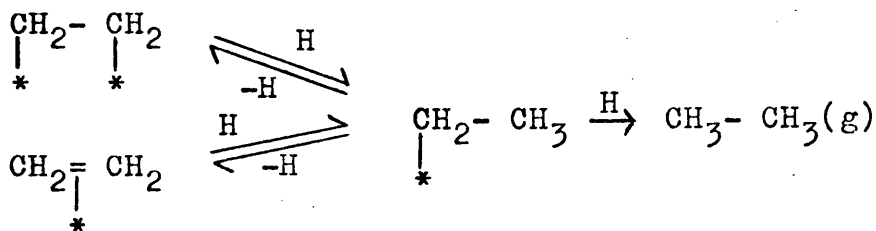


It was subsequently necessary, however, to accept that (V) was catalytically important.<sup>38</sup> The evidence for this type of intermediate was reviewed in 1963 by Rooney and Webb,<sup>37</sup> and they conclude that many hitherto unexplained reaction mechanisms and activity sequences were explicable in terms of  $\pi$ -bonded intermediates.

### 1.4.3 The Hydrogenation of Olefins.

It is generally agreed that olefin hydrogenation proceeds via a "half-hydrogenated state" first postulated by Horiuti and Polanyi<sup>32,33</sup> in a proposed mechanism for the hydrogenation of and exchange of ethylene. They assumed the ethylene was adsorbed by structure (IV) (Section 1.4.2),

whereas the development of the  $\pi$ -complex theory presumed structure (V): it is thought, however, that either could form the same intermediate, namely an adsorbed ethyl radical which could then react further to produce ethane, as shown in the reaction scheme below.



Larger hydrocarbons may also adsorb as structure (VI) ( $\pi$ -allyl) if they have an  $\alpha$ -hydrogen atom, but it is unlikely that this can react to form an alkyl radical; it is thus assumed the same mechanism operates for larger hydrocarbons as for ethylene. Twigg and Rideal<sup>34,39</sup> supported the concept of the "half-hydrogenated" intermediate, but argued that the hydrogen remained as a physically adsorbed molecule until it reacted, whereas Horiuti and Polanyi assumed the dissociative adsorption of hydrogen. They also proposed that addition of the second hydrogen atom was the rate-determining step.

A rather different mechanism was proposed by Beeck.<sup>25</sup> He considered that the acetylenic complex formed by dissociative adsorption was inactive, and suggested that reaction occurred between chemisorbed hydrogen and physically adsorbed ethylene. Eley,<sup>40</sup> however, pointed out several

shortcomings of this mechanism and subsequently it has not been seriously considered.

The reaction kinetics and activation energies have been measured for a number of olefins, but the bulk of the work has been carried out using ethylene; there is thus a corresponding shortage of results for higher olefins. It is generally accepted that the olefin is more strongly adsorbed than the hydrogen; the order in hydrogen is  $1.0 \pm 0.5$  on most metals, while the hydrocarbon order is generally zero or negative, although there are a number of cases where positive orders have been recorded.

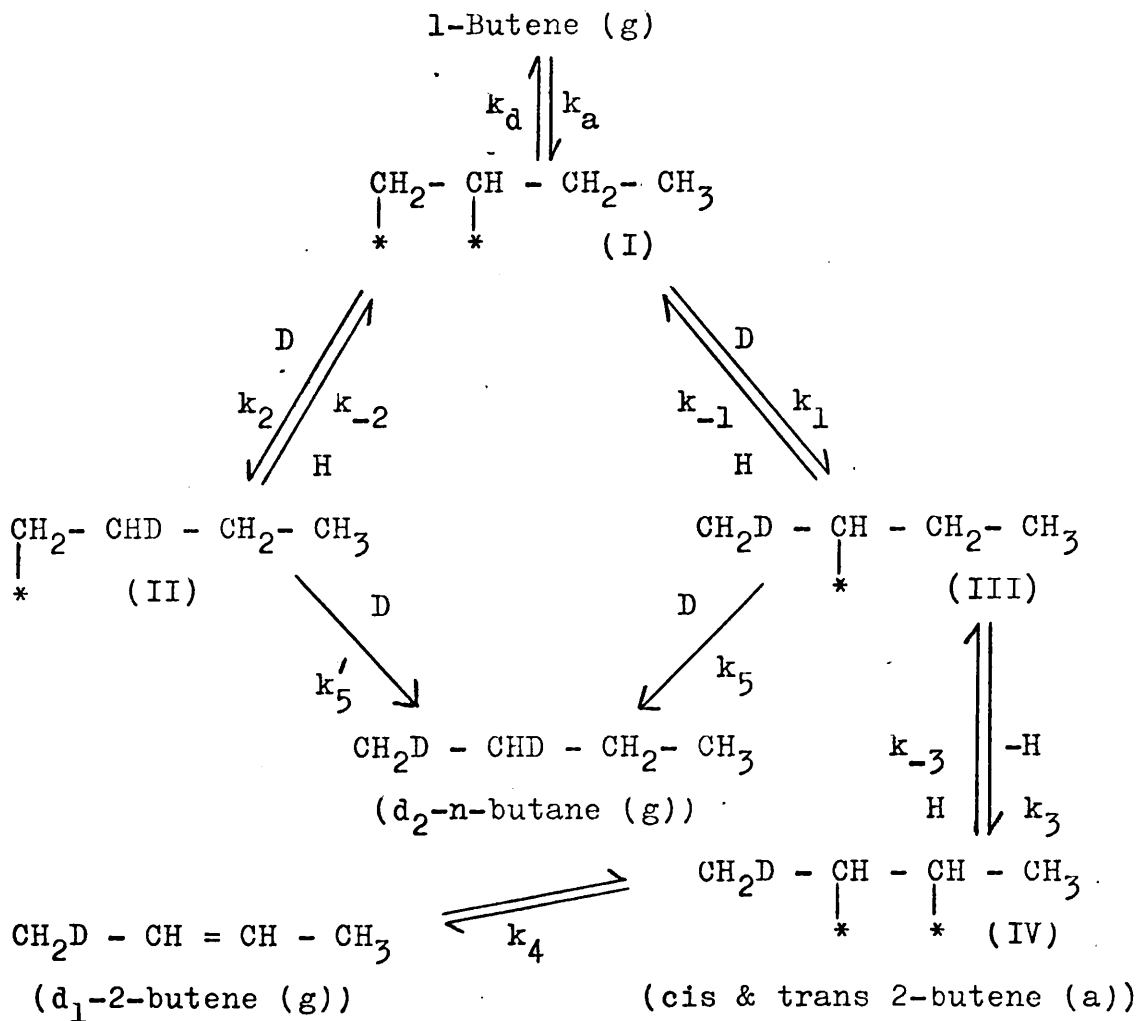
The hydrogenation of each of the n-butenes on nickel wire catalysts has been studied by Taylor and Dibeler.<sup>41</sup> Overall first order kinetics were obtained for the reaction of each butene but the orders in each reactant were not determined. The activation energies were found to be  $2.0 \text{ kcal.mole}^{-1}$  and  $3.5 \text{ kcal.mole}^{-1}$  for addition to 1-butene and 2-butene respectively, which is in striking agreement with results obtained by Twigg.<sup>42</sup> It is also interesting that the activation energy of hydrogenation falls from  $8-10 \text{ kcal.mole}^{-1}$  for ethylene to  $\sim 6 \text{ kcal.mole}^{-1}$  for propylene and  $\sim 3 \text{ kcal.mole}^{-1}$  for butene.<sup>41,42,43</sup>

#### 1.4.4 The Isomerisation and Exchange of Olefins on Metals.

If deuterium is employed in the hydrogenation of 1-butene, the reaction products at any intermediate stage generally include exchanged 1-butene and also deuterated 2-butenes. Likewise, the  $d_2$ -n-butane is rarely the sole product of the addition reaction. It is clear, then, that the reactant molecules are undergoing isomerisation and that equilibration of the available deuterium and hydrogen is occurring throughout the butene molecule. The mechanism most generally accepted for these processes is the "alkyl reversal" mechanism, first suggested by Horiuti and Polanyi<sup>32,33</sup> in 1934 to account for the exchange of ethylene. They postulated that the formation of the half-hydrogenated state (II and III), which was described in section 1.4.3, is reversible; the mechanism is shown below in the reaction scheme for butene isomerisation and exchange; H is used in the generic sense in the reverse reaction steps of this scheme.

The adsorbed radicals (II) and (III) may undergo the reverse reactions, steps -1 and -2. With structure (II) there is an equal probability that either H or D will be removed from the 2-carbon atom; the probability that H rather than D will be lost from (III) is 2/3. Thus, by desorption of the resulting 1,2-diadsorbed species (structure I),

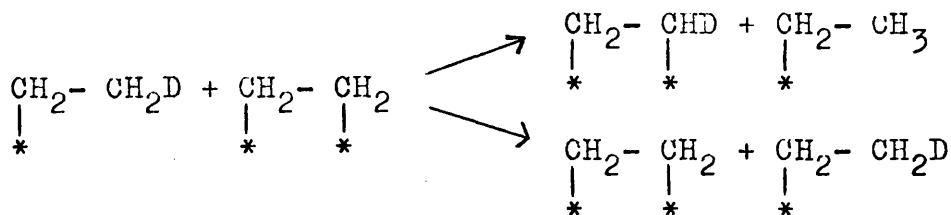
deuterium is incorporated into reactant 1-butene.



The reversal from adsorbed butyl to adsorbed butene may however proceed via step 3, in which case the 2,3-diadsorbed species (IV) is obtained; this may then be desorbed as cis or trans 2-butene. It is apparent that if  $k_{-1} > k_5$  and  $k_{-2} > k_5'$  exchange of the 1-butene will readily occur, while if  $k_3 > k_{-1}$  isomerisation will occur to a substantial

extent. Further, if  $k_{-3} > k_4$ , the isomerisation products will be considerably exchanged. Dependent upon the relative values of these rate constants, it is possible that all species of deuterated butenes, from  $d_0$  to  $d_8$ , may be obtained.

Bond,<sup>44</sup> in summarising the features of the mechanism, suggested that the alkyl intermediate may also undergo reactions such as disproportionation to adsorbed olefin and alkane, or direct atom exchange between adsorbed alkyl and olefin rather than requiring the hydrogen atom to be initially or finally in a chemisorbed state. There is evidence that this direct exchange is rapid, and it follows that

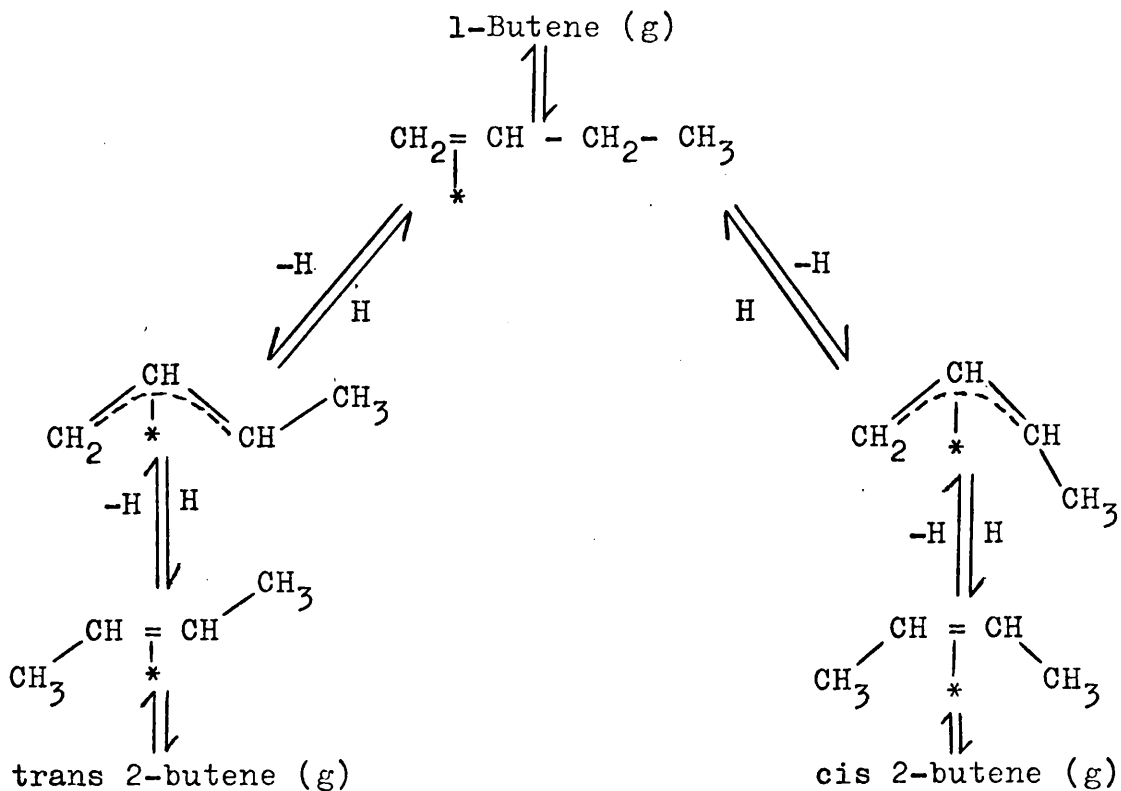


the majority of alkyl radicals will be  $d_0$  in the initial stages.

The advent of the  $\pi$ -complex theory introduced new mechanistic possibilities. Rooney and Webb<sup>36</sup> suggested that isomerisation might occur by one of two mechanisms, (i) interconversion between  $\pi$ -olefin and alkyl intermediates and (ii) interconversion between  $\pi$ -olefin and  $\pi$ -allyl complexes, the latter being an entirely new mechanism, while the former is a modification of the alkyl reversal mechanism. Mechanism (ii) is shown in the following reaction scheme for



the isomerisation of 1-butene.



The essential requirement for this mechanism to operate is an allylic hydrogen atom in the olefin; loss of this produces the syn or anti conformers of 1-methyl- $\pi$ -allyl, from which the trans and cis 2-butenes respectively are derived. There is also evidence, from cyclo-alkane exchange reactions,<sup>37</sup> that  $\pi$ -allylic complexes may react with either chemisorbed or molecular hydrogen, thus giving rise to the possibility of either Langmuir-Hinshelwood or Rideal-Eley type mechanisms respectively.

Some of the earliest work on butene isomerisation and

exchange was carried out by Twigg<sup>42</sup> and Taylor<sup>41</sup> on nickel wire catalysts. Twigg, following his earlier work on ethylene exchange,<sup>29</sup> predicted that double-bond migration would occur. He found this to be the case, and obtained the same reaction kinetics for both hydrogenation and isomerisation, i.e. rate =  $k p_{H_2}^{\frac{1}{2}} p_{1-B}^{\frac{1}{2}}$ . This is in agreement with his earlier calculation<sup>39</sup> that a metal surface could not be 100% covered by butene molecules owing to steric interaction, thus allowing non-competitive adsorption of hydrogen. The rate of double-bond migration was found to be 5-6 times faster than that of exchange, but it may be noted that there was no differentiation between olefin and hydrogen exchange.

Taylor and Dibeler,<sup>41</sup> however, obtained almost equal rates for the isomerisation and olefin exchange of 1-butene, which is of some mechanistic importance. They also found that the rates of appearance of one deuterium atom in 1-butene and cis 2-butene were similar, but formation of the  $d_2$ -2-butene was faster than the  $d_2$ -1-butene. The activation energies obtained are shown in table 1.1. One of their most significant results was the observation that the activation energy for double-bond migration rises from 5.0 to 7.8 kcal. if deuterium is used instead of hydrogen. At 60°C, the rate of double-bond migration with hydrogen is 4.0 times that with deuterium. This appears to be fairly

TABLE 1.1Activation Energies of Butene Hydrogenation, Exchange, and Isomerisation on Nickel Catalysts.

<u>Olefin</u>	<u>E<sub>h</sub></u>	<u>E<sub>e</sub></u>	<u>E<sub>i</sub></u>	<u>Ref.</u>
1-Butene	2.0	7.1	5.0	42
2-Butene	3.5	8.0	-	42
1-Butene	2.5	9.0	5.9	43

conclusive evidence that fission of a hydrogen bond is involved in the rate determining step. Their kinetic measurements were in agreement with those obtained by Twigg.<sup>42</sup>

It is of particular interest that an attempt was made to establish the position of exchange by mass spectroscopy. Slight evidence for initial exchange of 1-butene in 1-position was obtained, but it was concluded that insufficient knowledge of the fragmentation of butenes under electron bombardment was available to enable any definite conclusions to be reached. Taylor and Dibeler suggested that the "hydrogen switch" mechanism of Turkevich and Smith<sup>45</sup> explained most of their observations, but it is interesting to note their tentative suggestion of a  $\pi$ -allylic type of complex as an intermediate in isomerisation and exchange. This is perhaps the first reference to the concept of such a complex, although it was not developed until much later.

Bond and co-workers made a detailed study of reactions of various unsaturated hydrocarbons with deuterium on a series of alumina supported Group VIII metal catalysts. This and other work has recently been comprehensively reviewed by Bond and Wells.<sup>46</sup> By defining certain parameters in terms of the probabilities of "permitted" reaction steps, it was possible to evaluate for each metal theoretical values for these parameters, and deduce the most favoured steps.

Isomerisation and exchange reactions of ethylene and butene on palladium, rhodium, platinum, and iridium showed that palladium was the most active for both processes, although there was very little hydrogen exchange.  $d_0$ - and  $d_1$ -ethane and  $d_1$ -ethylene were the main exchanged products, a result similar to that obtained with nickel. The isomerised butenes were only lightly exchanged, the deuterium number being  $\sim 0.5$ , which may suggest an intramolecular hydrogen transfer mechanism for isomerisation. The main feature of the isomerisation of 1-butene on Pd/Al<sub>2</sub>O<sub>3</sub> was preferential formation of cis 2-butene; the initial trans/cis ratio was 1.9, compared with the thermodynamic equilibrium value of  $\sim 3.8$ . The isomerisation kinetics were zero order in each reactant, and were identical for each of the three n-butenes. This led Bond and Wells to suggest that butene desorption was the rate-controlling step.

Rhodium<sup>46,47</sup> was characterised by a temperature dependent isomerisation activity; at high temperatures isomerisation and exchange were rapid relative to hydrogenation, and the behaviour resembled that of nickel. The temperature effect is, however, less marked with the exchange than the isomerisation. This may indicate preferential formation of the adsorbed 1-butyl rather than 2-butyl species at low temperature.<sup>46</sup> In the reaction of 1-butene with deuterium, the 2-butenes were equally deuterated, but the deuterium number fell slightly with increasing temperature.

Platinum was found to have low isomerisation and exchange activity between 0° and 100°C, while iridium at 0°C was even less active, despite the fact that  $E_h < E_i$ .

Ruthenium and osmium<sup>48</sup> are of particular interest as their structure is close-packed-hexagonal, whereas the other noble Group VIII metals have a face-centred-cubic structure. Both metals have isomerisation and exchange activities intermediate between those of palladium, nickel, and high-temperature rhodium on the one hand, and platinum and iridium on the other.

It is therefore apparent that isomerisation and exchange activities follow the same pattern; this is reasonable evidence that the mechanisms for each are closely related. The order of activity of Group VIII metals is

Ni > Pd > Rh ~ Ru > Os > Pt > Ir. This contrasts with the suggested order of importance of  $\pi$ -allylic intermediates: Pd > Ni ~ Pt > Rh.<sup>37</sup>

#### 1.4.5 Isomerisation of n-Butenes on Acid Catalysts.

In some of the early studies of isomerisation on oxide catalysts it was assumed that the butenes isomerised in equilibrium proportions, but Lucchesi et al.<sup>49</sup> reported that cis 2-butene was preferentially formed in the isomerisation of 1-butene over silica-alumina. This selectivity has been found by many investigators to be a common occurrence; the present situation has recently been reviewed by Gerberich and Hall.<sup>50</sup>

The reactions of all three n-butenes on alumina and silica-alumina have been studied by micro-catalytic reactor and tracer techniques.<sup>51</sup> It was established that all six interconversion reactions occurred directly, contrary to Lucchesi's suggestion that formation of the trans isomer from 1-butene occurred only via cis 2-butene. The results obtained by different techniques showed consistent activities; the interconversion rates relative to rate of 1-butene  $\rightarrow$  cis 2-butene = 1.0 are shown in table 1.2.

The trends which are evident in table 1.2 are in agreement with the general observations of Brouwer;<sup>52</sup>

similar results were also obtained with n-pentenes. The isomerisation activity of alumina, however, was shown to depend upon the water content and pre-treatment of the catalyst.

TABLE 1.2  
Butene Interconversion Rates.<sup>51</sup>

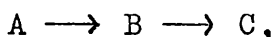
<u>Catalyst</u>	<u>Temperature</u>	<u>Relative rate constants.</u>					
		$\frac{k_{lc}}{k_{cl}}$	$\frac{k_{tl}}{k_{lt}}$	$\frac{k_{ct}}{k_{tc}}$	$\frac{k_{cl}}{k_{lc}}$	$\frac{k_{lt}}{k_{tl}}$	$\frac{k_{tc}}{k_{ct}}$
SiO <sub>2</sub> /Al <sub>2</sub> O <sub>3</sub>		1.0	0.24	0.06	0.96	0.38	0.10
Al <sub>2</sub> O <sub>3</sub>		1.0	0.21	0.03	0.48	1.0	0.28

Hall et al.<sup>51</sup> supported the classical secondary carbonium ion as an intermediate, but Brouwer rejected it as an explanation of his results, and suggested instead that selectivity was due to competition between a concerted "switch" mechanism (double-bond migration only) and carbonium ion formation (mainly cis-trans). Tung and McIninch<sup>53</sup> obtained similar results on alumina and silica, and postulated that isomerisation occurs on Lewis acid sites, while cracking and polymerisation occur on Brønsted sites. Bielikoff, Fraissard and Imelik<sup>54</sup> showed recently that the trans/cis ratio increased with the temperature of pretreatment of the catalyst, and concluded the Lewis acid strength was the determining factor in this.

#### 1.4.6 The Hydrogenation of Diolefins.

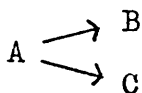
Diolefins may undergo the same general reactions as those described in section 1.4.1 for olefins. Diolefins, however, can undergo hydrogenation of only one double bond, forming the mono-olefin, or of both the double-bonds, forming the saturated compound. In consequence of this, there is a further reaction variable, namely the selectivity for mono-olefin formation, which is of use in the elucidation of the mechanisms of the surface reactions. With diolefins other than allene, there is also the possibility of the formation of isomeric mono-olefins. Thus the stereoselectivity exhibited by the catalyst is thus a further parameter to be considered.

Selectivity is caused by two main factors. If the reaction is shown schematically as



the chance of C being formed will depend upon the ability of B to adsorb, or remain adsorbed in competition with A. The selective formation of B thus depends on the relative adsorption strengths of A and B, and this is termed the "thermodynamic factor", denoted by  $S_t$ . If, however, products B and C are formed by two distinct routes,

i.e.

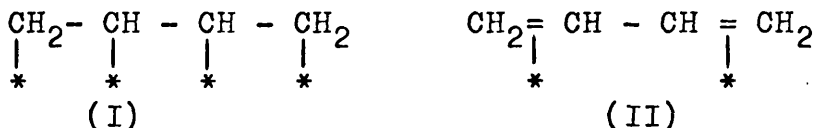




the selectivity for B will be determined by the relative rates of the two reactions. This is termed the "mechanistic factor", denoted by  $S_m$ .

On most metals, the results suggest that the adsorption strength of diolefins is greater than that of monoolefins,<sup>55</sup> and, in fact, that  $S_t$  is very high. This being so, the observed variation in selectivity is a measure of  $S_m$ <sup>56</sup>. Using the above example, selectivity is defined as  $S = \frac{B}{B+C}$ ; the values may therefore vary between zero and unity.

For a diolefin such as 1,3-butadiene to be more strongly adsorbed than the corresponding olefin, it is apparent that both the double bonds must be utilised in the adsorption. The adsorbed species may be written in two forms, one involving four carbon-metal  $\sigma$ -bonds (I), and the other, two olefinic  $\pi$ -complexes (II).



There is considerable evidence in favour of structure (II), as the  $sp^2$  hybridisation would cause no internal strain, while structure (I) could not be achieved without high internal strain produced by the  $sp^3$  hybridisation and the geometrical requirement of four metal sites at a suitable interatomic spacing.

There have been no reports of the hydrogenation of 1,3-butadiene on metal films, but the reaction has been thoroughly investigated by Bond et al. on a series of alumina supported Group VIII metal catalysts.<sup>55</sup> All the metals studied, with the exception of iridium, exhibited a high selectivity for butene formation at all temperatures and pressures used. The selectivity generally rose with increasing temperature, and, with the exception of palladium, was shown to fall slightly with increasing initial hydrogen pressure, and also with increasing conversion. The initial butene distribution and selectivities for a number of metals are shown in table 1.3.

It has been emphasised that selectivity is essentially characteristic of the metal only, and is virtually independent of the hydrocarbon used and the conditions under which the reaction was carried out.<sup>56</sup>

The hydrogenation kinetics were generally first order in hydrogen pressure and zero or negative order in 1,3-butadiene pressure. These values support the belief that the diolefin is adsorbed to the fullest extent. It is however feasible that hydrogen may also undergo limited non-competitive adsorption on sites unavailable to 1,3-butadiene due to steric effects.

The butene distributions obtained on alumina supported

TABLE 1.3

Dependence of Butene Distribution & Selectivity upon Temperature.

<u>Metal</u>	<u>Temp.</u> °C.	% Butene Distribution			<u>T/C</u>	<u>Sel.</u> <sup>y</sup>
		<u>l-B</u>	<u>t-2-B</u>	<u>c-2-B</u>		
Pd	0	64.4	33.2	2.4	13.8	1.000
"	43	59.4	36.8	3.8	9.7	1.000
Rh	16	51	32	17	1.9	0.743
"	82	48	32	20	1.6	0.906
Ru	0	69	19	12	1.6	0.736
"	49	61	23	16	1.4	0.835
Os	24	65	19	16	1.2	0.431
"	70	57	21	22	0.9	0.630
Pt-I	0	72	18	10	1.8	0.501
"	45	64	17	19	0.9	0.625
Pt-II	107	61	22	17	1.3	0.800
"	152	38	36	26	1.4	0.920
Ir	24	59	19	22	0.9	0.251
"	75	32	34	34	1.0	0.384

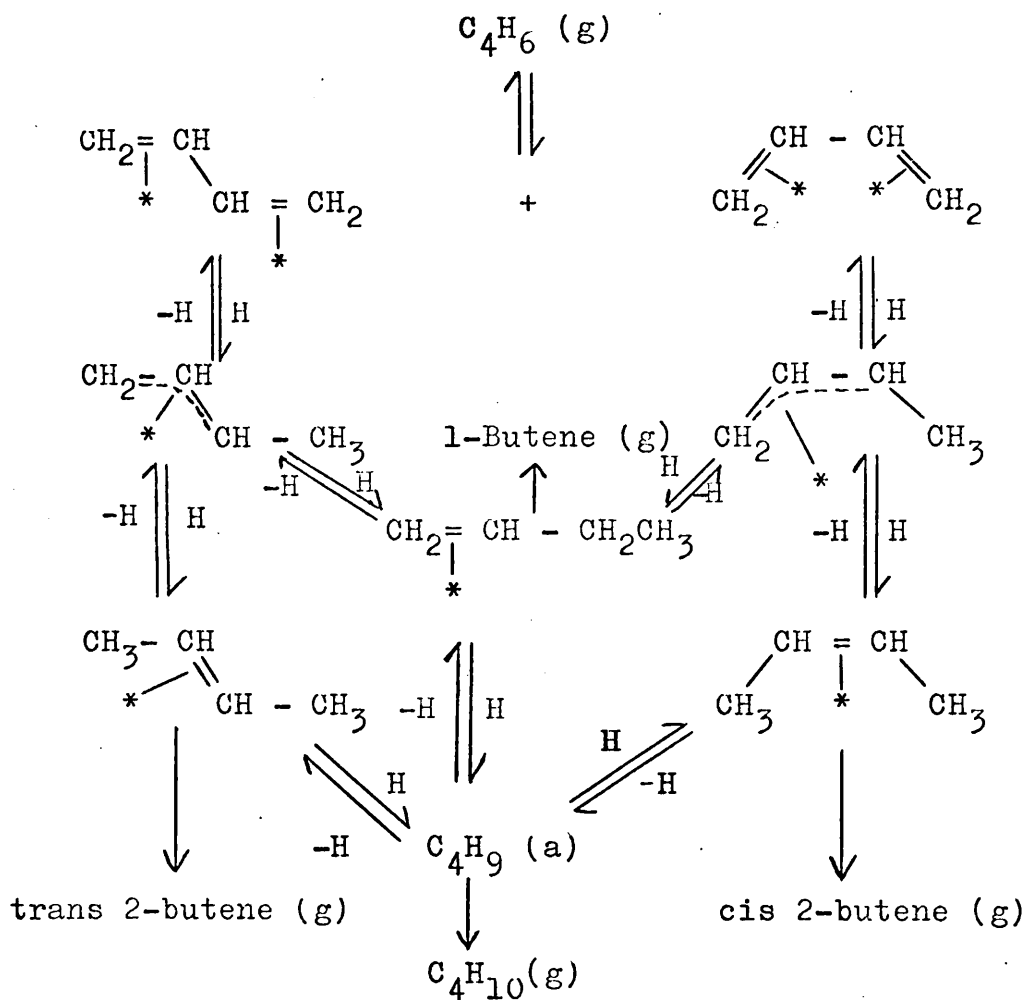
(l-B = l-butene; t-2-B = trans-2-butene; c-2-B = cis-2-butene; T/C = t-2-B/c-2-B).

metals,<sup>55,57</sup> and on platinum and palladium in 95% ethanol<sup>58</sup> show that l-butene is generally the principal product, particularly at low temperatures, and that the trans/cis

ratio falls with increasing temperature. On all the catalysts except rhodium, also, the distributions tended toward equilibrium proportions with increasing conversion. Two main mechanisms have been postulated to explain these features. First, the 1-butenes and 2-butenes may be produced by the independent operation of 1,2- and 1,4-addition. The relative amounts of 1,2- and 1,4-addition would be determined by the metal and the reaction conditions, while the trans/cis ratio would be expected to be determined by the relative proportions of the adsorbed 1,3-butadiene in the syn and anti conformations. The second mechanism involves the formation of 1-butene by 1,2 addition, and its subsequent isomerisation to produce the 2-butenes. The two mechanisms are shown in the reaction scheme below.

If the latter mechanism is operative, it may be expected that the trans/cis ratio would be similar to that obtained in the hydroisomerisation of 1-butene on the same catalysts; it is significant, therefore, that with the exception of palladium and cobalt, ( $T/C \sim 10$ ) all the metals studied show this interesting correlation. Bond and Wells<sup>46</sup> also pointed out that a good correlation exists between 1-butene isomerisation activity and 2-butene yield, and also their temperature dependence. In this context it is interesting also to note that palladium has a selectivity of

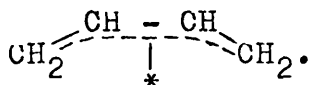
1.000 which implies there are virtually no adsorbed  $C_4H_9$  radicals, and thus no possibility of isomerisation - assuming that this would occur by an alkyl reversal mechanism.



It may therefore be suggested that at least part of the 2-butene yield is produced by 1,2-addition and subsequent isomerisation on all the Group VIII metals except palladium and cobalt. It is notable, however, that Bond et al.<sup>55</sup>

later suggested that 1,4-addition is appreciable on all metals on account of the general independence of the butene distribution upon the initial hydrogen pressure.

Where 1,4-addition operates, the trans/cis ratio must be determined by the proportions of each conformer on the surface. As the syn/anti ratio in gas-phase 1,3-butadiene is  $\sim 15$ , it is interesting to compare this with the trans/cis ratio on palladium. It is more probable, however, that the stability of the adsorbed species is more important than the gas-phase ratio, and it has been suggested that the anti conformer may be stabilised by electron delocalisation, viz.



The reaction of 1,3-butadiene with deuterium on palladium/alumina has been reported by Meyer and Burwell.<sup>57</sup> Diolefin exchange was very slow, and hydrogen exchange was severely inhibited. The most significant feature was the lower deuterium content of the cis 2-butene compared with the trans 2-butene and 1-butene. No acceptable explanation of this phenomenon has yet been put forward. Surface heterogeneity has been suggested as a possible cause, although Bond and Wells<sup>46</sup> claimed that there is no direct evidence for this.

Consideration of the above results shows certain well-

-defined trends:<sup>48</sup> selectivity and the trans/cis ratio decrease down each triad of Group VIII and increase from left to right, across each row, with the exception of iridium. Similar trends have been observed with other hydrocarbons including allene, acetylene and dimethylacetylene.

## 1.5 The Poisoning of Metal Catalysts.

### 1.5.1 Introduction.

A catalyst poison may be generally regarded as a substance which acts on a catalyst in such a way as to inhibit its activity for a certain reaction. It is thus only a relative term, and in practice a catalyst poison is so called only if it exhibits a toxic effect even if present in very small amounts. Reports of catalyst poisoning are many and varied, although in most cases systematic studies of the effects of the poison have not been carried out. Maxted et al., however, have studied the effects of poisoning on a number of reactions, and these studies have enabled a number of significant features to be defined. These, and a number of other results, together with the suggested mechanisms by which the poisons exert their effect, have been reviewed by Maxted.<sup>59</sup>

In general the poisoning effect is best explained by considering the existence of very strong adsorption bonds between the poison and the metal. Whilst the formation of these bonds may not be irreversible, the duration of one adsorption is much longer for a poison than for a reactant, with the result that the poison is concentrated in the adsorbed phase, and hence even trace amounts may be sufficient to poison a reaction. The nature of the adsorption bond



is therefore important to the understanding of the problem.

Catalyst poisons may be conveniently divided into three classes:<sup>59</sup>

- (i) molecules containing an element of Groups Vb or VIb, where the number of valencies of that element is less than the maximum;
- (ii) certain heavy metals, their ions, and compounds;
- (iii) molecules having multiple bonds, e.g. carbon monoxide.

The significant feature of each of these classes is the availability of filled non-bonding orbitals which may participate in the formation of the adsorption bonds. Poisons of type (i) achieve this by the use of  $sp^3$  hybridised filled, non-bonding orbitals, as in molecules such as hydrogen sulphide, thiols, phosphines, etc. With type (ii) poisons, the toxic heavy metals are shown<sup>59</sup> to have either filled or partly filled d-orbitals. Metals such as copper, zinc, silver, gold, mercury, and lead are therefore toxic, while Group I and II elements and also even a few at the start of each transition series, are non-toxic. Poisons of type (iii) such as carbon monoxide, and cyanides are of special interest as they have certain similarities with unsaturated reactant molecules. The poisoning effect of these molecules is caused not by the presence of a specific element, but rather by the strength of adsorption of the multiple bond.

Maxted<sup>59</sup> suggests that bonding is caused by a change of bond order, or by diadsorbed resonance hybridisation. It appears more probable, however, in the light of current thoughts on adsorption,<sup>37</sup> that a  $\pi$ -complex is involved, as with the adsorption of olefins on metals. The role of the poison is two-fold. (a) The physical size of the molecule prevents reactants adsorbing on the catalyst, and (b) by donation of electrons to the d-orbitals, the d-band vacancies thought to be responsible for catalytic activity are filled, thereby limiting the possibility of adsorption by a reactant.<sup>60</sup> Evidence for this comes from magnetic susceptibility measurements of methyl sulphide on palladium.<sup>61</sup>

Consideration will now be given to each of the poison types in turn.

### 1.5.2 Group Vb and VIb Poisons.

The ability of sulphur or sulphur compounds to poison the synthesis of ammonia on iron catalysts has been known for some time. It has been shown, however, that the toxic effect on hydrogenation could be eliminated if the compound were converted to one where all the sulphur valencies were used for bonding,<sup>62</sup> such as a sulphone or sulphuric acid. Similarly, the ammonium ion, does not inhibit hydrogenation on platinum, but ammonia which had been very carefully

dried was shown to inhibit the hydrogenation of cyclohexene in cyclohexane solution on a platinum block catalyst.<sup>63</sup>

The effect of molecular weight on the toxic power has been studied by a number of workers. If the rate of deactivation is assumed to be linear, which is generally true for at least the initial stages of poisoning, the poisoned reaction rate,  $k_c$ , may be related to the unpoisoned rate  $k_o$  by the expression  $k_c = k_o (1 - \alpha C)$ , where  $c$  is the concentration of the poison, and  $\alpha$  is a constant which represents the sensitivity of the catalyst and the reaction to the poison. The hydrogenation of crotonic acid on platinum block and nickel-kieselguhr was employed as a standard reaction, and the results for a number of poisons are shown in table 1.4.

TABLE 1.4

Relative toxicity per g. atom sulphur.<sup>64</sup>

<u>Poison</u>	<u>M.W.</u>	<u>Pt</u>	<u>Ni</u>
Hydrogen sulphide	34	1	1
Carbon disulphide	76	1.9	2.4
Thiophene	84	4.4	4.5
Cysteine	121	5.0	5.4

It is apparent that the poisoning effect increases with molecular weight, and also that a reaction may be poisoned to the same extent on platinum and nickel. This similarity

in magnitude may be related to the similarity of lattice constants for platinum and nickel.

Thiophene was found to be five times more effective than carbon disulphide in the inhibition of benzene hydrogenation on supported nickel catalysts.<sup>65</sup> Neither poison caused any change in the activation energy of the reaction. It was also observed that identical amounts of carbon disulphide were adsorbed on a series of supported nickel catalysts.

A series of homologous thiols and sulphides investigated by Maxted and Evans showed similar trends,<sup>66</sup> the sulphides ( $R-CH_2-S-CH_2-R'$ ), being more toxic than the thiols ( $R-CH_2-SH$ ). The effect of a molecule with two terminal sulphur atoms was shown to be significantly less than a similar molecule with only such atom, suggesting that adsorption of each end reduced the effective physical obstruction.

While these sulphur compounds are generally poisons, they may, however, themselves undergo reactions on the catalyst. Recent studies<sup>67</sup> show that thiophene and furan exchange with  $D_2O$  on a number of metals, often with a high degree of selectivity. Thiophene is deuterated most rapidly on  $PtO_2$ , while  $RuO_2$  catalyses selective exchange of the  $\alpha$ -position. With furan, the order of activity is.

$\text{IrO}_2 > \text{NiO}_2 > \text{RuO}_2 \sim \text{PtO}_2$ , and nickel exhibits  $\sim 100\%$   $\alpha$ -selectivity. It is suggested that adsorption may involve donation of ring  $\pi$ -orbitals to the metal, while electron repulsion between the hetero-atom and the oxygen in the metal oxide prevents the former adsorbing directly on the surface. Its effect is therefore limited to activation of the  $\alpha$ -position.

#### Poisoning of n-Butene Isomerisation.

Leftin and Stern<sup>68</sup> have recently investigated the hydrogen sulphide poisoning of the hydrogenation of cis-2-butene on alumina-supported nickel and produced what they believe to be the first direct evidence for the formation by a poison of a specific coordination complex on the catalyst surface. The reactions were carried out in an optical cell-catalytic reactor<sup>69</sup> which enabled the spectrum of the catalyst to be measured during the reaction. The background spectrum of the catalyst was measured, and no change was observed during the reaction, but when a small dose of hydrogen sulphide was added, an intense band developed at 4260 Å and a weak band in the 5700 Å region; this was considered as direct evidence for the formation of a specific complex. An attempt was made to extract the complex with methylene chloride and the resulting solution exhibited two clear bands at the same wavelengths, thus confirming

the existence and stability of the complex. By comparison of the spectral characteristics they suggest the complex formed is nickel bis (dithio-2,3-butanedione). The effect of the poison on the reaction is not reported, other than that the hydrogenation is inhibited.

### 1.5.3 Poisoning by Heavy Metals.

A study of the effect of small quantities of heavy metals was first carried out by Maxted et al.<sup>70,71</sup> The aforementioned metals (section 1.5.1) were shown to be toxic, and it was suggested that the main factor contributing to this effect was that they had filled d-orbitals.

Radiochemical techniques in catalytic studies were introduced by Campbell and Thomson,<sup>72</sup> who employed radioactive mercury in an investigation of the selective poisoning of cyclopropane hydrogenation on evaporated nickel films. The use of the radioisotope enabled the true surface concentration of the mercury to be measured, allowing a more quantitative correlation between deactivation and the degree of poisoning to be made. The mercury was introduced to the system from the manometer used to measure the pressure fall during the reaction. The hydrogenation of cyclopropane was found to be seriously inhibited by the mercury while the reaction of propylene was only minimally affected. It is significant, however, that in the latter case the total weight of mercury adsorbed was only 0.098mg.

compared with 0.568mg. in the former case. Adsorption studies showed that adsorption of mercury caused the displacement of cyclopropane at 25°C, but not of propylene; it had previously been shown that mercury could displace adsorbed hydrogen.<sup>73</sup> Adsorption of propylene was not, however, detected on a catalyst with pre-adsorbed mercury.

Some interesting results were obtained by Bond and Wells<sup>14</sup> from the study of the mercury poisoning of alumina-supported palladium for the hydrogenation of acetylene and ethylene. The mercury was again introduced to the catalyst vessel by allowing the vapour to diffuse in from a manometer. Two distinct types of deactivation patterns were observed. Type A: below 85°C, the activity for acetylene hydrogenation at first fell exponentially, and subsequently more rapidly, with increasing exposure to the mercury. Type B: at temperatures above 115°C, an immediate rapid deactivation, followed by immunity to further mercury, was observed. Above 115°C, the catalyst could not be completely poisoned. The kinetics varied considerably from type A to type B. The former exhibited normal orders of zero and unity for acetylene and hydrogen, while the latter exhibited orders ranging from zero to unity for each reactant, according to the degree of poisoning and partial pressure.

The ethylene hydrogenation reaction was more rapidly

poisoned than was the acetylene reaction, and it is significant that while successive ethylene hydrogenations had no effect on the activity, the admission of 50mm. acetylene to the reaction vessel for one minute produced some reactivation.

The reactions were studied in less detail over alumina supported platinum, rhodium and iridium.<sup>14</sup> Each metal exhibited trends very similar to those of palladium, except that platinum was not deactivated for ethylene hydrogenation.

The interpretation of the results of Campbell and Thomson and Bond and Wells is possible with the use of a geometrical model of the catalyst surface, and the assumption of random adsorption by mercury atoms. The immunity of the propylene hydrogenation may be accounted for by the strong adsorption of the propylene. The surface concentration of hydrogen is low, and the geometrical model shows the existence of sites which may adsorb only hydrogen when the surface is "covered" with mercury and propylene. The type B poisoning is not explained purely in terms of this statistical procedure, but it is suggested the heat of adsorption of mercury may fall, until the adsorption is reversible at higher temperatures.

The correlation between the experimental results and the statistical model interpretation is further



evidence in support of the suggestion that the poisoning mechanism of the mercury is mainly a surface blocking effect. The mercury concentration is insufficient to fill the d-band vacancies in the catalyst, and alloy formation is ruled out: investigation of the rhodium mercury system<sup>74</sup> showed that the mutual solubilities are very small, and the only stable homogeneous compounds had mercury/rhodium ratios greater than unity.

It has recently been noted<sup>75</sup> that not all heavy metals have an inhibiting effect. The effect of uranium oxide in the support for a nickel catalyst is shown in table 1.5.

TABLE 1.5

<u>Catalyst</u>	<u>Surface Area</u>
Ni/Al <sub>2</sub> O <sub>3</sub>	7.0 m. <sup>2</sup> g <sup>-1</sup> .
Ni/U <sub>3</sub> O <sub>8</sub> /Al <sub>2</sub> O <sub>3</sub>	12.0 "
U <sub>3</sub> O <sub>8</sub> /Al <sub>2</sub> O <sub>3</sub>	1.0 "

The adsorption of hydrogen and water is much stronger on the mixed catalyst, causing a change in the kinetics of the butane-steam reaction. It is suggested the uranium oxide forms a compound with the nickel having a greater surface area than the supported nickel.

#### 1.5.4 Poisons containing multiple-bonds.

Interest in this class of catalyst poison is concerned primarily with the nature of the adsorption bond, as was discussed briefly in section 1.5.1. Their similarity to many reactant molecules causes the division between poison and reactant to be rather diffuse; ethylene, for instance, may poison the conversion of p-hydrogen on nickel,<sup>28</sup> while benzene inhibits the hydrogenation of ethylene. As may be expected, the saturation of the poison molecule generally renders it non-toxic, and this principle may be used in the purification of reactants for a catalytic reactor, as, for instance, the conversion of carbon monoxide into methane or carbon dioxide.

#### 1.5.5 Further Features of Catalyst Poisoning.

The effect of a poison has been demonstrated to depend upon the physical form of the catalyst. It has been shown,<sup>76</sup> for example, in a series of experiments on zeolite supported metal catalysts that the ratio of the pore diameter to the size of the poison molecule, and the location of the metal, in a pore site or on an external surface site, are critical factors in determining the effect of a poison.

A recent report on the hydrogenation of dimethyl ethynyl carbinol on an acrylonitrile supported palladium catalyst produced an apparent anomaly in poisoning trends.<sup>77</sup>

The reactant, a doubly unsaturated species, is selectively hydrogenated to dimethylvinylcarbinol, and then to the fully saturated 2-methylbutan-2-ol, the accumulation of which poisons the reaction. The intermediate vinyl compound has no poisoning effect. This is in distinct contrast to the multiple bond poisons.

#### 1.5.6 Conclusion.

The nature of catalyst poisoning has been widely investigated, and a number of regular trends have become evident, but the interpretation of the poisoning effect varies from the physical obstruction of surface sites to the formation of specific complexes, and interaction with the bulk metal electron bands. The multiplicity of reaction systems allows wide scope for further work in this field.

CHAPTER 2OBJECTS OF PRESENT WORK.

The object of the present work was two-fold;

(1) to study the influence of the support on the catalytic behaviour of supported rhodium catalysts for the hydroisomerisation of 1-butene, and;

(2) to study the influence of a selective poison, namely, mercury, upon the catalytic properties of supported rhodium catalysts for the hydrogenation of 1,3-butadiene and the hydroisomerisation of 1-butene.

The effect of the support was studied by considering the interaction of 1-butene with hydrogen on alumina- and silica-supported rhodium with the following aims:

(i) to study the kinetic features of the hydrogenation and isomerisation reactions;

(ii) to determine the distribution of isomers in the initial stages of reaction;

(iii) to elucidate mechanisms for the hydrogenation and isomerisation reactions, and to investigate the influence, if any, of the support upon the mechanism.

The objects of study of the mercury poisoning of the rhodium - catalysed reaction of 1,3-butadiene with deuterium and 1-butene with deuterium were:

(i) to study the variation in distribution of products

as a function the degree of poisoning of the surface;

(ii) to study the variation in rates of addition, olefin exchange and hydrogen exchange reactions with progressive poisoning of the surface;

(iii) to attempt to establish the mechanism for formation of 1-butene and 2-butene in 1,3-butadiene hydrogenation, i.e. whether 2-butene is produced by (a) direct 1,4-addition of hydrogen to adsorbed 1,3-butadiene, or (b) by 1,2-addition to the 1,3-butadiene and subsequent isomerisation;

(iv) in 1-butene hydroisomerisation to attempt to establish whether hydrogenation and isomerisation are concomitant or independent reactions.

CHAPTER 3.EXPERIMENTAL3.1 Materials.

Rh/Al<sub>2</sub>O<sub>3</sub> catalyst. 5% (w/w) rhodium supported on Peter Spence Type A alumina was supplied by Johnson -Matthey Ltd.

Rh/SiO<sub>2</sub> catalyst. 5% (w/w) rhodium supported on silica was prepared by suspending 20g. "Aerosil" silica (purity 99.99%) (Degussa Ltd.) in a solution of 2.5g. Analar rhodium trichloride (RhCl<sub>3</sub>·3H<sub>2</sub>O) in ~100ml. water. The suspension was slowly evaporated to dryness, and the residue ground to a fine powder. A sample of the supported salt was then heated in an evacuated reaction vessel to 220°C for one hour. Reduction of the supported salt was carried out at 220°C using three successive volumes of hydrogen, each of 150mm. pressure, for periods of ½, 1½, and 17 hours respectively. During the initial period the pressure fell by ~12mm. The vessel was finally pumped out for one hour at 220°C, and allowed to cool.

Hydrogen. Cylinder hydrogen (British Oxygen Co.) was purified by diffusion through a palladium/silver alloy thimble into a degassed storage vessel. A temperature of ~200°C gave an initial diffusion rate of 300mm./hr.

Deuterium. Norsk Hydro deuterium was supplied by I.C.I. Ltd. and was quoted as being > 99.7% isotopically pure. This was checked by mass spectrometry, which gave a value of

99.92%. The oxygen content was < 10p.p.m., which was considered to be negligible, and hence no further purification was carried out.

1-Butene (Matheson Co. Inc.) was found by gas chromatography to contain 0.45% iso-butene, but as the 1-butene was preferentially hydrogenated and the iso-butene remained a constant fraction of the total hydrocarbon, there was no apparent need for its removal. The 1-butene was therefore merely degassed before use.

1,3-Butadiene (Matheson Co. Inc.) contained no impurities detectable by gas chromatography, and was merely degassed before use.

Radioactive mercury. ( $\text{Hg}^{197}$   $\text{Hg}^{203}$ ) was supplied in 2g. samples by the Isotope Production Unit, A.E.R.E., Harwell. Four weeks irradiation at a Pile Factor of 10 produced a total activity of 50mC.  $\text{Hg}^{203}$  and  $\sim 700\text{mC. Hg}^{197}$ .

### 3.2 Apparatus.

#### 3.2.1 The Vacuum System.

The apparatus used for carrying out all reactions was a conventional high-vacuum static system. It is shown in Fig. 3.1. The reaction section - from the cold trap T to the gas burette B, - the common lead to it from the four 2 litre storage vessels  $S_1$ - $S_4$ , and the high vacuum line A-A' formed a closed high-vacuum circuit, providing the facility of

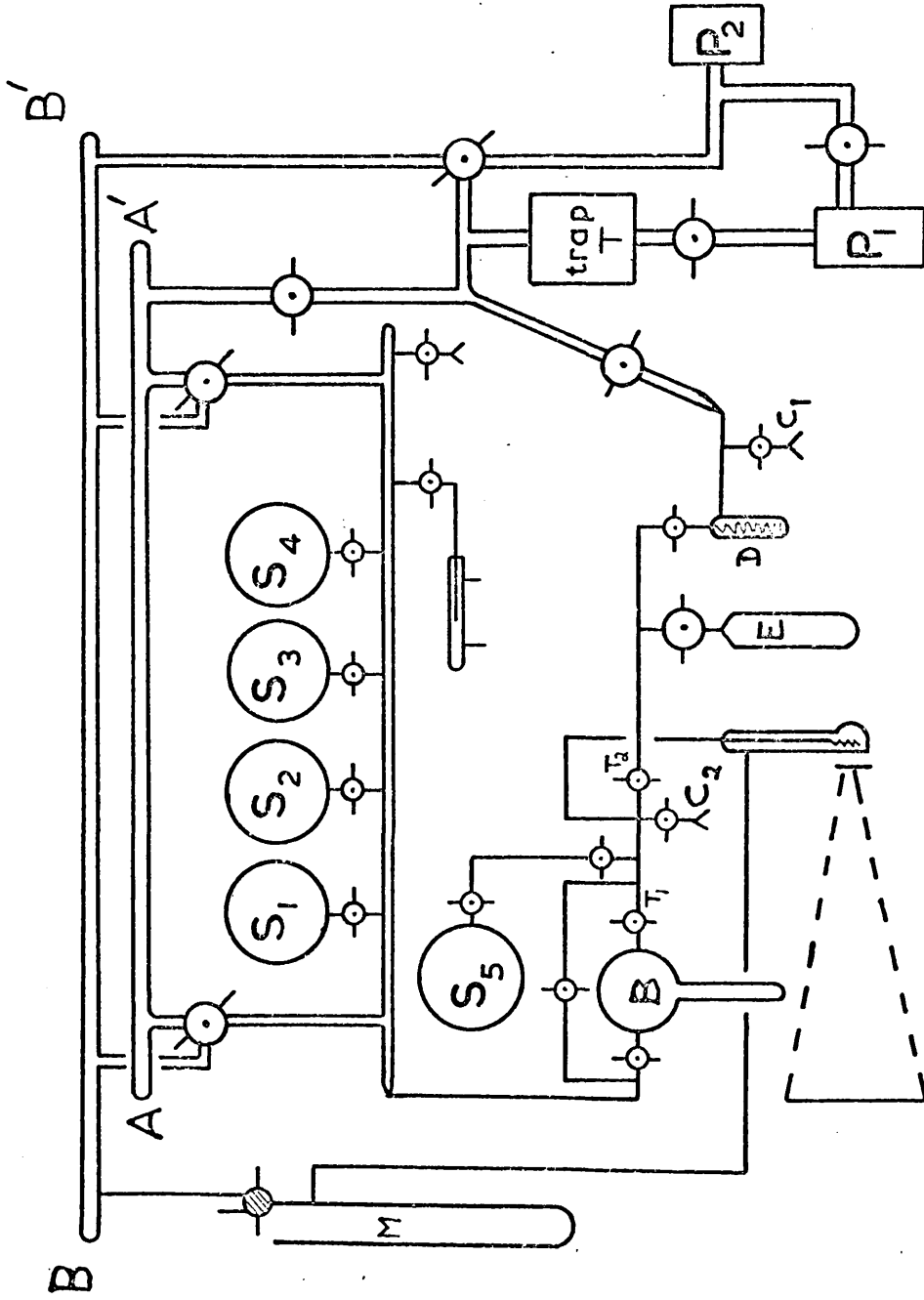


FIG. 3.1 The Vacuum System.

P<sub>1</sub> = diffusion pump P<sub>2</sub> = rotary pump M = manometer



evacuating from either side of the reaction section. This was of considerable practical convenience. Vacuum of  $10^{-4}$  torr and better was obtained by an oil-filled diffusion pump backed by a rotary oil-pump. The use of an oil-filled diffusion pump was necessary in order to prevent possible contamination of the reaction section by mercury, as this would interfere with the controlled poisoning of the catalysts. For the same reason, the use of a mercury filled manometer for pressure measurement in the reaction vessel was obviously unsuitable, and hence a calibrated Bourdon spiral gauge was used in conjunction with a spotlight and a graduated scale. The gauge was calibrated against a mercury-filled manometer which was evacuated only via the low-vacuum line B-B' by the rotary pump, thus avoiding any mercury contamination of the high-vacuum section.

To enable deuterium to be admitted directly to the reaction vessel, a storage vessel  $S_5$  was constructed with a separate lead to the reaction vessel.

All taps were greased with Apiezon N grease as this is inert to all the gases used. This, however, precluded the baking of the system for degassing; this was done by heating it gently with a light oxygen flame on parts away from taps.

### 3.2.2 The Reaction Vessel.

The design of the reaction vessels used for all experi-

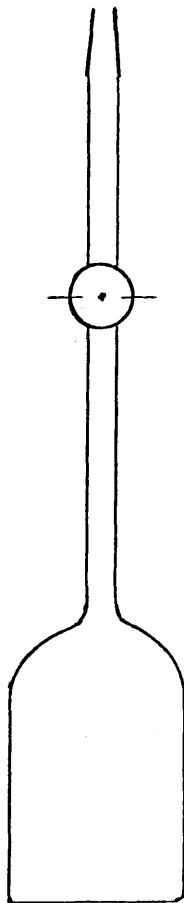


Fig. 3.2 The Reaction Vessel.

-ments on unpoisoned catalysts is shown in Fig. 3.2. It was made from "Pyrex" glass and consisted of a cylindrical vessel of  $\sim 120$  c.c. capacity with a 2mm. high-vacuum tap.

### 3.3 Experimental Procedure.

Any section of the high-vacuum section which had been open to air was degassed as described above at the start of a reaction series. Gas mixtures were made up by admitting a measured pressure of hydrocarbon to the gas burette, closing tap  $T_1$ , and condensing it in the cold finger of the burette. Hydrogen was then admitted to the required pressure,  $T_1$  closed, and the vessel allowed to warm up to ambient temperature. To ensure complete mixing, the hydrocarbon was partially condensed twice more, and then left for at least one hour for mixing to be complete.

Before each reaction series, the reaction vessel was cut open and washed in a mixture of equal volumes of concentrated hydrochloric and nitric acids for at least 30 min. It was thoroughly rinsed with distilled water, and dried. The required weight of catalyst was sealed in the vessel, which was then attached to the high-vacuum system by the B10 socket  $C_2$  and evacuated while the temperature was raised to  $220^\circ\text{C}$  by means of an electric furnace placed around the vessel. After degassing for 20 - 30 min. the catalyst was activated by admitting 150mm. hydrogen for 60 minutes at  $220^\circ - 225^\circ\text{C}$ .

Finally, the vessel was evacuated for 30 minutes at the reduction temperature, and allowed to cool under vacuum.

Reactions were carried out by admitting the required pressure of the reaction mixture to the reaction vessel, and measuring the pressure fall on the spiral gauge. At the required pressure fall, the reaction products were extracted into the expansion vessel E, then freed from unreacted hydrogen by condensing in the spiral trap D and pumping away the hydrogen. The hydrocarbon products were removed for analysis by warming up and condensing in an evacuated sample vessel connected to the apparatus at the B14 socket C<sub>1</sub>. Although the leads to the reaction vessel were kept as small as possible by the use of capillary tubing, the reaction vessel tap was closed immediately before extraction and the section between it and taps T<sub>1</sub> and T<sub>2</sub> evacuated. The temperature of the reaction vessel was maintained constant by surrounding it with an electric furnace or a Dewar flask containing ice, an ice-salt mixture, or water, as required. Temperatures were measured with a Pt - Pt/Rh thermocouple or a thermometer.

### 3.4 The Analysis of Reaction Products.

Quantitative analysis of the reaction products was achieved by gas chromatography and mass spectrometry.

#### 3.4.1 The Gas Chromatography System.

The analytical requirements were the separation of the

products of (i) the 1-butene hydroisomerisation, i.e. n-butane, 1-butene, trans 2-butene and cis 2-butene, and (ii) the hydrogenation of 1,3-butadiene, these being n-butane, 1-butene, trans 2-butene, cis 2-butene, and 1,3-butadiene.

For the first problem, a complex of silver nitrate with benzyl cyanide supported on 60 - 80 mesh Silocel firebrick was found to give complete separation of the products. 16.0g. silver nitrate were dissolved in 32.0g. benzyl cyanide and the solution diluted to 500ml. with absolute alcohol. 150g. firebrick were suspended in the solution, and the excess alcohol was evaporated off until the powder was free-running. Using a 20ft. column of 5 - 6mm. bore, the corrected retention volumes for n-butane, trans 2-butene, 1-butene, cis 2-butene were 250, 450, 575, and 700ml. respectively. These values decreased by  $\sim 10\%$  over the period of use. A typical trace is shown in Fig. 3.3 (a).

As the above column did not separate cis 2-butene and 1,3-butadiene, an alternative stationary phase was required for the second problem. A 40% (w/w) 2,5-hexadione (acetyl acetone) on firebrick column was found to be suitable. The column packing was prepared by dissolving 40g. acetyl acetone in 250ml. acetone and stirring in 103g. 60 - 80 mesh Silocel firebrick. The acetone was removed by evaporation until a dry, free-running powder was left. A 20ft. column

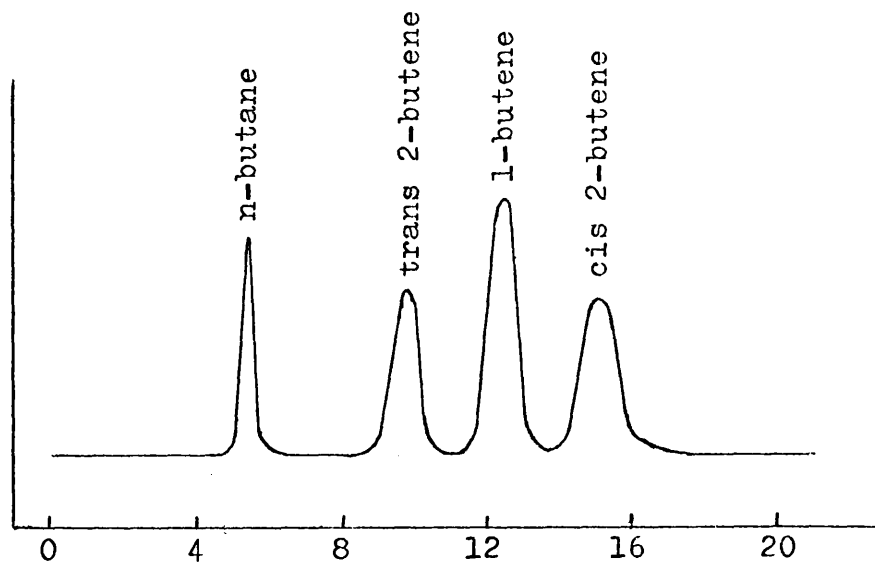
gave corrected retention volumes for n-butane, 1-butene, trans 2-butene, cis 2-butene, and 1,3-butadiene of 200, 385, 525, 650, and 990ml. respectively. These values decreased by ~50% with use, after which the column had to be repacked. A typical trace is shown in Fig. 3.3 (b).

TABLE 3.1

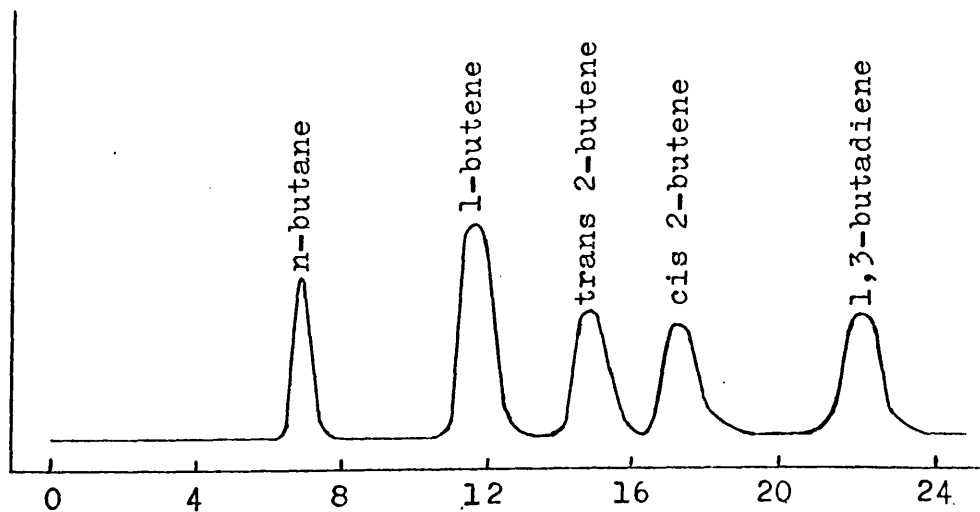
Operating Conditions for Silver Nitrate & Acetyl Acetone Columns.

Carrier gas	Nitrogen
Input pressure	1.6 atmos.
Flow rate	$50 \pm 1.5$ ml./min.
Temperature	$20^{\circ} \pm 3^{\circ}$ C.

An apparatus had to be designed with a sampling system which could accept gas samples transferred from the main reaction system. This was achieved with the sampling system shown in Fig. 3.4 (a). The U-tube between the three-way taps  $T_1$  and  $T_2$  formed a fixed sample volume of ~14ml., which, with the manometer M, was evacuated by a rotary oil-pump P. Samples were admitted to the system from sample vessels via the B10 socket C, the pressure being read from the manometer. If necessary, the whole sample could be condensed in the U-tube. During this operation the carrier gas flowed through the by-pass B, and by simultaneously

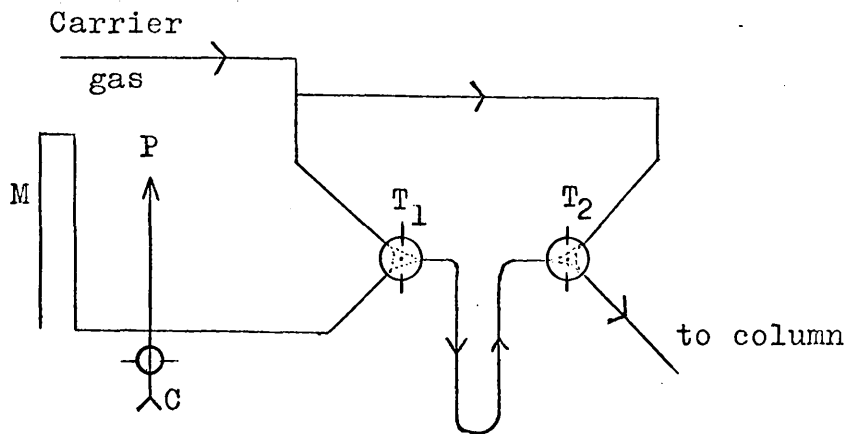


(a) Separation on silver nitrate benzyl cyanide column.

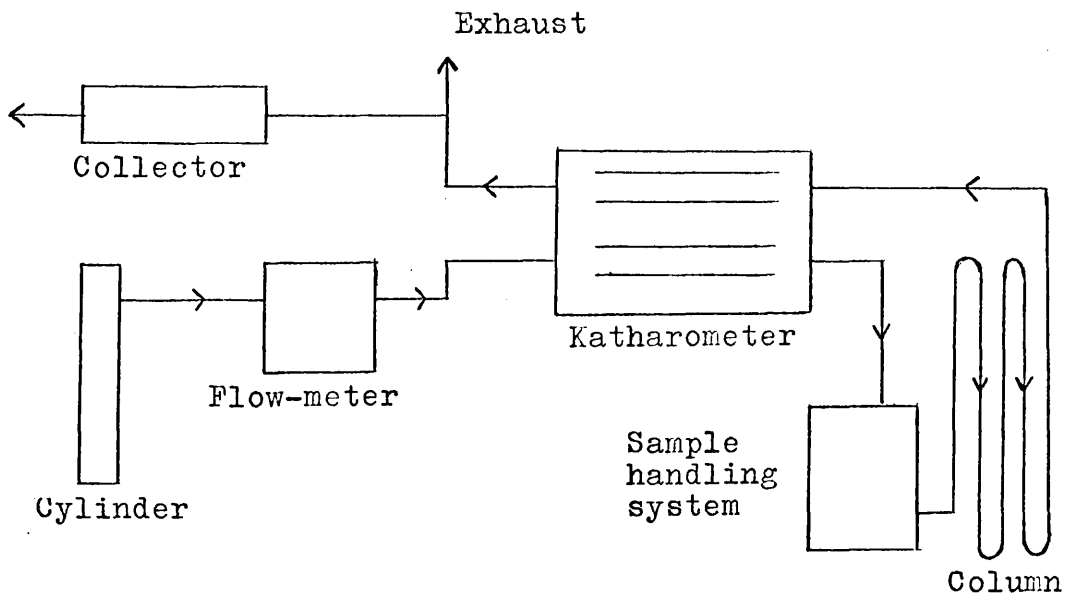


(b) Separation on acetonyl acetone column.

Fig. 3.3 Typical traces obtained from chromatography columns.



(a) The sampling system.



(b) Block Diagram of Apparatus.

Fig. 3.4 The Chromatography System.



turning both  $T_1$  and  $T_2$ , the gas was diverted through the U-tube, thus carrying the sample onto the column. The complete chromatography unit is shown diagrammatically in Fig. 3.4 (b).

The carrier gas flow rate was measured by means of a bubble flowmeter, and controlled by a Crawford Swagelock needle valve.

The detector used was a Gow-Mac hot-wire katharometer, the filament current being supplied by a 12v. battery. Initially a current of 90mA. was used but this was later increased to 150mA. to give greater sensitivity.

The output from the detector bridge circuit was recorded on a Servoscribe potentiometric chart recorder operated in most cases at 5mv. full scale deflection. Where small partial pressures were being measured, however, it was operated on the 2mv. range to give greater recorder response. The area under each peak is proportional to the corresponding partial pressure, and was measured initially with an Allbrit fixed-arm planimeter. The error introduced by this method was  $\sim \pm 3\%$  in the measurement alone, and it was soon realised that some form of electronic integration would be more efficient.

The recording system described above was therefore modified by feeding the bridge output directly to an

analogue to digital converter and measuring the digitised output on an Echo scaler. A continuous output corresponding to 2, 5, or 10mv. full-scale deflection was also taken from the integrating unit to the Servoscribe recorder. A plot of count rate against % deflection for the 5mv. range (Fig. 3.5) shows a linear relationship above 100c.p.m. The rate controlling potentiometer on the integrator was therefore adjusted so that 3% deflection on the recorder, normally used as the baseline, corresponded to a count rate of 100c.p.m. The baseline count rate was measured before and after each peak was eluted, and by noting the total counts and the time for which it was counted, the nett counts were obtained, corresponding to the peak area in arbitrary units.

#### 3.4.2 Mass Spectrometric Analysis.

The use of a non-destructive detector such as a katharometer allows each fraction of the chromatograph eluant to be retained for analysis of the deuterium content by mass spectrometry : this was achieved by passing the eluant through the collector (Fig. 3.4 (b)). This consisted of five traps lightly packed with glass wool, as shown in Fig. 3.6, placed in series after the detector. Each was surrounded by a Dewar vessel containing liquid air, and by directing the gas flow through the U-tube or by-pass, as appropriate, samples of each hydrocarbon in turn were con-

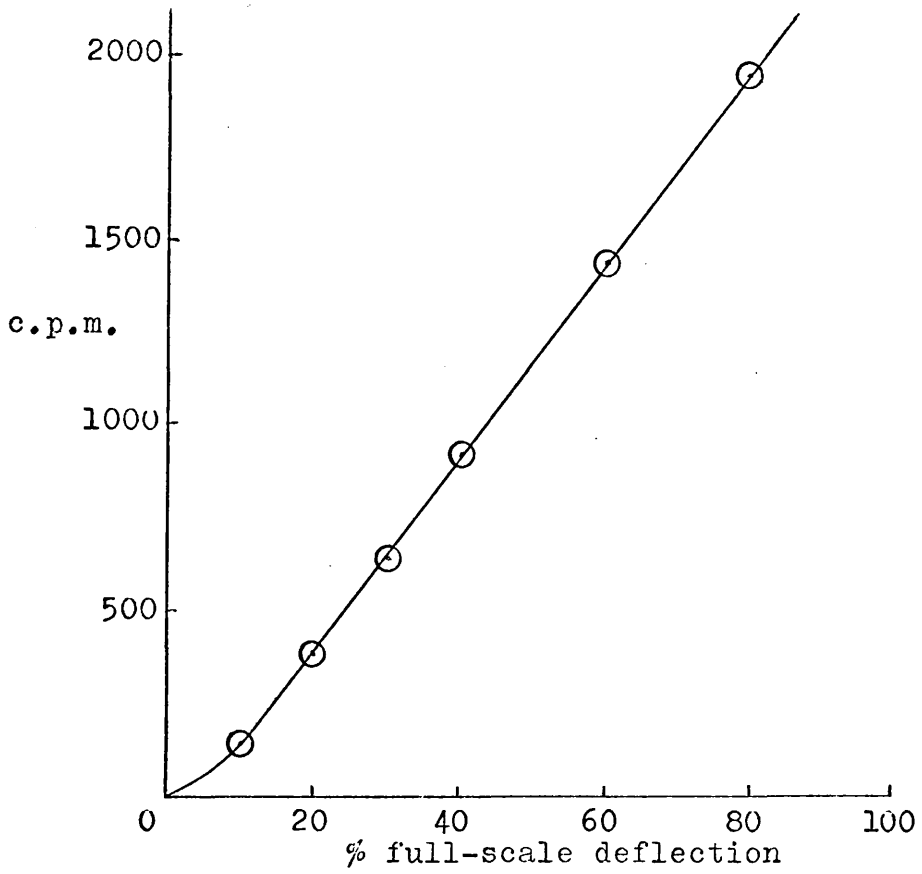
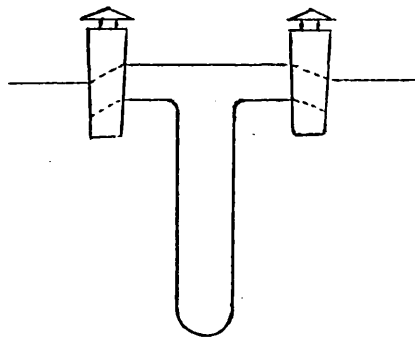


Fig. 3.5 Increase in integrator count with % deflection.

Fig. 3.6 A Collector.



-dense out of the carrier gas stream. The traps were evacuated and allowed to warm up, and the samples removed for analysis by condensing them into evacuated sample vessels.

The analyses were carried out with an A.E.I. MS10 mass spectrometer, using the following operating conditions:

	<u>Hydrocarbons</u>	<u>Hydrogen/Deuterium</u>
Ionising voltage	12e.v.	70e.v.
Trap current	50 A.	50 A.
Ion repeller	-1v.	-1v.

### 3.5 Apparatus & Procedure for Poisoning of Catalysts.

#### 3.5.1 Preparation of Mercury.

The irradiation of natural mercury to produce  $\text{Hg}^{203}$  also produces a large excess of  $\text{Hg}^{197}$  and the samples as received from Harwell contained  $\sim 50\text{mC.}$  activity  $\text{Hg}^{203}$  and  $\sim 700\text{mC.}$   $\text{Hg}^{197}$ . As the respective half-lives are however 47 days and 65 hours, and as the presence of only one active isotope is desirable for measurement purposes, the mercury was left for at least four weeks to allow the 197 - isotope to decay to negligible concentration. Purification of the mercury was carried out by vacuum distillation into break-seal ampoules.

#### 3.5.2 Modifications to the Reaction Vessel.

The problem of controlling access of the mercury vapour to the catalyst was overcome by modifying the reaction vessel

by the addition of a side-arm, as shown in Fig. 3.7. The catalyst vessel V was of the same design and size as in the original, while section A was of 5mm. bore glass tubing and was just long enough to enable a lead brick to be placed between the arm and a furnace or Dewar flask placed around the catalyst vessel. A subsidiary side-arm D was attached to the 12mm. section B, which was left open in order that the ampoule C containing the mercury below the breakseal could be sealed onto it.

### 3.5.3 The Counting Problem.

$\text{Hg}^{203}$  is a  $\beta$ - $\gamma$  emitter, the  $\beta$ -energy being 0.205MeV. and the  $\gamma$ -energy 0.286MeV. The advantage of the use of a  $\gamma$ -emitter for adsorption measurements is that it greatly facilitates the problem by permitting the counter to be situated externally, as the energy is sufficient for nearly all the radiation to pass through the glass vessel.

The counter used was a Mullard MX 168/01 Geiger-Muller tube, with a window thickness of  $1.4\text{mg.cm}^{-2}$ . The optimum position for the counter was immediately below and concentric with the catalyst vessel, but this, however, raised the problem of the means of having the counter in close proximity to the catalyst vessel consistent with the requirement of surrounding the latter with a suitable thermostat device, such as a Dewar flask. As this situation could not be

achieved with conventional Dewar flasks, one was designed and built for the purpose, as shown in Fig. 3.8. The silvered section was limited to the outer wall, and the base contained a well just wide enough to hold the G.M. tube. The vessel was placed concentrically around the catalyst vessel and clamped with the well firmly against the base of the catalyst vessel; it was then filled with water, ice, etc., as required. The distance between the counter and base was  $\sim \frac{1}{2}$ ". Temperatures above  $25^{\circ}\text{C}$  were maintained with the use of a cylindrical electric furnace with an open base, so that the counter could be clamped in place inside the furnace.

During early experiments it was observed that the catalyst tended to deposit around the outside edges of the base of the vessel, thus giving a less efficient counting geometry. This was improved by further modifying the reaction vessel by the introduction of a shallow well,  $\sim \frac{1}{8}$ " deep, and of the same diameter as the counter ( $\sim \frac{1}{2}$ "), in the base. This had the effect of keeping all the catalyst, and hence all the adsorbed mercury, directly above the counter. It had no effect on reaction rates.

Despite the advantage described above in using a  $\gamma$ -emitter, the  $\gamma$ -counting efficiency of a G.M. tube is fairly low compared with the  $\beta$ -efficiency. Use may be made, how-

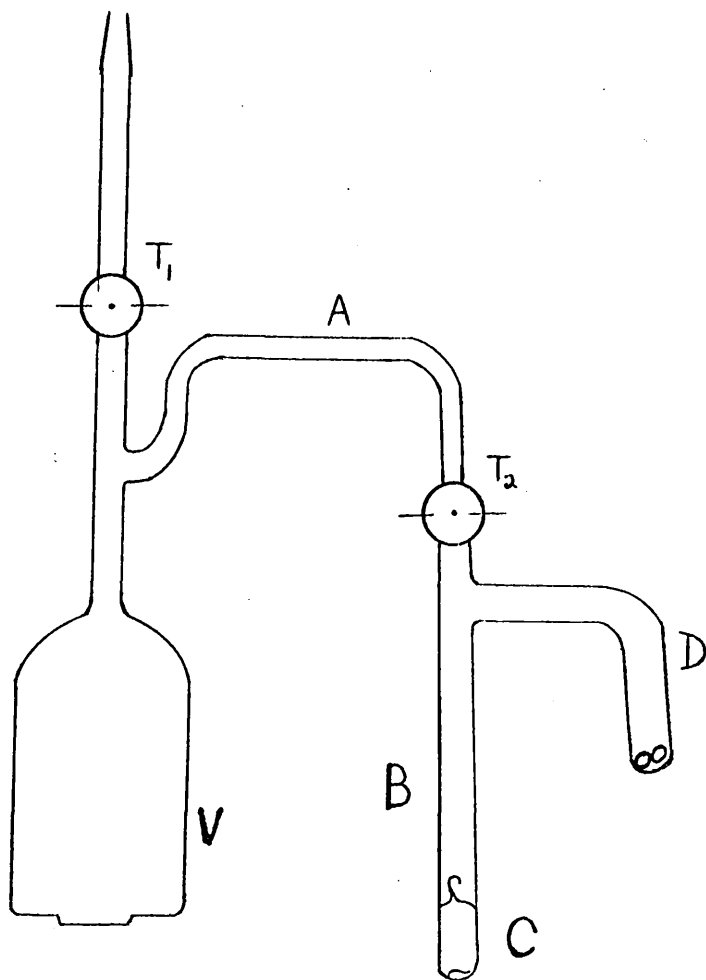


Fig. 3.7 Reaction vessel modified for mercury poisoning studies.

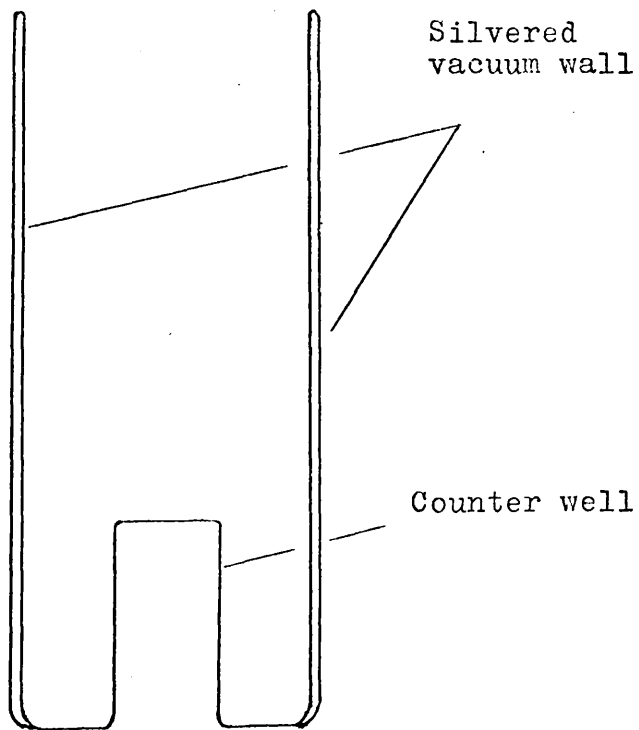


Fig. 3.8 Dewar flask for mercury counting studies.



-ever, of the secondary electron emission of  $\gamma$ -irradiated heavy elements e.g. lead. Provided there is no  $\beta$  absorber between the element and the counter, these electrons will be detected at a higher efficiency than would the  $\gamma$ -rays. If the  $\beta$ -source is too thick, however, the count rate will be reduced by self-absorption. This arrangement may be achieved in the system under consideration by interposing a lead foil of suitable thickness between the catalyst vessel and counter. An experiment was therefore carried out using a  $\text{Hg}^{203}$  source and a series of lead foils to determine the optimum thickness. The result is shown in Fig. 3.9 (a), and a foil of thickness  $120\text{mg./cm}^2$  was therefore used for all experimental measurements. The working voltage of the counter was previously determined in the normal manner. The plateau region was fairly short, as shown in Fig. 3.9 (b) and 375v. was selected as the most suitable working voltage.

#### 3.5.4 Procedure.

A mercury ampoule was sealed onto a reaction vessel containing a sample of catalyst as described in 3.5.2. The vessel was evacuated and degassed as far as the break-seal, and tap  $T_2$  closed. The catalyst was activated as described in section 3.3 and, where required, a series of reactions carried out on the unpoisoned catalyst.

The mercury ampoule was thermostated 10 - 20 degrees

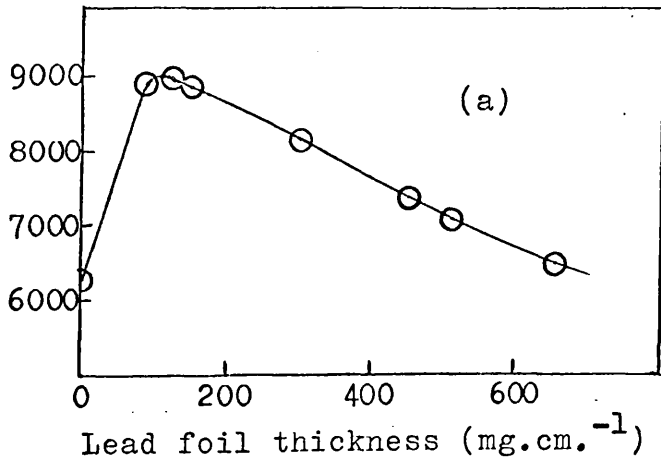
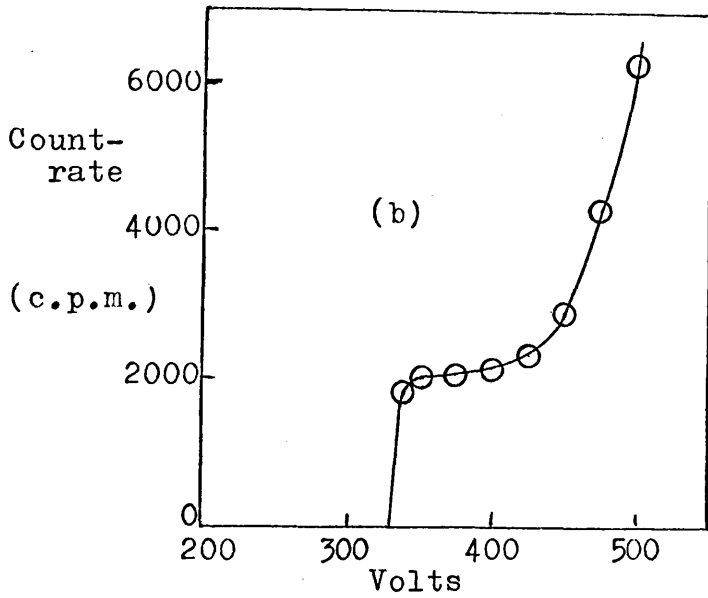


Fig. 3.9 (a) Effect of lead foils on count-rate by emission of secondary electrons.  
 (b) Determination of counter plateau and working voltage.

below the adsorption temperature of the catalyst vessel, and surrounded by 3/4" thick lead bricks. After measuring the background activity, and evacuating the reaction vessel, the break-seal was broken. With tap  $T_1$  closed,  $T_2$  was opened, allowing the mercury vapour to diffuse into the catalyst vessel. Counts were taken at regular intervals, and the adsorption could be stopped when required by closing  $T_2$ . Reactions were then carried out on the partially poisoned catalyst in the usual way. By successive adsorptions and series of reactions, the effect of progressive poisoning on the catalytic properties could be evaluated.

#### 3.5.5 Total Mercury Determination.

As the count rates measured by the system described in 3.5.3 gave only the relative amounts of mercury adsorbed on the catalyst, it was necessary to determine finally the total mass of mercury adsorbed. This was done by boiling the catalyst in ~50ml. 12N nitric acid for 30 - 40 minutes to dissolve the adsorbed mercury. The solution, evaporated to ~5ml., was washed into a 10ml. graduated flask and made up to the mark. A standard solution was prepared by dissolving a weighed globule of mercury of the same specific activity, and making the solution up to 50ml.

10ml. samples of each solution were counted initially on a Nuclear Enterprises well-crystal scintillation counter,

but the measurements so obtained were very unsatisfactory, as the ratios of the counts varied with the pulse height and slit width control settings. When no great degree of success could be achieved with this system, experiments were carried out with a liquid G.M. counter, and consistent results were obtained. All subsequent measurements were made with this system, and from the relative count rates the total mass of mercury was calculated.

In order to check that all the adsorbed mercury had been dissolved, the catalyst residue was treated a second time in the same manner, and the solution counted; in most cases it was found to have little activity.

## CHAPTER 4

### TREATMENT OF EXPERIMENTAL DATA.

#### 4.1 The Hydrogenation Reaction.

The pressure fall during hydrogenation was calculated by noting the instantaneous Bourdon gauge scale reading, and converting the scale reading directly to pressure from the previously determined calibration curve. The pressure fall was plotted against time; the gradient of the tangent to the curve at the origin, or the gradient of the line itself if it was linear, was measured and taken to be the initial rate of hydrogenation.

#### 4.2 The Butene Distribution.

##### 4.2.1 Interpretation of Gas Chromatography Traces.

The area under a peak in the chromatography traces was found to be proportional to the partial pressure of the corresponding gas, the ratio of peak area to partial pressure being termed the sensitivity coefficient for that gas. The columns were calibrated using samples of a standard mixture of all the gases to be encountered in the reaction analyses; a high degree of reproducibility was achieved, and the respective sensitivity coefficients were determined as the mean ratio obtained for each gas. A calibration check was carried out at regular intervals to allow for any

changes with usage.

The computation of the partial pressure of each reaction product and the percentage distribution, was first carried out by hand; at a later stage, computer programmes were written to evaluate these, together with the required product ratios, such as the trans/cis ratio, and the selectivity of 1,3-butadiene hydrogenation.

#### 4.2.2 The Initial Rate of Isomerisation.

The initial rates of isomerisation were calculated by the method developed by Twigg.<sup>42</sup> This is concerned only with double-bond migration, and leads to the following equation:<sup>48</sup>

$$r_i = [\log_{10}(1-y_{eq}) - \log_{10}(y-y_{eq})] \cdot 2.303(1-y_{eq})P_B/t;$$

where  $r_i$  = initial rate of isomerisation,

$y$  = fraction of reactant butene remaining,

$y_{eq}$  = thermodynamic equilibrium fraction of reactant butene,

$P_B$  = initial pressure of butene,

$t$  = time of reaction.

The main assumption required by this model is that the adsorption coefficients of 1-butene and 2-butenes are the same; this may not be valid, but the problem otherwise becomes very complex.

This equation was incorporated in the relevant computer programme, and by the use of a "fork" device, the programme would either calculate the rate from the computed butene distribution, plus extra data, as, for example, the time of reaction, or it would return to the start of the programme for the next set of data.

#### 4.3 Determination of Reaction Kinetics.

The dependence of reaction rates on the initial reactant pressures was calculated on the assumption that the rate expression is of the form:

$$\text{rate} = k p_{\text{H}_2}^x p_{\text{B}}^y$$

By alternately varying the initial pressure of one reactant while the pressure of the other was maintained constant, and plotting  $\log(\text{rate})$  against  $\log p_{\text{H}_2}$  and  $\log p_{\text{B}}$ , the kinetic orders with respect to hydrogen and butene respectively are determined.

#### 4.4 Determination of Activation Energies.

The relationship between reaction rates and temperature is conveniently expressed by the simple form of the Arrhenius equation, that is;

$$\text{rate} = A e^{-E_a/RT},$$

and hence,  $\ln (\text{rate}) = \text{constant} - \frac{E_a}{RT}$ ,

where  $E_a$  = activation energy,  $R = 1.986 \text{ cal. deg.}^{-1} \text{mole}^{-1}$ ,  
 $T$  = absolute temperature,  $A$  = a constant.

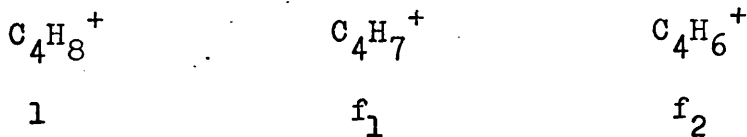
The initial rates were measured at a series of temperatures, and, by plotting  $\log (\text{rate})$  against  $1/T$ , the activation energy could be calculated, since the gradient of the line is equal to  $E_a/2.303R$ .

#### 4.5 Interpretation of Mass Spectra.

Mass spectrometric analysis were made of (i) the hydrocarbon products of the reactions of 1-butene and 1,3-butadiene with deuterium, and (ii) the residual hydrogen/deuterium from the same reactions.

##### 4.5.1 Analysis of Hydrocarbons.

At a beam voltage of 12.0ev. each of the hydrocarbons undergo both ionisation and fragmentation. The parent ion was always the most abundant, while the fragments were denoted by f-values (fractions relative to parent ion intensity equal to unity). With butene, for example, the relevant species are:



It is therefore apparent that in calculating the deuterio-butene distribution allowance must be made for these



fragments. It has been shown it is justifiable to assume that the fragmentation pattern of a deuterated butene is the same as for the light butene.<sup>89</sup> A set of simultaneous equations may therefore be derived to enable the true intensity of each deuterio-butene parent ion to be calculated. The ion current of a given mass is produced by (i) the parent ion of the same mass, and (ii) fragments from species of higher mass. The latter contribution is dependent upon (a) the f-values, which are determined by experiment, and (b) a statistical factor to account for the probability of the formation of the given species from each ion of higher mass, assuming no preferential splitting of C - H or C - D bonds. The intensities of each parent ion after correction for fragmentation are thus calculated. If the scheme is valid, it is apparent that the corrected intensities of the first and second fragments of the  $d_0$ -butene should each be zero. A check on this showed they were generally less than 2% of the highest intensity, which is acceptable within experimental error. The full equations used in the analysis of each hydrocarbon are given in Appendix A.

The parent ion intensities obtained from these equations were then corrected for the  $C^{13}$  content of each hydrocarbon by subtracting 4.4% of the intensity of the  $d_0$ -species from that of the  $d_1$ -species, then subtracting

4.4% of the  $C^{13}$  - corrected  $d_1$ -intensity from that of the  $d_2$ -species, and so on.

The deuterium distributions were calculated by expressing each of the final corrected intensities as a percentage of the total. The mean number of deuterium atoms contained in the molecule, known as the deuterium number, was calculated from the expression

$$D.N. = \sum_{i=1}^n id_i$$

where  $d_i$  is the fractional abundance of the species containing  $i$  deuterium atoms.

#### 4.5.2 Analysis of Hydrogen/Deuterium.

The analysis of the hydrogen content of the residual deuterium was carried out at 70ev. Assuming that the probability of ionisation of  $D_2$  and HD are the same, the measured ion current was used to calculate the proportion of each isotope directly. No evidence was found for the occurrence of mass 2 in the reaction samples.

RESULTS - SECTION A.CHAPTER 5.REACTIONS OF 1-BUTENE ON UNPOISONED CATALYSTS.5.1 Reaction of 1-Butene with Hydrogen on Rh/Al<sub>2</sub>O<sub>3</sub>.

The reaction of 1-butene with hydrogen on Rh/Al<sub>2</sub>O<sub>3</sub> was studied at temperatures between -20° and 153°C, using catalyst samples weighing between 1.0 and 15.5mg. All reactions were carried out with equal pressures of hydrogen and butene at a total initial pressure of 60mm.

The pressure fall against time curves were found to be independent of temperature; a typical curve is shown in Fig.5.1, along with the first order plot derived from it. Since the latter plots are linear, the overall order of reaction for hydrogenation is unity.

The isomerisation reaction was studied by carrying out a series of reactions at varying conversions to n-butane at each temperature, and observing the change in butene distribution with conversion. The analysis figures, together with the trans/cis ratio (T/C) and the time ( $t_{ex}$ ) at which the products were extracted for analysis, are shown in table 5.1. The n-butane yield is expressed as a percentage of total hydrocarbon, while each butene is given as a percentage of total butene yield. The terms n-butane,

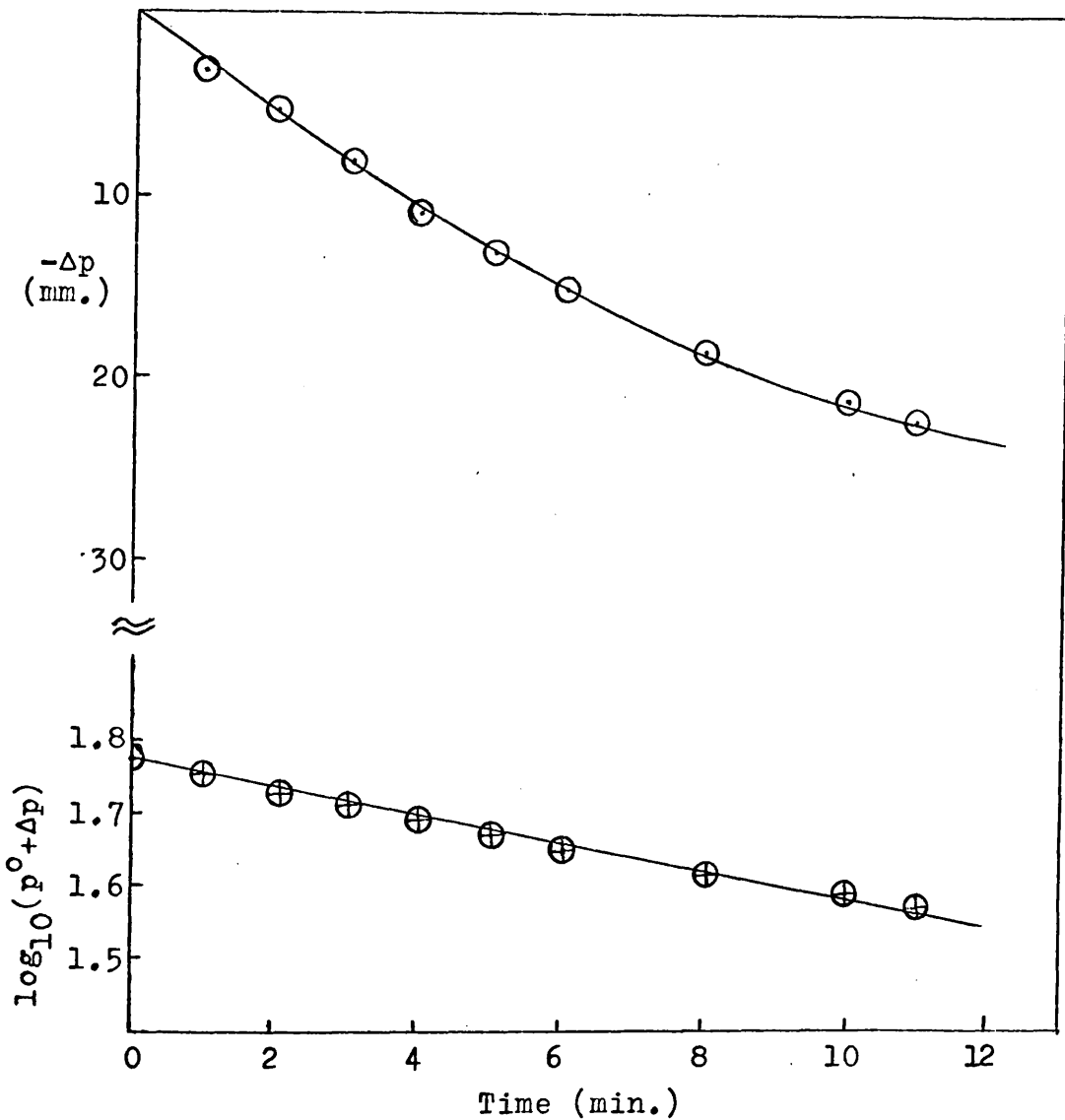


Fig. 5.1 Pressure fall against time curve for 30.0mm. 1-butene and 30.0mm. hydrogen at 0°C. First order function plot shown below.

1-butene, trans 2-butene and cis 2-butene are abbreviated to n-B, l-B, t-2-B, c-2-B for use in all tables. The results are illustrated graphically in Figs. 5.2 - 5.8. The equilibrium proportions of the butenes are shown for each temperature at the right hand side of the plot.

An interesting feature may be noted from the extraction times ( $t_{ex}$ ). At lower temperatures, notably in series A and B and to a lesser extent series C, the deactivation of the catalyst with each reaction is much more marked than at higher temperatures. At  $-20^{\circ}\text{C}$  this self-poisoning effect was sufficient to require a short reactivation with 150mm. hydrogen after reaction A/4 : it is apparent that reaction A/5 proceeded to a much higher conversion (70.5% compared with 26.8%) in a time (30.5min.) only slightly longer than that of A/4 (26.5min.). In series D, reaction D/7 was carried out some time after the rest of the series, and after the catalyst had been stored in 40mm. hydrogen, which accounts for the greater activity exhibited. Series E and F, at  $67^{\circ}$  and  $153^{\circ}\text{C}$  respectively, show no sign of deactivation by self-poisoning.

The dominant features to emerge from the butene distribution pattern are the great increase in isomerisation relative to hydrogenation at higher temperatures, and the initial preferential formation of the cis isomer, which

occurs over the whole temperature range, but to a greater extent at low temperatures. As the plots for series C and D appeared to be somewhat inconsistent, series A2 was carried out at 30°C using the same sample of catalyst as was employed at -20°C.

#### The Effect of Reaction Number on Product Ratios.

In order to determine if there were any systematic changes in the hydrogenation/isomerisation or trans/cis ratios with successive reactions, a series of reactions to constant conversion was carried out at 22°C on 7.5mg.Rh/Al<sub>2</sub>O<sub>3</sub>. Fig. 5.9(a) shows the percentage 1-butene against conversion to n-butane, the reaction number being shown beside each point. Reactions 4, 6, and 8 were not analysed. It is observed that a regular trend toward increasing isomerisation emerges but it is nevertheless very slight, and is almost within the experimental precision of the chromatograph. The plot of the trans/cis ratio, Fig. 5.9(b), shows a similar trend towards increased cis formation.

It can therefore be concluded that, while there may be slight changes in the directions indicated, these will be insignificant compared to changes caused by conversion or temperature.

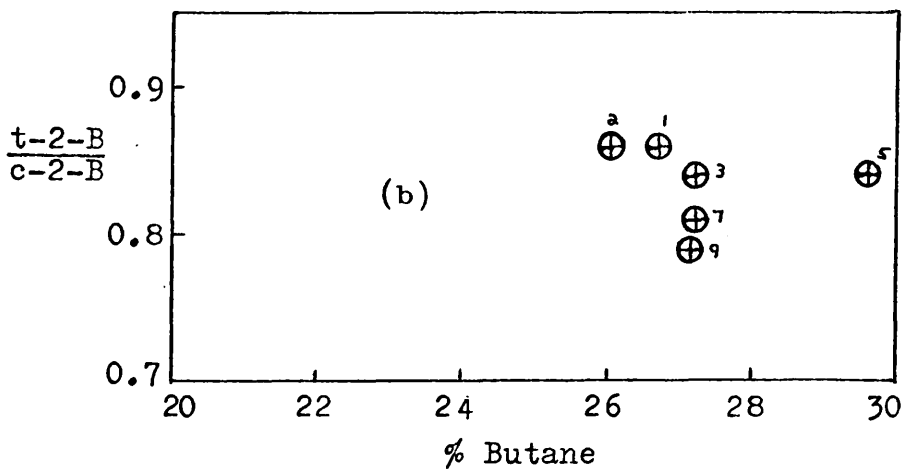
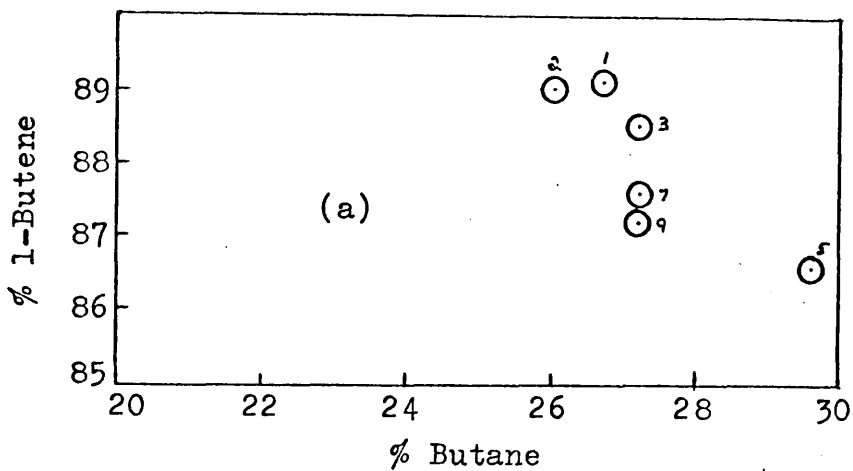


Fig. 5.9 Effect of reaction number on product ratios.  
 (a) Variation of isomerisation/hydrogenation ratio.  
 (b) Variation of trans/cis ratio.  
 Reaction numbers are shown beside corresponding points.

TABLE 5.1

Variation of Butene Distribution with Conversion and Temperature on Rh/Al<sub>2</sub>O<sub>3</sub>.

Initial  $p_{H_2} = p_{1-B} = 30.0 \pm 0.6$  mm.

Reaction	Wt. of Catalyst (mg.)	Temperature °C	% Butene Distribution				T/C	$t_{ex}$ (min.)
			$\%n-B$	$\%1-B$	$\%t-2-B$	$\%c-2-B$		
A/3	7.5	-20	3.9	99.0	0.4	0.7	0.53	2.0
A/2	"	"	12.5	97.7	1.1	1.2	0.89	5.3
A/4	"	"	26.8	90.7	4.2	5.1	0.84	26.5
A/6	"	"	50.5	76.5	11.6	11.9	0.98	28.5
A/5	"	"	70.5	49.9	27.0	23.1	1.17	30.5
A/1	"	"	80.7	26.0	43.8	30.2	1.46	40.7
B/5	15.5	0	7.8	98.1	0.7	1.2	0.64	1.0
B/4	"	"	17.4	94.3	2.4	3.3	0.74	2.3
B/3	"	"	26.9	91.5	3.8	4.7	0.82	5.2
B/2	"	"	40.1	86.7	6.7	6.6	1.03	6.5
B/1	"	"	87.8	8.8	62.6	28.6	2.20	11.5
C/5	5.7	25.5	8.7	92.2	3.8	4.0	0.94	2.5
C/4	"	"	12.8	81.5	8.8	9.7	0.92	4.2
C/3	"	"	26.5	67.1	16.4	16.5	0.99	7.0
C/2	"	"	39.3	23.2	43.3	33.5	1.30	14.3
C/1	"	"	76.7	7.4	72.6	20.0	3.62	26.5



TABLE 5.1 (Cont'd)

D/6	3.0	45	5.4	97.1	1.4	1.5	0.90	0.2
D/4	"	"	15.8	86.9	6.4	6.7	0.95	2.4
D/3	"	"	32.3	70.7	13.5	15.8	0.86	3.6
D/2	"	"	47.7	52.4	22.8	24.8	0.92	5.6
D/7	"	"	53.2	39.0	35.0	26.0	1.34	4.5
D/1	"	"	82.3	4.1	77.5	18.4	4.20	15.7
E/6	2.0	67	4.1	90.5	4.6	4.9	0.94	0.5
E/5	"	"	11.3	65.9	17.6	16.5	1.06	1.4
E/4	"	"	25.0	24.7	44.2	31.1	1.42	3.6
E/3	"	"	37.7	6.6	63.0	30.4	2.08	5.3
E/2	"	"	53.5	4.1	70.5	25.4	2.78	8.5
E/1	"	"	80.5	5.7	68.8	25.5	2.70	18.5
F/6	1.0	153	2.1	78.5	12.2	9.3	1.31	0.5
F/5	"	"	8.7	16.6	53.6	29.8	1.80	3.2
F/4	"	"	16.2	10.2	59.8	30.0	2.00	7.5
F/3	"	"	29.7	9.6	60.6	29.8	2.04	14.4
F/1	"	"	56.2	9.2	61.1	29.7	2.07	30.5
A2/4	7.5	30	4.7	96.4	1.6	2.0	0.77	0.5
A2/3	"	"	10.8	90.7	4.5	4.8	0.94	1.7
A2/2	"	"	23.4	78.9	10.5	10.6	1.00	3.0
A2/1	"	"	67.3	4.1	65.5	30.4	2.14	10.0

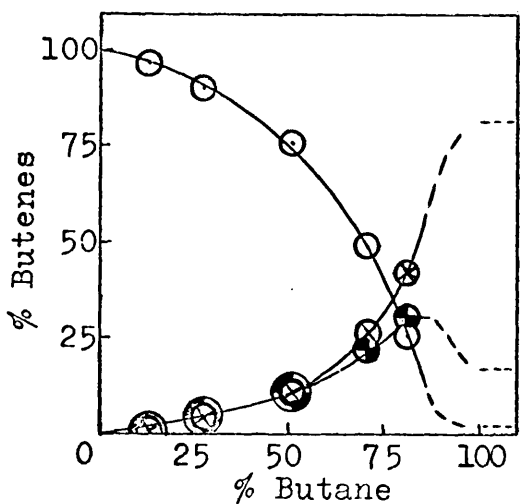


Fig. 5.2  $-20^{\circ}\text{C}.$

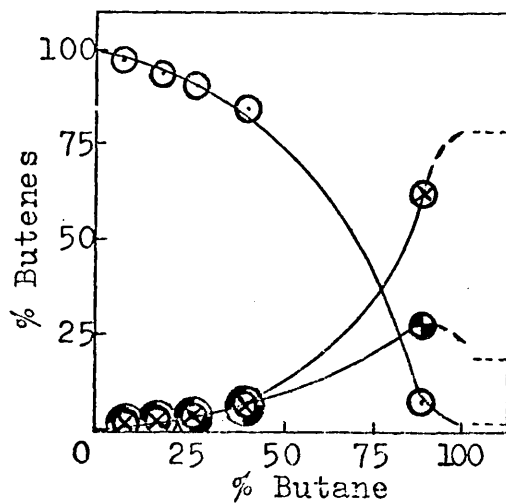


Fig. 5.3  $0^{\circ}\text{C}.$

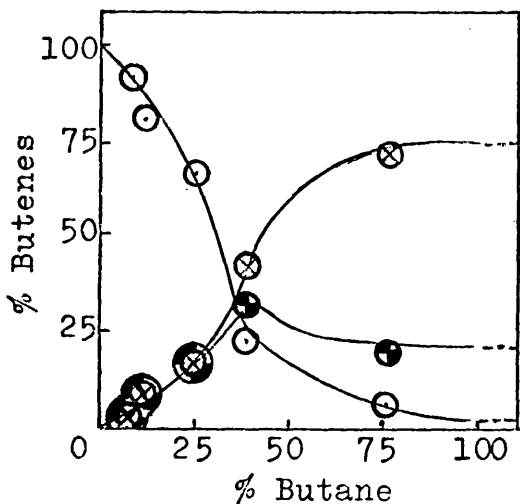


Fig. 5.4  $25.5^{\circ}\text{C}$

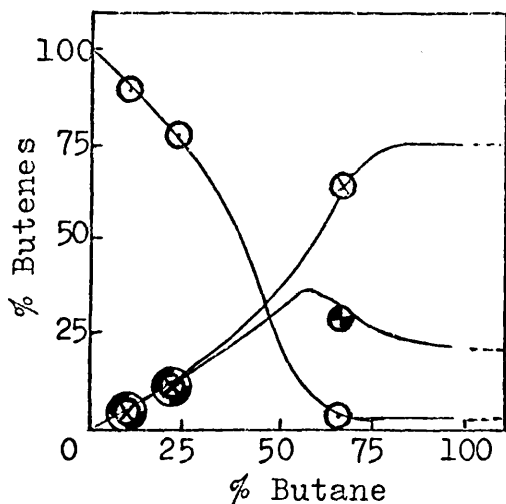


Fig. 5.5  $30^{\circ}\text{C}$

Figs. 5.2 - 5.5 Variation of butene distribution with conversion on  $\text{Rh}/\text{Al}_2\text{O}_3$ .

(  $\circ$  - 1-B       $\otimes$  - t-2-B       $\bullet$  - c-2-B)

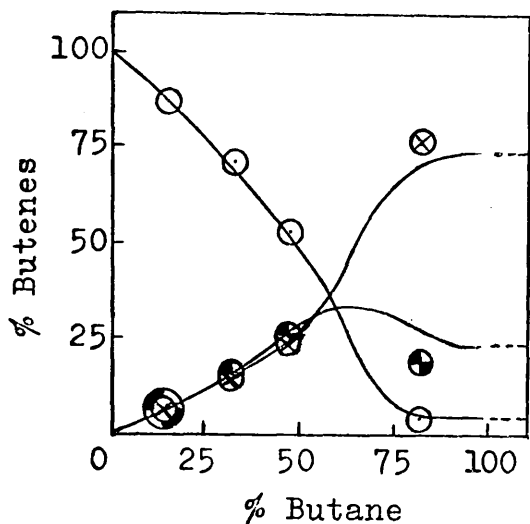


Fig. 5.6

45°C

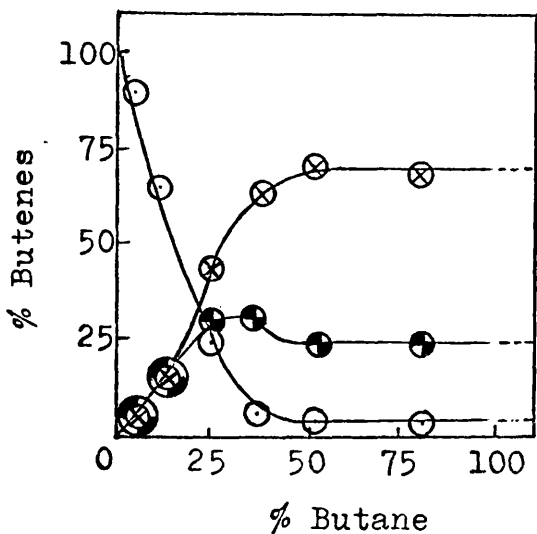


Fig. 5.7

67°C

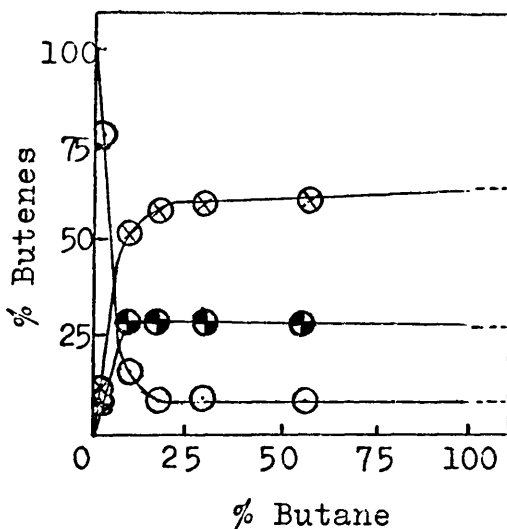


Fig. 5.8

153°C

Figs. 5.6 - 5.8 Variation of butene distribution with conversion on Rh/Al<sub>2</sub>O<sub>3</sub>.

(○ - 1-B

⊗ - t-2-B

● - c-2-B)

## 5.2 Reaction of 1-Butene with Hydrogen on Rh/SiO<sub>2</sub>.

The reaction of 1-butene with hydrogen on Rh/SiO<sub>2</sub> was studied over the temperature range -16° to 75°C with samples of catalyst weighing from 1.8 to 14.3mg. The characteristics of the pressure fall against time plots were independent of temperature, and are very similar to those of the reaction on Rh/Al<sub>2</sub>O<sub>3</sub>. A typical example is shown in Fig. 5.10, together with the corresponding first order plot.

Series of reactions were carried out at five temperatures as described in section 5.1, the complete analysis results being shown in table 5.2. They are also illustrated graphically in Figs. 5.11 - 5.15.

Deactivation of the catalyst with successive reactions was appreciable at lower temperatures, while at 75°C the activity appeared to be virtually constant. The sample of catalyst employed for series H1 was found also to have a suitable activity at 25°C (series H2.). After completion of H1, the catalyst vessel was evacuated, allowed to warm up to ambient temperature, and was allowed to stand under 120mm. hydrogen for 45 minutes. The hydrogen was then pumped away, and the catalyst was stored overnight under 80mm. hydrogen at room temperature.

The two series J1 and J2 were carried out on the same sample of catalyst without reactivation, other than that

brought about by storage for several days under 80mm. hydrogen at room temperature. Both sets of points are shown on the same plot (Fig. 5.14) and it may be noted that the results of the two series are in close agreement.

It can be seen from the course of reaction plots that the rate of isomerisation increases rather more rapidly with temperature than does the rate of hydrogenation. The isomerisation reaction also exhibits strong preferential formation of the cis isomer, particularly at low temperatures.

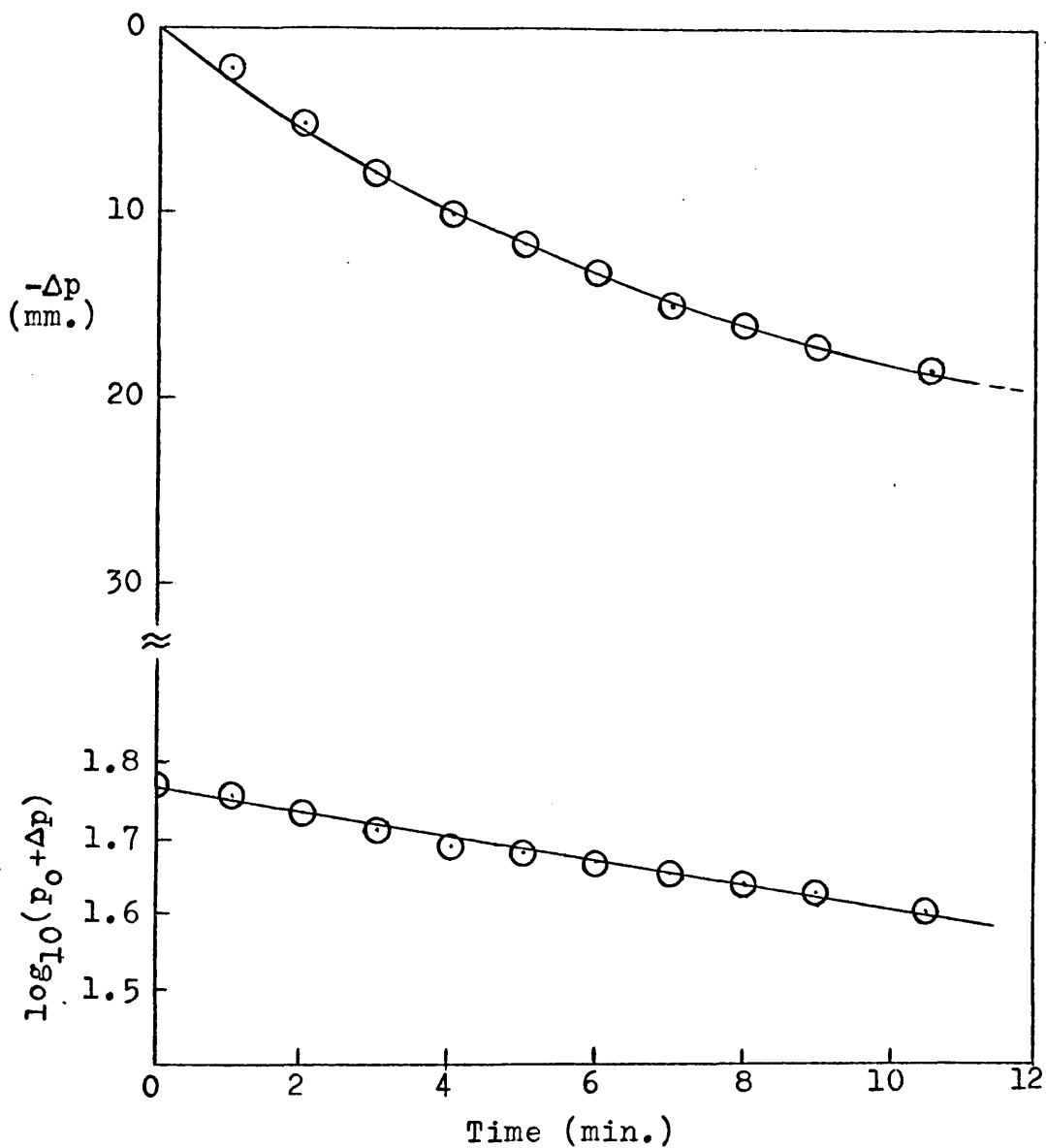


Fig. 5.10 Pressure fall against time curve for 30.0mm. 1-butene with 30.0mm. hydrogen at 43°C. First order function plot shown below.

TABLE 5.2

Variation of Butene Distribution with Conversion and Temperature on Rh/SiO<sub>2</sub>.Initial PH<sub>2</sub> = P<sub>1-B</sub> = 30.0 ± 0.5 mm.

Reaction	Wt. of Catalyst (mg.)	Temperature °C	% Butene Distribution				T/C	t <sub>ex</sub> (min.)
			%n-B	l-B	t-2-B	c-2-B		
I/6	14.3	-16	6.2	95.9	1.1	3.0	0.37	1.0
I/5	"	"	16.6	83.4	4.4	12.2	0.36	4.5
I/2	"	"	26.3	73.6	8.3	18.1	0.46	5.0
I/4	"	"	45.2	37.9	21.5	40.6	0.53	12.5
I/3	"	"	59.3	9.6	40.6	49.8	0.82	13.5
I/1	"	"	78.5	2.8	81.0	16.2	5.00	22.5
HL/6	8.0	0	3.8	96.0	1.2	2.8	0.40	1.0
HL/4	"	"	15.2	81.6	6.8	12.6	0.54	5.5
HL/3	"	"	28.9	61.4	15.0	23.6	0.63	9.3
HL/2	"	"	43.0	30.6	31.3	38.1	0.82	12.3
HL/5	"	"	55.2	2.9	63.7	33.4	1.91	28.0
HL/1	"	"	84.7	4.4	84.0	11.6	7.27	20.5
H2/6	8.0	25	4.6	92.6	2.4	5.0	0.48	0.5
H2/5	"	"	14.7	76.6	9.5	13.9	0.68	2.0
H2/4	"	"	25.1	53.0	21.3	25.7	0.83	3.7
H2/3	"	"	39.7	14.9	45.7	39.4	1.16	7.5
H2/2	"	"	57.2	12.5	72.4	25.1	2.90	12.5
H2/1	"	"	76.5	3.0	77.9	19.1	4.07	20.3

TABLE 5.2 (Cont'd.)

J1/5	4.0	43	16.7	70.5	14.5	15.0	0.97	1.3
J1/4	"	"	35.4	34.9	35.2	29.9	1.18	2.8
J1/3	"	"	40.0	23.2	43.4	33.4	1.30	3.5
J1/2	"	"	59.0	4.0	67.2	28.8	2.34	5.5
J2/4	"	"	5.91	91.7	3.6	4.7	0.76	0.2
J2/3	"	"	24.7	53.0	23.0	24.0	0.95	1.8
J2/2	"	"	44.8	12.9	52.9	34.2	1.54	4.0
J2/1	"	"	74.1	3.6	77.4	19.0	4.06	9.5
K/6	1.8	75	6.5	81.1	10.0	8.9	1.11	0.6
K/5	"	"	14.9	52.6	26.2	21.2	1.24	1.3
K/3	"	"	19.6	33.6	36.4	30.0	1.22	1.7
K/4	"	"	25.8	18.8	48.4	32.8	1.46	2.3
K/2	"	"	43.0	6.9	66.7	26.4	2.52	4.0
K/1	"	"	65.8	5.3	72.2	22.5	3.22	7.5



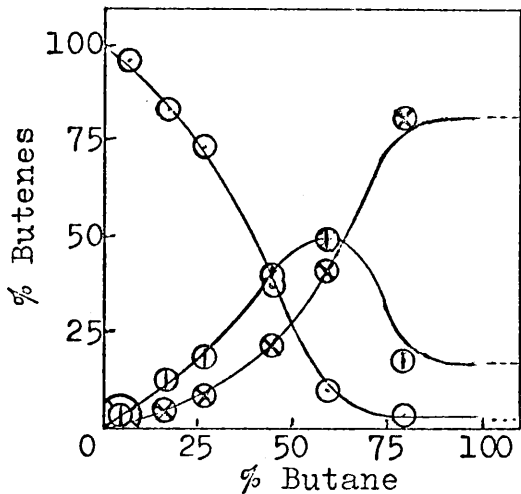


Fig. 5.11  $-16^{\circ}\text{C}$

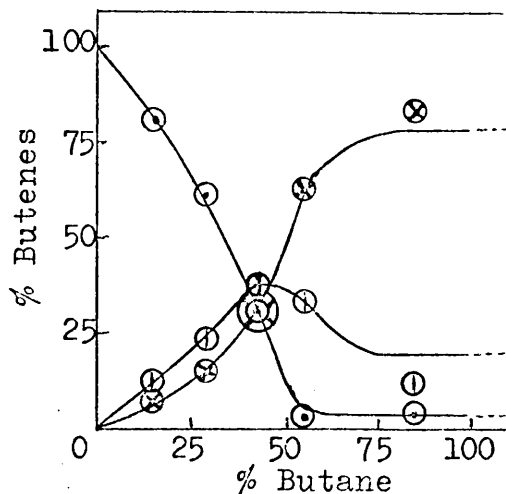


Fig. 5.12  $0^{\circ}\text{C}$

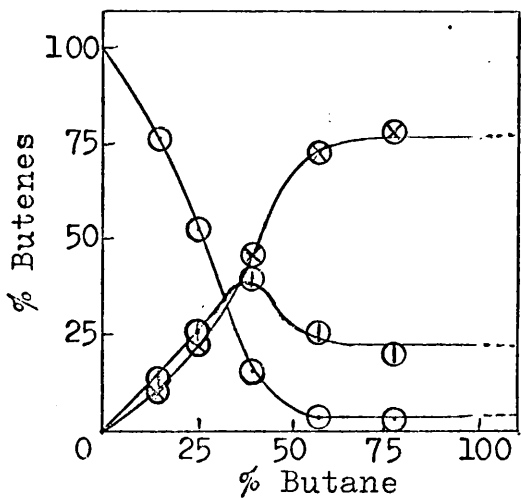


Fig. 5.13  $25^{\circ}\text{C}$

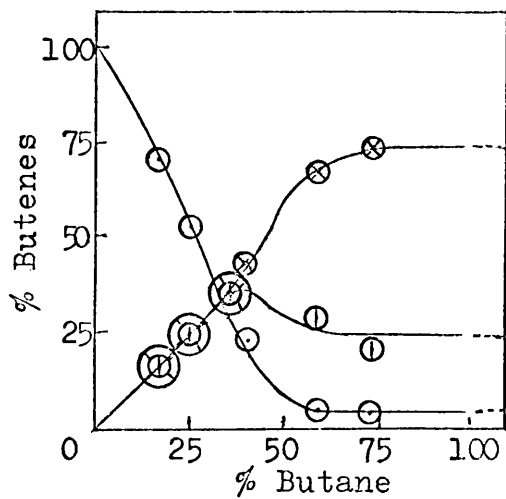


Fig. 5.14  $43^{\circ}\text{C}$

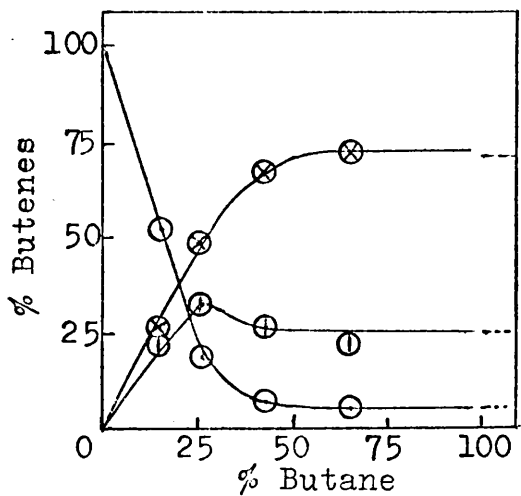


Fig. 5.15  $75^{\circ}\text{C}$

Figs. 5.11-5.15 Variation of butene distribution with conversion on  $\text{Rh}/\text{SiO}_2$ . Broken lines show thermodynamic equilibrium values.

- 1-B
- ⊗ t-2-B
- ⊙ c-2-B

### 5.3 Kinetics & Activation Energies of 1-Butene Hydrogenation & Isomerisation.

#### 5.3.1 Reaction Kinetics on Rh/Al<sub>2</sub>O<sub>3</sub>.

The dependence of the initial reaction rates and the product distributions upon the initial hydrogen pressure was determined from two series of reactions at 0° and 66°C in which the initial 1-butene pressure was maintained constant at 30.0mm. and the initial hydrogen pressure was varied from 14.2mm. to 124.5mm. Likewise, the effect of varying the initial butene pressure was determined in a third series, at 66°C, in which the initial hydrogen pressure was maintained at 30.0mm. and the 1-butene pressure varied from 10.2mm. to 149.8mm. In the first two series, the products were extracted for analysis at constant conversion, and in the third at a constant hydrogen uptake.

As discussed briefly in sections 5.1 and 5.2, a gradual deactivation of the catalyst was seen to occur during a course of reactions. If this occurred during a series intended specifically to determine the variation of reaction rates with initial pressures, the observed variation would be the result of both the reaction conditions and the deactivation. There are two means of overcoming this problem. First, the catalyst could be reactivated by some standard process after each reaction; but there would still be no guarantee of its activity until the succeeding reaction

was carried out. It is conceivable that continual reactivation might alter the catalyst's characteristics, and thus defeat its own purpose. A second and probably more sound method was to define particular conditions as a "standard reaction", and to carry out such reactions at regular intervals during the series. By this means, a plot could be obtained of the change of "standard" activity with reaction number, and hence by interpolation the rate  $r'_n$  of a hypothetical standard reaction number  $n$  could be estimated. The measured rate  $r_n$  of reaction  $n$  was converted to the corrected rate  $R_n$  by multiplying by the activity correction factor  $f$ , where  $f = \frac{R_0}{r_n}$ ,  $R_0$  being the standard rate for the series, and generally equal to the measured rate of the first (standard) reaction of the series. Thus  $R_n = r_n \cdot \frac{R_0}{r_n}$ .

The results of the series at  $0^\circ\text{C}$  to determine the dependence on initial hydrogen pressure are shown in table 5.3, and the corresponding reaction rates and activity correction factors are shown in table 5.4. All reaction rates are quoted in units of  $\text{mm}\cdot\text{min}^{-1}$ . In these and all subsequent tables the symbols  $r$  and  $R$  refer to measured and corrected rates respectively, and the subscripts  $h$  and  $i$  refer to hydrogenation and isomerisation reactions respectively. The plot of  $\log R_n$  against  $\log p_{\text{H}_2}$  (Fig. 5.16) produces a reasonably good straight line, from the

gradient of which an order of  $1.0 \pm 0.1$  for hydrogenation is obtained. Fig. 5.17 similarly exhibits the linear relationship between  $\log R_i$  and  $\log p_{H_2}$ , from which an isomerisation order of  $0.25 \pm 0.05$  is derived.

During this series, reactions G1/8, 9, 11, 12 were not analysed, and accordingly no data is available from them for isomerisation. The other points lie on a straight line with the exception of G1/3 but it may be significant that this reaction was inadvertently extracted at a higher conversion, and thus the isomerisation data may not allow a valid comparison to be made.

Tables 5.5 and 5.6 show the dependence on the initial hydrogen pressure of the product distributions and initial rates at  $66^\circ\text{C}$ . The plot of  $\log R_h$  against  $\log p_{H_2}$  (Fig. 5.18) produces a very good straight line of gradient  $1.0 \pm 0.05$  and hence a hydrogenation order of unity. No activity correction was required for the  $r_i$  values, as the rates of Q/3, Q/5, and Q/8 were virtually constant. Thus  $R_i = r_i$ , with the exception of Q/1, and in the plot of  $\log R_i$  against  $\log p_{H_2}$  (Fig. 5.19) two points are plotted separately for the standard hydrogen pressure. The spread of points is wider than in series G, but there is a small but steady positive gradient. The isomerisation order derived from it is  $0.05 \pm 0.1$ .

TABLE 5.3

Variation of Butene Distribution on Rh/Al<sub>2</sub>O<sub>3</sub> with Initial Hydrogen Pressure.

Temperature = 0°C. Wt. of catalyst = 7.5mg.

Initial 1-butene pressure = 30.0 ± 0.6mm.

% Butene Distribution

Reaction	p <sub>H<sub>2</sub></sub> (mm.)	%n-B	l-B	t-2-B	c-2-B	T/C	t <sub>ex</sub> (min.)
G1/1	30.0	30.0	84.2	7.2	8.6	0.83	4.0
G1/2	15.2	26.8	74.8	11.4	13.8	0.83	11.2
G1/3	88.0	38.0	85.0	8.0	7.0	1.14	3.5
G1/4	30.0	27.0	82.6	8.1	9.3	0.87	8.0
G1/5	59.6	29.5	87.6	5.9	6.5	0.91	6.0
G1/6	120.0	27.3	91.6	3.8	4.6	0.83	4.0
G1/7	30.2	25.0	84.7	7.3	8.0	0.90	12.0
G1/10	91.0	27.4	89.5	4.6	5.9	0.79	8.0

TABLE 5.4

Variation of Initial Reaction Rates on Rh/Al<sub>2</sub>O<sub>3</sub> at 0°C with Initial Hydrogen Pressure.

Reaction	p <sub>H<sub>2</sub></sub> (mm.)	Hydrogenation			Isomerisation		
		r <sub>h</sub>	f <sub>h</sub>	R <sub>h</sub>	r <sub>i</sub>	f <sub>i</sub>	R <sub>i</sub>
G1/1	30.0	1.60	1.00	1.60	1.04	0.99	1.00
G1/2	15.2	0.50	1.20	0.60	0.73	1.12	0.82
G1/3	88.0	2.00	1.60	3.20	1.22	1.27	1.55
G1/4	30.0	0.75	2.10	1.60	0.69	1.44	1.00
G1/5	59.6	1.10	2.50	2.70	0.67	1.67	1.12
G1/6	120.0	1.80	2.90	5.30	0.67	1.98	1.34
G1/7	30.2	0.52	3.20	1.60	0.42	2.41	1.00
G1/8	40.6	0.55	3.25	1.80	-	-	-
G1/9	30.0	0.48	3.34	1.60	-	-	-
G1/10	91.0	0.78	5.0	3.90	-	-	-
G1/11	30.5	0.25	6.40	1.60	-	-	-
G1/12	60.3	0.44	7.0	3.10	-	-	-

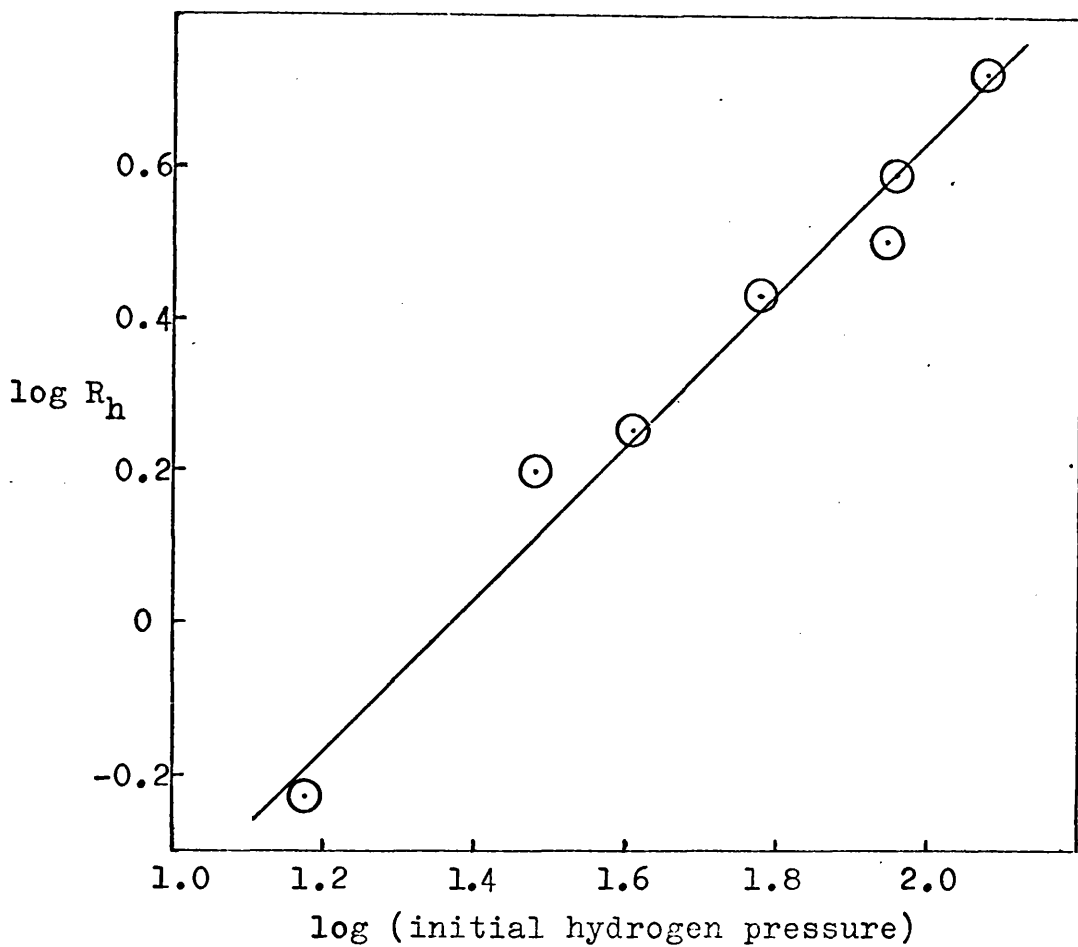


Fig. 5.16 The variation of  $\log R_h$  with  $\log p_{H_2}$  on Rh/Al<sub>2</sub>O<sub>3</sub> at 0°C.

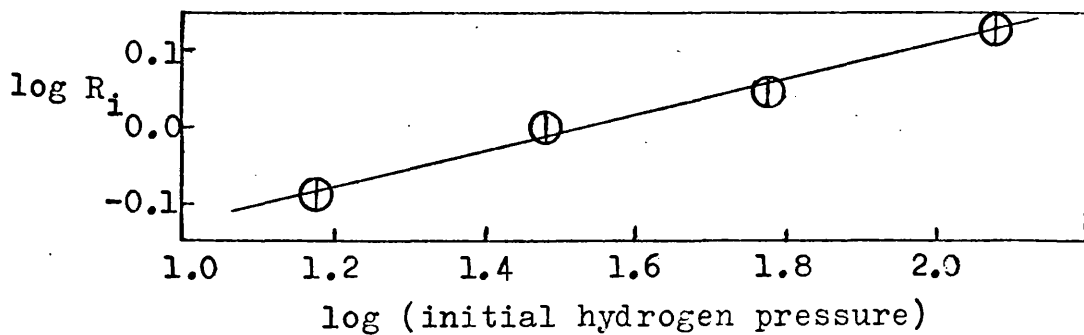


Fig. 5.17 The variation of  $\log R_i$  with  $\log p_{H_2}$  on Rh/Al<sub>2</sub>O<sub>3</sub> at 0°C.

TABLE 5.5

Variation of Butene Distribution on Rh/Al<sub>2</sub>O<sub>3</sub> with Initial Hydrogen Pressure.

Temperature = 66°C. Wt. of catalyst = 1.5mg.

Initial 1-butene pressure = 30.0 ± 0.5mm.

% Butene Distribution

Reaction	$p_{H_2}$ (mm.)	%n-B	1-B	t-2-B	c-2-B	T/C	$t_{ex}$ (min.)
Q/1	30.6	16.2	86.1	7.9	6.0	1.32	6.3
Q/2	14.2	17.8	72.0	13.5	14.5	0.93	20.0
Q/3	30.0	21.2	82.9	8.5	8.6	0.99	9.8
Q/4	87.6	24.7	91.5	3.8	4.7	0.80	3.5
Q/5	30.3	21.4	81.6	9.8	8.6	1.14	10.3
Q/6	60.8	22.2	90.8	5.0	4.2	1.18	5.0
Q/7	124.5	26.1	94.7	2.9	2.4	1.24	3.0
Q/8	31.0	22.8	81.1	10.5	8.4	1.26	11.0
Q/9	105.6	26.1	93.3	3.8	2.9	1.30	3.5

TABLE 5.6

Variation of Initial Reaction Rates at 66°C with Initial Hydrogen Pressure.

Reaction	$p_{H_2}$ (mm.)	Hydrogenation			Isomerisation		
		$\bar{r}_h$	$\bar{f}_h$	$\bar{R}_h$	$\bar{r}_i$	$\bar{f}_i$	$\bar{R}_i$
Q/1	30.6	0.86	1.16	1.00	0.72	-	-
Q/2	14.2	0.31	1.56	0.48	0.50	-	-
Q/3	30.0	0.48	2.08	1.00	0.58	-	-
Q/4	87.6	1.60	2.04	3.26	0.80	-	-
Q/5	30.3	0.50	2.00	1.00	0.59	-	-
Q/6	60.8	1.00	2.08	2.08	0.59	-	-
Q/7	124.5	1.80	2.12	3.82	0.54	-	-
Q/8	31.0	0.46	2.18	1.00	0.57	-	-
Q/9	105.6	1.60	2.22	3.55	0.64	-	-

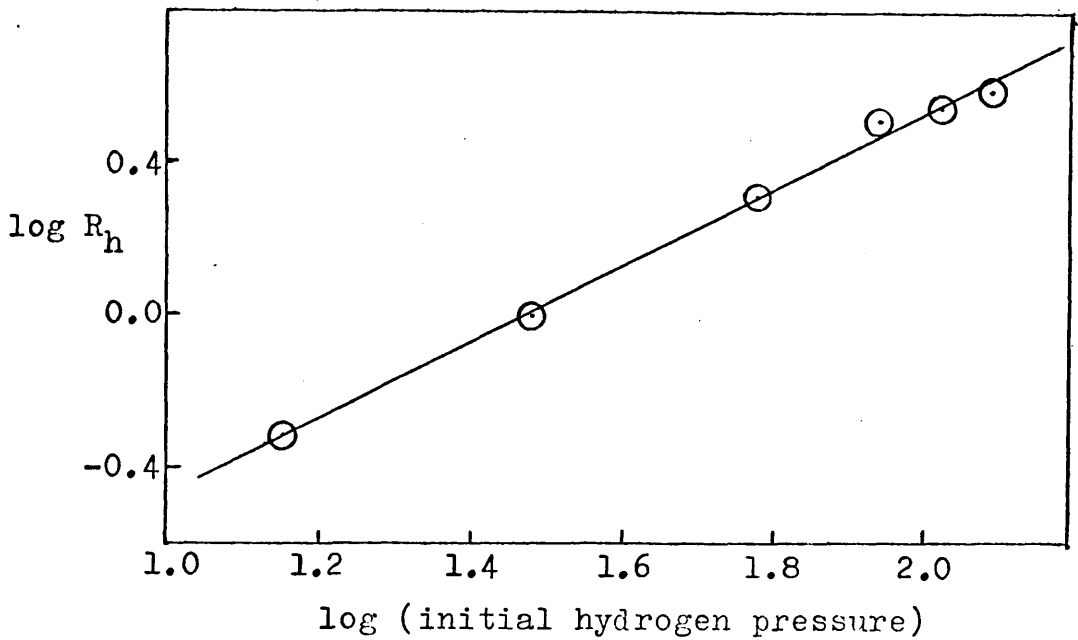


Fig. 5.18 The variation of  $\log R_h$  with  $\log p_{H_2}$  on  $\text{Rh}/\text{Al}_2\text{O}_3$  at  $66^\circ\text{C}$ .

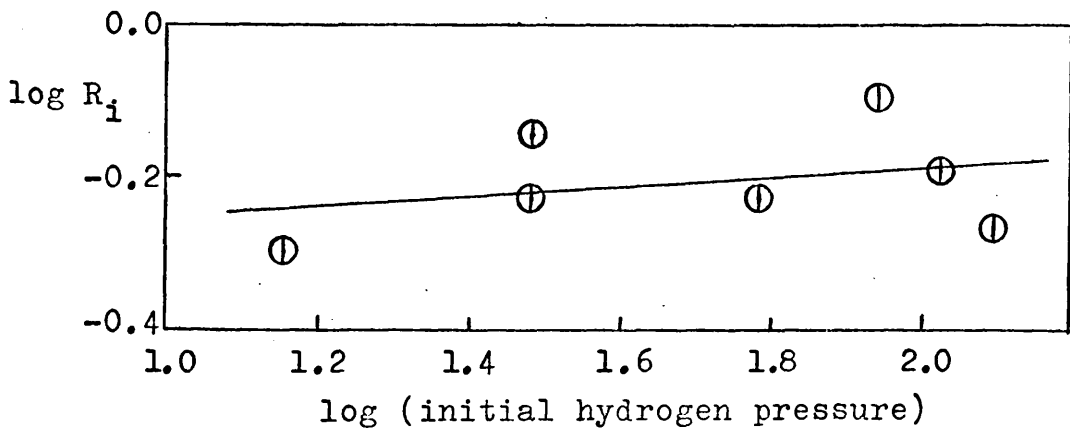


Fig. 5.19 The variation of  $\log R_i$  with  $\log p_{H_2}$  on  $\text{Rh}/\text{Al}_2\text{O}_3$  at  $66^\circ\text{C}$ .



TABLE 5.7

Variation of Butene Distribution on Rh/Al<sub>2</sub>O<sub>3</sub> with Initial 1-Butene Pressure.

Temperature = 66°C. Wt. of catalyst = 1.7mg.

Initial hydrogen pressure = 30.0 ± 0.8mm.

% Butene Distribution

<u>Reaction</u>	<u>p<sub>1-B</sub></u> (mm.)	<u>%n-B</u>	<u>l-B</u>	<u>t-2-B</u>	<u>c-2-B</u>	<u>T/C</u>	<u>t<sub>ex</sub></u> (min.)
R/1	30.4	25.5	83.5	8.8	7.7	1.14	4.0
R/2	91.8	8.0	92.6	3.1	4.3	0.72	7.5
R/3	29.7	25.8	82.6	10.6	6.8	1.56	5.8
R/4	16.1	77.8	59.8	24.3	15.9	1.40	6.0
R/5	30.4	26.1	77.8	11.1	11.1	1.00	5.8
R/6	10.2	77.6	35.2	40.9	23.9	1.71	6.3
R/7	149.8	4.2	95.9	1.6	2.5	0.64	10.0
R/8	31.5	23.6	75.6	12.8	11.6	1.11	7.5
R/9	10.2	74.5	27.4	35.8	36.8	0.97	7.5

TABLE 5.8

Variation of Initial Reaction Rates at 66°C with Initial 1-Butene Pressure.

<u>Reaction</u>	<u>p<sub>1-B</sub></u> (mm.)	<u>Hydrogenation</u>			<u>Isomerisation</u>		
		<u>r<sub>h</sub></u>	<u>f<sub>h</sub></u>	<u>R<sub>h</sub></u>	<u>r<sub>i</sub></u>	<u>f<sub>i</sub></u>	<u>R<sub>i</sub></u>
R/1	30.4	1.55	0.97	1.50	1.38	1.09	1.50
R/2	91.8	0.96	1.37	1.32	0.95	1.34	1.27
R/3	29.7	1.00	1.50	1.50	0.99	1.51	1.50
R/4	16.1	1.00	1.50	1.50	1.40	1.20	1.68
R/5	30.4	1.00	1.50	1.50	1.32	1.14	1.50
R/6	10.2	0.92	1.67	1.54	1.76	1.18	2.08
R/7	149.8	0.74	1.84	1.36	0.63	1.22	0.77
R/8	31.5	0.78	1.92	1.50	1.18	1.27	1.50
R/9	10.2	0.80	1.95	1.56	1.86	1.30	2.41

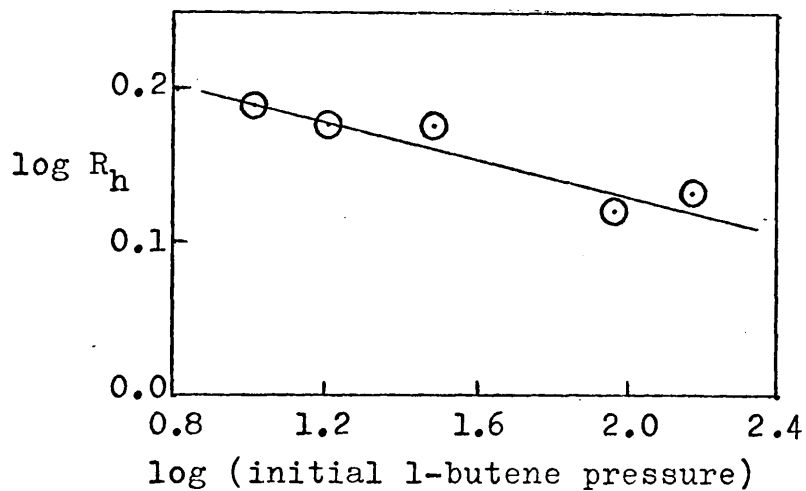


Fig. 5.20 Variation of  $\log R_h$  with  $\log p_{1-B}$  on  $\text{Rh}/\text{Al}_2\text{O}_3$  at  $66^\circ\text{C}$ .

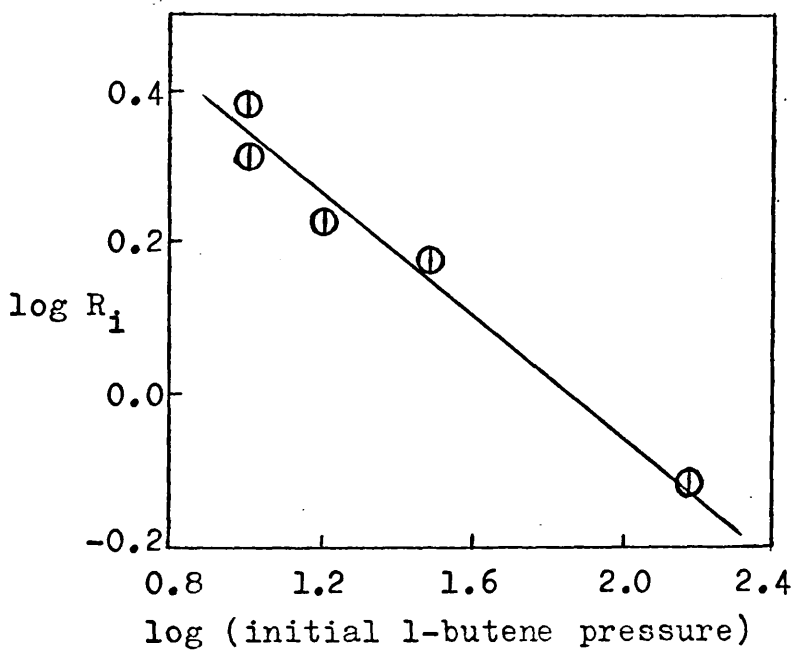


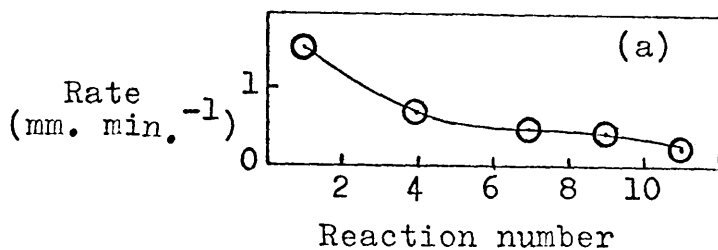
Fig. 5.21 Variation of  $\log R_i$  with  $\log p_{1-B}$  on  $\text{Rh}/\text{Al}_2\text{O}_3$  at  $66^\circ\text{C}$ .

The influence of initial 1-butene pressure at 66°C is shown in tables 5.7 and 5.8. It is apparent that both hydrogenation and isomerisation rates are reduced by increasing 1-butene pressure, and Figs. 5.20 and 5.21 show plots of  $\log R_h$  and  $\log R_i$  respectively against  $\log p_{1-B}$ . The orders derived from them for hydrogenation and isomerisation are  $-0.06 \pm 0.05$  and  $-0.4 \pm 0.1$  respectively.

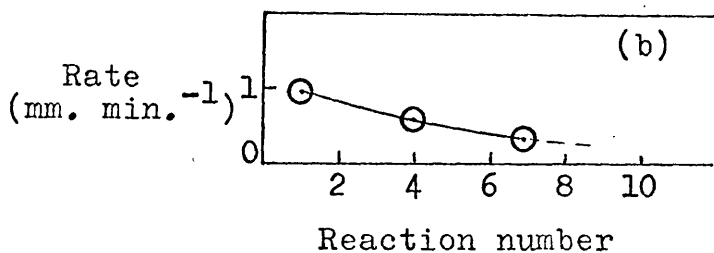
The tables of f-values and initial rates under standard conditions illustrate the relative deactivation of each reaction at the two temperatures; they are generally concordant with the findings in section 5.1 that deactivation is greater at the lower temperatures. It is also observed that deactivation of the hydrogenation reaction is slightly greater than of the isomerisation, again in agreement with the trend reported in section 5.1. These features are illustrated in the plots of  $r_h$  and  $r_i$  (for standard reactions) against reaction number (Fig. 5.22).

### 5.3.2 Reaction Kinetics on Rh/SiO<sub>2</sub>.

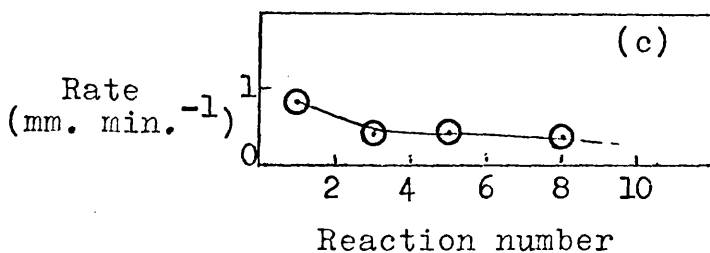
The initial rate kinetics of the reactions on Rh/SiO<sub>2</sub> were determined by three series of reactions which paralleled those on Rh/Al<sub>2</sub>O<sub>3</sub>. The effect of varying the initial hydrogen pressure from 14.6mm. to 121.6mm. was studied at 0° and 54°C and the effect of varying the 1-butene pressure from 19.0mm. to 149.5mm. at 54°C. Activity corrections were



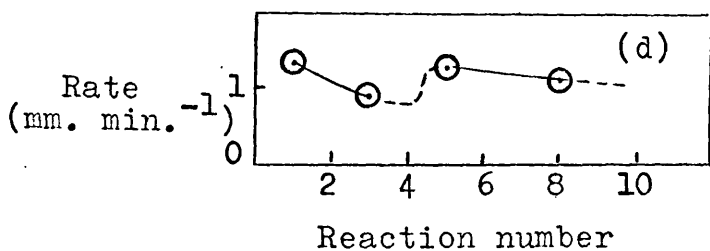
Series G1



Series G1



Series Q1



Series R1

Fig. 5.22 Variation of "standard reaction" initial rates with reaction number on Rh/Al<sub>2</sub>O<sub>3</sub>. (a) Hydrogenation at 0°C, (b) isomerisation at 0°C, (c) hydrogenation at 66°C, (d) isomerisation at 66°C.

applied as described in the previous section.

The dependence of the product distribution at 0°C on the initial hydrogen pressure is shown in table 5.9, and the corresponding reaction rates, in units of  $\text{mm}\cdot\text{min}^{-1}$ , and activity correction factors in table 5.10. The rate of hydrogenation is seen to rise linearly with increasing hydrogen pressure, and the plot of  $\log R_h$  against  $\log p_{\text{H}_2}$  (Fig. 5.23) produces a good straight line, from which an order of  $0.95 \pm 0.1$  is obtained for hydrogenation. The plot of  $\log R_i$  against  $\log p_{\text{H}_2}$  in Fig. 5.24 shows a fairly regular trend with the exception of the point corresponding to 121.6mm. hydrogen. It may be noted this same point is also rather low in Fig. 5.23, which may imply some inaccuracy in the measured rates for that reaction. The hydrogenation reaction was, however, very fast and it is possible the reaction may have been partly diffusion controlled, which would thus account for a lower rate of isomerisation. An order of  $0.05 \pm 0.05$  for isomerisation is obtained from these results.

The results of the equivalent series at 54°C are shown in tables 5.11 and 5.12. Consideration of the  $r_h$  values shows that no activity correction is required, and accordingly Fig. 5.25 is a plot of  $\log R_h (= \log r_h)$  against  $\log p_{\text{H}_2}$ . The linear relationship is clearly shown, an order of  $1.0 \pm 0.05$  being obtained for hydrogenation. The

plot of  $\log R_i$  against  $\log p_{H_2}$  (Fig. 5.26) is a fairly good straight line with the exception of the point corresponding to P1/2, but it is to be noted that the butene distribution in that reaction was approaching equilibrium proportions, and hence the validity of the equation used in the rate calculation must be in doubt. The point corresponding to P1/9 is lower than expected, and it may be significant that this reaction was inadvertently carried out with a 1-butene pressure of only 28.5mm. Ignoring P1/2, the order of the isomerisation reaction is found to be  $0.10 \pm 0.05$ .

The dependence of the butene distribution and initial rates on the 1-butene pressure is shown in tables 5.13 and 5.14 respectively. It is readily apparent that the trends exhibited are very similar to those on Rh/Al<sub>2</sub>O<sub>3</sub>. The plot of  $\log R_h$  against  $\log p_{1-B}$  (Fig. 5.27) displays a good straight line from which an order of  $-0.08 \pm 0.05$  for hydrogenation is obtained. Fig. 5.28 illustrates the relation between  $\log R_i$  and  $\log p_{1-B}$ , an order of  $-0.4 \pm 0.1$  being obtained, ignoring reaction P2/6.

The  $f$  values and standard reaction rates (Fig. 5.29) provide some contrasts with the reactions on Rh/Al<sub>2</sub>O<sub>3</sub>. The extent of the deactivation appears to be rather less on Rh/SiO<sub>2</sub> at 0°C; reactivation is also more easily achieved, as shown by series L2, where a large excess of hydrogen, as

TABLE 5.9

Variation of Butene Distribution on Rh/SiO<sub>2</sub> with Initial Hydrogen Pressure.

Temperature = 0°C. Wt. of catalyst = 4.7mg.

Initial 1-butene pressure = 30.0 ± 0.4mm.

% Butene Distribution

<u>Reaction</u>	<u>p<sub>H<sub>2</sub></sub> (mm.)</u>	<u>%n-B</u>	<u>l-B</u>	<u>t-2-B</u>	<u>c-2-B</u>	<u>T/C</u>	<u>t<sub>ex</sub></u> (min.)
L2/1	29.9	25.9	88.6	5.3	6.1	0.87	2.8
L2/2	15.5	26.5	77.9	10.6	11.5	0.92	6.8
L2/3	29.6	26.9	87.8	5.0	7.2	0.70	4.0
L2/4	90.0	27.7	93.3	2.8	3.9	0.70	1.7
L2/5	29.9	26.0	87.9	5.2	6.9	0.76	3.4
L2/6	39.9	26.4	88.9	4.7	6.4	0.73	3.3
L2/7	30.1	27.1	85.2	6.4	8.4	0.76	4.6
L2/8	121.6	25.4	95.3	1.9	2.8	0.68	1.5
L2/9	29.7	27.4	86.8	5.4	7.8	0.70	3.9

TABLE 5.10

Variation of Initial Reaction Rates at 0°C with Initial Hydrogen Pressure.

<u>Reaction</u>	<u>p<sub>H<sub>2</sub></sub> (mm.)</u>	<u>Hydrogenation</u>			<u>Isomerisation</u>		
		<u>r<sub>h</sub></u>	<u>f<sub>h</sub></u>	<u>R<sub>h</sub></u>	<u>r<sub>i</sub></u>	<u>f<sub>i</sub></u>	<u>R<sub>i</sub></u>
L2/1	29.9	2.20	0.91	2.00	1.30	1.17	1.50
L2/2	15.5	1.00	1.06	1.06	1.11	1.29	1.44
L2/3	29.6	1.50	1.33	2.00	0.99	1.52	1.50
L2/4	90.0	4.00	1.40	5.60	1.24	1.38	1.71
L2/5	29.9	1.65	1.21	2.00	1.12	1.33	1.50
L2/6	39.9	1.85	1.33	2.47	1.06	1.40	1.48
L2/7	30.1	1.40	1.43	2.00	1.06	1.42	1.50
L2/8	121.6	4.00	1.55	6.20	0.95	1.50	1.43
L2/9	29.7	1.55	1.29	2.00	1.10	1.36	1.50

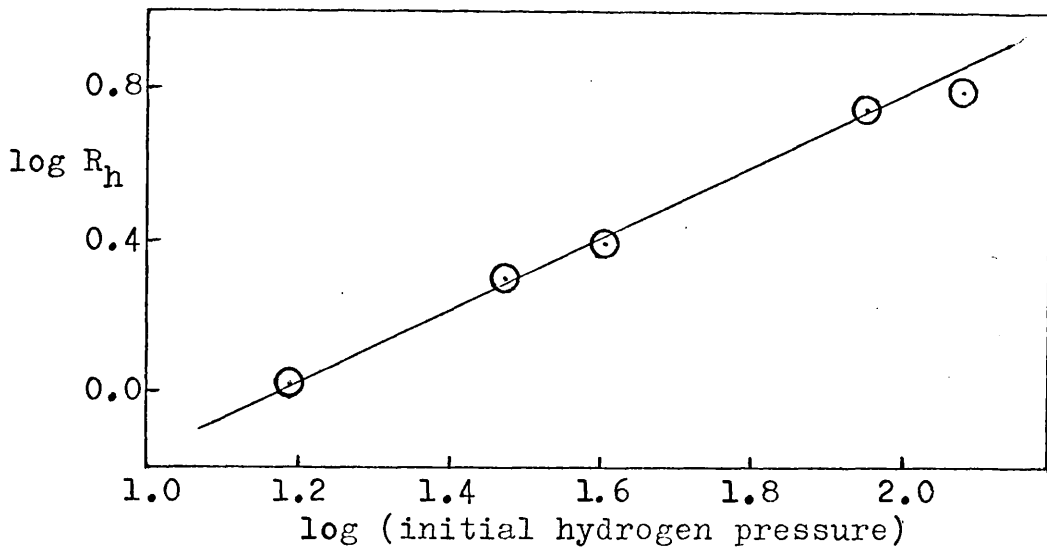


Fig. 5.23 Variation of  $\log R_h$  with  $\log p_{H_2}$  on Rh/SiO<sub>2</sub> at 0°C.

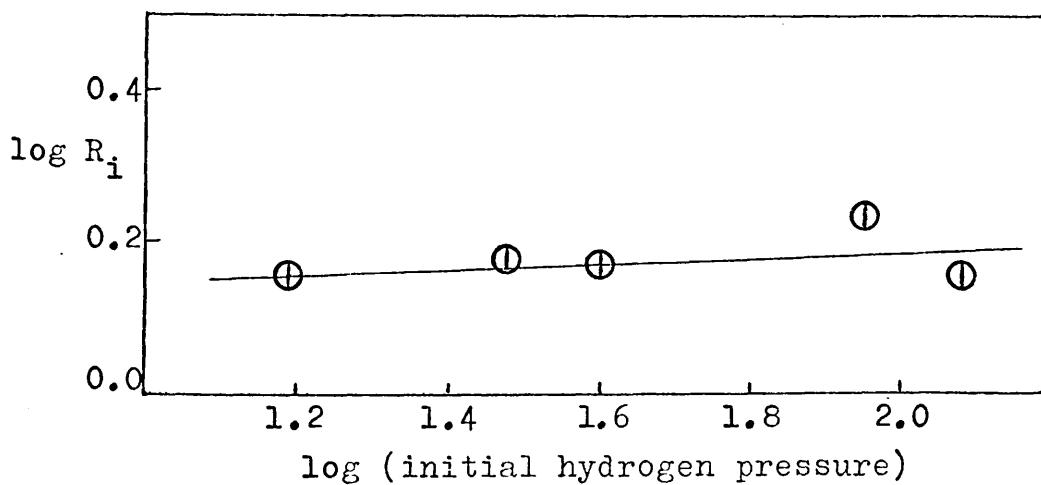


Fig. 5.24 Variation of  $\log R_i$  with  $\log p_{H_2}$  on Rh/SiO<sub>2</sub> at 0°C.



TABLE 5.11

Variation of Butene Distribution on Rh/SiO<sub>2</sub> with Initial Hydrogen Pressure.

Temperature = 54°C. Wt. of catalyst = 1.1mg.

Initial 1-butene pressure = 30.0 ± 0.5mm.

% Butene Distribution

<u>Reaction</u>	<u>p<sub>H<sub>2</sub></sub> (mm.)</u>	<u>%n-B</u>	<u>l-B</u>	<u>t-2-B</u>	<u>c-2-B</u>	<u>T/C</u>	<u>t<sub>ex</sub></u> (min.)
P1/1	30.6	23.2	35.4	31.4	33.2	0.94	4.5
P1/2	14.6	25.9	16.6	57.6	35.8	1.61	12.0
P1/3	29.6	25.7	34.3	33.5	32.2	1.04	4.8
P1/4	91.2	32.7	62.9	19.4	17.7	1.10	1.8
P1/5	30.4	27.7	28.9	37.8	33.3	1.14	5.7
P1/6	40.7	34.4	42.0	30.4	27.6	1.10	3.8
P1/7	20.2	26.6	18.1	45.9	36.0	1.27	8.8
P1/8	30.3	26.0	29.2	36.8	34.0	1.08	5.8
P1/9	121.0	26.0	76.9	10.1	13.0	0.77	1.2
P1/10	60.8	28.0	53.5	24.1	22.4	1.07	2.3

TABLE 5.12

Variation of Initial Reaction Rates at 54°C with Initial Hydrogen Pressure.

<u>Reaction</u>	<u>p<sub>H<sub>2</sub></sub> (mm.)</u>	<u>Hydrogenation</u>			<u>Isomerisation</u>		
		<u>r<sub>h</sub></u>	<u>f<sub>h</sub></u>	<u>R<sub>h</sub></u>	<u>r<sub>i</sub></u>	<u>f<sub>i</sub></u>	<u>R<sub>i</sub></u>
P1/1	30.6	1.00	-	-	7.32	1.02	7.50
P1/2	14.6	0.55	-	-	8.99	1.04	9.34
P1/3	29.6	1.10	-	-	7.09	1.06	7.50
P1/4	91.2	3.48	-	-	7.66	1.07	8.20
P1/5	30.4	1.00	-	-	6.92	1.08	7.50
P1/6	40.7	1.40	-	-	6.89	1.09	7.50
P1/7	20.2	0.70	-	-	6.30	1.10	6.93
P1/8	30.3	1.00	-	-	6.79	1.11	7.50
P1/9	121.0	5.0	-	-	6.43	1.12	7.20
P1/10	60.8	2.10	-	-	8.15	1.12	9.12

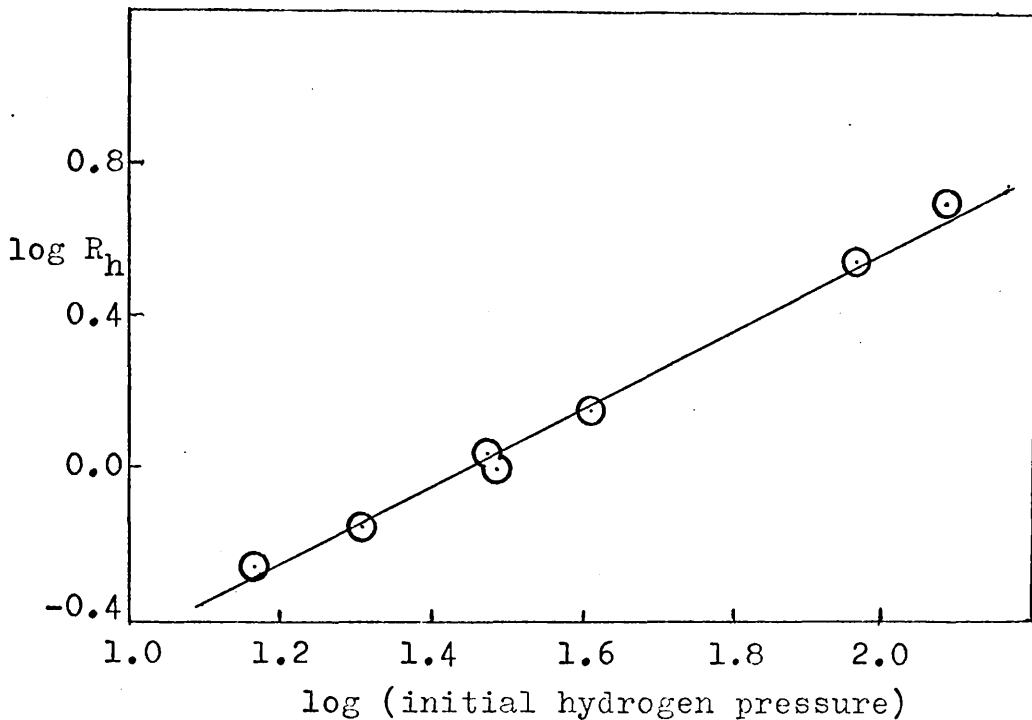


Fig. 5.25 Variation of  $\log R_h$  with  $\log p_{H_2}$  on Rh/SiO<sub>2</sub> at 54°C.

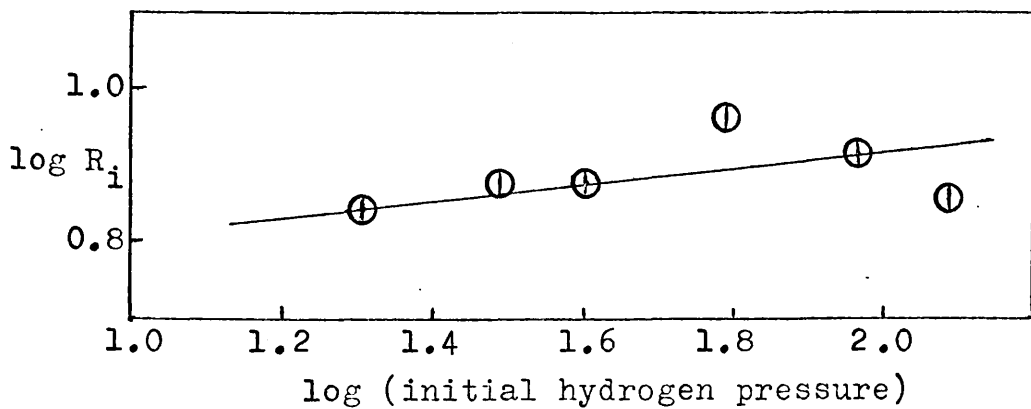


Fig. 5.26 Variation of  $\log R_i$  with  $\log p_{H_2}$  on Rh/SiO<sub>2</sub> at 54°C.

TABLE 5.13

Variation of Butene Distribution on Rh/SiO<sub>2</sub> with Initial 1-Butene Pressure.

Temperature = 54°C. Wt. of catalyst = 1.mg.

Initial hydrogen pressure = 30.0 ± 0.6mm.

% Butene Distribution

<u>Reaction</u>	<u>p<sub>1-B</sub></u> (mm.)	<u>%n-B</u>	<u>1-B</u>	<u>t-2-B</u>	<u>c-2-B</u>	<u>T/C</u>	<u>t<sub>ex</sub></u> (min.)
P2/1	30.0	24.1	37.6	31.8	30.6	1.04	3.5
P2/2	90.4	8.8	74.7	10.6	14.7	0.72	4.5
P2/3	30.6	25.4	43.0	29.2	27.8	1.05	4.0
P2/4	40.0	18.8	49.2	24.0	26.8	0.90	5.2
P2/5	31.0	25.5	35.9	32.1	32.0	1.00	5.8
P2/6	19.0	46.5	8.0	60.0	32.0	1.88	6.3
P2/7	149.5	5.1	83.3	6.8	9.9	0.69	8.7
P2/8	30.2	27.7	35.7	33.8	30.5	1.11	6.0

TABLE 5.14

Variation of Initial Reaction Rates at 54°C with Initial 1-Butene Pressure.

<u>Reaction</u>	<u>p<sub>1-B</sub></u> (mm.)	<u>Hydrogenation</u>			<u>Isomerisation</u>		
		<u>r<sub>h</sub></u>	<u>f<sub>h</sub></u>	<u>R<sub>h</sub></u>	<u>r<sub>i</sub></u>	<u>f<sub>i</sub></u>	<u>R<sub>i</sub></u>
P2/1	30.0	1.50	1.00	1.50	8.66	1.03	9.00
P2/2	90.4	1.30	1.04	1.35	5.91	1.19	7.03
P2/3	30.6	1.40	1.07	1.50	6.63	1.36	9.00
P2/4	40.0	1.00	1.36	1.36	5.62	1.49	8.36
P2/5	31.0	0.92	1.63	1.50	5.63	1.60	9.00
P2/6	19.0	0.96	1.63	1.56	9.42	1.64	15.4
P2/7	149.5	0.80	1.63	1.30	3.15	1.67	5.25
P2/8	30.2	1.00	1.50	1.50	5.37	1.68	9.00

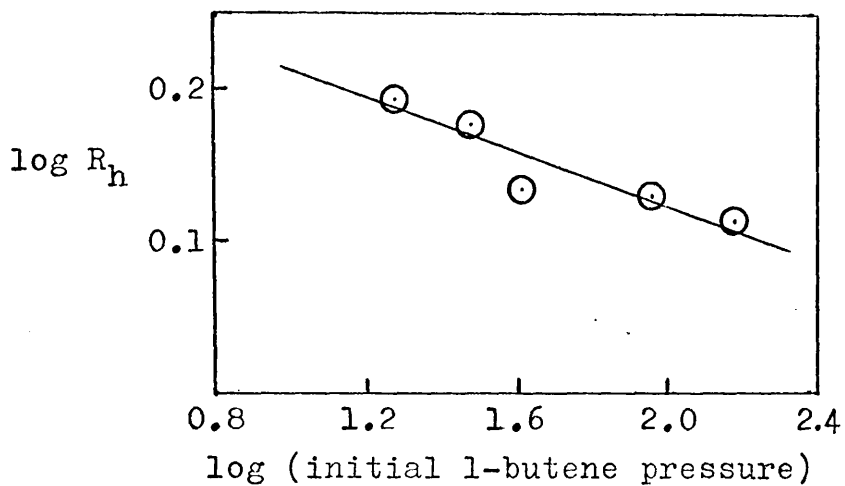


Fig. 5.27 Variation of  $\log R_h$  with  $\log p_{1-B}$  on Rh/SiO<sub>2</sub> at 54°C.

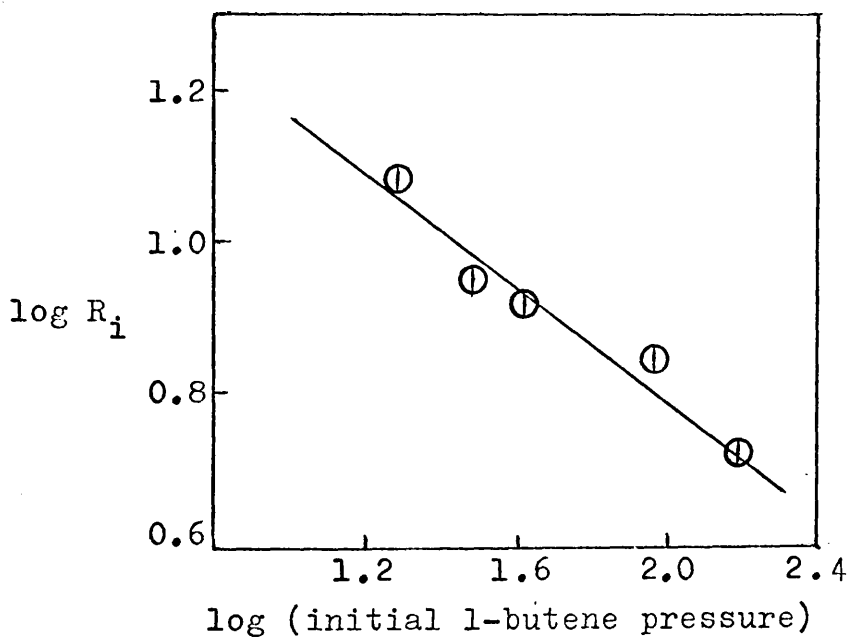
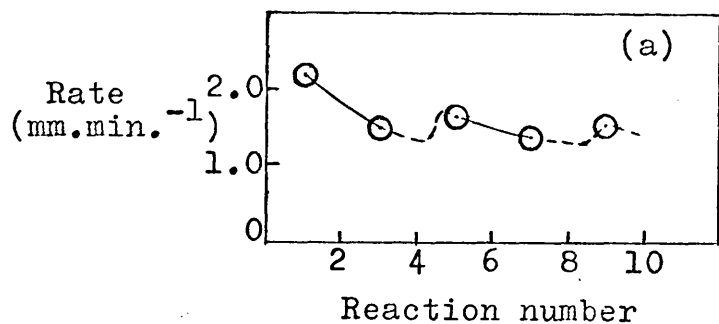
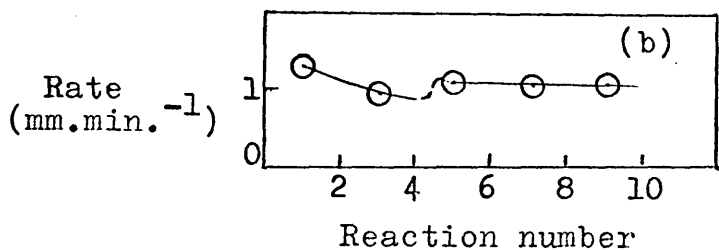


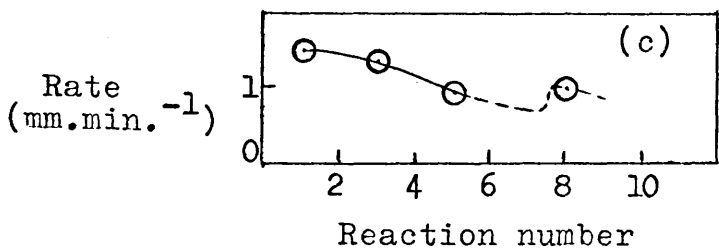
Fig. 5.28 Variation of  $\log R_i$  with  $\log p_{1-B}$  on Rh/SiO<sub>2</sub> at 54°C.



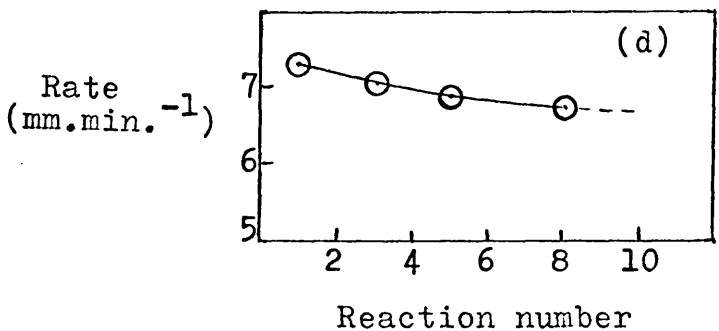
Series L2



Series L2



Series P2



Series P1

Fig. 5.29 Variation of "standard reaction" initial rates on Rh/SiO<sub>2</sub>. (a) Hydrogenation at 0°C, (b) isomerisation at 0°C, (c) hydrogenation at 54°C, (d) isomerisation at 54°C.

in reactions 4 and 8, caused a distinct increase in the standard activity.

A summary of the hydrogenation and isomerisation kinetics is given in table 5.15.

TABLE 5.15

Summary of Kinetics of 1-Butene Reactions.

<u>Catalyst</u>	<u>Temperature</u> °C	<u>Hydrogenation</u>		<u>Isomerisation</u>	
		Hydrogen	1-Butene	Hydrogen	1-Butene
Rh/Al <sub>2</sub> O <sub>3</sub>	0	1.0	-	0.25	-
"	66	1.0	-0.06	0.05	-0.4
Rh/SiO <sub>2</sub>	0	0.95	-	0.05	-
"	54	1.0	-0.08	0.10	-0.4

5.3.3 Effect of Temperature on Reactions on Rh/Al<sub>2</sub>O<sub>3</sub>.

The effect of temperature on the butene distribution and initial rates of the hydrogenation and isomerisation of 1-butene on Rh/Al<sub>2</sub>O<sub>3</sub> was studied using 7.5mg. of catalyst (-18° to 27.5°C) and 2mg. of catalyst (56° to 105°C). The principal reason for carrying out two series of reactions was that the increase in activity with temperature was such that the desired range could not be adequately investigated using one sample only. As the catalysts exhibited the same deactivation features as in the kinetics series, the same technique was applied of carrying out alternate reactions under standard conditions, and activity correction

factors were calculated as described as in section 5.3.1. The standard conditions for each series were around the median temperatures of the ranges covered, these being  $0^{\circ}$  and  $76^{\circ}\text{C}$ . All reactions were carried out with equal initial pressures ( $30.0 \pm 0.5\text{mm.}$ ) of hydrogen and 1-butene and were extracted for analysis at 25% conversion to n-butane.

The analysis results and initial rates for the low temperature series are shown in tables 5.16 and 5.17 respectively. It is apparent that isomerisation occurs to a greater extent at the high temperatures, in agreement with the findings of section 5.1. Fig. 5.30 shows the Arrhenius plots of  $\log R_h$  and  $\log R_i$  against  $1/T$ . The activation energies calculated from the gradient of each line are  $6.0 \text{ kcal.mole}^{-1}$  and  $10.0 \text{ kcal.mole}^{-1}$  for hydrogenation and isomerisation respectively. The point of intersection of the two plots corresponds to a temperature of  $39^{\circ}\text{C}$ , and thus at this temperature, the initial rates of hydrogenation and isomerisation should be identical.

The butene distributions and initial rates calculated from the high temperature series are shown in tables 5.18 and 5.19. The  $\log R$  against  $1/T$  plots are also shown in Fig. 5.30. The activation energies derived from these plots are  $4.8 \text{ kcal.mole}^{-1}$  and  $10.0 \text{ kcal.mole}^{-1}$  for hydrogenation and isomerisation respectively. By extrapolation

TABLE 5.16

Variation of Butene Distribution on Rh/Al<sub>2</sub>O<sub>3</sub> with Temperature.

Wt. of catalyst = 7.5mg.

% Butene Distribution

<u>Reaction</u>	<u>Temperature</u> °C	<u>%n-B</u>	<u>l-B</u>	<u>t-2-B</u>	<u>c-2-B</u>	<u>T/C</u>	<u>t<sub>ex</sub></u> (min.)
G2/1	0	28.9	91.0	4.9	4.1	1.19	3.3
G2/2	-18	25.2	94.1	3.1	2.8	1.11	10.0
G2/3	0	23.4	90.9	4.6	4.5	1.02	4.0
G2/4	18	25.2	85.0	7.4	7.6	0.98	3.5
G2/5	0	25.2	89.1	5.3	5.6	0.93	7.3
G2/6	11	25.4	85.5	7.2	7.3	0.98	6.8
G2/7	27.5	24.4	78.9	10.0	11.1	0.89	4.5
G2/8	0	23.8	88.4	5.5	6.1	0.90	13.0

TABLE 5.17

Variation of Initial Rates on Rh/Al<sub>2</sub>O<sub>3</sub> with Temperature.

Hydrogenation

Isomerisation

<u>Reaction</u>	<u>Temperature</u> °C	<u>r<sub>h</sub></u>	<u>f<sub>h</sub></u>	<u>R<sub>h</sub></u>	<u>r<sub>i</sub></u>	<u>f<sub>i</sub></u>	<u>R<sub>i</sub></u>
G2/1	0	1.94	1.03	2.00	0.85	0.94	0.80
G2/2	-18	0.64	1.25	0.80	0.18	1.05	0.19
G2/3	0	1.30	1.54	2.00	0.71	1.13	0.80
G2/4	18	1.84	1.93	3.54	1.40	1.37	1.92
G2/5	0	0.84	2.38	2.00	0.48	1.68	0.80
G2/6	11	0.86	2.82	2.42	0.70	1.98	1.38
G2/7	27.5	1.30	3.40	4.42	1.58	2.36	3.73
G2/8	0	0.50	4.00	2.00	0.28	2.82	0.80



TABLE 5.18

Variation of Butene Distribution on Rh/Al<sub>2</sub>O<sub>3</sub> with Temperature.

Wt. of catalyst = 2.0mg.

% Butene Distribution

<u>Reaction</u>	<u>Temperature</u> °C	<u>%n-B</u>	<u>1-B</u>	<u>t-2-B</u>	<u>c-2-B</u>	<u>T/C</u>	<u>t<sub>ex</sub></u> (min.)
E2/1	76	26.4	44.5	32.0	23.5	1.36	4.3
E2/2	56	24.1	54.3	24.7	21.0	1.18	9.0
E2/3	76	23.7	30.3	42.1	27.6	1.53	7.0
E2/4	95	24.8	14.2	55.2	30.6	1.80	5.3
E2/5	76	24.6	28.2	44.6	27.2	1.63	6.8
E2/6	87	24.1	18.3	52.0	29.7	1.75	6.5
E2/7	105	22.8	11.4	58.6	30.0	1.95	5.0
E2/8	76	23.8	25.2	45.8	29.0	1.58	7.3

TABLE 5.19

Variation of Initial Rates on Rh/Al<sub>2</sub>O<sub>3</sub> with Temperature.

Hydrogenation

Isomerisation

<u>Reaction</u>	<u>Temperature</u> °C	<u>r<sub>h</sub></u>	<u>f<sub>h</sub></u>	<u>R<sub>h</sub></u>	<u>r<sub>i</sub></u>	<u>f<sub>i</sub></u>	<u>R<sub>i</sub></u>
E2/1	76	1.40	1.43	2.00	5.72	1.05	6.00
E2/2	56	0.60	1.94	1.16	2.16	1.09	2.36
E2/3	76	0.90	2.28	2.00	5.42	1.11	6.00
E2/4	95	1.05	2.35	2.47	13.20	1.05	13.90
E2/5	76	0.80	2.50	2.00	6.04	1.00	6.00
E2/6	87	0.83	2.50	2.08	8.76	0.98	8.63
E2/7	105	1.18	2.50	2.95	17.0	0.98	16.7
E2/8	76	0.80	2.50	2.00	6.15	0.98	6.00

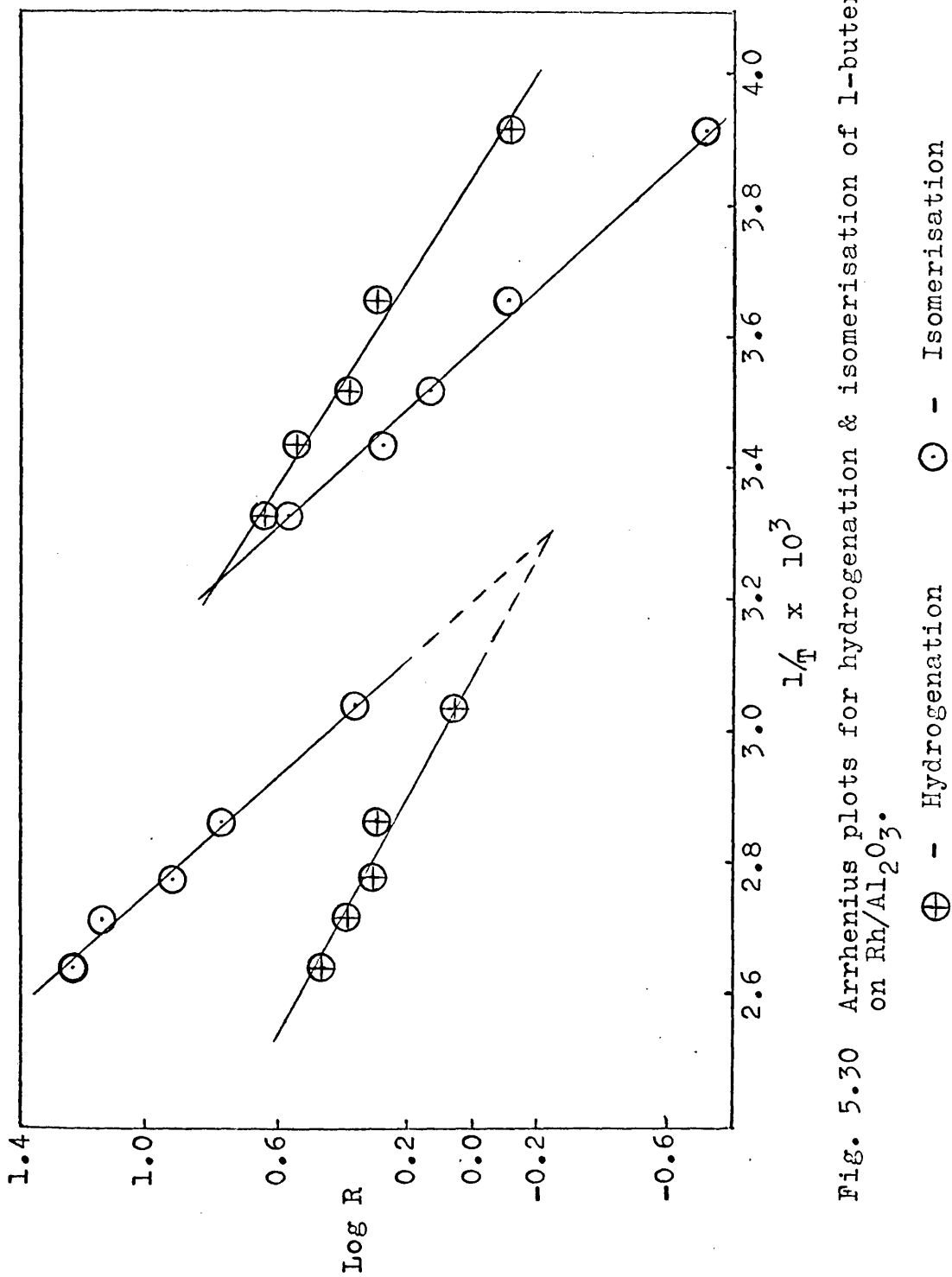


Fig. 5.30 Arrhenius plots for hydrogenation & isomerisation of 1-butene on Rh/Al<sub>2</sub>O<sub>3</sub>.

$\oplus$  - Hydrogenation       $\ominus$  - Isomerisation

the two lines intersect at a point corresponding to 29°C, in close agreement with the low temperature plots.

The rates of the standard reactions display characteristics similar to those described in sections 5.1. The deactivation is greater for hydrogenation than for isomerisation. The only exception to the regularity is the high temperature isomerisation, where there is a marked increase in activity between reactions 3 and 5.

#### 5.3.4 Effect of Temperature on Reactions on Rh/SiO<sub>2</sub>.

The temperature dependence of the butene distribution and initial reaction rates on Rh/SiO<sub>2</sub> was studied using catalyst samples weighing 4.7mg. (-20° to 18°C) and 1.2mg. (41° to 86°C). The initial pressures of hydrogen and 1-butene were each 30.6 ± 0.5mm. and the products were extracted at ~25% conversion to n-butane.

The results of the low temperature series are shown in tables 5.20 and 5.21. Plots of log R<sub>h</sub> and log R<sub>i</sub> against 1/T (Fig. 5.31) produce two straight lines of similar gradient, from which activation energies of 9.2 kcal.mole<sup>-1</sup> for hydrogenation and 11.3 kcal.mole<sup>-1</sup> for isomerisation were calculated.

The apparent discontinuity in standard reaction rates - and thus also in f values - between L1/6 and L1/7 is due to the regeneration of activity by 10mm. hydrogen for a

TABLE 5.20

Variation of Butene Distribution on Rh/SiO<sub>2</sub> with Temperature.

Wt. of catalyst = 4.7mg.

% Butene Distribution

<u>Reaction</u>	<u>Temperature</u> °C	<u>%n-B</u>	<u>1-B</u>	<u>t-2-B</u>	<u>c-2-B</u>	<u>T/C</u>	<u>t<sub>ex</sub></u> (min.)
L1/1	0	25.4	86.7	5.9	7.4	0.79	3.5
L1/2	-20	22.3	90.0	4.3	5.7	0.76	14.8
L1/3	0	25.3	82.7	7.2	10.1	0.71	5.2
L1/4	18	26.1	78.9	10.3	10.8	0.95	2.0
L1/5	0	26.5	85.1	7.0	7.9	0.87	5.3
L1/6	7	25.4	81.4	8.6	10.0	0.86	3.8
L1/7	0	23.8	87.6	5.0	7.4	0.75	2.8
L1/8	15	24.5	80.1	8.6	11.3	0.75	2.3
L1/9	0	25.0	85.3	7.0	7.7	0.91	5.7

TABLE 5.21

Variation of Initial Rates on Rh/SiO<sub>2</sub> with Temperature.

Hydrogenation

Isomerisation

<u>Reaction</u>	<u>Temperature</u> °C	<u>r<sub>h</sub></u>	<u>f<sub>h</sub></u>	<u>R<sub>h</sub></u>	<u>r<sub>i</sub></u>	<u>f<sub>i</sub></u>	<u>R<sub>i</sub></u>
L1/1	0	1.95	1.03	2.00	1.25	1.20	1.50
L1/2	-20	0.37	1.25	0.46	0.22	1.27	0.26
L1/3	0	1.15	1.74	2.00	1.12	1.34	1.50
L1/4	18	3.00	1.82	5.46	3.60	1.44	5.18
L1/5	0	1.10	1.82	2.00	0.94	1.59	1.50
L1/6	7	1.40	1.90	2.66	1.62	1.68	2.72
L1/7	0	2.00	1.00	2.00	1.50	1.00	1.50
L1/8	15	2.20	1.47	3.68	3.04	1.50	4.56
L1/9	0	1.00	2.00	2.00	0.86	1.74	1.50

TABLE 5.22  
Variation of Butene Distribution on Rh/SiO<sub>2</sub>  
with Temperature.

Wt. of catalyst = 1.2mg.

% Butene Distribution

<u>Reaction</u>	<u>Temperature</u> °C	<u>%n-B</u>	<u>1-B</u>	<u>t-2-B</u>	<u>c-2-B</u>	<u>T/C</u>	<u>t<sub>ex</sub></u> (min.)
M/1	60	27.1	41.2	31.2	27.6	1.14	3.5
M/2	41	24.6	48.8	23.8	27.4	0.87	7.8
M/3	60	25.0	48.1	26.9	25.0	1.08	4.8
M/4	75	31.0	30.5	39.7	29.8	1.33	3.6
M/5	60	26.9	42.2	28.7	29.1	0.99	5.7
M/6	60	26.4	50.6	25.1	24.3	1.04	4.0
M/7	70	26.2	43.5	29.8	26.7	1.12	3.8
M/8	60	25.2	49.6	25.4	25.0	1.02	5.3
M/9	86	28.2	36.2	36.7	27.1	1.33	3.0
M/10	60	25.8	37.4	32.4	30.2	1.07	6.8

TABLE 5.23

Variation of Initial Rates on Rh/SiO<sub>2</sub> with Temperature.

<u>Reaction</u>	<u>Temperature</u> °C	<u>Hydrogenation</u>			<u>Isomerisation</u>		
		<u>r<sub>h</sub></u>	<u>f<sub>h</sub></u>	<u>R<sub>h</sub></u>	<u>r<sub>i</sub></u>	<u>f<sub>i</sub></u>	<u>R<sub>i</sub></u>
M/1	60	1.75	1.14	2.00	7.87	1.02	8.00
M/2	41	0.70	1.43	1.00	2.85	1.21	3.46
M/3	60	1.10	1.82	2.00	4.73	1.69	8.00
M/4	75	1.80	1.96	3.53	9.47	1.69	16.00
M/5	60	0.96	2.02	2.00	4.71	1.70	8.00
M/6	60	1.60	1.25	2.00	5.24	1.53	8.00
M/7	70	1.50	1.67	2.50	6.84	1.77	12.10
M/8	60	1.00	2.00	2.00	4.19	1.91	8.00
M/9	86	2.15	2.35	5.05	10.7	1.95	20.9
M/10	60	0.85	2.35	2.00	4.61	1.74	8.00

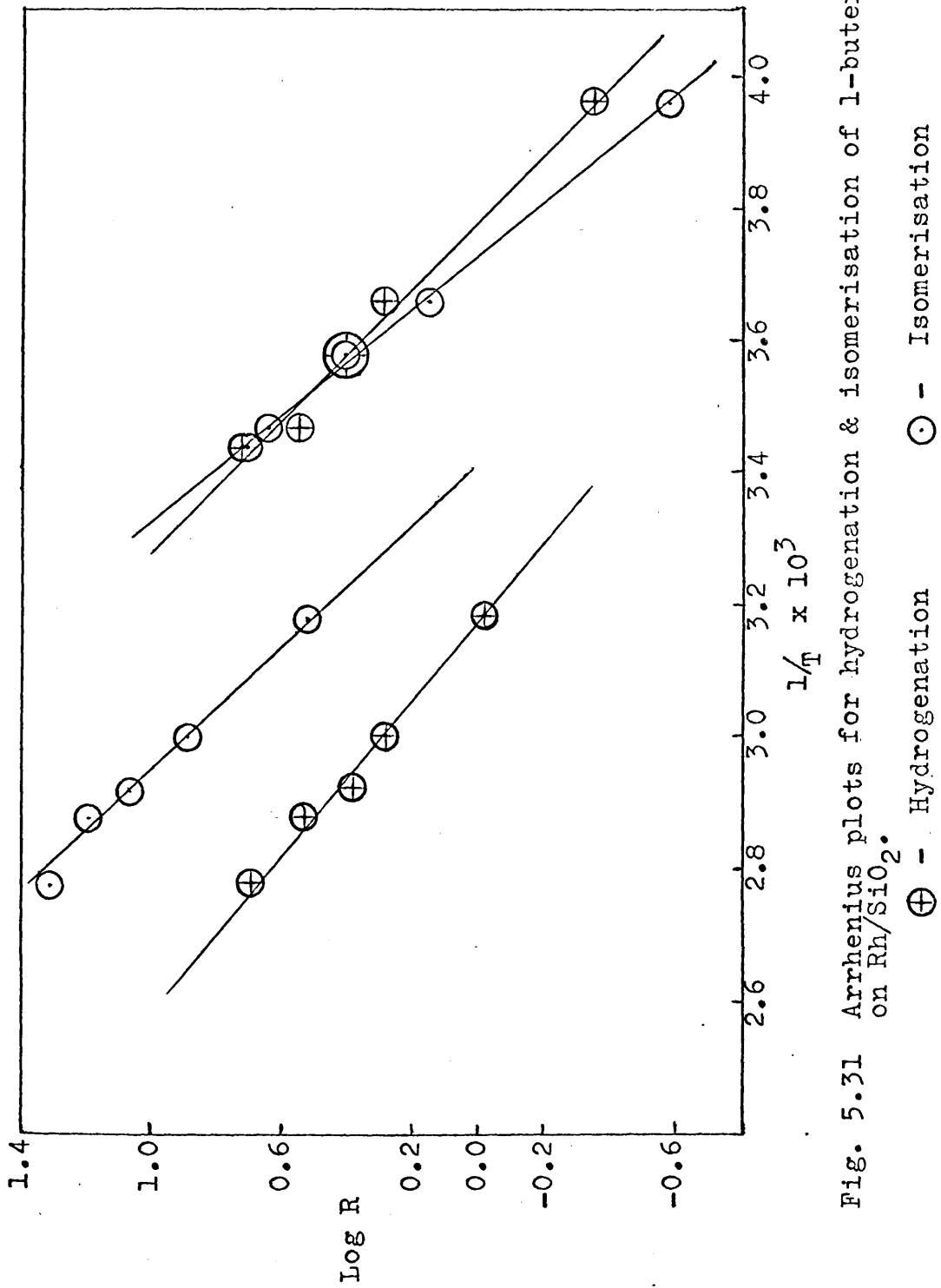


Fig. 5.31 Arrhenius plots for hydrogenation & isomerisation of 1-butene on Rh/SiO<sub>2</sub>.  $\oplus$  - Hydrogenation  $\odot$  - Isomerisation

period of 15 minutes at 15°C. This treatment caused the activity for both reactions to return to the original values, but the regeneration was apparently only temporary, as indicated by subsequent reactions.

The results of the high temperature series are shown in tables 5.22 and 5.23. Reaction M/4 was allowed to proceed beyond the normal extraction point, but as the isomerisation had not reached equilibrium proportions, the  $r_i$  value may be considered as valid. Fig. 5.31 shows the plots of  $\log R_h$  and  $\log R_i$  against  $1/T$  and activation energies of 8.1 kcal.mole<sup>-1</sup> and 9.9 kcal.mole<sup>-1</sup> are obtained for hydrogenation and isomerisation respectively.

The measured standard reaction rates on Rh/SiO<sub>2</sub> exhibit some interesting features, dependent upon the temperatures of the preceding reactions. After reaction M/5 the catalyst vessel was evacuated, and the catalyst was allowed to stand under 60mm. hydrogen for 8 minutes at 60°C. This regenerated the catalyst to almost its original activity, as shown by reaction M/6. The general trends for Rh/SiO<sub>2</sub> show that deactivation of both addition and isomerisation reactions is rather less than on Rh/Al<sub>2</sub>O<sub>3</sub>.

A summary of activation energies is given in table 5.24.

TABLE 5.24

Summary of Activation Energies

<u>Catalyst</u>	<u>Temperature Range</u>	<u>E<sub>h</sub></u> (kcal.mole <sup>-1</sup> )	<u>E<sub>i</sub></u> (kcal.mole <sup>-1</sup> )
Rh/Al <sub>2</sub> O <sub>3</sub>	-18° to 27.5°C	6.0 ± 0.5	10.0 ± 0.5
"	56° " 105°	4.8 ± 0.5	10.0 ± 0.5
Rh/SiO <sub>2</sub>	-20° to 18°C	9.2 ± 0.5	11.3 ± 0.5
"	41° " 86°	8.1 ± 1.0	9.9 ± 0.5



#### 5.4 Reaction of 1-Butene in Absence of Molecular Hydrogen.

There are three possible reactions which 1-butene may be expected to undergo on a catalyst in the absence of hydrogen. These are (i) isomerisation to the 2-butenes, (ii) disproportionation, leading to n-butane and 1,3-butadiene, and (iii) cracking to smaller molecules. There is no apparent reason why (iii) should occur in the absence of hydrogen when it does not occur in its presence, and (ii) seems unlikely, but possible. Thus, interest is focussed mainly on (i), the isomerisation, as it is possible to write mechanisms for isomerisation which do not require the presence of hydrogen. A catalyst activated in hydrogen will almost certainly have some residual adsorbed hydrogen, and therefore an improved procedure was required in order to remove as much residual hydrogen as possible from the catalyst surface.

##### 5.4.1 Reaction on Rh/Al<sub>2</sub>O<sub>3</sub>.

The catalyst used for this series was Rh-G (7.5mg.), and after activation in the usual way at 220°C, the temperature was raised to 295°C, and the catalyst vessel evacuated for 6 hours, before cooling to ambient temperature. A series of reactions was then carried out at two temperatures, 26.5° and 116°C, with 1-butene pressures of 30.5 ± 0.5mm. The results, together with the reaction

times ( $t_{\text{ex}}$ ) are shown in table 5.25.

TABLE 5.25

Butene Isomerisation on Rh/Al<sub>2</sub>O<sub>3</sub> in Absence of Hydrogen.

<u>Reaction</u>	<u>Temperature</u> (°C)	<u>t<sub>ex</sub></u> (hr.)	<u>r<sub>i</sub></u> (mm./min) x10 <sup>-3</sup>	% Butene Distribution			<u>T/C</u>
				<u>l-B</u>	<u>t-2-B</u>	<u>c-2-B</u>	
G3/1	26.5	1.0	3.5	99.2	0.3	0.5	0.65
G3/2	26.5	1.0	0.0	100	Trace	Trace	-
G3/3	116	1.0	42.5	92.0	4.3	3.7	1.14
G3/4	116	1.0	13.5	97.4	1.4	1.2	1.19
G3/5	116	11.0	8.6	83.5	9.4	7.1	1.32
G3/6	115	1.0	2.6	99.5	0.2	0.24	0.93
G3/7	26	21.0	0.0	100	Trace	Trace	-

It is apparent that isomerisation is much faster at the higher temperatures, as may be anticipated, but over the whole temperature range it is very much slower than in the presence of hydrogen. There were no detectable amounts of n-butane or 1,3-butadiene, or of hydrocarbons of lower molecular weight, and thus only the isomerisation process was occurring.

The deactivation of the catalyst at 26.5°C is very rapid, as can be seen from the relative rates of reactions 1 and 2, despite evacuation of the catalyst vessel at

26.5°C for one hour. Between reactions 2 and 3, the catalyst was pumped for a total of 4½ hours at ~116°C, and each high temperature reaction was followed by 40 minutes evacuation. G3/7 produced even a smaller trace of isomerised products than did G3/2, and hence, even at the higher temperature, pumping alone was insufficient to remove all the residue from the catalyst.

#### 5.4.2 Reaction on Rh/SiO<sub>2</sub>.

The reaction of 1-butene on Rh/SiO<sub>2</sub> was investigated in a manner similar to that described for Rh/Al<sub>2</sub>O<sub>3</sub> but the experiment was extended in two ways. The activation of the catalyst was carried out with deuterium, and the reaction products were then examined by mass spectrometry to determine the extent of the role played by residual adsorbed "hydrogen". After completion of the series, one reaction was carried out with a 1:1 :: 1-butene:deuterium mixture.

The reactions were carried out on a 9.8mg. sample of Rh/SiO<sub>2</sub> and after activation in deuterium at 225°C, the catalyst was evacuated for 8½ hours at 295°C, before cooling to room temperature. The initial pressure of 1-butene in each reaction was 30.5 ± 0.5mm. The analysis results and extraction times are shown in table 5.26, with the exception of reaction 1, the products of which were accidentally lost during extraction.

TABLE 5.26

<u>Reaction</u>	<u>Temperature</u> (°C)	<u>t<sub>ex</sub></u> (hr.)	<u>r<sub>i</sub></u> (mm./min)	% Butene Distribution			<u>T/C</u>
				<u>1-B</u>	<u>t-2-B</u>	<u>c-2-B</u>	
S/2	27	1.25	0.01	96.6	3.0	0.4	8.92
S/3	115	1.0	0.17	72.0	19.0	9.0	2.11
S/4	114	10.0	0.04	50.8	30.4	18.8	1.62
S/5	114	1.0	0.01	98.1	0.9	1.0	0.91
S/6	28	1.0	0.00	100	0.0	0.0	-

No trace of n-butane or 1,3-butadiene was found in the reaction products nor were any lighter hydrocarbons observed. The disproportionation and cracking reactions are thus eliminated. It is unfortunate that the products of S/1 were lost, but it is nevertheless apparent that isomerisation proceeds more readily on Rh/SiO<sub>2</sub> than on Rh/Al<sub>2</sub>O<sub>3</sub>; the deactivation of the former with successive reactions is also very much less, but despite this the activity was virtually zero by S/6.

The addition of a 1:1 mixture of deuterium and 1-butene at 28°C after completion of the series produced an interesting result. The initial rate of hydrogenation was 0.4mm.min.<sup>-1</sup> but this increased with time, and after 15 minutes, the total pressure fall was 15.2mm., suggesting a partial regeneration by the deuterium.

The extent of the incorporation of deuterium into the butenes is shown in table 5.27.

TABLE 5.27

Distribution of Deutero-butenes in Series S.

<u>Reaction</u>	$d_0$	$d_1$	$d_2$	$d_3$	$d_4$	$d_5$	$d_6$	$d_7$	$d_8$	<u>D.N.</u>
$\frac{S1/2}{1-B}$	99.0	0.1	0.7	0.1	0.06	0.02	-	-	-	0.022
t-2-B	79.5	6.6	9.1	2.5	1.4	0.5	0.3	0.1	0.03	0.427
$\frac{S/3}{c-2-B}$	88.3	2.5	3.8	2.2	1.4	0.9	0.5	0.3	0.1	0.324

All other samples showed no trace of deuteration, although the yield of cis 2-butene from reaction S/2 was apparently too small to be detected by the MS10, and hence no spectrum is available for it. It is notable that exchange of the reactant 1-butene extends to the  $d_5$  species in reaction 2, and to the  $d_8$  species in the 2-butene isomerisation products of reactions 2 and 3. It must therefore be assumed that considerable exchange occurred in the first reaction, thus showing that, while molecular hydrogen was not present, the reactions were occurring in the presence of a substantial amount of adsorbed hydrogen, and this has to be taken account of when considering mechanisms.<sup>10,85</sup>

CHAPTER 6INVESTIGATION OF SUPPORT EFFECT.6.1 Introduction.

The results of Chapter 5 showed there are a number of significant features in which the products of 1-butene hydroisomerisation and the catalyst reactivity differ considerably on Rh/Al<sub>2</sub>O<sub>3</sub> and Rh/SiO<sub>2</sub> respectively. The cause of this effect must lie in the change from one support to the other, and it was therefore relevant to carry out an investigation of the possible effects of the support material upon the reaction.

This problem was approached in two different ways. The possibility that the support materials might themselves catalyse the reactions was investigated by series of reactions at a number of temperatures on pure alumina and pure silica. Second, the possible effect on Rh/SiO<sub>2</sub> of the separate addition of alumina and silica was studied at 0°C, as at that temperature the rates of hydrogenation and isomerisation were comparable and thus any change would be more apparent. The alumina used in these experiments was supplied by Johnson-Matthey and was of the same source as that used in the preparation of the rhodium catalyst. The silica was Degussa "Aerosil", as used in the preparation of the Rh/SiO<sub>2</sub>.

6.2 Reactions on Al<sub>2</sub>O<sub>3</sub>.

A 50mg. sample of alumina was given exactly the same pretreatment as was employed for the metal catalysts, (i.e. heating in an atmosphere (150mm.) of hydrogen at 220°C for one hour). A series of reactions was carried out with initial hydrogen and 1-butene pressures each of 30.0 ± 0.5mm. The results are shown in table 6.1.

TABLE 6.1Reaction of 1-Butene with Hydrogen on Al<sub>2</sub>O<sub>3</sub>.

Wt. of catalyst = 50mg.

<u>Reaction</u>	<u>Temperature</u> °C	<u>t<sub>ex</sub></u> (min.)	<u>%n-B</u>	<u>% Butene Distribution</u>			<u>T/C</u>
				<u>1-B</u>	<u>t-2-B</u>	<u>c-2-B</u>	
1	100	30	2.0	39.7	37.6	22.7	1.65
2	100	180	14.6	6.9	65.5	27.6	2.40
3	21.5	30	Trace	99.3	~0.3	~0.4	~0.7
4	52	30	Trace	98.1	0.9	1.0	0.86

The detection of n-butane in reaction 3 was very doubtful; it could only have been present in very small quantities, as even at 52°C only trace quantities were produced. It may be noted that the butene distribution from reaction 2 was equal to the thermodynamic equilibrium distribution.

No attempt was made to determine if the activity decreased with successive reactions. Initial rates of

isomerisation were calculated for reactions 1, 3, and 4 and, without any activity correction, the Arrhenius plot gave an activation energy of  $\sim 13.4 \text{ kcal.mole}^{-1}$ . This must inevitably be subject to a large systematic error, as it is based on only three points with no activity corrections, but it is nevertheless not dissimilar to the values of  $E_1$  obtained on  $\text{Rh/Al}_2\text{O}_3$  and  $\text{Rh/SiO}_2$ .

No attempt was made to measure the rate of hydrogenation, as this was almost imperceptible.

### 6.3 Reactions on $\text{SiO}_2$ .

300mg. silica were treated with hydrogen (150mm.) for 19 hours, thereby reproducing the conditions of the first stage of the preparation of the  $\text{Rh/SiO}_2$  catalyst. Two samples of this silica, weighing 40mg. and 22mg., were used for separate series of reactions, after activation by the standard treatment (150mm. of hydrogen for one hour at  $220^\circ\text{C}.$ ) The initial pressures of 1-butene and hydrogen were each  $30.0 \pm 0.5\text{mm}.$  The results are shown in table 6.2.



TABLE 6.2

Reaction of 1-Butene with Hydrogen on SiO<sub>2</sub>.

Weights of catalyst A = 40mg.

B = 22mg.

<u>Reaction</u>	<u>Temperature</u> °C	<u>t<sub>ex</sub></u> (min.)	<u>%n-B</u>	<u>% Butene Distribution</u>			<u>T/C</u>
				<u>1-B</u>	<u>t-2-B</u>	<u>c-2-B</u>	
A/1	97	30	Trace	99.4	0.2	0.4	0.50
A/2	0	720	0.0	100	Trace	Trace	-
B/1	100	30	0.0	100	0.0	0.0	-
B/2	100	212	0.0	100	0.0	0.0	-
B/3	154	30	0.0	100	0.0	0.0	-

It is apparent that hydrogenation does not occur on silica, and that the degree of isomerisation is very much less than on alumina.

6.4 Reactions on Mixed Catalysts.

Four series of reactions were carried out on mixed catalysts at 0°C as follows.

Series A1	7.2mg. Rh/SiO <sub>2</sub>
" A2	7.2mg. " + 9.4mg. Al <sub>2</sub> O <sub>3</sub> .
" B1	7.0mg. "
" B2	7.0mg. " + 8.0mg. SiO <sub>2</sub> .

The results of series A1 and A2 were identical, within experimental error, while series B2 produced a small rise in the proportion of isomerised products from B1. The magnitude of the change, however, was insufficient to enable any major conclusions to be drawn from it.

#### 6.5 Conclusion.

It was apparent from sections 6.2 and 6.3 that alumina is able to catalyse the isomerisation, and, to a lesser extent, the hydrogenation of 1-butene in the presence of hydrogen, while silica is virtually inactive for either isomerisation or hydrogenation.

R E S U L T S - S E C T I O N BCHAPTER 7THE REACTION OF 1-BUTENE WITH DEUTERIUM ON MERCURY POISONED  
Rh/SiO<sub>2</sub> CATALYSTS.

The choice of Rh/SiO<sub>2</sub> as the catalyst for the studies of mercury poisoning was made for two main reasons. First, it was apparent from the results presented in chapter 6 that silica is a catalytically inactive support for butene hydroisomerisation. Second, the activation energies for hydrogenation and isomerisation of 1-butene on Rh/SiO<sub>2</sub> were such that the hydrogenation/isomerisation ratio would change more gradually with temperature than it would on Rh/Al<sub>2</sub>O<sub>3</sub>. If the adsorption of mercury on the catalyst were to produce a change in this ratio, it would thus be relatively greater than the temperature induced change with Rh/SiO<sub>2</sub> than with Rh/Al<sub>2</sub>O<sub>3</sub>.

Before commencing the study of reactions on Rh/SiO<sub>2</sub> catalysts poisoned by the adsorption of mercury, it was necessary to make a survey of the adsorption characteristics of mercury on Rh/SiO<sub>2</sub>.

7.1.1 The Adsorption of Mercury on Rh/SiO<sub>2</sub>.

This study was carried out by a three-stage continuous adsorption on a 10.6mg. sample of catalyst which had pre-

-viously been activated at  $225^{\circ}\text{C}$  in the usual manner. The results are shown in Fig. 7.1. In stage 1, from 0-17 hours, the mercury ampoule was thermostatted at  $0^{\circ}\text{C}$ , and the catalyst vessel surrounded by a water jacket maintained at  $12 \pm 2^{\circ}\text{C}$ ; under these isothermal conditions the rate of adsorption is rapid initially and falls gradually until an equilibrium is reached. During stage 2, from 17-38 hours, when few readings were available, the temperature of the water jacket rose to  $18^{\circ}\text{C}$  and that of the mercury source remained at  $0^{\circ}\text{C}$  and it may be significant that count rates at this temperature are slightly higher than at  $12^{\circ}\text{C}$ . Before the final three counts were taken, the water was again cooled to  $10^{\circ}\text{C}$ . In stage 3, from 38-60 hours, the catalyst vessel and mercury source were thermostatted at  $27 \pm 1^{\circ}\text{C}$  and  $22 \pm 0.5^{\circ}\text{C}$  respectively, and it is observed that further adsorption occurs, with the formation of a new equilibrium. During the first 12 hours of adsorption, counts were taken over 5 minute periods, and subsequently over 10 minutes or longer; the statistical accuracy of the measurements thus increases with the length of adsorption.

### 7.1.2 Determination of Gas-Phase Count-Rate.

While the saturated vapour pressure of mercury is very low ( $1.2 \times 10^{-3}$  mm. at  $20^{\circ}\text{C}$ ) it was necessary to determine if the mercury present in the catalyst vessel as vapour during

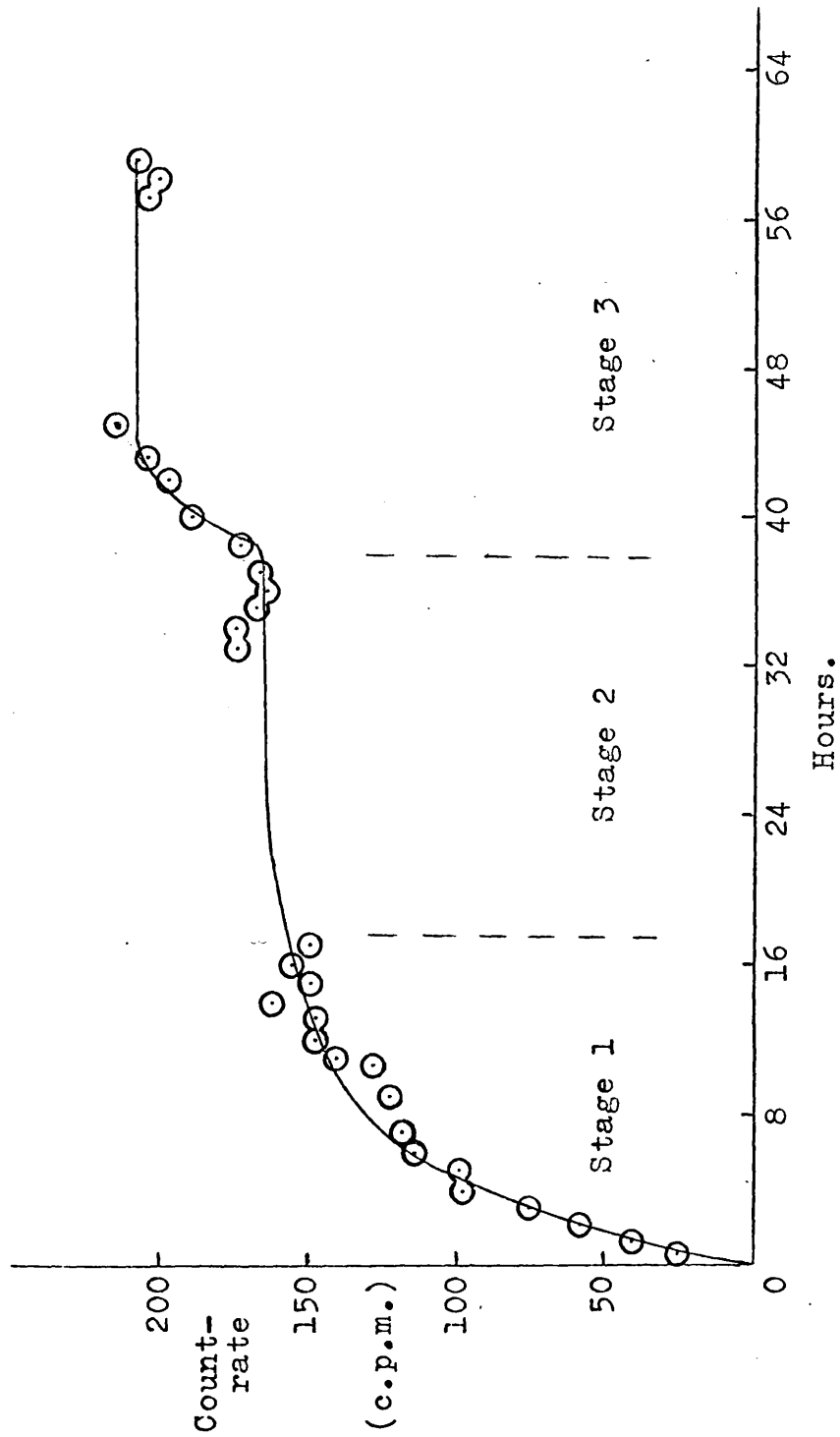


Fig. 7.1 Adsorption isotherm ( $0^{\circ}\text{C}$ ) for mercury on  $\text{Rh/SiO}_2$ .

an adsorption were sufficient to contribute to the measured count-rate. This was done by allowing the mercury vapour to diffuse into an evacuated vessel containing no catalyst, and comparing the count-rate so obtained with the previously measured background. This was carried out at two temperatures and it is apparent from the results shown in table 7.1 that the gas-phase contribution to the count rate is negligible. In run 1, the mercury source was thermostatted at  $0^{\circ}\text{C}$  and the catalyst vessel at  $20 \pm 1^{\circ}\text{C}$ , and in run 2 at  $19.6 \pm 0.2^{\circ}\text{C}$  and  $44 \pm 0.5^{\circ}\text{C}$  respectively.

TABLE 7.1

Count-Rates obtained from "blank" Mercury Adsorptions.

<u>Run 1.</u>		<u>Run 2.</u>	
Background : $25 \pm 0.4\text{c.p.m.}$		Background : $78.7 \pm 0.8\text{c.p.m.}$	
<u>Duration</u> (hrs.)	<u>Count-Rate</u> (c.p.m.)	<u>Duration</u> (hrs.)	<u>Count-Rate</u> (c.p.m.)
0.5	$27.4 \pm 1.6$	0.1	$79.9 \pm 2.8$
1.0	$25.1 \pm 1.3$	0.5	$79.5 \pm 2.8$
2.0	$23.7 \pm 0.9$	0.75	$79.5 \pm 1.6$
3.0	$25.1 \pm 1.2$	1.4	$81.0 \pm 2.9$
6.25	$25.1 \pm 1.3$	1.75	$75.5 \pm 2.2$
8.0	$25.5 \pm 1.3$	2.25	$78.3 \pm 2.2$
9.0	$24.1 \pm 1.1$	2.5	$77.8 \pm 2.0$
20.25	$26.6 \pm 0.9$	3.0	$79.7 \pm 1.6$

In all subsequent adsorption measurements the total nett

count was assumed to be due to mercury adsorbed on the catalyst.

### 7.1.3 Effect of Temperature on Adsorbed Mercury.

The behaviour of pre-adsorbed mercury with increasing temperature was studied from 0°C to 300°C. A continuous trace of the activity of the adsorbed mercury was obtained with the use of an I.D.L. type 649A probe unit and an I.D.L. type 550 ratemeter which provided digitised and continuous outputs to an electronic scaler and chart recorder respectively.

A 5.2mg. sample of Rh/SiO<sub>2</sub> was activated in the standard way, and a series of reactions of hydrogen and 1-butene (series A) carried out at 0°C. This was followed by continuous adsorption of mercury for eight hours at 0°C, by which time the activity of adsorbed mercury had virtually reached the plateau; it must therefore have been >95% monolayer cover. The count-rate was  $2.4 \pm 0.3$  c.p.s. A second series of reactions (series B) was carried out at 0°C on the poisoned catalyst, and it was apparent from the ratemeter trace that no desorption of mercury occurred during the series.

The catalyst vessel was then evacuated continuously as the temperature was raised to 25°C over a period of three hours. No desorption occurred, nor during four reactions carried out at 25°C. Again it was apparent from the rate-

-meter trace that the reactions had no effect on the adsorbed mercury. The ice/water bath was then replaced by the furnace, necessitating a change of geometry for the counter; the new count-rate was 3.15c.p.s. at 25°C. The temperature was raised to 60°C, and after ten hours evacuation at that temperature and a further series of reactions, the count-rate was undiminished. Thereafter evacuation was continued while the temperature was steadily raised to 303°C over four hours. However, at 128°C, the counter ceased to function. Up to 120°C, the count rate remained steady on 3.15c.p.s. but from 120° - 128°C, a slight drop to 2.85c.p.s. was observed. This may be due to one of two possible causes, (i) desorption of mercury, or (ii) the counter characteristics changing with the temperature.

After evacuating for one hour at 303°C, the catalyst vessel was allowed to cool. The counter was restarted at ~125°C and the count-rate remained steady on  $0.9 \pm 0.1$ c.p.s. as the temperature was lowered to 0°C. A post-desorption series of reactions (series C) was carried out to determine the subsequent catalytic activity. The relative nett count-rates, after correction for decay, of the activity before and after desorption are shown below.



Initial rate at 25°C	=	117.5 ± 4.0c.p.m.
Final rate at 0°C	=	18.2 ± 2.2 "
Mean residual activity	=	15.5 ± 2.5%

Thus ~85% of the adsorbed mercury was removed at temperatures between 120° and 300°C. The rates of hydrogenation and isomerisation for reactions extracted at 15% conversion in each series are shown in table 7.3 and the complete analyses of each series are shown in table 7.2.

TABLE 7.2

Butene Distribution at 0°C before and after Desorption.

Initial  $p_{H_2} = p_{1-B} = 30.0 \pm 0.5$ mm.

% Butene Distribution

<u>Reaction</u>	<u>%n-B</u>	<u>1-B</u>	<u>t-2-B</u>	<u>c-2-B</u>	<u>T/C</u>	<u>t<sub>ex</sub></u> (min.)
A/2	15.6	93.4	4.2	2.4	1.77	2.5
A/1	28.1	85.2	9.5	5.3	1.81	4.0
A/4	50.5	61.2	24.9	13.9	1.80	7.3
A/3	60.6	45.3	35.9	18.8	1.91	7.5
B/1	14.4	82.6	7.6	9.8	0.77	14.3
B/4	31.1	56.2	23.3	20.5	1.14	25.8
B/3	47.8	17.6	49.2	33.2	1.48	42.5
B/2	62.7	2.1	68.8	29.1	2.37	53.5
C/3	14.7	91.4	3.4	5.2	0.66	8.5
C/1	33.9	73.4	12.0	14.6	0.82	15.3
C/4	49.9	43.0	28.0	29.0	0.97	29.0
C/2	64.6	9.6	53.4	37.0	1.45	36.0

TABLE 7.3

Initial Reaction Rates at 0°C before and after Desorption.

<u>Reaction</u>	<u>%n-B</u>	<u>r<sub>h</sub></u> (mm. min. <sup>-1</sup> )	<u>r<sub>i</sub></u>	<u>r<sub>i</sub>/r<sub>h</sub></u>
A/2	15.6	1.30	0.82	0.63
B/1	14.4	0.22	0.39	1.77
C/3	14.7	0.38	0.32	0.84

## 7.2 Reaction of 1-Butene with Deuterium on Poisoned and Unpoisoned Catalysts.

The effect of adsorbed mercury upon the reaction of 1-butene with deuterium on  $\text{Rh}/\text{SiO}_2$  was studied by carrying out series of reactions at several stages of mercury adsorption at each of three temperatures. The addition and isomerisation reactions were studied simultaneously in the same way as described in chapter 5, the initial pressures of deuterium and 1-butene each being 30.0mm. As only deuterium was used in the reactions to be described in this chapter, the term "deuteration" will be taken to imply the addition reaction.

The products of each reaction were separated and collected for mass spectrometric analysis to enable the olefin exchange reaction to be studied. Where the yield was very low, however, the sensitivity of the instrument was sometimes insufficient for a spectrum to be obtained. Thus, as the sensitivity to n-butane was less than that for each of the butenes, no spectrum was obtained for the n-butane from low conversion reactions. Similarly, on occasions no spectra were obtained for 1-butene if the isomerisation reaction had proceeded almost to equilibrium.

### 7.3.1 Hydrogenation and Isomerisation at 0°C.

The hydrogenation and isomerisation reactions were

studied at 0°C on a 12.6mg. sample of catalyst at mercury coverages ranging from zero to almost 100% monolayer. The pressure fall against time curves were similar to those of sections 5.1 and 5.2; that is, they were initially first order in overall kinetics. With the exception of the initial series on the unpoisoned catalyst, however, no reactions were allowed to proceed beyond approximately 28% conversion.

The isomerisation reaction was studied at each stage by series of reactions extracted for analysis at different conversions. As the amount of mercury was increased, however, fewer reactions per series were carried out, as it was found from the results that the relative poisoning effects on the hydrogenation and isomerisation reactions were such as to allow the butenes to isomerise to equilibrium proportions at much lower conversions. The results are shown in table 7.5.

The extent of mercury adsorption at each stage is shown in table 7.4 by the decay corrected count-rate and  $\theta_{\text{Hg}}$ , the percentage of monolayer coverage of mercury. The total mass of mercury adsorbed on the catalyst, determined by solution counting, was 0.0206mg., corresponding to a mercury/rhodium ratio of ~1:60 (0.0168).

The poisoning effect on initial reaction rates is

TABLE 7.4

Summary of Mercury Count-rates & Percentage Adsorption  
on Rh-9.

Temperature of catalyst vessel =  $25 \pm 1^\circ\text{C}$ .

Temperature of mercury source =  $10 \pm 1^\circ\text{C}$ .

Wt. of catalyst = 12.6mg.

Total wt. of mercury adsorbed = 0.0206mg.

<u>Series</u>	<u>Count Rate</u> (c.p.m.)	<u>% Final Rate</u> ( $\theta_{\text{Hg}}$ )	<u>Atom ratio.</u> $\frac{\text{Hg/Rh}}{(\times 10^{-3})}$
A	0.0	0.0	0.0
D	$26.4 \pm 1.5$	13.3	2.2
F	$57.1 \pm 1.0$	28.8	4.8
H	$90.9 \pm 0.5$	45.8	7.7
J	$144.0 \pm 2.5$	72.5	12.2
L	$193.1 \pm 1.0$	97.4	16.4
(Final)	198.5	100.0	16.8

shown in table 7.8 and it is apparent that hydrogenation is affected to a much greater extent than is isomerisation. The only apparent exception to the trend to decreasing rates is the rate of hydrogenation for reaction 9H/2, but this is explained by the catalyst having been stored for three hours under 20mm. hydrogen at  $0^\circ\text{C}$  between the two reactions of that series. It is thus apparent that hydrogen may partially regenerate the activity of the poisoned catalyst. As no

TABLE 7.5

1-Butene Product Distribution on Poisoned Catalyst at 0°C.Initial  $p_{D_2} = p_{1-B} = 29.8 \pm 0.3$ mm.

% Butene Distribution

<u>Reaction</u>	$\theta_{Hg}$	<u>%n-B</u>	<u>1-B</u>	<u>t-2-B</u>	<u>c-2-B</u>	<u>T/C</u>	$t_{ex}$ (min.)
9A/4	0.0	11.2	64.9	12.3	22.8	0.54	4.0
9A/2	"	26.0	21.1	36.9	42.0	0.88	7.5
9A/1	"	52.1	2.2	76.6	21.2	3.61	13.5
9A/3	"	86.5	6.0	78.9	15.1	5.23	32.5
9D/2	13.3	12.0	67.3	13.6	19.1	0.71	4.2
9D/1	"	29.0	25.0	36.4	38.6	0.94	11.5
9F/2	28.8	10.8	64.0	14.7	21.3	0.69	11.8
9F/1	"	27.1	16.4	42.4	41.3	1.03	21.5
9H/2	45.8	11.8	64.1	15.3	20.6	0.74	11.3
9H/1	"	26.5	11.1	48.5	40.4	1.20	35.6
9J/2	72.5	10.8	58.5	18.3	23.2	0.79	27.0
9J/1	"	24.3	10.0	49.6	40.4	1.23	56.0
9K/1	97.4	7.2	41.5	28.5	30.0	0.95	296.0

desorption of the mercury occurs, however, it would appear the effect of the hydrogen is limited to overcoming self-poisoning by hydrocarbon residues. It is also noticeable that while the hydrogenation activity was increased by this treatment, the rate of isomerisation continued to decrease. The decrease in reaction rate with  $\theta_{Hg}$  is illustrated in

### 7.3.2 Deuterium Exchange Reactions of 1-Butene at 0°C.

The experimental procedure and conditions for these reactions have been described in sections 7.2 and 7.3.1.

The variation of deuterium content in the exchanged products with increasing conversion to n-butane was studied by series of reactions using a 1:1 :: 1-butene:deuterium mixture at each stage of the mercury adsorption. The deuterium distributions of the products of the unpoisoned reactions (series 9A) are shown in table 7.6; distributions from the succeeding series are shown in table 7.7. No analyses of the hydrogen content of the residual deuterium were available for series 9H, 9J, or 9K.

In series 9A the most significant feature of the deuterio-butane distribution is the proportion of the  $d_0$ - and  $d_1$ -species, indicating considerable addition of exchanged hydrogen. In none of the samples did the exchange products extend beyond the  $d_7$  species. Of the butenes, the cis and trans isomers have similar distributions; in both there is more exchange than in the parent 1-butene.

On the poisoned catalysts the same trends are apparent, but the deuterium content of the n-butane is significantly greater than in series 9A, as is the extent of the exchange in the butenes. Only in the sample of n-butane from

TABLE 7.6

Distribution of deuterio-butanes &amp; deuterio-butenes at 0°C. I Unpoisoned.

Initial  $p_{D_2} = p_{1-B} = 29.8 \pm 0.3$ mm.

<u>Reaction</u>	<u>d<sub>0</sub></u>	<u>d<sub>1</sub></u>	<u>d<sub>2</sub></u>	<u>d<sub>3</sub></u>	<u>d<sub>4</sub></u>	<u>d<sub>5</sub></u>	<u>d<sub>6</sub></u>	<u>d<sub>7</sub></u>	<u>d<sub>8</sub></u>	<u>D.N.</u>
<u>9A/4</u>	Conversion = 11.2% Final H.N. = 0.090									
1-B	95.0	4.3	0.6	0.1	0.02	0.0	0.0	0.0	0.0	0.058
t-2-B	91.4	4.7	2.8	1.0	0.01	0.0	0.0	0.0	0.0	0.134
c-2-B	92.9	5.9	0.9	0.3	0.07	0.0	0.0	0.0	0.0	0.088
<u>9A/2</u>	Conversion = 26.0% Final H.N. = 0.156									
t-2-B	89.4	9.4	0.9	0.3	0.01	0.0	0.0	0.0	0.0	0.123
c-2-B	88.2	10.1	1.4	0.2	0.05	0.0	0.0	0.0	0.0	0.138
<u>9A/1</u>	Conversion = 52.1% Final H.N. = 0.346									
n-B	30.0	29.3	27.6	6.3	4.2	1.2	0.4	0.1	0.0	1.289
c-2-B	78.2	17.1	3.6	0.7	0.3	0.04	0.0	0.0	0.0	0.281
<u>9A/3</u>	Conversion = 86.5% Final H.N. = 0.732									
n-B	23.1	27.2	34.1	10.7	4.3	0.7	0.0	0.0	0.0	1.478
t-2-B	63.3	25.2	8.3	2.1	0.9	0.2	0.0	0.0	0.0	0.528
c-2-B	65.8	26.0	7.1	0.9	0.3	0.0	0.0	0.0	0.0	0.437



TABLE 7.7

Distribution of deuterio-butanenes &amp; deuterio-butenes at 0°C. II Poisoned.

Initial  $p_{D_2} = p_{1-B} = 30.0 \pm 0.5$ mm.Series D :  $\theta_{Hg} = 13.3\%$ Series F :  $\theta_{Hg} = 28.8\%$ 

Reaction	$d_0$	$d_1$	$d_2$	$d_3$	$d_4$	$d_5$	$d_6$	$d_7$	$d_8$	D.N.
Final H.N. = 0.080										
<u>9D/2</u>	Conversion = 12.0%									
n-B	37.1	27.8	30.0	4.5	0.7	0.0	0.0	0.0	0.0	1.038
l-B	93.3	5.8	0.8	0.1	0.02	0.0	0.0	-	-	0.077
t-2-B	89.3	9.6	1.0	0.1	0.02	0.0	0.0	-	-	0.119
c-2-B	89.2	8.8	1.6	0.4	0.1	0.0	0.0	-	-	0.133
Final H.N. = 0.158										
<u>9D/1</u>	Conversion = 29.0%									
l-B	83.8	12.9	2.2	0.8	0.2	0.08	0.0	0.0	0.0	0.210
t-2-B	81.8	14.3	3.1	0.4	0.3	0.08	0.02	0.0	0.0	0.235
c-2-B	80.9	14.8	3.4	0.8	0.1	0.05	0.0	-	-	0.245
Final H.N. = 0.084										
<u>9F/2</u>	Conversion = 10.8%									
l-B	86.1	12.1	1.3	0.2	0.1	0.05	0.04	0.03	0.03	0.167
t-2-B	83.9	12.4	2.2	0.8	0.3	0.1	0.1	0.1	0.1	0.231
c-2-B	85.5	10.9	2.6	0.6	0.2	0.1	0.05	0.06	0.03	0.201
Final H.N. = 0.158										
<u>9F/1</u>	Conversion = 27.1%									
n-B	19.2	29.8	32.4	9.1	2.3	1.8	1.3	1.0	0.4	1.840
l-B	67.9	24.2	6.0	1.1	0.4	0.2	0.1	0.1	0.1	0.439
t-2-B	74.3	19.1	4.8	1.1	0.4	0.1	0.1	0.07	0.03	0.356
c-2-B	75.0	18.4	4.8	1.1	0.4	0.1	0.06	0.06	0.04	0.347

TABLE 7.7 (Cont'd.)

<u>Reaction</u>	Series J : $\theta_{\text{Hg}} = 72.5\%$										<u>D.N.</u>
	$\frac{d_0}{d_1}$	$\frac{d_1}{d_2}$	$\frac{d_2}{d_3}$	$\frac{d_3}{d_4}$	$\frac{d_4}{d_5}$	$\frac{d_5}{d_6}$	$\frac{d_6}{d_7}$	$\frac{d_7}{d_8}$			
<u>9J/2</u>	Conversion = 10.8%										
n-B	27.1	27.4	31.9	7.2	3.1	0.9	1.0	0.8	0.1	0.1	1.453
l-B	88.2	10.4	1.4	0.0	0.0	0.0	0.0	0.0	0.0	0.0	0.131
t-2-B	83.3	12.0	2.5	0.9	0.6	0.6	0.1	0.0	0.0	0.0	0.257
c-2-B	86.3	9.8	2.3	0.5	0.4	0.2	0.2	0.2	0.2	0.2	0.220
<u>9J/1</u>	Conversion = 24.3%										
n-B	24.2	26.5	34.2	8.9	3.6	1.3	0.8	0.3	0.2	0.2	1.514
l-B	66.4	22.5	8.5	1.9	0.7	0.1	0.0	0.0	0.0	0.0	0.483
t-2-B	75.2	19.8	3.8	1.0	0.2	0.0	0.0	0.0	0.0	0.0	0.312
c-2-B	78.0	15.7	4.1	1.2	0.4	0.3	0.1	0.1	0.1	0.07	0.327

reaction 9J/2, however, were traces ( $\sim 0.1\%$ ) of  $d_9$ - and  $d_{10}$ -deutero-butanes found. The deuterium content of the 1-butene rises with  $\theta_{\text{Hg}}$ , with the exception of the 9J/2 sample, which appears to be anomalous.

TABLE 7.8

Initial Reaction Rates of 1-Butene on Poisoned Catalyst at 0°C.

<u>Reaction</u>	$\theta_{\text{Hg}}$	$\%n\text{-B}$	$\underline{r}_h$ (mm.min. <sup>-1</sup> )	$\underline{r}_i$ (mm.min. <sup>-1</sup> )	$\underline{r}_e$ (x10 <sup>-3</sup> )
9A/4	0.0	11.2	1.00	3.26	14.5
9A/2	"	26.0	0.85	6.36	-
9A/1	"	52.1	0.77	-	-
9A/3	"	86.5	0.67	3.24	-
9D/2	13.3	12.0	0.60	3.65	18.3
9D/1	"	29.0	0.60	2.98	18.2
9F/2	28.8	10.8	0.30	2.60	13.2
9F/1	"	27.1	0.25	1.14	20.4
9H/2	45.8	11.8	0.21	1.97	-
9H/1	"	26.5	0.28	1.18	-
9J/2	72.5	10.8	0.13	1.31	4.9
9J/1	"	24.3	0.12	0.60	8.6
9K/1	97.4	7.2	0.009	0.09	-

The initial rate of exchange of the reactant 1-butene is shown in table 7.8 together with  $\theta_{\text{Hg}}$  and the rates of hydrogenation and isomerisation. The fall of the exchange rate with  $\theta_{\text{Hg}}$  for the 10% conversion reactions is shown in

Fig. 7.5.

### 7.3.3 The Hydrogen Exchange Reaction at 0°C.

The appearance of hydrogen in the residual deuterium is apparently unaffected by the adsorption of mercury. The fraction of exchanged hydrogen increased with increasing conversion at a slightly increasing rate; this trend was observed for all values of  $\theta_{\text{Hg}}$ .

### 7.4.1 Hydrogenation & Isomerisation Reactions at 21°C.

A 6.4mg. sample of catalyst was used to study the reactions at 21°C; the general procedure was the same as that described in section 7.3.1.

The hydrogenation reaction was followed almost to completion only on the unpoisoned catalyst, and it was found to exhibit overall first order kinetics. On the poisoned catalyst, however, the rate tended to increase during the first few minutes, and then remain very steady, suggesting a zero order reaction in the initial stages. A typical pressure vs. time plot is shown in Fig. 7.2.

The influence of the mercury on the relative rates of the hydrogenation and isomerisation reactions is shown in table 7.10, where it is clearly evident that isomerisation becomes more predominant at each stage of poisoning. At 93% monolayer poisoning, the butenes isomerised to equi-

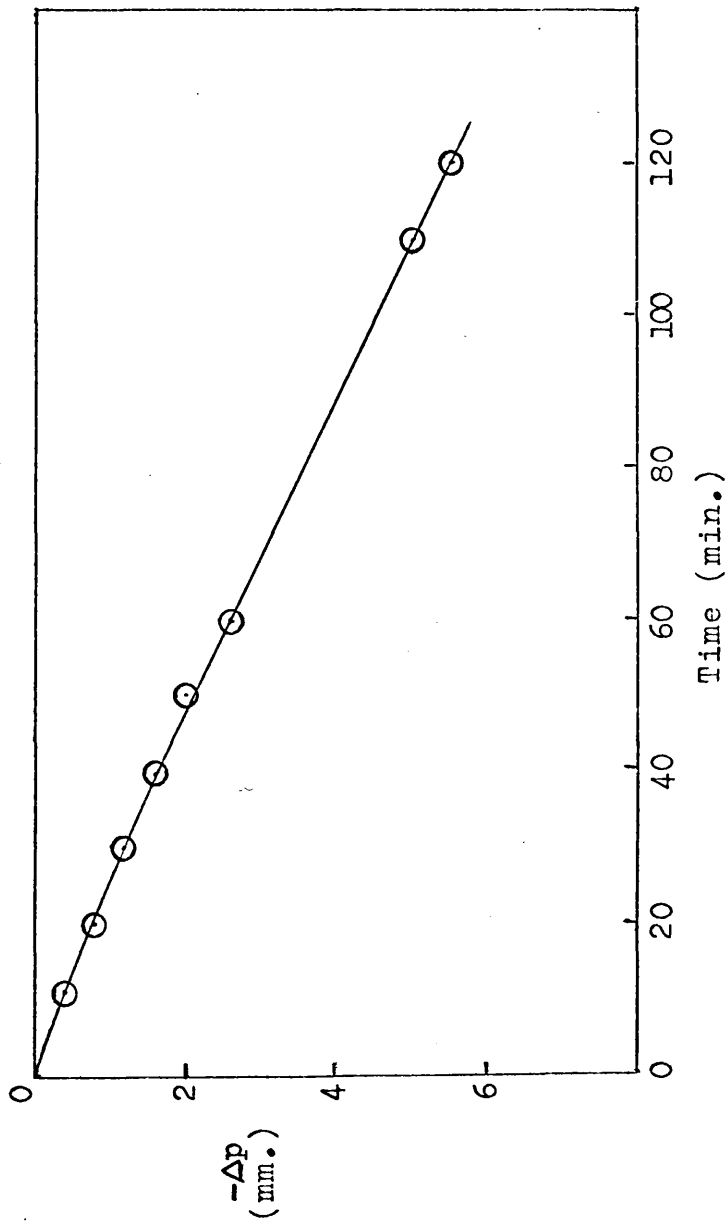


Fig. 7.2 Initial pressure fall against time curve for reaction of 30.0mm. 1-butene with 30.0mm. deuterium on mercury poisoned catalyst.  $\theta_{\text{Hg}} = 78.6\%$  Temperature = 21°C.

-librium proportions at only 6.5% conversion to n-butane.

The total mass of mercury adsorbed on the catalyst was 0.103mg., corresponding to a Hg/Rh atom ratio of  $\sim 1/6$  (.1647). The experimental conditions for the adsorption, together with the count-rate and coverage at each stage are shown in table 7.9

TABLE 7.9

Summary of Mercury Count-Rates & Percentage Adsorption  
on Rh-5.

Temperature of catalyst vessel =  $48 \pm 1^\circ\text{C}$ .

Temperature of mercury source =  $20 \pm 1^\circ\text{C}$ .

Wt. of catalyst = 6.4mg.

Total wt. of mercury adsorbed = 0.103mg.

<u>Series</u>	<u>Count Rate</u> (c.p.m.)	<u>% Final Rate</u> ( $\theta_{\text{Hg}}$ )	<u>Atom ratio.</u> <u>Hg/Rh</u> ( $\times 10^{-3}$ )
A	0.0	0.0	0.0
D	$86.1 \pm 2.0$	39.5	65.1
F	$171.2 \pm 2.0$	78.6	129.5
H	$202.8 \pm 3.0$	93.1	153.4
(Final)	217.7	100.0	164.7

The initial reaction rates corresponding to each value of  $\theta_{\text{Hg}}$  are shown in table 7.13. The fractional deactivation is of the same order as at  $0^\circ\text{C}$ , but it is noteworthy that the ratio of mercury to rhodium is greater by a factor of 10 at

21°C. Within each series, further deactivation is observed to occur with successive reactions. The initial rates of hydrogenation and isomerisation obtained from the 10% conversion reactions are plotted against  $\theta_{\text{Hg}}$  in Figs. 7.3 and 7.4 respectively.

TABLE 7.10

1-Butene Product Distributions on Poisoned Catalyst at 21°C.

Initial  $p_{\text{D}_2} = p_{1\text{-B}} = 30.0 \pm 0.8\text{mm.}$

% Butene Distribution

<u>Reaction</u>	<u><math>\theta_{\text{Hg}}</math></u>	<u>%n-B</u>	<u>1-B</u>	<u>t-2-B</u>	<u>c-2-B</u>	<u>T/C</u>	<u><math>t_{\text{ex}}</math></u> (min.)
5A/3	0.0	10.3	88.9	5.1	6.1	0.84	2.8
5A/1	"	26.5	68.1	15.5	16.4	0.95	4.9
5A/4	"	41.1	29.3	41.2	29.5	1.39	7.0
5A/2	"	57.9	15.6	56.1	28.3	1.98	10.3
5A/6	"	81.7	3.6	79.2	17.2	4.62	22.0
5D/2	39.5	10.0	60.9	19.8	19.3	1.03	9.0
5D/4	"	25.4	13.9	50.4	35.7	1.41	24.3
5D/1	"	41.1	2.5	72.3	25.2	2.87	24.0
5D/3	"	56.0	1.3	79.4	19.3	4.12	53.8
5F/1	78.6	11.1	7.9	58.6	33.5	1.75	50.0
5F/2	"	18.1	2.0	73.4	26.6	2.98	140.0
5H/1	93.1	3.8	12.8	54.4	32.7	1.66	284.0
5H/2	"	6.5	3.1	70.9	25.9	2.74	960.0

7.4.2 Deuterium Exchange Reactions of 1-Butene at 21°C.

The reaction conditions for these series have been described in section 7.4.1.

Mass spectra were obtained for each hydrocarbon during this run, but no measurements were made of the hydrogen content of the residual deuterium.

The variation of the deuterium distributions with conversion on an unpoisoned catalyst is shown in table 7.11. The n-butane samples all exhibit exchange to the  $d_{10}$  species and have a maximum at  $d_2$ . This maximum, however, decreases as the spectrum broadens with increasing conversion although the overall deuterium number continues to rise. It may be noted that all the butenes, except at low conversion, contain all species from  $d_0$  to  $d_8$ . It is interesting that the deuterium content of the 1-butene rises linearly with conversion, while that of the 2-butenes remains steady until 60% conversion.

The deuterio-product distributions on the poisoned catalyst are shown in table 7.12, and they exhibit a number of definite trends. The cis and trans 2-butenes continue to have similar distributions, but as  $\theta_{Hg}$  increases, their deuterium content is slightly diminished, and is considerably exceeded by that of the 1-butene. The n-butane appears to suffer little change; the apparent increase in the maximum at  $d_2$  in series 5H may not be significant.

The rate of 1-butene exchange and its dependence on the degree of poisoning are shown in table 7.13 and Fig.7.5.



TABLE 7.11

Distribution of deutero-butanes & deutero-butenes at 21°C. I Unpoisoned.

Initial  $P_{D_2} = P_{1-B} = 30.0 \pm 0.9\text{mm.}$

<u>Reaction</u>	$d_0$	$d_1$	$d_2$	$d_3$	$d_4$	$d_5$	$d_6$	$d_7$	$d_8$	$d_9$	$d_{10}$	<u>D.N.</u>
<u>5A/3</u>	Conversion = 10.3%											
n-B	22.5	27.7	34.6	9.5	3.3	1.2	0.6	0.3	0.2	0.08	0.02	1.527
1-B	91.5	6.6	1.4	0.3	0.1	0.05	0.02	0.0	0.0	-	-	0.112
t-2-B	61.5	23.9	9.6	3.0	1.3	0.4	0.2	0.1	0.06	-	-	0.612
c-2-B	54.6	36.9	5.3	1.9	0.7	0.2	0.1	0.07	0.04	-	-	0.589
<u>5A/1</u>	Conversion = 26.5%											
n-B	22.4	29.0	32.2	10.4	3.4	1.3	0.5	0.3	0.2	0.1	0.2	1.543
1-B	85.5	11.7	2.3	0.3	0.2	0.06	0.03	0.0	0.0	-	-	0.184
t-2-B	63.1	24.5	8.5	2.6	0.8	0.3	0.1	0.06	0.02	-	-	0.556
c-2-B	66.0	23.5	7.3	2.1	0.7	0.3	0.1	0.05	0.02	-	-	0.495
<u>5A/4</u>	Conversion = 41.1%											
n-B	17.4	30.3	29.9	12.5	5.2	2.4	0.9	0.5	0.4	0.4	0.2	1.780
1-B	75.7	18.0	4.4	1.1	0.4	0.2	0.1	0.08	0.03	-	-	0.338
t-2-B	56.6	28.0	10.3	3.3	1.1	0.4	0.2	0.1	0.06	-	-	0.669
c-2-B	59.3	27.5	9.2	2.7	0.8	0.3	0.1	0.08	0.05	-	-	0.603

TABLE 7.11 (Cont'd)

<u>Reaction</u>	<u>d<sub>0</sub></u>	<u>d<sub>1</sub></u>	<u>d<sub>2</sub></u>	<u>d<sub>3</sub></u>	<u>d<sub>4</sub></u>	<u>d<sub>5</sub></u>	<u>d<sub>6</sub></u>	<u>d<sub>7</sub></u>	<u>d<sub>8</sub></u>	<u>d<sub>9</sub></u>	<u>d<sub>10</sub></u>	<u>D.N.</u>
<u>5A/2</u>	Conversion = 57.9%											
n-B	19.2	28.1	30.4	13.3	5.3	2.0	0.8	0.4	0.2	0.2	0.1	1.718
l-B	70.9	20.4	6.1	1.7	0.5	0.2	0.06	0.04	0.02	-	-	0.417
t-2-B	65.1	20.5	9.5	3.1	1.1	0.5	0.2	0.1	0.04	-	-	0.575
c-2-B	53.5	29.9	10.9	3.78	1.2	0.5	0.2	0.07	0.02	-	-	0.718
<u>5A/6</u>	Conversion = 81.7%											
n-B	16.6	27.7	29.8	15.2	6.5	2.5	0.9	0.4	0.2	0.2	0.06	1.830
l-B	57.4	19.7	11.0	6.2	3.3	1.4	0.5	0.3	0.1	-	-	0.867
t-2-B	37.2	33.9	17.2	7.5	2.6	1.0	0.3	0.2	0.08	-	-	1.102
c-2-B	35.1	32.8	18.0	8.7	3.4	1.3	0.4	0.2	0.1	-	-	1.198

TABLE 7.12

Distribution of deutero-butanes &amp; deutero-butenes at 21°C. II Poisoned.

Initial  $P_{D_2} = P_{1-B} = 30.0 \pm 0.8\text{mm.}$ Series D :  $\theta_{Hg} = 39.5\%$ 

Reaction	$d_0$	$d_1$	$d_2$	$d_3$	$d_4$	$d_5$	$d_6$	$d_7$	$d_8$	$d_9$	$d_{10}$	D.N.
<u>5D/2</u> Conversion = 10.0%												
n-B	27.3	29.1	32.2	7.7	2.2	0.9	0.6	0.1	0.0	0.0	0.0	1.339
1-B	85.6	12.1	1.8	0.3	0.1	0.04	0.01	0.0	0.0	-	-	0.175
t-2-B	79.7	14.7	3.7	1.1	0.4	0.2	0.1	0.05	0.02	-	-	0.290
c-2-B	80.0	14.5	3.8	1.0	0.4	0.2	0.1	0.06	0.04	-	-	0.288
<u>5D/4</u> Conversion = 25.4%												
n-B	23.3	28.4	29.7	10.6	4.2	1.9	1.0	0.5	0.2	0.07	0.04	1.583
1-B	61.6	28.9	6.9	1.7	0.5	0.2	0.1	0.02	0.0	-	-	0.516
t-2-B	70.4	21.1	6.0	1.7	0.5	0.2	0.1	0.04	0.02	-	-	0.421
c-2-B	68.9	21.8	6.5	1.8	0.6	0.2	0.1	0.05	0.02	-	-	0.447
<u>5D/1</u> Conversion = 41.1%												
n-B	21.2	27.4	28.5	12.7	5.1	2.3	1.3	0.7	0.4	0.3	0.1	1.741
t-2-B	61.8	25.5	8.3	2.8	1.0	0.4	0.2	0.1	0.03	-	-	0.581
c-2-B	57.5	27.3	9.8	3.5	1.2	0.5	0.2	0.1	0.04	-	-	0.666
<u>5D/3</u> Conversion = 56.0%												
n-B	19.0	27.1	28.9	13.2	6.9	3.0	1.2	0.4	0.2	0.06	0.01	1.795
1-B	48.1	24.1	15.2	7.1	3.4	1.4	0.6	0.1	0.0	-	-	1.011
t-2-B	50.1	29.1	13.3	4.8	1.7	0.6	0.2	0.1	0.06	-	-	0.824
c-2-B	46.1	31.0	14.7	5.5	1.8	0.6	0.2	0.1	0.06	-	-	0.895

TABLE 7.12 (Cont'd).

Series F :  $\theta_{\text{Hg}} = 78.6\%$

Series H :  $\theta_{\text{Hg}} = 93.2\%$

Reaction	$d_0$	$d_1$	$d_2$	$d_3$	$d_4$	$d_5$	$d_6$	$d_7$	$d_8$	$d_9$	$d_{10}$	D.M.
<u>5F/1</u> Conversion = 11.1%												
n-B	26.0	27.4	34.4	7.8	2.8	1.0	0.4	0.1	0.03	0.0	0.0	1.396
l-B	63.2	26.6	7.3	1.8	0.7	0.2	0.1	0.06	0.0	-	-	0.516
t-2-B	84.1	11.9	2.9	0.7	0.2	0.1	0.04	0.01	0.01	-	-	0.216
c-2-B	81.8	13.5	3.4	0.9	0.3	0.1	0.05	0.03	0.02	-	-	0.253
<u>5F/2</u> Conversion = 18.1%												
n-B	22.1	27.6	32.6	10.8	4.3	1.5	0.7	0.2	0.06	0.03	0.02	1.566
l-B	58.5	24.1	10.6	3.8	1.6	0.6	0.6	0.2	0.07	-	-	0.711
t-2-B	73.5	19.3	5.2	1.4	0.4	0.2	0.07	0.03	0.01	-	-	0.370
c-2-B	69.0	21.4	6.6	1.9	0.6	0.2	0.1	0.04	0.02	-	-	0.452
<u>5H/1</u> Conversion = 3.8%												
n-B	17.8	18.2	47.2	7.4	4.3	2.1	0.8	0.5	0.5	0.6	0.6	1.859
l-B	83.0	13.2	2.7	0.6	0.2	0.1	0.8	0.06	0.02	-	-	0.230
t-2-B	90.3	7.6	1.5	0.4	0.2	0.06	0.04	0.02	0.01	-	-	0.130
c-2-B	88.9	8.4	1.8	0.5	0.2	0.1	0.04	0.03	0.02	-	-	0.152
<u>5H/2</u> Conversion = 6.5%												
n-B	16.8	19.1	45.5	9.8	4.2	1.7	0.6	0.5	0.6	0.7	0.6	1.887
l-B	69.4	20.7	6.8	2.1	0.9	0.2	0.04	0.0	0.0	-	-	0.450
t-2-B	82.0	12.4	3.9	1.0	0.4	0.2	0.1	0.06	0.03	-	-	0.267
c-2-B	79.2	14.3	4.4	1.2	0.5	0.2	0.1	0.07	0.04	-	-	0.309

TABLE 7.13

Initial Reaction Rates of 1-Butene on Poisoned Catalyst at 21°C.

<u>Reaction</u>	$\theta_{\text{Hg}}$	$\%n\text{-B}$	$\bar{r}_h$ (mm.min. <sup>-1</sup> )	$\bar{r}_i$ (mm.min. <sup>-1</sup> )	$\bar{r}_e$ (x10 <sup>-3</sup> )
5A/3	0.0	10.3	1.15	1.25	39.5
5A/1	"	26.5	1.30	2.42	37.4
5A/4	"	41.1	1.40	-	48.0
5A/2	"	57.9	1.40	-	40.7
5A/6	"	81.7	1.34	-	39.4
5D/2	39.5	10.0	0.36	1.65	19.5
5D/4	"	25.4	0.30	2.61	21.3
5D/1	"	41.1	0.70	-	-
5D/3	"	56.0	0.33	-	18.9
5F/1	78.6	11.1	0.065	1.68	10.3
5F/2	"	18.1	0.041	-	5.1
5H/1	93.1	3.8	0.004	0.23	0.8
5H/2	"	6.5	0.003	0.17	0.5

#### 7.5.1 Hydrogenation & Isomerisation Reactions at 69°C.

The reactions were studied at 69°C on a 2.0mg. sample of catalyst (Rh-8); the general procedure has been described in section 7.3.1.

The characteristics of the pressure fall against time curves on the unpoisoned catalyst were the same as obtained at 0° and 21°C, namely first order overall. At each stage

of poisoning, the pressure fall varied linearly with time, and there was virtually no induction period. The pressure fall against time plots were comparable to that shown in Fig. 7.2.

TABLE 7.14

Summary of Mercury Count-Rates & Percentage Adsorption  
on Rh-8.

Temperature of catalyst vessel =  $83 \pm 2^{\circ}\text{C}$ .

Temperature of mercury source =  $22 \pm 1^{\circ}\text{C}$ .

Wt. of catalyst = 2.0mg.

Total wt. of mercury adsorbed = 0.027mg.

<u>Series</u>	<u>Count Rate</u> (c.p.m.)	<u>% Final Rate</u> ( $\theta_{\text{Hg}}$ )	<u>Atom ratio</u> <u>Hg/Rh</u> ( $\times 10^{-3}$ )
A	0.0	0.0	0.0
D	$31.1 \pm 0.5$	23.2	32.4
F	$59.5 \pm 0.5$	44.0	62.1
H	$90.4 \pm 4.0$	67.5	94.4
J	$108.7 \pm 1.0$	81.0	113.2
L	$125.8 \pm 1.5$	93.7	131.0
(Final)	134.0	100.0	139.8

The analysis results in table 7.15 show the product distributions for each series on Rh-8; isomerisation is again shown to predominate as  $\theta_{\text{Hg}}$  increases. The total

weight of mercury adsorbed on the catalyst was 0.0272mg., corresponding to a Hg/Rh atom ratio of  $\sim 1/7$  (0.1398). Details of the adsorption conditions and count-rates for each level of poisoning are summarised in table 7.14.

The initial reaction rates in each series are shown in table 7.18, and their variation with  $\theta_{\text{Hg}}$  is shown graphically in Figs. 7.3 and 7.4. The deactivation of the isomerisation reaction is very slight at this temperature, and thus the whole increase in the isomerisation/hydrogenation ratio is caused by poisoning of the hydrogenation reaction alone.

#### 7.5.2 Deuterium Exchange Reactions at 69°C.

The general procedure and experimental conditions for these reactions have been outlined in section 7.5.1. The deuterium distribution in each of the products of reactions on unpoisoned catalysts is shown in table 7.16; the variation of the distributions with  $\theta_{\text{Hg}}$  is shown in table 7.17. The deuterium content of the n-butane is unknown as none of the samples was obtained in sufficient yield for a spectrum to be determined.

Exchange of the butenes beyond  $d_4$  is seen to be unusual at this temperature. In series A, the 2-butenes have undergone much greater exchange at low conversion than has the 1-butene, but as  $\theta_{\text{Hg}}$  is increased, 1-butene exchange

appears to become predominant. The rates of 1-butene exchange and the corresponding values of  $\theta_{Hg}$  are shown in table 7.18 and Fig. 7.5.

TABLE 7.15

1-Butene Product Distribution on Poisoned Catalyst at 69°C.

Initial  $p_{D_2} = p_{1-B} = 30.0 \pm 0.5$ mm.

% Butene Distribution

<u>Reaction</u>	$\theta_{Hg}$	<u>%n-B</u>	<u>1-B</u>	<u>t-2-B</u>	<u>c-2-B</u>	<u>T/C</u>	<u>t<sub>ex</sub></u> (min.)
8A/4	0.0	5.8	86.0	6.2	7.8	0.80	1.3
8A/3	"	11.0	67.1	15.8	17.1	0.92	2.5
8A/1	"	28.4	32.7	37.1	30.2	1.23	5.3
8A/2	"	51.3	8.6	65.7	25.7	2.56	12.0
8D/3	23.2	6.5	64.7	16.7	18.6	0.90	4.0
8D/1	"	14.4	37.2	32.4	30.4	1.07	7.3
8D/2	"	28.7	10.0	55.6	34.4	1.62	15.3
8F/3	44.4	5.8	51.3	24.5	24.2	1.01	6.0
8F/1	"	11.1	22.9	48.6	28.5	1.71	8.0
8F/2	"	25.0	4.1	65.0	30.9	2.11	24.5
8H/2	67.5	5.7	29.0	40.0	31.0	1.29	10.5
8H/1	"	12.2	12.9	54.3	32.8	1.65	14.0
8J/2	81.0	5.8	18.6	46.4	35.1	1.32	16.0
8J/1	"	10.8	5.9	61.4	32.7	1.87	24.0
8L/1	93.7	5.3	12.4	54.0	33.6	2.80	26.0



TABLE 7.16

Distribution of deuterio-butanes & deuterio-butenes at 69°C. I Unpoisoned.

Initial  $P_{D_2} = P_{1-B} = 30.0 \pm 0.8\text{mm.}$

<u>Reaction</u>	<u>d<sub>0</sub></u>	<u>d<sub>1</sub></u>	<u>d<sub>2</sub></u>	<u>d<sub>3</sub></u>	<u>d<sub>4</sub></u>	<u>d<sub>5</sub></u>	<u>d<sub>6</sub></u>	<u>d<sub>7</sub></u>	<u>d<sub>8</sub></u>	<u>D.N.</u>
Final H.N. = 0.144										
<u>8A/4</u>	Conversion = 5.8%									
t-2-B	91.7	6.9	1.2	0.2	0.02	0.0	0.0	0.0	0.0	0.099
c-2-B	87.6	10.7	1.4	0.2	0.02	0.0	0.0	0.0	0.0	0.143
Final H.N. = 0.226										
<u>8A/3</u>	Conversion = 11.0									
1-B	96.5	2.9	0.4	0.1	0.02	0.0	0.0	0.0	0.0	0.041
t-2-B	87.5	10.2	1.9	0.3	0.06	0.02	0.0	0.0	0.0	0.152
c-2-B	84.3	12.9	2.3	0.4	0.1	0.02	0.0	0.0	0.0	0.193
Final H.N. = 0.446										
<u>8A/1</u>	Conversion = 28.4									
t-2-B	60.2	27.0	8.9	3.0	0.8	0.1	0.0	0.0	0.0	0.573
c-2-B	79.4	15.8	4.0	0.7	0.1	0.02	0.0	0.0	0.0	0.264
Final H.N. = 0.818										
<u>8A/2</u>	Conversion = 51.3									
1-B	69.8	20.7	6.4	2.3	0.4	0.3	0.06	0.0	0.0	0.438
t-2-B	67.9	23.1	6.8	1.6	0.4	0.1	0.02	0.02	0.01	0.440
c-2-B	69.6	22.5	6.2	1.3	0.4	0.08	0.02	0.0	0.0	0.407

TABLE 7.17

Distribution of deutero-butanes &amp; deutero-butenes at 69°C. II Poisoned.

Initial  $p_{D_2} = p_{1-B} = 30.0 \pm 0.5$  mm.Series D :  $\theta_{Hg} = 23.2\%$   
Series F :  $\theta_{Hg} = 44.4\%$ 

Reaction	$d_0$	$d_1$	$d_2$	$d_3$	$d_4$	$d_5$	$d_6$	$d_7$	$d_8$	D.N.
<u>8D/3</u>	Conversion = 6.5%      Final H.N. = 0.184									
1-B	92.1	7.3	0.5	0.02	0.01	0.0	0.0	0.0	0.0	0.085
t-2-B	90.4	8.0	1.4	0.08	0.06	0.01	0.0	0.0	0.0	0.113
c-2-B	89.2	9.0	1.5	0.2	0.1	0.01	0.0	0.0	0.0	0.129
<u>8D/1</u>	Conversion = 14.4%      Final H.N. = 0.316									
1-B	86.8	11.3	1.6	0.2	0.03	0.01	0.0	0.0	0.0	0.155
t-2-B	81.7	14.9	2.7	0.6	0.02	0.01	0.0	0.0	0.0	0.223
c-2-B	82.8	14.2	2.4	0.5	0.1	0.03	0.0	0.0	0.0	0.210
<u>8D/2</u>	Conversion = 28.7%      Final H.N. = 0.632									
1-B	74.4	19.7	4.2	0.8	0.8	0.07	0.01	0.0	0.0	0.341
t-2-B	71.7	21.0	5.3	1.4	0.6	0.06	0.01	0.0	0.0	0.383
c-2-B	75.8	19.6	3.4	0.8	0.4	0.1	0.02	0.0	0.0	0.309
<u>8F/3</u>	Conversion = 5.8%      Final H.N. = 0.182									
1-B	90.2	8.0	1.4	0.2	0.1	0.03	0.01	0.0	0.0	0.121
t-2-B	86.3	10.9	2.6	0.2	0.02	0.0	0.0	0.0	0.0	0.167
c-2-B	87.5	10.0	2.1	0.3	0.1	0.02	0.0	0.0	0.0	0.158

TABLE 7.17 (Cont'd.)

Reaction	$d_0$	$d_1$	$d_2$	$d_3$	$d_4$	$d_5$	$d_6$	$d_7$	$d_8$	D.N.
	Series H : $\theta_{Hg} = 67.5\%$ " J : $\theta_{Hg} = 81.0\%$ " L : $\theta_{Hg} = 93.7\%$									
<u>8F/1</u>	Final H.N. = 0.386									
1-B	80.9	15.8	2.7	0.4	0.2	0.0	0.0	0.0	0.0	0.231
t-2-B	78.8	17.8	2.8	0.9	0.4	0.1	0.1	0.0	0.0	0.281
c-2-B	82.9	12.7	3.1	0.8	0.3	0.08	0.09	0.0	0.0	0.234
<u>8F/2</u>	Final H.N. = 0.674									
t-2-B	67.0	22.7	6.8	2.1	0.7	0.4	0.1	0.1	0.05	0.497
c-2-B	65.0	23.7	8.2	2.0	0.8	0.1	0.1	0.0	0.0	0.509
<u>8H/2</u>	Final H.N. = 0.204									
1-B	87.5	10.7	1.6	0.1	0.06	0.0	0.0	0.0	0.0	0.145
t-2-B	85.1	10.3	2.6	0.9	0.7	0.2	0.1	0.0	0.0	0.227
c-2-B	88.0	10.0	1.8	0.2	0.04	0.0	0.0	0.0	0.0	0.144
<u>8H/1</u>	Final H.N. = 0.338									
1-B	78.8	17.4	3.7	0.1	0.07	0.0	0.0	0.0	0.0	0.254
t-2-B	82.2	13.4	2.2	1.8	0.4	0.0	0.0	0.0	0.0	0.247
c-2-B	83.8	12.7	2.7	0.7	0.05	0.0	0.0	0.0	0.0	0.205

TABLE 7.17 (Cont'd.)

<u>Reaction</u>	<u>d<sub>0</sub></u>	<u>d<sub>1</sub></u>	<u>d<sub>2</sub></u>	<u>d<sub>3</sub></u>	<u>d<sub>4</sub></u>	<u>d<sub>5</sub></u>	<u>d<sub>6</sub></u>	<u>d<sub>7</sub></u>	<u>d<sub>8</sub></u>	<u>D.N.</u>
		Series J : $\theta_{Hg} = 81.0\%$ " L : $\theta_{Hg} = 93.7\%$								
<u>8J/2</u>	Final H.N. = 0.216									
1-B	88.5	5.9	5.8	0.0	0.0	0.0	0.0	0.0	0.0	0.168
t-2-B	90.7	7.3	1.8	0.2	0.03	0.0	0.0	0.0	0.0	0.115
<u>8J/1</u>	Final H.N. = 0.216									
c-2-B	90.4	8.4	1.0	0.2	0.0	0.0	0.0	0.0	0.0	0.110
<u>8L/1</u>	Final H.N. = 0.088									
1-B	84.3	12.6	2.39	0.44	0.20	0.0	0.0	0.0	0.0	0.195
t-2-B	88.2	9.75	1.58	0.24	0.18	0.02	0.0	0.0	0.0	0.144
c-2-B	90.5	7.9	1.4	0.2	0.04	0.0	0.0	0.0	0.0	0.113

TABLE 7.18

Initial Rates of 1-Butene Reactions at 69°C.

<u>Reaction</u>	$\theta_{\text{Hg}}$	$\%n\text{-B}$	$\underline{r}_h$ (mm.min. <sup>-1</sup> )	$\underline{r}_i$ (mm.min. <sup>-1</sup> )	$\underline{r}_e$ (x10 <sup>-3</sup> )
8A/4	0.0	5.8	1.33	3.37	-
8A/3	"	11.0	1.40	4.95	16.4
8A/1	"	28.4	1.40	6.71	-
8A/2	"	51.3	1.40	-	36.5
8D/3	23.2	6.5	0.45	3.18	21.2
8D/1	"	14.4	0.50	4.17	21.2
8D/2	"	28.7	0.50	5.46	22.3
8F/3	44.0	5.8	0.32	3.4	20.2
8F/1	"	11.1	0.50	6.0	28.9
8F/2	"	25.0	0.32	-	-
8H/2	67.5	5.7	0.17	3.7	13.8
8H/1	"	12.2	0.25	5.04	18.1
8J/2	81.0	5.8	0.12	3.46	10.5
8J/1	"	10.8	0.18	5.44	-
8L/1	93.7	5.3	0.07	2.80	7.5

7.5.3 The Hydrogen Exchange Reaction at 69°C.

The extent of hydrogen exchange at 69°C is directly proportional to the conversion on both poisoned and unpoisoned catalyst surfaces. As the mercury coverage was increased, the extent of the exchange increased relative to the con-

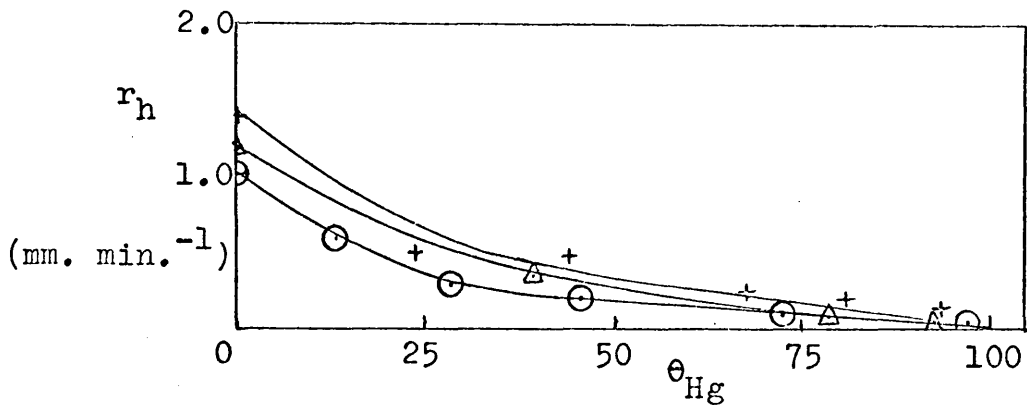


Fig. 7.3 Poisoning of catalyst for l-butene hydrogenation

( $\odot$  -  $0^\circ\text{C}$      $\Delta$  -  $21^\circ\text{C}$     + -  $69^\circ\text{C}$ )

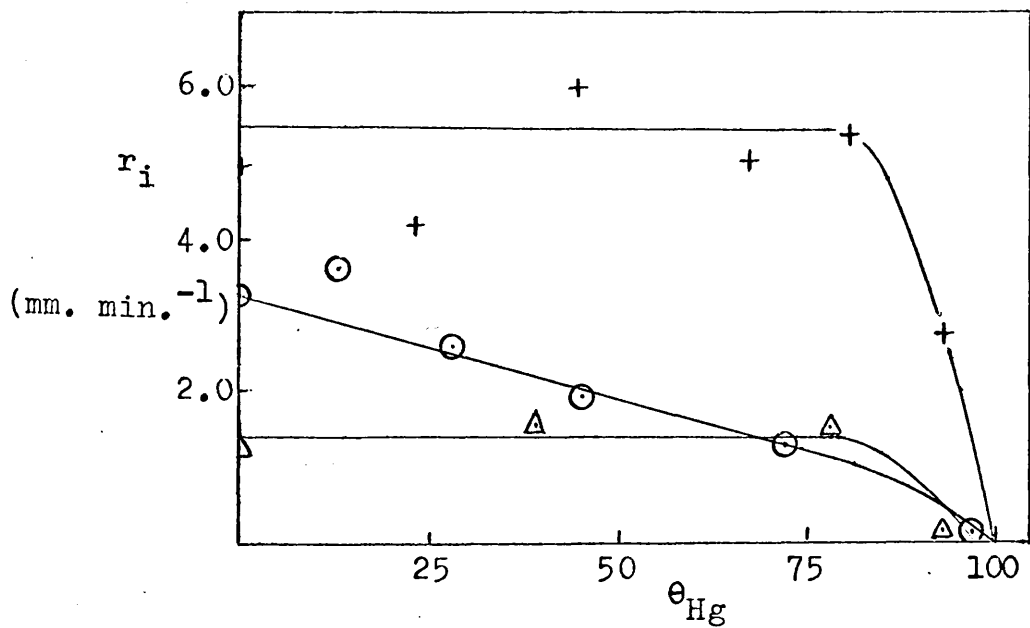


Fig. 7.4 Poisoning of catalyst for l-butene isomerisation

(Symbols as in Fig. 7.3)

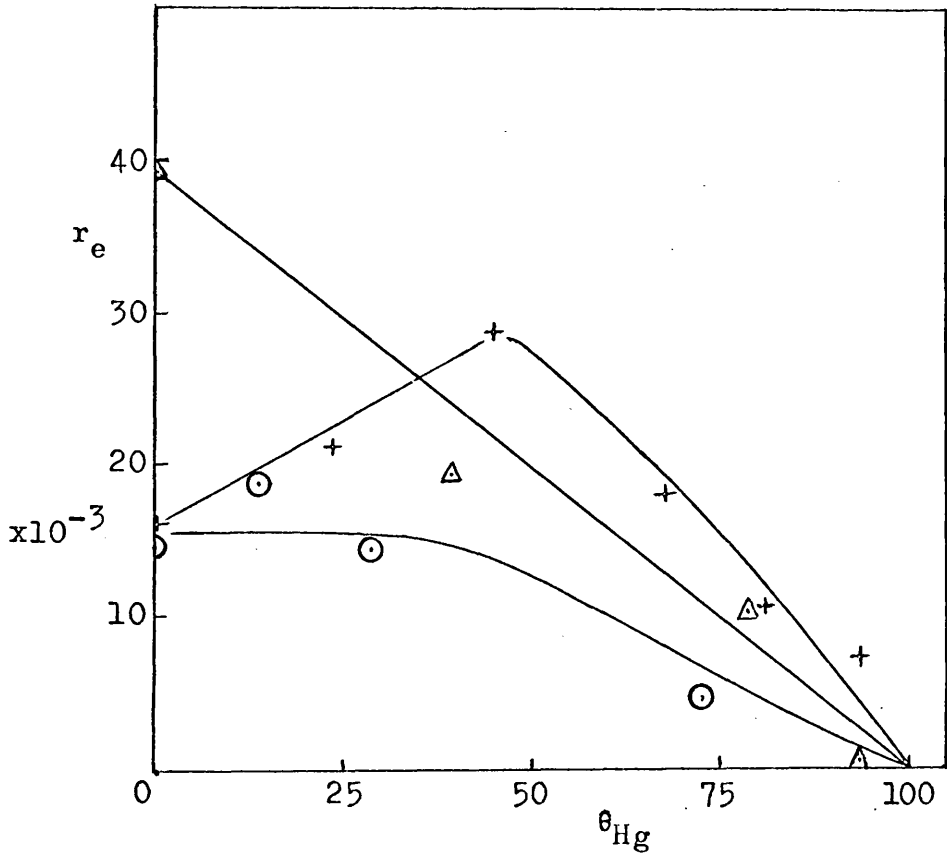


Fig. 7.5 Poisoning of catalyst for 1-butene exchange.

○ - 0°C    Δ - 21°C    + - 69°C

-version, until  $\sim 50\%$  monolayer coverage. Further adsorption of mercury produced no further change in the exchange/hydrogenation ratio.

#### 7.6 The Mass Balance.

The absolute amounts of deuterium and hydrogen in the reaction products were calculated from the partial pressure and hydrogen and deuterium numbers of each product. The final totals, in units of mm.atoms, were compared with the initial amounts of each in order to obtain the balance of hydrogen and deuterium over the reaction. The calculation and result for reaction 9D/2 is shown below, and it is apparent that the balance is fairly satisfactory. There is small deuterium deficiency in the products, but this may be within experimental error.



MASS BALANCE - REACTION 9D/2.

	<u>Partial Pressure</u> (mm.)	<u>D.N.</u>	<u>H.N.</u>	<u>Total D</u> (mm. atoms)	<u>Total H</u> (mm. atoms)
<u>Initial:</u>					
D <sub>2</sub>	29.9	1.994	0.006	59.6	0.18
l-B	29.9	0.00	8.00	0.00	239.20
				<hr/>	<hr/>
Total				59.62	239.38
				<hr/>	<hr/>

Final:

n-B	3.59	1.038	8.962	3.72	32.13
l-B	17.71	0.077	7.923	1.36	140.29
t-2-B	3.58	0.119	7.881	0.43	28.18
c-2-B	5.03	0.133	7.867	0.67	39.58
H/D	26.31	1.920	0.080	50.53	2.11
				<hr/>	<hr/>
				57.70	242.29
				<hr/>	<hr/>

Summary:

	<u>Initial</u>	<u>Final</u>
Hydrogen	239.38	242.29
Deuterium	59.62	57.70
	<hr/>	<hr/>
Total	299.00	299.99
	<hr/>	<hr/>

CHAPTER 8THE POISONING OF THE REACTION OF 1,3-BUTADIENE WITH DEUTERIUM  
ON Rh/SiO<sub>2</sub>.8.1 Introduction.

The interaction between 1,3-butadiene and deuterium over Rh/SiO<sub>2</sub> catalysts was studied in series of reactions at 25°, 48°, and 83°C using three samples of catalyst of different weights. Each of these series on the unpoisoned catalysts was followed by alternate adsorption of mercury and further series of reactions under the same conditions of temperature and initial reactant pressure. This enabled the effects of the mercury on the reactions to be observed at coverages between zero and almost 100% monolayer at each of the above temperatures. As deuterium was used for all the reactions with 1,3-butadiene, the term "deuteration" will be taken to imply the addition reaction.

Each reaction was carried out using initial pressures of deuterium and 1,3-butadiene of 60.0mm. and 30.0mm. respectively. In order to ensure that each reaction was taking place on a surface on which only deuterium (and possibly hydrocarbon residue) was initially present, the catalyst was allowed to stand under 30mm. deuterium for up to five minutes after each reaction to allow any exchangeable hydrogen on the surface to equilibrate with

the deuterium.

In each reaction series, the products of each reaction were extracted for analysis at varying conversions, thus enabling the variation with conversion of the butene distributions and the selectivity to be observed. The conversion may be defined as the number of moles of hydrogen taken up per mole of 1,3-butadiene, expressed as a percentage. Thus, for complete reaction, the conversion is 200%. In the subsequent tables of product distributions, each of the butenes will be shown as a percentage of the total butene yield, together with the trans/cis ratio, the selectivity, and the conversion.

All the reaction products were separated and collected for mass spectrometric analysis, but owing to the small yields of n-butane from most reactions, it was generally impossible to obtain mass spectra for these samples, and hence any variations in the deuterobutane distributions could not be systematically studied. In certain reactions, the yields of some of the butenes were also too low to provide a measurable spectrum.

## 8.2 Reactions of 1,3-Butadiene at 25°C.

### 8.2.1 The Deuteration Reaction.

The reactions were studied at 25°C on a 12.6mg. sample of catalyst (Rh-9). The full course of a reaction

was followed only on the unpoisoned catalyst, and the pressure fall against time curve showed a gradual decrease in the rate. There is a noticeable acceleration in the rate of pressure fall at a point corresponding to the uptake of 1.2 moles of hydrogen per mole of 1,3-butadiene. A typical pressure fall vs. time plot and the corresponding first order plot are shown in Fig. 8.1. On a partially poisoned catalyst, the pressure fall vs. time curves showed similar characteristics to those with the unpoisoned catalyst for reactions taken to  $\sim 50\%$  conversion.

The experimental conditions for the adsorption of the mercury are given in table 8.1, together with the extent of adsorption and decay corrected count-rate at each stage, and the corresponding rates of deuteration ( $r_d$ ). The total weight of mercury adsorbed was 0.021mg. or 0.0168mg. Hg per mg. Rh, corresponding to a mercury/rhodium atom ratio of  $\sim 1/60$ .

Table 8.2 shows the product distributions and olefin selectivities with increasing conversion. The selectivity factors decrease slightly with increasing conversion, but they are apparently unaffected by the adsorption of mercury. The butene distributions show that within each series there is a gradual increase in the proportion of 2-butenes, with increasing conversion, while the trans/cis

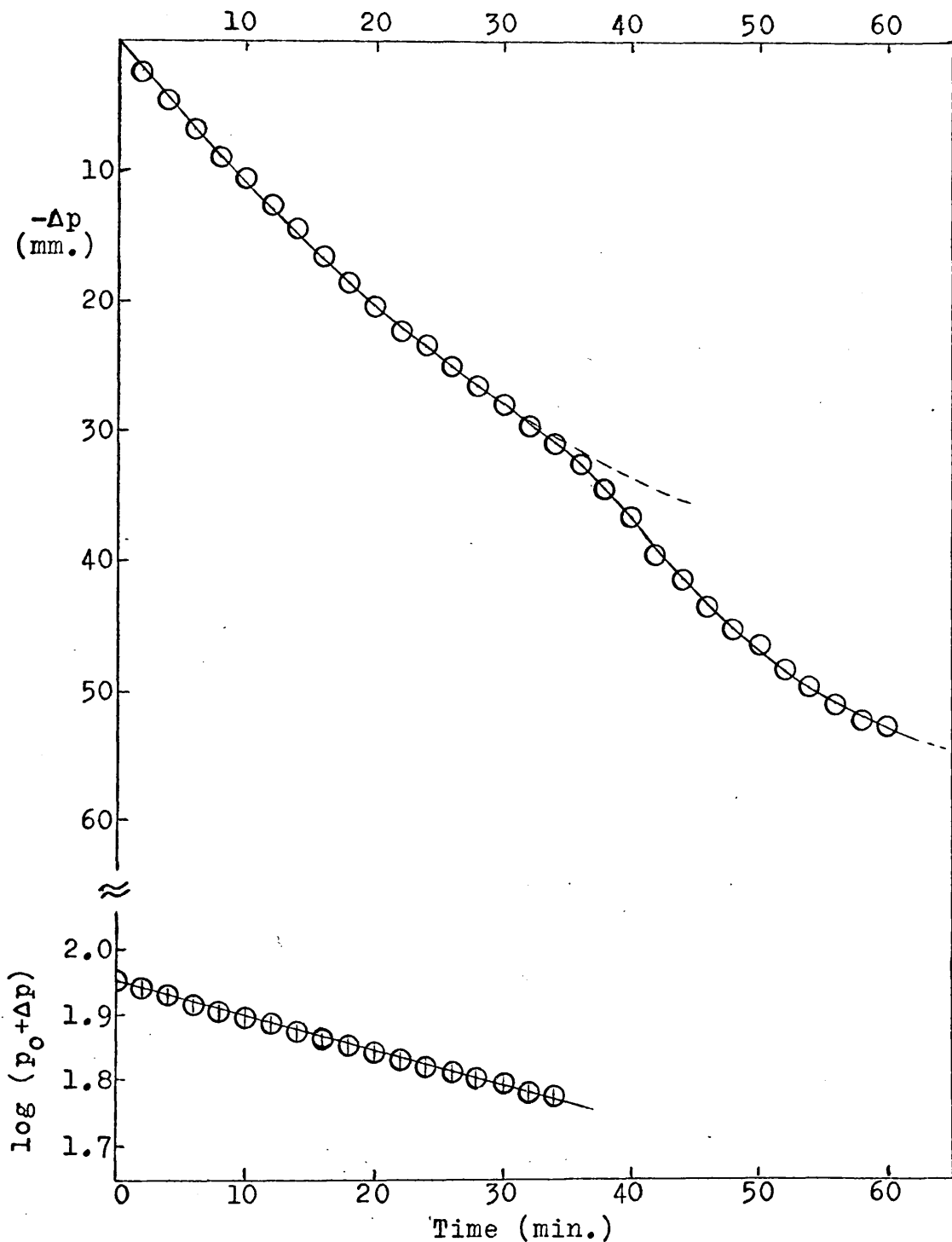


Fig. 8.1 Pressure fall against time curve for reaction of 60.0mm. 1,3-butadiene with 30.0mm. deuterium on Rh/SiO<sub>2</sub> at 25°C. First order plot is shown below.

ratio remains approximately constant. As  $\theta_{\text{Hg}}$  increases, however, the trans/cis ratio falls markedly, while the ratio of 1-butene : 2-butenes remains unchanged. The distribution of reaction products on the unpoisoned catalyst is shown in Fig. 8.2, and the decline in the rate of deuteration at each stage of poisoning in Fig. 8.3.

TABLE 8.1

Summary of Mercury Adsorption & Rates of Deuteration on Rh-9.

Temperature of mercury source =  $10 \pm 1^{\circ}\text{C}$

Temperature of catalyst vessel =  $25 \pm 1^{\circ}\text{C}$

<u>Series</u>	<u>Count-Rate</u> (c.p.m.)	$\theta_{\text{Hg}}$ (%)	Atom ratio <u>Hg/Rh</u> ( $\times 10^{-3}$ )	$\bar{r}_d$ (mm.min. <sup>-1</sup> )
B	0.0	0.0	0.0	1.50
C	$26.4 \pm 1.5$	13.3	2.2	1.00
E	$57.1 \pm 1.0$	28.8	4.8	0.70
G	$90.9 \pm 0.5$	45.8	7.7	0.55
I	$150.7 \pm 2.5$	76.0	12.8	0.30
K	$193.1 \pm 1.0$	97.4	16.4	0.03
(Final)	198.5	100.0	16.8	

TABLE 8.2

1,3-Butadiene Product Distributions at 25°C.Initial  $p_{D_2} = 60.0 \pm 0.8\text{mm.}$ Initial  $p_{1,3-B} = 30.0 \pm 0.6\text{mm.}$ 

<u>Reaction</u>	$\theta_{\text{Hg}}$	<u>Conv.</u> %	% Butene Distribution			<u>T/C</u>	<u>Sel.</u>
			<u>1-B</u>	<u>t-2-B</u>	<u>c-2-B</u>		
9B/4	0.0	12.6	55.3	32.4	12.3	2.64	0.962
9B/2	"	21.4	51.5	34.1	14.4	2.37	0.955
9B/1	"	49.1	50.6	36.4	13.0	2.80	0.945
9B/5	"	64.3	50.4	33.2	16.3	2.03	0.914
9B/3	"	91.0	46.5	38.5	15.0	2.57	0.882
9C/3	13.3	11.3	56.8	30.2	13.0	2.32	0.989
9C/1	"	23.2	54.9	30.9	14.2	2.17	0.972
9C/2	"	48.3	50.7	33.0	16.3	2.02	0.932
9E/3	28.8	11.7	59.2	28.3	12.5	2.27	0.986
9E/1	"	22.6	54.0	31.5	14.5	2.17	0.972
9E/2	"	47.2	52.0	31.9	16.1	1.99	0.936
9G/3	45.8	11.3	58.4	28.0	13.6	2.05	0.976
9G/1	"	20.6	55.4	30.5	14.1	2.16	0.984
9G/2	"	47.1	52.7	31.7	15.6	2.04	0.948
9I/3	76.0	13.4	56.9	27.4	15.7	1.74	0.962
9I/1	"	21.4	55.1	28.8	16.1	1.79	0.960
9I/2	"	49.2	52.2	30.2	17.6	1.71	0.945
9K/1	97.4	12.6	55.4	23.5	21.1	1.11	0.975

### 8.2.2 The Exchange Reactions.

The distribution of deutero-butanenes and deutero-butenes in the products of the reactions on the unpoisoned catalyst are shown in table 8.3; the results for the series on the poisoned catalyst are shown in table 8.4. Mass spectra were not obtained for the hydrocarbon products of series 9G and 9K. The deuterium content of each of the butenes rises slightly with increasing conversion in series 9B, while on the poisoned catalyst the content is higher than on the unpoisoned, but does not increase greatly with the conversion. The exchange of the 1,3-butadiene increases with conversion on the unpoisoned catalyst (Fig. 8.5); the effect of mercury is generally to increase the deuterium content, but its dependence upon conversion appears to vary irregularly from one series to another. The rate of exchange of the 1,3-butadiene at each value of  $\theta_{\text{Hg}}$  is shown in Fig. 8.4. The n-butane from reaction 9B/5 was exchanged as far as the  $d_8$  species, but no systematic study of the deutero-butanenes is possible for the reasons given above.

### 8.2.3 The Hydrogen Exchange Reaction.

The hydrogen content of the residual deuterium was found to rise linearly with conversion, and to be virtually unaffected by the adsorption of mercury.



TABLE 8.3

Distribution of 1,3-Butadiene Deuterated Products at 25°C. I Unpoisoned.

Initial  $p_{D_2} = 60.0 \pm 0.6\text{mm.}$

Initial  $p_{1,3-B} = 30.0 \pm 0.6\text{mm.}$

Reaction	$d_0$	$d_1$	$d_2$	$d_3$	$d_4$	$d_5$	$d_6$	$d_7$	$d_8$	<u>D.N.</u>
<u>9B/4</u>	Conversion = 12.7%									
	Final H.N. = 0.052									
t-2-B	12.0	30.0	47.8	8.1	1.4	0.5	0.1	0.0	0.0	1.589
c-2-B	16.2	31.5	41.8	7.5	2.3	0.5	0.2	0.0	0.0	1.502
1,3-B	99.6	0.2	0.1	0.03	0.04	0.0	0.0	-	-	0.007
<u>9B/2</u>	Conversion = 21.4%									
	Final H.N. = 0.054									
1-B	15.7	26.3	46.1	9.3	2.1	0.4	0.0	0.0	0.0	1.569
t-2-B	20.8	30.7	40.5	6.6	0.4	0.7	0.1	0.06	0.0	1.383
1,3-B	99.3	0.3	0.2	0.07	0.08	0.03	0.0	-	-	0.014
<u>9B/1</u>	Conversion = 49.1%									
	Final H.N. = 0.076									
c-2-B	18.1	30.7	42.3	7.2	1.5	0.3	0.03	0.0	0.0	1.442
1,3-B	96.7	2.5	0.6	0.1	0.1	0.0	0.0	-	-	0.045

TABLE 8.3 (Cont'd).

<u>Reaction</u>	<u>d<sub>0</sub></u>	<u>d<sub>1</sub></u>	<u>d<sub>2</sub></u>	<u>d<sub>3</sub></u>	<u>d<sub>4</sub></u>	<u>d<sub>5</sub></u>	<u>d<sub>6</sub></u>	<u>d<sub>7</sub></u>	<u>d<sub>8</sub></u>	<u>D.N.</u>
<u>9B/5</u>	Conversion = 64.2%      Final H.N. = 0.132									
n-B	10.6	8.7	15.1	25.0	23.0	10.1	4.9	1.8	0.7	3.042
l-B	9.0	28.5	46.1	11.9	3.4	0.7	0.1	0.04	0.0	1.751
t-2-B	11.2	31.2	46.4	8.1	2.6	0.5	0.1	0.0	0.0	1.616
c-2-B	12.6	33.5	43.3	7.8	1.9	0.4	0.3	0.2	0.06	1.565
1,3-B	94.5	4.7	0.4	0.2	0.2	0.04	0.02	-	-	0.072
<u>9B/3</u>	Conversion = 91.0%      Final H.N. = 0.154									
l-B	12.4	27.1	40.8	14.3	3.6	1.3	0.2	0.05	0.0	1.750
t-2-B	11.5	31.3	44.9	8.8	2.8	0.6	0.2	0.0	0.0	1.626
c-2-B	13.1	32.2	41.8	8.8	2.5	1.1	0.4	0.2	0.04	1.613
1,3-B	91.8	6.3	0.8	0.4	0.5	0.1	0.02	-	-	0.119

TABLE 8.4

Distribution of Butadiene Deuterated Products at 25°C. II Poisoned.Initial  $P_{D_2}$  = 60.0 ± 0.8mm.Series C :  $\theta_{Hg}$  = 13.3%Initial  $P_{1,3-B}$  = 30.0 ± 0.6mm.Series E :  $\theta_{Hg}$  = 28.8%

Reaction	$d_0$	$d_1$	$d_2$	$d_3$	$d_4$	$d_5$	$d_6$	$d_7$	$d_8$	$d_9$	$d_{10}$	D.N.
<u>9C/1</u>	Conversion = 23.1%											
	Final H.N. = 0.058											
1-B	12.4	24.4	49.4	9.9	2.9	0.7	0.2	0.06	0.0	-	-	1.694
t-2-B	12.4	31.4	47.4	6.4	1.8	0.4	0.1	0.0	0.0	-	-	1.554
c-2-B	16.9	28.2	43.5	7.1	3.5	0.6	0.2	0.0	0.0	-	-	1.547
1,3-B	99.4	0.3	0.2	0.06	0.08	0.01	0.0	-	-	-	-	0.012
<u>9C/2</u>	Conversion = 48.3%											
	Final H.N. = 0.092											
t-2-B	13.1	29.0	47.1	7.9	2.7	0.3	0.02	0.0	0.0	-	-	1.591
c-2-B	15.1	28.7	42.7	7.7	3.4	1.9	0.4	0.08	0.0	-	-	1.632
1,3-B	97.0	2.4	0.3	0.07	0.2	0.04	0.02	-	-	-	-	0.043
<u>9E/3</u>	Conversion = 11.7%											
	Final H.N. = 0.048											
1-B	7.0	22.8	45.1	15.1	6.6	2.1	0.9	0.3	0.2	-	-	2.040
t-2-B	6.4	21.8	48.2	13.2	5.3	2.1	0.7	0.3	0.2	-	-	2.010
c-2-B	7.2	21.7	47.3	14.6	5.0	2.6	1.1	0.4	0.2	-	-	2.033
1,3-B	99.0	0.3	0.2	0.1	0.2	0.05	0.03	-	-	-	-	0.026

TABLE 8.4 (Cont'd).

Series I :  $\theta_{Hg} = 76.0\%$

<u>Reaction</u>	$d_0$	$d_1$	$d_2$	$d_3$	$d_4$	$d_5$	$d_6$	$d_7$	$d_8$	$d_9$	$d_{10}$	<u>D.N.</u>
<u>9E/1</u>	Final H.N. = 0.052											
	Conversion = 22.6%											
n-B	2.2	0.8	5.0	5.9	32.8	19.7	17.6	7.7	6.5	1.9	0.03	4.866
l-B	7.4	20.3	48.8	14.2	6.0	2.0	0.8	0.3	0.1	-	-	2.027
t-2-B	8.4	22.4	46.0	14.1	5.7	2.0	0.9	0.3	0.1	-	-	1.978
l,3-B	98.6	0.8	0.3	0.1	0.2	0.05	0.01	-	-	-	-	0.028

9E/2 Conversion = 47.2% Final H.N. = 0.090

n-B	2.2	2.6	5.8	26.2	28.2	23.6	6.1	5.8	1.1	0.07	0.2	4.067
l-B	6.8	20.7	44.9	17.1	6.2	2.8	0.7	0.6	0.1	-	-	2.102
t-2-B	5.3	27.7	39.6	16.2	4.3	4.0	1.3	1.0	0.6	-	-	2.121
c-2-B	7.7	19.9	46.6	14.3	5.0	4.1	1.4	0.7	0.3	-	-	2.120
l,3-B	98.5	0.4	0.4	0.2	0.3	0.1	0.03	-	-	-	-	0.037

9I/3 Conversion = 13.4%

n-B	12.9	7.7	8.0	14.4	23.1	15.6	9.6	5.1	2.6	0.9	0.3	3.621
l-B	10.0	19.8	46.2	14.6	4.8	2.5	1.6	0.6	0.0	-	-	2.009
t-2-B	7.9	17.9	56.2	10.3	6.0	1.2	0.7	0.0	0.0	-	-	1.947
c-2-B	12.7	21.9	44.5	11.4	5.2	2.1	1.4	0.3	0.4	-	-	1.907
l,3-B	97.4	1.8	0.3	0.1	0.2	0.1	0.04	-	-	-	-	0.046

TABLE 8.4 (Cont'd).

Series I :  $\theta_{Hg} = 76.0\%$

<u>Reaction</u>	<u>d<sub>0</sub></u>	<u>d<sub>1</sub></u>	<u>d<sub>2</sub></u>	<u>d<sub>3</sub></u>	<u>d<sub>4</sub></u>	<u>d<sub>5</sub></u>	<u>d<sub>6</sub></u>	<u>d<sub>7</sub></u>	<u>d<sub>8</sub></u>	<u>d<sub>9</sub></u>	<u>d<sub>10</sub></u>	<u>D.N.</u>
<u>9I/1</u> Conversion = 21.4%												
n-B	12.3	4.6	10.9	13.1	20.1	15.5	12.3	4.8	2.3	2.4	1.8	3.886
l-B	17.4	16.7	42.8	13.1	4.7	3.6	1.2	0.4	0.0	-	-	1.887
t-2-B	16.1	20.2	46.4	10.7	3.4	2.7	0.4	0.0	0.0	-	-	1.750
c-2-B	19.1	19.1	41.5	10.8	6.2	1.1	1.0	1.0	0.4	-	-	1.801
l,3-B	96.5	2.4	0.4	0.2	0.4	0.1	0.07	-	-	-	-	0.061
<u>9I/2</u> Conversion = 49.2%												
n-B	9.9	4.6	7.8	21.7	27.0	9.4	8.9	6.8	1.3	1.5	1.0	3.753
l-B	6.8	18.7	46.8	17.3	6.4	2.5	1.2	0.4	0.0	-	-	2.120
t-2-B	5.7	20.9	51.0	13.6	4.4	3.1	0.8	0.5	0.2	-	-	2.058
c-2-B	9.9	21.7	45.3	13.6	4.5	2.7	1.0	0.5	0.8	-	-	2.007
l,3-B	92.5	4.5	0.8	0.7	1.1	0.4	0.2	-	-	-	-	0.152

### 8.3 Reactions of 1,3-Butadiene at 48°C.

#### 8.3.1 The Deuteration Reaction.

The reactions were carried out at 48°C on a 6.4mg. sample of catalyst (Rh-5). The details of the mercury adsorption and percentage coverages, together with the rate of deuteration ( $r_d$ ) at each stage are summarised in table 8.5 (See also Fig. 8.3.)

TABLE 8.5

Summary of Mercury Adsorption & Rates of Deuteration on Rh-5.

Temperature of mercury source = 20 ± 1°C

Temperature of catalyst vessel = 48 ± 1°C

<u>Series</u>	<u>Count-Rate</u> (c.p.m.)	$\theta_{\text{Hg}}$ (%)	Atom ratio $\frac{\text{Hg}}{\text{Rh}}$ ( $\times 10^{-3}$ )	$r_d$ (mm.min. <sup>-1</sup> )
B	0.0	0.0	0.0	0.96
C	86.1 ± 2.0	39.5	65.1	0.40
E	171.2 ± 2.0	78.6	129.5	0.10
G	202.8 ± 3.0	93.2	153.4	0.027
(Final)	217.7	100.0	164.7	

The final weight of mercury adsorbed, 0.103mg., or 0.321mg. per mg. Rh corresponded to a mercury/rhodium ratio of  $\sim 1/6$ .

The pressure fall against time curves showed a general first order reduction in rate on the unpoisoned

catalyst. At  $\theta_{\text{Hg}} = 79\%$ , the rate was linear with time for the first 15% conversion, and thereafter was first order in nature. A slight acceleration in the rate of pressure fall was observed at  $\sim 110\%$  conversion.

The product distributions obtained from the deuteration reactions are shown in table 8.6; the variation with conversion in series 5B, on the unpoisoned catalyst, is illustrated in Fig. 8.2. It is apparent that the butene ratios are generally unchanged within each series during the first stage of the reaction (up to 60% conversion), but that successive adsorptions of mercury caused the trans/cis ratio to fall sharply. The ratio of 1-butene : 2-butene is unchanged, with the exception of series 5G. The deactivation of the catalyst for the deuteration reaction is illustrated in Fig. 8.3.

The selectivity for butene formation is very high, and declines only slightly with increasing conversion; there was little apparent change on the poisoned catalyst.

### 8.3.2 The Exchange Reactions.

There are a number of interesting features in the distributions of deuterio-butanenes and deuterio-butenes obtained using catalyst Rh-5, and which are shown in tables 8.7 and 8.8.

It is notable that all the deuteration products con-

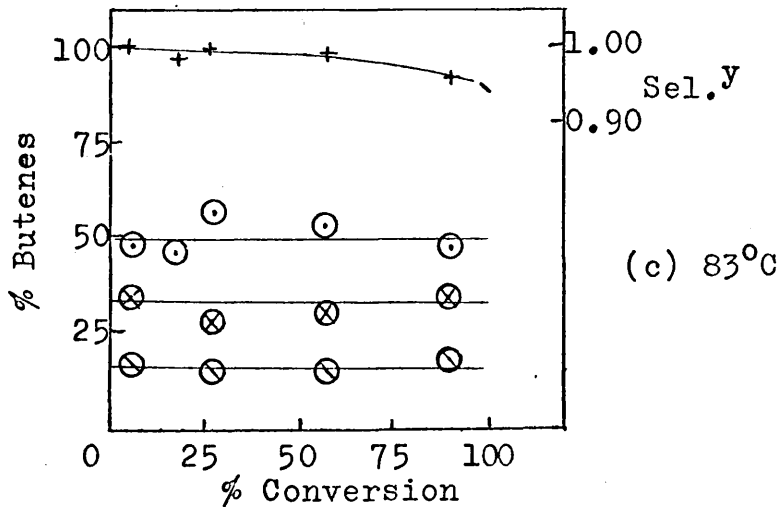
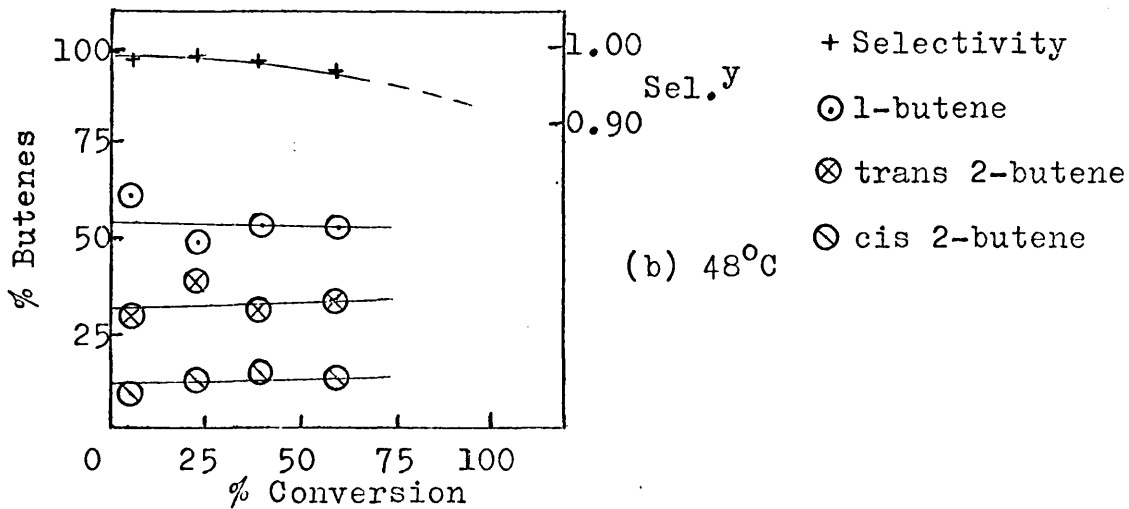
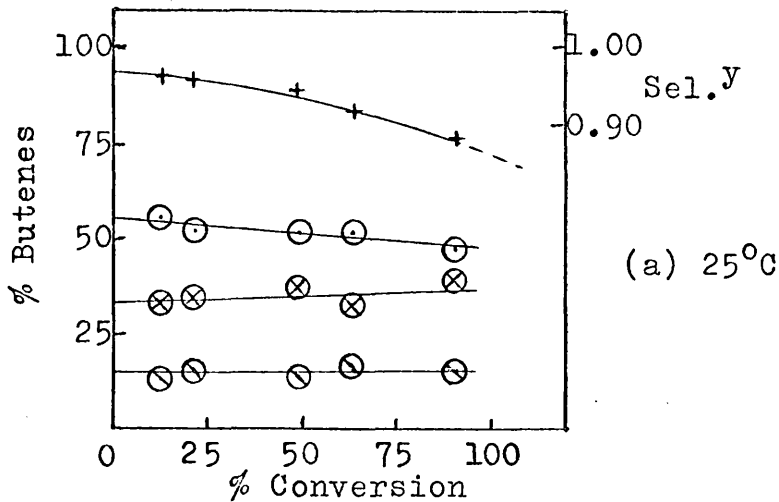


Fig. 8.2 Variation of selectivity and butene distribution on Rh/SiO<sub>2</sub>. (a) 25°C, (b) 48°C, (c) 83°C.



TABLE 8.6

1,3-Butadiene Product Distributions at 48°C.Initial  $p_{D_2}$  = 60.0  $\pm$  1.0mm.Initial  $p_{1,3-B}$  = 30.0  $\pm$  0.7mm.

% Butene Distribution

<u>Reaction</u>	$\theta_{Hg}$	<u>Conv.</u> %	<u>1-B</u>	<u>t-2-B</u>	<u>c-2-B</u>	<u>T/C</u>	<u>Sel.</u>
5B/3	0.0	5.6	61.1	29.9	9.0	3.33	0.988
5B/1	"	22.2	49.4	38.3	12.3	3.12	0.994
5B/5	"	39.1	53.7	31.6	14.7	2.16	0.980
5B/4	"	58.7	52.2	33.9	13.9	2.44	0.973
5B/2	"	126.4	7.3	64.4	28.4	2.27	0.727
5C/3	39.5	7.9	62.6	21.0	16.3	1.29	0.992
5C/1	"	21.4	55.9	26.8	17.3	1.55	0.997
5C/2	"	39.2	54.7	26.5	18.8	1.41	0.988
5C/4	"	55.2	54.4	27.6	18.0	1.53	0.975
5E/1	78.6	6.9	51.2	26.1	22.7	1.15	0.995
5E/2	"	19.5	55.1	22.7	22.2	1.02	0.992
5E/3	"	38.5	54.0	23.2	22.8	1.02	0.990
5G/2	93.2	4.8	89.0	5.1	5.9	0.87	1.000
5G/1	"	13.1	61.8	14.6	23.7	0.61	0.997

TABLE 8.7

Distribution of 1,3-Butadiene Deuterated Products at 48°C. I Unpoisoned.

Initial P<sub>D<sub>2</sub></sub> = 60.5 ± 0.5mm. Initial P<sub>1,3-B</sub> = 30.0 ± 0.6mm.

Reaction	d <sub>0</sub>	d <sub>1</sub>	d <sub>2</sub>	d <sub>3</sub>	d <sub>4</sub>	d <sub>5</sub>	d <sub>6</sub>	d <sub>7</sub>	d <sub>8</sub>	d <sub>9</sub>	d <sub>10</sub>	D.N.
5B/3 Conversion = 5.6%												
1-B	11.6	17.9	45.0	15.7	5.6	2.2	1.1	0.5	0.3	-	-	2.013
t-2-B	6.1	22.8	52.3	11.5	4.6	1.6	0.7	0.2	0.1	-	-	1.951
c-2-B	5.6	23.2	46.6	13.6	6.1	2.8	1.2	0.5	0.3	-	-	2.092
1,3-B	98.6	0.9	0.4	0.1	0.03	0.0	0.0	-	-	-	-	0.022
5B/1 Conversion = 22.2%												
n-B	1.9	2.5	8.8	19.1	27.7	16.3	11.0	5.4	3.4	2.1	1.7	4.365
t-2-B	5.1	24.9	53.5	10.7	3.9	1.1	0.5	0.2	0.07	-	-	1.903
c-2-B	6.3	22.4	50.3	12.2	5.1	2.1	1.0	0.4	0.2	-	-	2.011
1,3-B	97.2	2.0	0.4	0.2	0.2	0.04	0.01	-	-	-	-	0.043
5B/5 Conversion = 39.1%												
n-B	6.6	4.3	8.6	16.7	23.0	18.2	10.4	5.2	2.8	2.7	1.4	4.150
1-B	7.5	19.6	46.8	16.4	6.3	2.2	0.9	0.3	0.1	-	-	2.068
t-2-B	6.7	21.7	51.3	12.6	4.7	1.8	0.8	0.3	0.1	-	-	1.972
c-2-B	5.5	20.2	52.9	11.9	5.4	2.4	1.0	0.4	0.3	-	-	2.063
1,3-B	95.3	2.8	0.5	0.5	0.7	0.2	0.04	-	-	-	-	0.094

TABLE 8.7 (Cont'd).

<u>Reaction</u>	<u>d<sub>0</sub></u>	<u>d<sub>1</sub></u>	<u>d<sub>2</sub></u>	<u>d<sub>3</sub></u>	<u>d<sub>4</sub></u>	<u>d<sub>5</sub></u>	<u>d<sub>6</sub></u>	<u>d<sub>7</sub></u>	<u>d<sub>8</sub></u>	<u>d<sub>9</sub></u>	<u>d<sub>10</sub></u>	<u>D.N.</u>
<u>5B/4</u>	Conversion = 58.7%											
n-B	1.6	3.1	9.6	18.9	26.4	17.5	10.1	5.7	3.4	2.2	1.4	4.337
l-B	6.3	20.0	46.7	16.8	6.6	2.3	0.8	0.3	0.1	-	-	2.098
t-2-B	6.7	25.2	48.6	12.0	4.8	1.7	0.7	0.2	0.1	-	-	1.928
c-2-B	6.9	25.1	43.3	14.1	6.0	2.6	1.3	0.6	0.3	-	-	2.046
l,3-B	93.5	4.6	0.8	0.4	0.5	0.2	0.04	-	-	-	-	0.106
<u>5B/2</u>	Conversion = 126.4%											
n-B	2.1	5.1	13.6	22.3	23.8	15.2	9.1	4.4	2.4	1.3	0.7	3.935
l-B	4.7	16.3	33.8	24.4	12.8	5.3	1.8	0.6	0.2	-	-	2.520
t-2-B	6.0	21.1	38.5	18.6	9.7	3.9	1.6	0.4	0.1	-	-	2.257
c-2-B	5.5	18.5	34.5	21.6	11.9	5.3	1.9	0.7	0.2	-	-	2.437

TABLE 8.8

## Distribution of Butadiene Deuterated Products at 48°C. II Poisoned.

Initial  $p_{D_2}$  = 60.0 ± 1.0mm.  
 Initial  $p_{1,3-B}$  = 30.0 ± 0.7mm.

Series C :  $\theta_{Hg}$  = 39.5%

Reaction	$d_0$	$d_1$	$d_2$	$d_3$	$d_4$	$d_5$	$d_6$	$d_7$	$d_8$	$d_9$	$d_{10}$	<u>D.N.</u>
<u>5C/3</u> Conversion = 7.9%												
1-B	18.2	17.8	44.4	11.9	4.8	1.7	0.8	0.2	0.1	-	-	1.776
t-2-B	6.4	23.2	52.3	11.0	4.5	1.6	0.7	0.2	0.1	-	-	1.929
c-2-B	6.7	23.5	50.8	11.0	4.4	1.9	1.0	0.4	0.2	-	-	1.962
1,3-B	98.2	0.4	0.4	0.3	0.5	0.1	0.08	-	-	-	-	0.052
<u>5C/1</u> Conversion = 21.4%												
1-B	12.4	20.0	46.5	12.9	5.3	1.8	0.8	0.2	0.1	-	-	1.887
t-2-B	6.0	25.0	49.8	11.7	4.5	1.8	0.8	0.2	0.1	-	-	1.942
c-2-B	6.7	24.9	48.6	11.8	4.4	2.0	0.9	0.4	0.2	-	-	1.954
1,3-B	97.2	1.6	0.4	0.2	0.5	0.1	0.04	-	-	-	-	0.055
<u>5C/2</u> Conversion = 39.2%												
n-B	3.2	2.7	9.1	17.3	27.6	17.3	9.4	6.0	3.5	2.0	2.0	4.334
1-B	8.9	20.1	48.0	14.1	5.6	2.0	0.9	0.2	0.1	-	-	1.985
t-2-B	6.1	24.5	51.2	10.9	4.7	1.6	0.7	0.2	0.1	-	-	1.930
c-2-B	7.2	24.4	48.5	11.5	4.8	2.0	0.9	0.4	0.3	-	-	1.956
1,3-B	96.6	2.1	0.4	0.3	0.4	0.1	0.02	-	-	-	-	0.062

TABLE 8.8 (Cont'd).

Series E :  $\theta_{Hg} = 78.6\%$

Reaction	$d_0$	$d_1$	$d_2$	$d_3$	$d_4$	$d_5$	$d_6$	$d_7$	$d_8$	$d_9$	$d_{10}$	D.N.
5C/4												
	Conversion = 55.2%											
n-B	2.8	3.0	9.4	19.2	27.4	15.6	10.2	5.8	3.0	2.0	1.6	4.266
l-B	8.2	20.6	47.0	14.5	6.0	2.2	1.0	0.3	0.2	-	-	2.028
t-2-B	6.5	24.7	49.4	11.8	4.9	1.7	0.8	0.2	0.1	-	-	1.939
c-2-B	7.8	25.3	47.1	11.5	4.8	2.0	0.9	0.4	0.2	-	-	1.929
l,3-B	95.0	3.3	0.5	0.4	0.6	0.1	0.06	-	-	-	-	0.090

5E/1 Conversion = 6.9%

l-B	13.0	18.6	48.6	11.7	4.8	1.8	1.0	0.3	0.1	-	-	1.884
t-2-B	5.3	23.5	53.8	11.0	3.9	1.4	0.7	0.2	0.1	-	-	1.931
c-2-B	7.8	22.5	51.5	10.9	4.0	1.8	1.0	0.4	0.2	-	-	1.936
l,3-B	99.1	0.4	0.3	0.07	0.1	0.02	0.0	-	-	-	-	0.018

5E/2 Conversion = 19.5%

l-B	8.9	20.4	51.0	12.4	4.8	1.6	0.7	0.2	0.07	-	-	1.924
t-2-B	6.9	23.9	51.7	11.1	4.2	1.4	0.6	0.1	0.07	-	-	1.893
c-2-B	6.7	24.9	52.5	10.1	3.6	1.4	0.6	0.2	0.1	-	-	1.872
l,3-B	98.2	1.1	0.3	0.2	0.3	0.04	0.0	-	-	-	-	0.035

TABLE 8.8 (Cont'd).

Series G :  $\theta_{Hg} = 93.2\%$

<u>Reaction</u>	<u>d<sub>0</sub></u>	<u>d<sub>1</sub></u>	<u>d<sub>2</sub></u>	<u>d<sub>3</sub></u>	<u>d<sub>4</sub></u>	<u>d<sub>5</sub></u>	<u>d<sub>6</sub></u>	<u>d<sub>7</sub></u>	<u>d<sub>8</sub></u>	<u>d<sub>9</sub></u>	<u>d<sub>10</sub></u>	<u>D.N.</u>
<u>5E/3</u>	Conversion = 38.5%											
1-B	8.4	20.9	48.4	13.6	5.5	2.0	0.9	0.2	0.1	-	-	1.981
t-2-B	7.4	24.5	48.9	11.9	4.5	1.7	0.8	0.2	0.1	-	-	1.915
c-2-B	7.5	24.2	49.1	11.7	4.2	1.8	0.9	0.3	0.2	-	-	1.928
1,3-B	96.9	1.9	0.5	0.3	0.4	0.07	0.03	-	-	-	-	0.056
<u>5G/2</u>	Conversion = 4.8%											
t-2-B	18.7	19.8	45.1	9.1	3.4	2.2	1.0	0.5	0.3	-	-	1.731
c-2-B	10.6	20.3	53.5	9.2	3.2	1.5	0.8	0.5	0.3	-	-	1.862
1,3-B	99.0	0.2	0.5	0.08	0.15	0.02	0.01	-	-	-	-	0.022
<u>5G/1</u>	Conversion = 13.1%											
1-B	30.3	13.4	42.0	8.2	3.4	1.4	0.7	0.3	0.2	-	-	1.505
t-2-B	25.2	17.9	43.0	8.1	3.2	1.3	0.8	0.3	0.2	-	-	1.560
c-2-B	12.8	19.7	53.3	8.4	3.1	1.2	0.8	0.4	0.3	-	-	1.798
1,3-B	98.3	1.0	0.4	0.1	0.2	0.02	0.0	-	-	-	-	0.028

-tain at least a small fraction of fully exchanged molecules. Each butene shows very little change in the deuterium distribution other than a gradual broadening of the spectrum as the conversion increases. The total deuterium content is unchanged up to  $\sim 100\%$  conversion. As the value of  $\theta_{\text{Hg}}$  rises, however, there is a very slight trend toward lower deuterium content, although there is no significant change in the percentages of  $d_0$ , and  $d_1$ -species.

It is of interest that the initially produced butanes have a deuterium number greater than four and as the conversion increases, its value drops slightly owing to a relative increase in the fraction of  $d_1$ - and  $d_2$ -n-butane.

The results of the exchange reaction of the 1,3-butadiene on the unpoisoned catalyst are shown in Fig.8.5; its rate of exchange declines with increasing  $\theta_{\text{Hg}}$  (Fig.8.4) but on the poisoned catalyst the deuterium content at comparable conversion is only marginally reduced. The hydrogen exchange reaction was not studied on Rh-5.

#### 8.4 Reactions of 1,3-Butadiene at 83°C.

##### 8.4.1 The Deuteration Reaction.

The study of the reaction of 1,3-butadiene with deuterium at 83°C was made using a 2mg. sample of Rh/SiO<sub>2</sub> (Rh-8). The total weight of mercury adsorbed at this temperature was 0.0272mg., or 0.272mg. per mg. rhodium, corresponding to an atom ratio mercury : rhodium :: 1 : 7.

The details of the adsorption conditions, the count-rates at each stage, and the percentage of monolayer coverage, together with the corresponding rates of deuteration, are shown in table 8.9. The decrease in the reaction rate with increasing  $\theta_{\text{Hg}}$  is also shown in Fig. 8.3.

The pressure fall against time characteristics were observed on the unpoisoned catalyst up to 133% conversion, during which stage a uniform first order rate was obtained, and no acceleration of the reaction occurred. On the mercury poisoned catalyst, however, the pressure fall was initially linear with time, and then first order, the transition occurring at  $\sim 40\%$  conversion when  $\theta_{\text{Hg}} = 81\%$ .

The deuteration products for each reaction are shown in table 8.10; the distribution for series 8B (unpoisoned) is shown in Fig. 8.2. The principal features which emerge from these results are the very high selectivity factors, and the significant changes in distributions of the butene products. As at  $25^{\circ}$  and  $48^{\circ}\text{C}$ , the 1-butene : 2-butene and trans/cis ratios do not vary greatly within each series; as the mercury coverage increases, however, there is a decrease in the trans/cis ratio, but not so marked as at the lower temperatures. There is also a slight decrease in the 1-butene/2-butene ratio, which was not observed at either of the lower temperatures.



TABLE 8.9Summary of Mercury Adsorption & Rates of Deuteration on Rh-8.

Temperature of mercury source =  $83 \pm 1^{\circ}\text{C}$

Temperature of catalyst vessel =  $21 \pm 2^{\circ}\text{C}$

<u>Series</u>	<u>Count-Rate</u> (c.p.m.)	$\theta_{\text{Hg}}$ (%)	Atom ratio $\frac{\text{Hg}}{\text{Rh}}$ ( $\times 10^{-3}$ )	$r_d$ ( $\text{mm}\cdot\text{min}^{-1}$ )
B	0.0	0.0	0.0	2.35
C	$31.5 \pm 0.5$	23.2	32.4	1.60
E	$59.5 \pm 0.5$	44.4	62.1	1.07
G	$90.4 \pm 4.0$	67.5	94.4	0.50
I	$108.7 \pm 1.0$	81.0	113.2	0.33
K	$125.8 \pm 1.5$	93.7	131.0	0.22
Final	134.0	100.0	139.8	

8.4.2 The Exchange Reactions.

The distributions of deuterio-butanenes and deuterio-butenes in series 8B are shown in table 8.11, and those for the series on the poisoned catalyst in table 8.12.

The n-butene products exhibit a number of features common to each. Their deuterium numbers vary somewhat with the conversion, but there is no systematic trend. As the mercury coverage increases, however, the deuterium content rises; this is mainly due to a rise in the  $d_2$  maximum, and a fall in the proportion of  $d_0$  and  $d_1$  species, rather than

TABLE 8.10

1,3-Butadiene Product Distributions at 83°C.Initial  $p_{D_2}$  = 60.0  $\pm$  0.8mm.Initial  $p_{1,3-B}$  = 30.0  $\pm$  0.5mm.

% Butene Distribution

<u>Reaction</u>	<u><math>\theta_{Hg}</math></u>	<u>Conv.</u> %	<u>1-B</u>	<u>t-2-B</u>	<u>c-2-B</u>	<u>T/C</u>	<u>Sel.</u>
8B/5	0.0	5.3	48.3	34.6	17.1	2.02	1.000
8B/2	"	17.4	46.4	24.8	28.7	0.87	0.984
8B/3	"	25.5	57.2	28.4	14.4	1.98	0.996
8B/1	"	56.9	53.8	30.8	15.3	2.01	0.986
8B/4	"	89.8	47.7	34.5	17.8	1.94	0.961
8C/3	23.2	5.5	55.9	25.6	18.5	1.38	1.000
8C/1	"	13.3	54.6	25.0	20.3	1.23	0.997
8C/2	"	27.8	54.0	28.4	17.6	1.62	0.994
8E/3	44.4	13.8	50.8	27.7	21.5	1.29	0.996
8E/1	"	23.3	53.3	27.0	19.7	1.37	1.000
8E/2	"	53.1	51.1	28.3	20.6	1.37	0.995
8G/3	67.5	14.2	48.2	30.4	21.4	1.42	1.000
8G/1	"	27.7	40.3	32.8	26.9	1.22	1.000
8G/2	"	52.0	49.0	27.2	23.7	1.15	0.995
8I/3	81.0	13.5	50.4	28.6	21.0	1.36	1.000
8I/1	"	24.5	49.1	27.4	23.5	1.17	0.998
8I/2	"	49.4	47.5	28.6	23.9	1.20	0.996
8K/1	93.7	24.0	48.9	27.9	23.2	1.20	1.000

TABLE 8.11

Distribution of 1,3-Butadiene Deuterated Products at 83°C. I Unpoisoned.

Initial  $p_{D_2} = 60.0 \pm 0.4$  mm. Initial  $p_{1,3-B} = 30.0 \pm 0.4$  mm.

<u>Reaction</u>	$d_0$	$d_1$	$d_2$	$d_3$	$d_4$	$d_5$	$d_6$	$d_7$	$d_8$	<u>D.N.</u>
<p><u>8B/5</u> Conversion = 5.3% Final H.N. = 0.034</p>										
t-2-B	17.9	32.7	41.2	6.8	1.3	0.1	0.02	0.0	0.0	1.414
c-2-B	18.6	20.7	41.4	12.9	5.4	1.0	0.02	0.0	0.0	1.688
1,3-B	99.7	0.1	0.1	0.01	0.02	0.0	0.0	-	-	0.004
<p><u>8B/2</u> Conversion = 17.4% Final H.N. = 0.052</p>										
1-B	22.8	32.2	36.9	6.6	1.5	0.0	0.0	0.0	0.0	1.318
t-2-B	26.4	33.7	33.5	5.0	1.1	0.1	0.1	0.03	0.0	1.216
c-2-B	27.3	33.3	33.4	4.3	1.2	0.2	0.1	0.04	0.0	1.202
1,3-B	99.0	0.7	0.1	0.05	0.04	0.01	0.01	-	-	0.014
<p><u>8B/3</u> Conversion = 25.5% Final H.N. = 0.080</p>										
1-B	28.8	31.5	31.9	5.6	1.7	0.3	0.1	0.01	0.0	1.214
t-2-B	21.1	34.6	37.0	5.7	1.3	0.2	0.02	0.0	0.0	1.323
c-2-B	24.4	34.4	33.8	5.6	1.3	0.4	0.1	0.03	0.0	1.265
1,3-B	99.6	0.3	0.2	0.08	0.07	0.01	0.0	-	-	0.013

TABLE 8.11 (Cont'd).

<u>Reaction</u>	<u>d<sub>0</sub></u>	<u>d<sub>1</sub></u>	<u>d<sub>2</sub></u>	<u>d<sub>3</sub></u>	<u>d<sub>4</sub></u>	<u>d<sub>5</sub></u>	<u>d<sub>6</sub></u>	<u>d<sub>7</sub></u>	<u>d<sub>8</sub></u>	<u>D.N.</u>
<u>8B/1</u>	Conversion = 56.9% Final H.N. = 0.138									
1-B	17.2	32.0	38.8	9.2	2.2	0.5	0.1	0.01	0.0	1.490
1,3-B	96.6	2.0	0.7	0.3	0.3	0.06	0.01	-	-	0.059
<u>8B/4</u>	Conversion = 89.8% Final H.N. = 0.246									
1-B	20.9	34.7	32.0	9.3	2.5	0.6	0.04	0.02	0.0	1.399
t-2-B	24.2	35.8	30.3	6.7	2.0	0.6	0.2	0.2	0.04	1.299
c-2-B	25.3	35.8	28.5	7.2	2.2	0.7	0.2	0.1	0.04	1.287
1,3-B	92.5	4.6	0.9	0.9	0.9	0.2	0.05	-	-	0.139

TABLE 8.12

Distribution of 1,3-Butadiene Deuterated Products at 83°C. II Poisoned.

Initial  $p_{D_2}$  = 60.0 ± 0.8mm.      Series C :  $\theta_{Hg}$  = 23.2%  
 Initial  $p_{1,3-B}$  = 30.0 ± 0.5mm.

<u>Reaction</u>	<u>d<sub>0</sub></u>	<u>d<sub>1</sub></u>	<u>d<sub>2</sub></u>	<u>d<sub>3</sub></u>	<u>d<sub>4</sub></u>	<u>d<sub>5</sub></u>	<u>d<sub>6</sub></u>	<u>d<sub>7</sub></u>	<u>d<sub>8</sub></u>	<u>D.N.</u>
<u>8C/3</u>	Final H.N. = 0.048									
	Conversion = 5.5%									
t-2-B	21.3	37.4	34.2	4.8	1.7	0.5	0.03	0.0	0.0	1.298
c-2-B	24.6	36.0	34.3	4.0	0.9	0.2	0.05	0.0	0.0	1.215
1,3-B	99.5	0.3	0.1	0.04	0.05	0.0	0.0	-	-	0.007
<u>8C/1</u>	Final H.N. = 0.056									
	Conversion = 13.3%									
1-B	26.0	27.5	35.4	7.6	2.3	0.8	0.4	0.03	0.02	1.369
t-2-B	19.6	33.5	40.1	6.2	0.5	0.2	0.0	0.0	0.0	1.350
c-2-B	25.4	33.5	36.2	4.5	0.3	0.2	0.0	0.0	0.0	1.214
1,3-B	99.5	0.2	0.2	0.02	0.03	0.0	0.0	-	-	0.008
<u>8C/2</u>	Final H.N. = 0.082									
	Conversion = 27.8%									
1-B	17.3	32.0	41.9	7.4	1.1	0.3	0.0	0.0	0.0	1.440
t-2-B	22.0	33.6	37.6	5.3	1.2	0.2	0.06	0.0	0.0	1.311
c-2-B	22.4	32.6	37.1	5.8	1.9	0.2	0.06	0.0	0.0	1.330
1,3-B	99.3	0.3	0.2	0.08	0.1	0.02	0.0	-	-	0.014

TABLE 8.12 (Cont'd).

Reaction	$d_0$	$d_1$	$d_2$	$d_3$	$d_4$	$d_5$	$d_6$	$d_7$	$d_8$	D.N.
	Conversion = 13.8%									
8E/3										
1-B	11.5	24.9	53.2	8.6	1.4	0.3	0.0	0.0	0.0	1.643
t-2-B	17.9	30.5	44.3	4.5	2.6	0.2	0.0	0.0	0.0	1.441
c-2-B	17.9	34.6	40.8	5.0	1.4	0.2	0.06	0.0	0.0	1.384
1,3-B	99.3	0.5	0.1	0.03	0.01	0.0	0.0	-	-	0.010
8E/1										
	Conversion = 23.3%									
t-2-B	26.2	33.4	35.8	3.2	1.3	0.2	0.0	0.0	0.0	1.205
c-2-B	25.7	34.1	35.6	3.6	1.0	0.1	0.0	0.0	0.0	1.203
1,3-B	99.1	0.6	0.2	0.05	0.05	0.01	0.0	-	-	0.014
8E/2										
	Conversion = 53.1%									
1-B	15.0	29.0	44.0	8.4	2.4	0.6	0.03	0.03	0.0	1.558
t-2-B	13.8	31.8	43.5	7.6	1.9	0.9	0.3	0.1	0.0	1.563
c-2-B	17.1	31.2	42.4	6.6	1.9	0.6	0.1	0.04	0.0	1.474
1,3-B	98.3	1.1	0.2	0.1	0.2	0.02	0.0	-	-	0.027
8G/3										
	Conversion = 14.2%      Final H.N. = 0.052									
c-2-B	18.6	28.5	39.7	10.6	2.6	0.0	0.0	0.0	0.0	1.498
1,3-B	99.2	0.7	0.1	0.03	0.04	0.0	0.0	-	-	0.011

Series E :  $\theta_{Hg}$  = 44.4%  
 Series G :  $\theta_{Hg}$  = 67.5%

TABLE 8.12 (Cont'd).

Reaction	$d_0$	$d_1$	$d_2$	$d_3$	$d_4$	$d_5$	$d_6$	$d_7$	$d_8$	D.N.
	Final H.N. = 0.096									
<u>8G/2</u>	Conversion = 52.0%									
1-B	8.6	26.5	52.4	8.5	3.0	0.5	0.4	0.2	0.06	1.750
t-2-B	9.7	26.8	50.7	8.7	3.7	0.4	0.0	0.0	0.0	1.710
c-2-B	9.4	30.1	41.0	7.2	2.0	0.2	0.0	0.0	0.0	1.631
1,3-B	97.9	1.3	0.3	0.2	0.3	0.05	0.04	-	-	0.040
<u>8I/1</u>	Conversion = 24.5%									
1-B	13.1	25.6	51.7	7.0	2.2	0.4	0.0	0.0	0.0	1.607
c-2-B	9.5	28.0	54.6	5.9	1.7	0.3	0.07	0.0	0.0	1.634
1,3-B	98.6	0.9	0.2	0.1	0.2	0.06	0.02	-	-	0.027
<u>8I/2</u>	Conversion = 49.4%									
1-B	13.3	26.4	50.0	7.0	2.9	0.5	0.0	0.0	0.0	1.609
t-2-B	12.9	27.5	46.4	8.2	2.7	1.8	0.5	0.0	0.0	1.677
1,3-B	98.3	1.1	0.2	0.1	0.3	0.05	0.0	-	-	0.032
<u>8K/1</u>	Conversion = 24.0%									
1-B	13.4	26.0	52.4	5.8	1.9	0.4	0.0	0.0	0.0	1.577
c-2-B	11.0	22.8	59.3	5.4	1.2	0.2	0.0	0.0	0.0	1.638
1,3-B	99.1	0.5	0.1	0.08	0.1	0.0	0.0	-	-	0.016

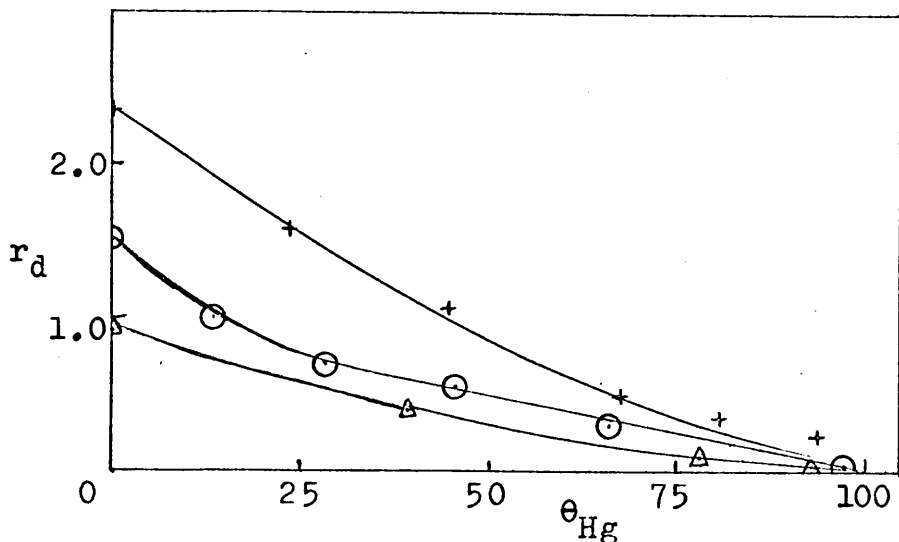


Fig. 8.3 Decrease of the rate of deuteration of 1,3-butadiene with mercury poisoning.  
 $\odot$  - 25°C       $\Delta$  - 48°C      + - 83°C

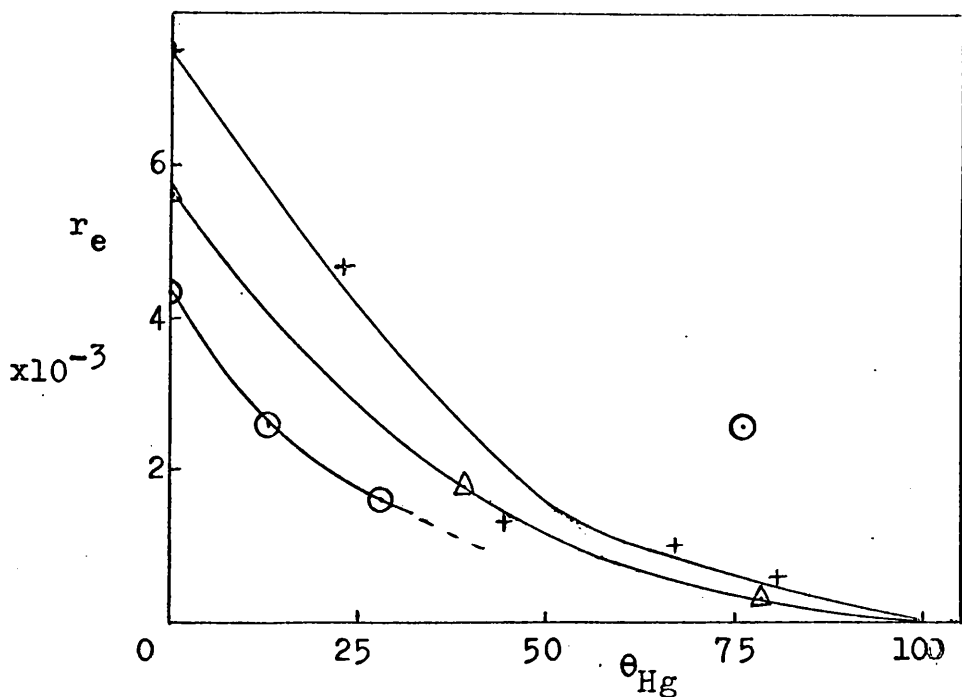


Fig. 8.4 Decrease of the rate of 1,3-butadiene exchange with mercury poisoning.  
 (Symbols as in Fig. 8.3)



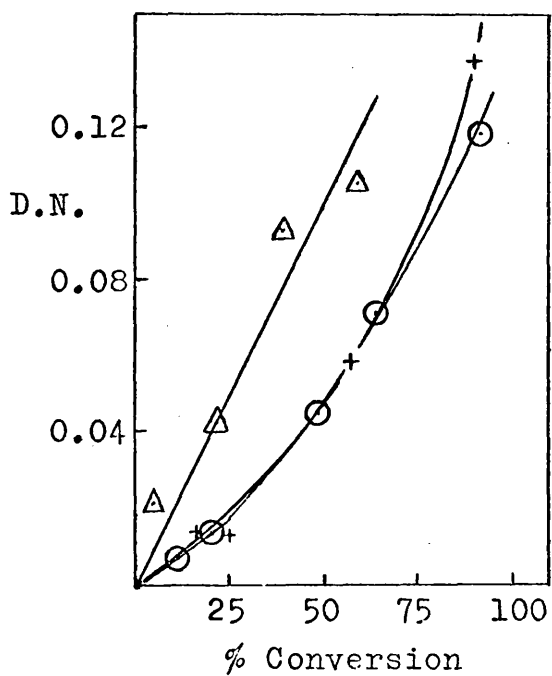


Fig. 8.5 Variation of 1,3-butadiene deuterium number with conversion on Rh/SiO<sub>2</sub>.

○ — 25°C

△ — 48°C

+ — 83°C

to any broadening of the spectrum. The heights of the respective  $d_2$  maxima for each reaction are apparently similar to each other, but the deuterium content of the 1-butene is generally slightly greater than the mean of the 2-butene values. This difference may not be significant, however. It is also notable that at low values of  $\theta_{\text{Hg}}$ , certain of the butenes have a maximum at  $d_1$  rather than  $d_2$ .

The distribution of deuterium in the 1,3-butadiene appears to vary rather irregularly. While the total content increases with conversion in each series, the characteristics of the increase vary from one series to another, and the effect of the mercury is thus more difficult to estimate.

#### 8.4.3 The Hydrogen Exchange Reaction.

The hydrogen exchange reaction on the unpoisoned catalyst is relatively rapid during the first 10% of conversion, and thereafter is rather slower. The total amount of exchanged hydrogen increased linearly with conversion. As  $\theta_{\text{Hg}}$  increases, two effects may be discerned. The rapid initial exchange becomes relatively faster, at least at low mercury coverage, but above 10% conversion, the reaction is increasingly inhibited by the successive adsorptions of mercury. The total exchanged hydrogen content, however, continued to increase linearly with conversion.

## 8.5 The Mass Balance.

The total hydrogen and deuterium content of each product was calculated where the results allowed this, and the balance of the initial and final content of each obtained. The results for reaction 9E/2 are shown below; a small deficit of deuterium and excess of hydrogen in the final products is apparent, but the initial and final totals are the same within experimental error. It may be reasonably assumed that the balance is applicable also to those reactions for which a mass spectrum was not obtained for one or more of the products.

MASS BALANCE - REACTION 9E/2.

	<u>Partial Pressure</u> (mm.)	<u>D.N.</u>	<u>H.N.</u>	<u>Total D</u> (mm. atoms)	<u>Total H</u> (mm. atoms)
<u>Initial:</u>					
D <sub>2</sub>	59.4	1.994	0.006	118.44	0.36
1,3-B	30.4	0.00	6.00	-	182.40
Total				<u>118.44</u>	<u>182.76</u>

Final:

n-B	0.86	4.067	5.933	3.49	5.09
l-B	6.58	2.102	5.898	13.83	38.80
t-2-B	4.04	2.121	5.879	8.56	23.73
c-2-B	2.03	2.120	5.880	4.31	11.96
1,3-B	16.89	0.037	5.963	0.63	100.73
H/D	44.04	1.910	0.090	85.44	3.96
Total				<u>116.25</u>	<u>184.28</u>

Summary:

	<u>Initial</u>	<u>Final</u>
Hydrogen	182.76	184.28
Deuterium	<u>118.44</u>	<u>116.25</u>
Total	<u>301.20</u>	<u>300.53</u>

D I S C U S S I O NCHAPTER 9DISCUSSION OF THE HYDROISOMERISATION OF 1-BUTENE.

In the ensuing discussion of the results of the hydroisomerisation of 1-butene on Rh/Al<sub>2</sub>O<sub>3</sub> and Rh/SiO<sub>2</sub> catalysts an attempt will be made to correlate the results for each catalyst, and to derive reaction mechanisms which are consistent with each of them, but which will also explain a number of contrasting features of the two catalysts.

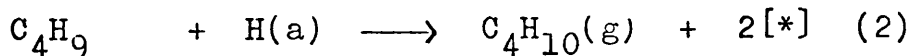
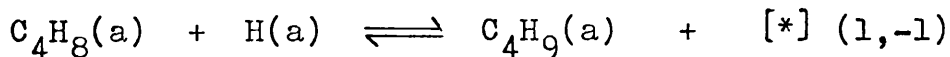
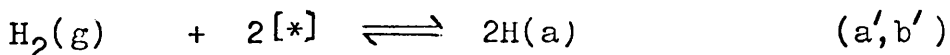
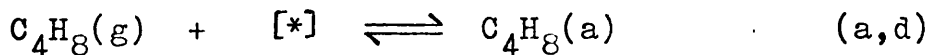
Consideration of the principal features which emerge from the results presented in chapter 5 shows that in many respects the reactions are fundamentally very similar over each catalyst. The butene distributions, for example, follow essentially similar trends, while the respective kinetic orders are the same, and  $E_h < E_i$  on both catalysts. Further, a marked preference for the formation of cis 2-butene is observed with each. There are, however, a number of interesting differences between the respective results, as, for example, the different values of  $(E_i - E_h)$ , the stronger preference of Rh/SiO<sub>2</sub> for the formation of cis 2-butene, and the faster isomerisation of 1-butene in the absence of hydrogen on Rh/SiO<sub>2</sub> than on Rh/Al<sub>2</sub>O<sub>3</sub>.

9.1 The Hydrogenation of 1-Butene./

## 9.1 The Hydrogenation of 1-Butene.

The mechanism most generally accepted for hydrogenation reactions involves the formation of a "half-hydrogenated state," i.e. an alkyl radical, as described in section 1.4. There are two principal mechanisms whereby this intermediate can be formed; first, the Langmuir-Hinshelwood mechanism involves dissociatively adsorbed hydrogen, viz.

Reaction Scheme A.



The observed kinetics of the hydrogenation reaction on both Rh/Al<sub>2</sub>O<sub>3</sub> and Rh/SiO<sub>2</sub> indicate that the hydrocarbon was strongly adsorbed and that hydrogen was comparatively weakly adsorbed, possibly on sites unavailable for 1-butene adsorption due to geometrical factors. Assuming competitive adsorption, however, the Langmuir adsorption isotherms for 1-butene and hydrogen are:

$$\theta_{\text{C}_4\text{H}_8} = \frac{b_B p_B}{1 + b_B p_B + b_H^{\frac{1}{2}} p_H^{\frac{1}{2}}}$$

$$\theta_H = \frac{b_H p_H}{1 + b_B p_B + b_H^{1/2} p_H^{1/2}}$$

where  $B = C_4H_8$ . Under the conditions described above, these simplify to  $\theta_{C_4H_8} \approx 1$  and  $\theta_H \propto p_{H_2}^{1/2}$ .

Consideration of the kinetics of each step in reaction scheme A shows that if step 2 is rate-determining, the rate expression is:

$$\text{rate} = k_2 \theta_{C_4H_9} \theta_H$$

A steady state analysis with respect to  $\theta_{C_4H_9}$  shows that

$$\theta_{C_4H_9} = \frac{k_1 \theta_{C_4H_8} \theta_H}{k_2 \theta_H + k_{-1}}. \quad \text{Substitution of this in the rate}$$

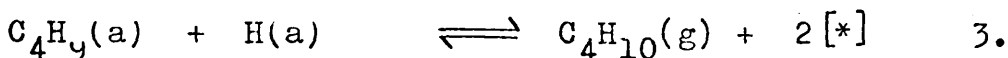
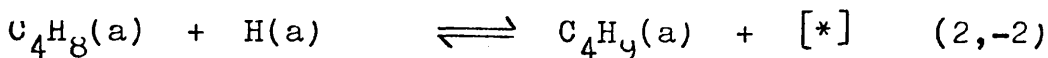
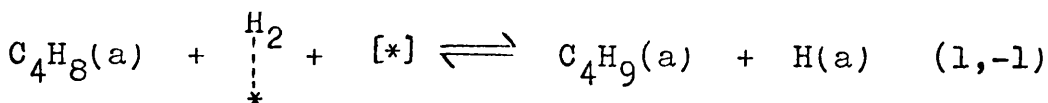
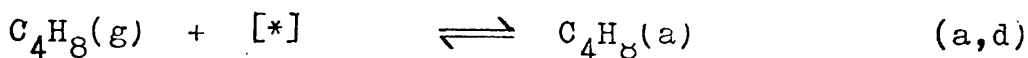
expression for step 2 shows that the overall rate is given by:

$$\text{rate} = \frac{k_1 k_2 \theta_{C_4H_8} \theta_H^2}{k_2 \theta_H + k_{-1}}.$$

Thus, assuming that  $k_{-1} \gg k_2 \theta_H$ ,  $\text{rate} \propto p_{H_2}$ , which is in agreement with the observed kinetics. No other step can give the same overall kinetics.

The second mechanism generally considered for hydrogenation is a Rideal-Eley mechanism, involving reaction of adsorbed 1-butene with molecular hydrogen, viz.

Reaction Scheme B./

Reaction Scheme B

A steady state analysis shows that:

$$\theta_{C_4H_9} = \left( \frac{k_1 k_2 P_{H_2}}{k_{-2}(k_{-1} + k_3)} \right)^{\frac{1}{2}} \quad \text{and} \quad \theta_H = \left( \frac{k_1 k_{-2} P_{H_2}}{k_2(k_{-1} + k_3)} \right)^{\frac{1}{2}}$$

If step 3 is rate-determining it is apparent that an order of unity in hydrogen is obtained. Similarly, if step 1 is rate-determining, then:

$$\text{rate} = k_1 \theta_{C_4H_8} P_{H_2}$$

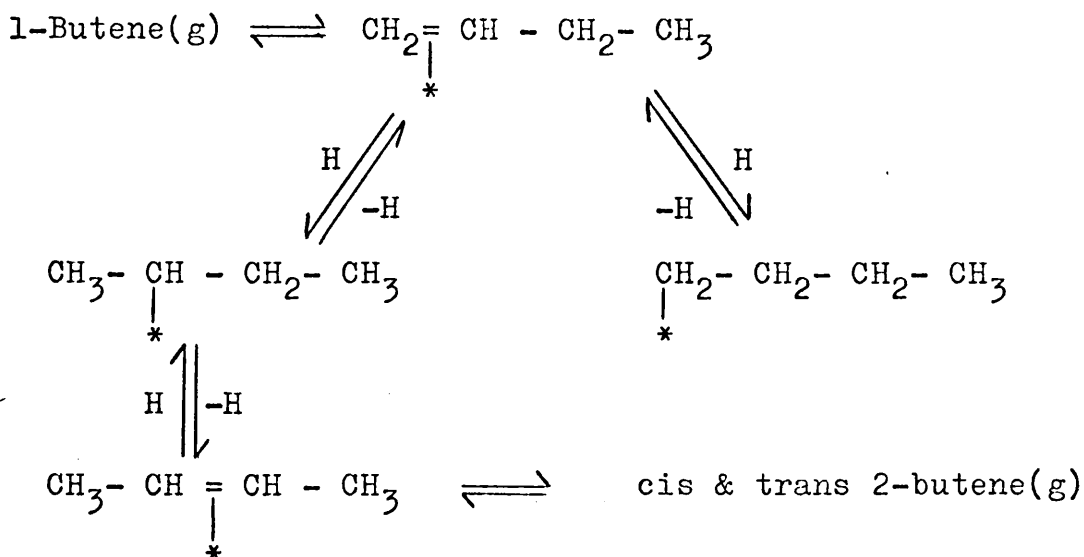
It is therefore evident that kinetic orders of zero in butene and unity in hydrogen may be obtained for hydrogenation with both the Langmuir-Hinshelwood and Rideal-Eley mechanisms, and thus it is impossible to distinguish between them on kinetic evidence alone.

## 9.2 The Isomerisation of 1-Butene.

The isomerisation results will be discussed with regard



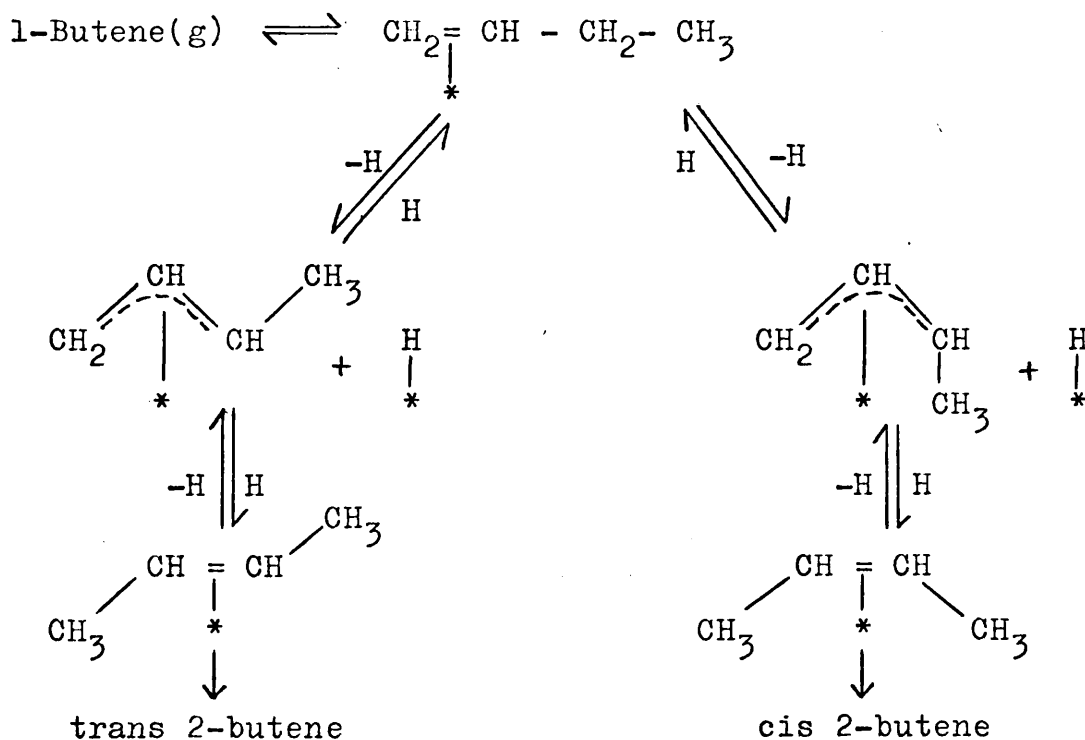
to the two general isomerisation mechanisms described in section 1.4.4, namely, those proceeding via adsorbed alkyl or  $\pi$ -allylic intermediates respectively. It is assumed, in the light of the discussion on the hydrogenation reaction, that  $C_4H_9$  radicals exist on the surface, and therefore the possibility of alkyl reversal must be considered, viz.



The observed kinetics of isomerisation are effectively zero order in hydrogen on both catalysts; the reaction rate is therefore independent of  $\theta_H$ , which suggests that butene desorption might be the rate-determining step. Two factors make this improbable. First, if desorption is rate-determining, it might be expected that  $E_i < E_h$ , and, second, the order of the reaction with respect to 1-butene might be expected to be zero or positive. Each of these suppositions is contrary to the experimental observations, and

it thus appears that alkyl reversal does not satisfactorily explain the isomerisation mechanism.

The alternative mechanism, whereby the reaction proceeds via a 1-methyl- $\pi$ -allyl intermediate is shown in the reaction scheme below.



The rate-determining step of this reaction might be expected to be formation of the 1-methyl- $\pi$ -allyl intermediate as it involves rupture of a carbon-hydrogen bond; the rate may be written as  $\text{rate} = k \theta_{\text{C}_4\text{H}_8}$ , and hence it is independent of hydrogen coverage. This is in agreement with the observed zero order in hydrogen pressure. The negative order in the 1-butene pressure may be interpreted as im-

-plying that  $\theta_{C_4H_8}$  rises slightly with increasing pressure, and therefore reduces the availability of sites for adsorption of the  $\alpha$ -hydrogen atom. It may be noted the hydrogenation reaction also exhibits a very slightly negative order ( $\sim -0.07$ ), which similarly suggests that increasing 1-butene pressure decreases the hydrogen coverage slightly. The rate-determining step of this mechanism involves fission of a carbon-hydrogen bond, and a reasonable explanation is therefore given of the observation that  $E_i > E_h$ <sup>36</sup>.

It has been shown, therefore, that a  $\pi$ -allylic mechanism is consistent with the experimental observations: there are several important implications inherent in this postulate, and the extent to which these are in accord with the observed results will be a strong indication of its validity.

First, if isomerisation does not occur by alkyl reversal, the butyl intermediates formed in the hydrogenation of 1-butene must be 1-butyl rather than 2-butyl. The implication of this is that butene exchange should occur independently of isomerisation, and it is thus significant that Bond et al. have found that  $Rh/Al_2O_3$  is more efficient for exchange than for isomerisation at low temperatures. As will be shown in chapter 11, similar results have also been obtained with  $Rh/SiO_2$  catalysts, and thus the prediction

of the postulate appears to be fulfilled. In order to test fully the validity of the postulate however, it would be necessary to determine the position of the exchanged deuterium atoms, or alternatively to obtain a mass spectrum for the terminal methylene group.

Second, the yields of the cis and trans 2-butenes are determined by the relative proportions of the adsorbed anti and syn conformations of the 1-methyl- $\pi$ -allyl intermediate. As the cis isomer is initially produced in excess of the trans at temperatures up to  $\sim 75^{\circ}\text{C}$  on both Rh/Al<sub>2</sub>O<sub>3</sub> and Rh/SiO<sub>2</sub>, it is apparent that the product trans/cis ratio is determined by a factor other than the thermodynamic equilibrium proportions, and it is probable that the stability of the  $\pi$ -allyl-metal complex formed by each conformer is the relevant factor. The preferential formation of the cis isomer continues until beyond its equilibrium proportion on both Rh/Al<sub>2</sub>O<sub>3</sub> and Rh/SiO<sub>2</sub> up to at least  $75^{\circ}\text{C}$ . While the height of the cis maximum remained constant at  $\sim 30\%$  on Rh/Al<sub>2</sub>O<sub>3</sub>, irrespective of the temperature, and varied around 35 - 40% above  $0^{\circ}\text{C}$ , and was as high as 50% at  $-16^{\circ}\text{C}$  on Rh/SiO<sub>2</sub>, it is apparent from the trans/cis ratios that the cis isomer is more strongly preferred at low temperatures; Rh/SiO<sub>2</sub> also exhibits a stronger directing effect than Rh/Al<sub>2</sub>O<sub>3</sub>. It can therefore be postulated that the relative

surface concentrations of the adsorbed 1-methyl- $\pi$ -allyl intermediates are the reverse of the equilibrium gas-phase proportions of the corresponding 2-butenes. The lower is the temperature, the greater therefore is the tendency to produce cis 2-butene until considerably in excess of the gas-phase equilibrium proportion. It is significant, in the light of this postulate, that evidence has been found elsewhere for preferential formation of the cis isomer in rhodium catalysed reactions, such as the  $\text{RhCl}_3^-$  catalysed isomerisation of 1-pentene,<sup>78,79</sup> the  $[\text{acac Rh}(\text{C}_2\text{H}_4)_2]-\text{HCl}$  or  $[(\text{C}_2\text{H}_4)_2 \text{RhCl}]_2-\text{HCl}$  catalysed isomerisation of 1-butene,<sup>80</sup> and the  $\text{RhCl}_3$  catalysed hydrogenation of 1-hexene.<sup>81</sup> It is also consistent with the observation that increasing temperature favours the syn conformation of the complex  $(\pi-\text{C}_4\text{H}_7)\text{Co}(\text{CO})_3$ .<sup>82</sup>

There are a number of reports of similar phenomena on other metals, and also on metal oxides,<sup>49,51,83</sup> where carbonium ion mechanisms have been postulated,<sup>52,83</sup> although not accepted by all workers in the field.<sup>51</sup> If such ions are in fact intermediates in butene isomerisation, it is apparent that the  $\text{C}_4\text{H}_7$  radical, and the  $\text{C}_4\text{H}_7^+$  carbonium ion have strong structural similarities and it may reasonably be accepted that similar product distributions might be obtained with each. In contrast, the 2-butyl intermediate

has a quite different structure, and consideration of the most stable adsorbed conformation leads to the conclusion that the minimum trans/cis ratio should be unity.<sup>84</sup> Furthermore, on these geometrical considerations one would expect the (trans/cis) ratio to decrease with increasing temperature.

A third feature of the postulated  $\pi$ -allyl mechanism is that one might predict that the reaction could occur in the absence of molecular hydrogen by intra- or intermolecular hydrogen transfer, whereas it is readily apparent that the alkyl reversal mechanism could not be initiated without a source of hydrogen atoms.

The results presented in section 5.4 show that on Rh/Al<sub>2</sub>O<sub>3</sub> the isomerisation of 1-butene in the absence of molecular hydrogen is slower by a factor of 10<sup>-3</sup> than when hydrogen is present. On Rh/SiO<sub>2</sub>, it is slower by a factor 10<sup>-2</sup>, with the result that the isomerisation proceeds rather further in the absence of hydrogen on Rh/SiO<sub>2</sub> than on Rh/Al<sub>2</sub>O<sub>3</sub>. The occurrence of the isomerisation reaction on both catalysts in the absence of hydrogen is apparently firm evidence in favour of the former mechanism. There are, however, two factors which detract considerably from the value of this evidence. First, the reduction of the rate by a factor of 10<sup>-2</sup> - 10<sup>-3</sup> is apparently inconsistent with a zero order dependence on hydrogen pressure.

It is possible, however, that the rate may be dependent upon  $\theta_{\text{H}}$ , and hence also on  $p_{\text{H}_2}$ , at very low pressures, and that the order decreases to zero only at pressures of the same order as those used in the hydroisomerisation studies. It is therefore improbable that isomerisation by intramolecular hydrogen transfer occurs to any significant extent.

The second factor is the problem of determining the extent of residual hydrogen on the surface. This was partially investigated on  $\text{Rh}/\text{SiO}_2$  by activating the catalyst in deuterium; it is apparent from the results shown in table 5.27 that the procedure employed removed only a part of the adsorbed deuterium, and that the residual amount was available to exchange with the butenes. This result is consistent with observations made on the effect of flowing helium over a tritiated catalyst.<sup>10</sup> The implication of this is that isomerisation does not necessarily occur by intra- or inter-molecular exchange of hydrogen atoms. The availability of a surface pool of hydrogen atoms must therefore assist the isomerisation reaction, and, as the total surface hydrogen increases with the pressure, it must be concluded that the ability of the pool to promote isomerisation reaches a limit at a low hydrogen pressure. This is identical to the earlier postulate, namely, that isomerisation is only zero order in hydrogen above a certain pressure.

It is apparent, however, from the results of the reactions on Rh/SiO<sub>2</sub>, that a study of reactions in the total initial absence of hydrogen is impracticable with the standard techniques used in the present study. It was stated initially that the results apparently confirmed the operation of a  $\pi$ -allyl mechanism: it is now seen, however, that the results neither support nor refute either mechanism.

### 9.3 Deactivation of the Catalysts.

It was observed in chapter 5 that both Rh/Al<sub>2</sub>O<sub>3</sub> and Rh/SiO<sub>2</sub> suffered progressive deactivation with successive reactions. This became apparent in the "course of reaction" series (tables 5.1 and 5.2) but could be observed on a more quantitative basis by the decrease in the measured rates of the standard reactions in the series to determine the kinetics and activation energies. A number of regular trends emerge from a consideration of all of these results. First, deactivation is greater at low temperatures. This is particularly evident in the contrast between series A (-20°C) and series E and F (67° and 153°C respectively) for Rh/Al<sub>2</sub>O<sub>3</sub>, where a short reactivation was required after four reactions at -20°C, whereas virtually no deactivation occurred at 67° or 153°C.

The effect of carrying out successive reactions at different temperatures is seen in tables 5.17, 5.19, 5.21



and 5.23. The deactivation is apparently similar in both the low and high temperature series, but within each series there is generally less deactivation after a reaction at a temperature above the standard. An analogous situation is obtained in each of the series to determine the reaction kinetics; less deactivation results from a reaction with a high initial hydrogen/1-butene ratio, and vice-versa.

It is reasonable to assume that the deactivation is caused by the accumulation on the surface of very strongly adsorbed hydrocarbon residues; these reduce the adsorption of reactants in successive reactions, and most probably react at a slow rate with the fresh reactants. That they must react to some extent is apparent from the regeneration of catalytic activity by brief treatment with hydrogen. More conclusive evidence is obtained from the reaction carried out on Rh/SiO<sub>2</sub> with equal pressures of deuterium and 1-butene immediately following the series of reactions in the absence of hydrogen (deuterium); the rate was initially very slow, but increased considerably over a period of 15 minutes. It is interesting to note also that reactivation is brought about more by reactions with a high initial hydrogen/1-butene ratio than by reactions at higher temperatures.

It may therefore be concluded that the deactivation is caused by the formation of hydrocarbon residues on the

surface, principally through there being insufficient hydrogen. Residue formation is greater at low temperatures, as their reaction with available hydrogen during a reaction is presumably slower at low temperature. Regeneration by evacuation has only a limited value unless preceded by hydrogen treatment, the effect of this being greater at high temperature. The situation is therefore analogous to that discussed in section 9.2, where deuterium could not be desorbed from Rh/SiO<sub>2</sub> by thermal evacuation, but could interact with other adsorbed species.

#### 9.4 The Support Effect.

Reactions were carried out on the pure support materials to investigate (i) the possibility of a reaction on the support contributing to the total reaction products, and (ii) the possibility of synergistic effects. The results presented in chapter 6 show that on SiO<sub>2</sub>, hydrogenation is negligible, while isomerisation is virtually so. On Al<sub>2</sub>O<sub>3</sub>, however, isomerisation is considerable, and a small amount of hydrogenation occurs. Even on Al<sub>2</sub>O<sub>3</sub>, however, the specific rates are negligible compared with those on the rhodium catalysts, and the main conclusion from this section is that any reaction on the support itself makes a negligible contribution to the products of the metal catalysed reaction.

The possibility must be considered, however, that in the supported metal catalysts the support may nevertheless play a significant role, and may even be activated in some way by the presence of the metal. It is evident from the different values of  $(E_i - E_h)$  and the relative preferences for cis 2-butene formation, on the two supported catalysts that the support must have some influence on the reaction.

Further evidence of this may be obtained from the results presented in section 5.4.2 on the exchange of 1-butene with residual surface deuterium, in the absence of gas-phase deuterium. The total number of deuterium atoms incorporated in the hydrocarbon from the catalyst is  $4.3 \times 10^{18}$  and  $3.6 \times 10^{18}$  for reactions S1/2 and S1/3 respectively. As the products of reaction S1/1 were lost during extraction, it is necessary to assume that their total deuterium content was in proportion to the succeeding reactions, i.e.  $5.1 \times 10^{18}$  atoms. The total number of deuterium atoms removed from the catalyst by exchange with the butenes is therefore  $1.3 \times 10^{19}$ . This compares with only  $0.29 \times 10^{19}$  rhodium atoms, and, further, as the mercury adsorption results suggest that only 1 in 8 of the rhodium atoms are available for adsorption, the number available from hydrogen adsorption may be as low as  $0.04 \times 10^{19}$ . It is thus apparent there is a large excess of adsorbed deuterium atoms over available rhodium atoms, and it must be

concluded that adsorption is therefore occurring on the support. It is also possible that exchange occurs with the hydroxyl groups in the support.

A number of major assumptions were made in the calculation of the adsorbed deuterium atoms, viz. (i) that the value of S1/1 was in proportion to the succeeding reactions, (ii) that the deuterium numbers of the cis and trans 2-butenes in reaction S1/2 were the same, and (iii) that the observation that the 1-butene and trans 2-butene in S1/3 contained no deuterium was valid. It is thus apparent that the value of  $1.3 \times 10^{19}$  is somewhat approximate, and is likely to be an underestimate.

It is significant that the residual deuterium corresponds to  $1.3 \times 10^{21}$  deuterium atoms per gram of catalyst; this figure is very close to values obtained in studies of residual tritium on a number of supported metal catalysts.<sup>10,85</sup>

## 9.5 Conclusions.

The results of the hydroisomerisation reaction lead us to the conclusion that isomerisation occurs via a 1-methyl- $\pi$ -allyl intermediate on both Rh/Al<sub>2</sub>O<sub>3</sub> and Rh/SiO<sub>2</sub>; this mechanism satisfactorily explains most of the characteristics of the reaction and its product distribution, and there is no evidence which contradicts this postulate.

The results are in general agreement with those of Bond et al.,<sup>46,84</sup> who suggested that Rh/Al<sub>2</sub>O<sub>3</sub> was a "good" isomerisation catalyst at high temperatures ( $\sim 100^{\circ}\text{C}$ ) and a "poor" one at low temperatures ( $\sim 0^{\circ}\text{C}$ ). These studies show conclusively, however, that this effect is caused only by the fact that  $E_i - E_h \approx 5 \text{ kcal.mole}^{-1}$ ; the mechanism remains the same on both catalysts over the temperature range studied. As  $E_i - E_h \approx 1.5 \text{ kcal.mole}^{-1}$  for Rh/SiO<sub>2</sub>, its isomerisation activity, relative to hydrogenation, is retained, to much lower temperatures.

It is also evident that the presence of the rhodium is essential to the reaction. Nevertheless, it appears certain that adsorption of hydrogen on the support occurs to a large extent, although the influence this has on the value of  $\theta_H$ , and therefore the reaction kinetics, cannot yet be established.

CHAPTER 10DISCUSSION OF MERCURY ADSORPTION.10.1 Characteristics of Mercury Adsorption.

The salient features of the adsorption of mercury on Rh/SiO<sub>2</sub> are the rapid initial adsorption until monolayer coverage is approached, and the dependence of the total adsorbed mercury upon temperature.

The isothermal adsorption characteristics are comparable with those obtained for the adsorption of e.g. ethylene, hydrogen, or nitrogen, on metal films, where the rate falls gradually from its initial high value as the equilibrium coverage is approached. As was discussed briefly in chapter 1, the term "monolayer coverage" may be open to more than one real meaning, but, if the concept of adsorption on all the surface sites is taken to imply saturation of the available sites, the term may be applied to the equilibrium coverage obtained on Rh/SiO<sub>2</sub>.

The use of the monolayer concept enabled intermediate coverages to be readily defined as a percentage of monolayer for that temperature. It did not, however, take account of any variation in the absolute mercury/rhodium ratio with temperature. Evidence that such a variation occurs comes from two sources, (i) stages 2 and 3 of the "isothermal" adsorption in Fig. 7.1, and (ii) the mercury/rhodium ratios

obtained at 25°, 48° and 83°C.

During stage 1 (Fig. 7.1), true isothermal adsorption occurred, and a monolayer corresponding to ~160c.p.m. was reached. It was noted, however, that the first two counts in stage 2, at 33 and 34 hours respectively, were ~175c.p.m., and that the temperature of the catalyst vessel was 18°C, compared to 12°C in stage 1. The temperature of the catalyst vessel was then lowered to ~10°C, and it is interesting to note that the count-rate returned to ~165c.p.m. It is unlikely, however, in view of the results of section 7.1.3, that desorption occurred at this temperature; it is also significant that the statistical error on these count-rates is  $\pm 4$ c.p.m. It is, however, possible to infer from the results of stage 2 that mercury adsorption may increase with increasing catalyst temperature.

This trend is shown much more impressively in the results of stage 3. This is effectively an isothermal adsorption at 27°C, and it may be noted (Fig. 7.1) that the coverage increases in a manner comparable to the latter part of stage 1, to a final count-rate of ~205c.p.m. It is reasonable to conclude, then, that a new equilibrium is reached at this temperature, corresponding to the saturation of, and thus the availability of, ~25% more adsorption sites.

The mercury adsorption studies at 25°, 48°, and 83°C, for which absolute mercury/rhodium ratios were obtained, are in broad qualitative agreement with the above results. The ten-fold increase ( $\frac{1}{60}$  to  $\frac{1}{6}$ ) from 25° to 48°C is rather larger than expected on the basis of the previous results, but there is no reason to doubt its validity. The slight ratio decrease at 83°C (1/7) may be within experimental error of the value at 48°C, and therefore cannot necessarily be regarded as being of great significance.

The study of the behaviour of adsorbed mercury during continuous increase in temperature produced some interesting results. First, it was apparent that no desorption occurred at temperatures below 120°C. There is evidence to suggest that slight desorption occurred immediately above that temperature, but this is inconclusive. Between 120° and 300°C, however, 85% adsorbed mercury was desorbed under vacuum. No mercury desorption was induced by carrying out 1-butene hydrogenation reactions at temperatures between 0° and 60°C, while in the systematic reaction series on poisoned catalysts, no desorption was observed after reactions performed at temperatures up to 83°C.

Consideration of tables 7.2 and 7.3 shows that the catalytic activity after the high-temperature desorption treatment is intermediate between the pre- and post-adsorp-



-tion activities. This is best illustrated by the butene distributions, and the rates of hydrogenation. The isomerisation rates are apparently inconsistent, but the  $r_i/r_h$  values exhibited the expected behaviour.

## 10.2 Conclusion.

An interpretation of the results discussed in this chapter must account primarily for the increase in total adsorption with temperature, and the resistance to desorption; a secondary consideration is the small decrease in adsorption between  $48^\circ$  and  $83^\circ\text{C}$ .

It is evident that, at temperatures between  $25^\circ$  and  $83^\circ\text{C}$ , mercury is very strongly adsorbed, and that desorption does not occur. It is possible that adsorption is an activated process; it is more probable, however, that adsorption itself requires no activation energy, and that it is a random process. As surface migration involves partial desorption, it is necessarily an activated step, and thus migration of the adsorbed atoms would increase with temperature. If it is assumed that this leads to clustering of the mercury atoms, or possibly the adsorption of mercury on sites which otherwise would be unavailable for it, it is to be expected that the total extent of adsorption will increase with temperature. It may be noted that evidence for clustering of mercury atoms on palladium has previously

been reported.<sup>14</sup> The value of  $E_d$  is considerable, as no desorption occurs until the temperature  $\geq 120^\circ\text{C}$ .

The effect of varying the temperature of the catalyst vessel while maintaining the mercury source at a constant temperature was not studied as a separate experiment. It has previously been suggested that the result of this is to decrease the amount of adsorption as the temperature difference increases.<sup>86</sup> The adsorption ratios obtained at  $48^\circ$  and  $83^\circ\text{C}$  are in agreement with this behaviour, but, as the vapour pressure of mercury over the catalyst must be constant in such circumstances, it is difficult to reconcile this with the concept of temperature dependent availability of adsorption sites. Further, the count-rates in Fig. 7.1, stage 2, contradict the application of this suggestion to the results presented in chapter 7. It is more probable that the monolayer coverage is determined by the temperature of the catalyst vessel alone, and the rate of attainment of the monolayer by both the catalyst vessel temperature and the vapour pressure of the mercury, i.e. the temperature of mercury source.

## CHAPTER 11

### DISCUSSION OF THE REACTION OF 1-BUTENE WITH DEUTERIUM IN THE PRESENCE & ABSENCE OF MERCURY.

A number of very significant trends emerge from the results presented in chapter 7. First, it is evident that as the mercury coverage is increased, the hydrogenation reaction is inhibited to a much greater extent than is the isomerisation. Second, the dependence of the rate of isomerisation upon mercury coverage varies considerably according to the temperature.

#### 11.1 Poisoning of the Catalyst for Hydrogenation.

The decrease in the rate of hydrogenation with increasing  $\theta_{\text{Hg}}$  was illustrated in Fig. 7.3, where it is seen that the rate falls uniformly at each temperature and the catalytic activity is reduced to zero only at  $\theta_{\text{Hg}} = 100\%$ . The presence of the mercury may be considered to exert one or more of the following effects.

- (i) By occupying surface sites, it inhibits adsorption of 1-butene and hydrogen, and thus lowers  $\theta_{\text{C}_4\text{H}_8}$  and  $\theta_{\text{H}}$ .
- (ii) As 1-butene is more strongly adsorbed than hydrogen, it is possible that competitive adsorption of each on a partially poisoned surface restricts adsorption of hydrogen more than the

- (ii) 1-butene. The effect of this would be to lower  $\theta_{\text{H}}$  by a relatively greater amount than  $\theta_{\text{C}_4\text{H}_8}$ .
- (iii) Irrespective of the dependence of  $\theta_{\text{C}_4\text{H}_8}$  and  $\theta_{\text{H}}$  upon  $\theta_{\text{Hg}}$ , the interaction of the adsorbed species may be hindered by physical obstruction of the surface, assuming that the species are mobile.
- (iv) In the event of non-competitive adsorption of 1-butene and hydrogen at higher values of  $\theta_{\text{Hg}}$ , adsorption of hydrogen would become relatively more favourable than adsorption of 1-butene.

It will be assumed for this discussion that all the adsorbed mercury atoms are on surface rhodium sites (chapter 10). It is therefore apparent that the mercury must exert at least a physical blocking action on the surface, even if electronic factors are unimportant, and thus it must be considered that (i) will occur. The courses of reactions on the poisoned catalysts suggest there is little change in the reaction kinetics with increasing  $\theta_{\text{Hg}}$ , except for a possible trend for reactions to be initially zero order. It may therefore be assumed that 1-butene is more strongly adsorbed than hydrogen on both poisoned and unpoisoned surfaces, but there is no direct evidence to suggest whether or not their relative strengths of adsorption are altered by the mercury, and hence no definite conclusions may be

drawn at this stage on effect (ii). Similarly, there is insufficient information available to determine if the inhibition of the catalyst is due solely to a reduction of  $\theta_{C_4H_8}$  and  $\theta_H$ , or if the interaction on the surface (iii) of the respective species is also obstructed. It was shown by Campbell & Thomson that hydrogen may be displaced from nickel films by mercury,<sup>73</sup> whereas propylene could not,<sup>72</sup> and thus it is improbable that hydrogen adsorption may be favoured over butene adsorption at high mercury coverage. Further, if it were to occur, it might be expected that the decrease of the reaction rate would be halted at high values of  $\theta_{Hg}$ . As this is not in accord with the experimental observations it may be concluded that effect (iv) does not operate. Thus, the inhibition is caused by the reduction of  $\theta_{C_4H_8}$  and  $\theta_H$ .

It was shown in chapter 9 that the reaction kinetics on the unpoisoned catalyst were consistent with the reaction of adsorbed 1-butene with either adsorbed hydrogen atoms or molecular hydrogen. It may be anticipated that the presence of the poison might increase the probability of reaction with molecular hydrogen, i.e. a Rideal-Eley mechanism, but the only new feature of the reactions on the poisoned catalyst was an apparent trend for the reactions to be initially zero order.

## 11.2 Poisoning of the Catalyst for Isomerisation.

### 11.2.1 The Rate of Isomerisation.

It was shown in chapter 9 that the observed features of the isomerisation on unpoisoned Rh/SiO<sub>2</sub> were consistent with a mechanism involving an adsorbed  $\pi$ -allylic intermediate. The results of the reactions on the poisoned catalysts will now be considered to determine if they support the same mechanism, or if a change of mechanism is induced by the poison.

It is observed, first, that the decrease in the rate with increasing  $\theta_{\text{Hg}}$  is almost linear at 0°C, while at 69°C there is no decrease at all until  $\theta > 80\%$ . A similar situation to the latter holds at 21°C. It has previously been suggested that "crowding" of mercury atoms may occur during the hydrogenation of acetylene on Pd/Al<sub>2</sub>O<sub>3</sub>.<sup>14</sup> The above observations may therefore be explained in terms of this effect; it would be expected "crowding" would be greatest at high temperature, and this is in accord with the experimental observations. According to the  $\pi$ -allyl mechanism, rate  $\propto \theta_{\text{C}_4\text{H}_8}$ , and thus only an adsorbed 1-butene molecule and a vacant adsorption site adjacent to it are required for the reaction to occur. This compares with a statistical treatment, which shows that linear deactivation is consistent with the reaction

requiring only one site.<sup>88</sup> It is also significant that, particularly at high temperatures, the rate is virtually unaffected by the mercury, while the hydrogenation is greatly inhibited. This is evident from Figs. 7.3 and 7.4, and also in the plot of  $r_i/r_h$  vs.  $\theta_{\text{Hg}}$  (Fig. 11.1). It may therefore be inferred that, while the interaction of adsorbed 1-butene with hydrogen is retarded, loss of the allylic hydrogen atom is able to occur virtually unhindered. This may be understood if it is assumed that 1-butene cannot cover every adsorption site, owing to geometric restrictions, and thus the probability of there being a suitable vacant site remains high until  $\theta_{\text{Hg}}$  approaches unity. As the poisoning of hydrogenation implies a diminution of  $\theta_{\text{C}_4\text{H}_9}$ , isomerisation by alkyl reversal would necessarily be somewhat inhibited also.

It may be further inferred that, as 1-butene continues to be adsorbed on the poisoned catalyst, adsorption of hydrogen is prevented by the mercury to a relatively greater extent than is adsorption of 1-butene.

### 11.2.2 The Trans/Cis Ratio.

Consideration of the trans/cis ratios in the 2-butene products shows an apparent trend for the ratio to increase with  $\theta_{\text{Hg}}$ , that is, for the trans isomer to be favoured at higher mercury coverages. It may be shown, however, that

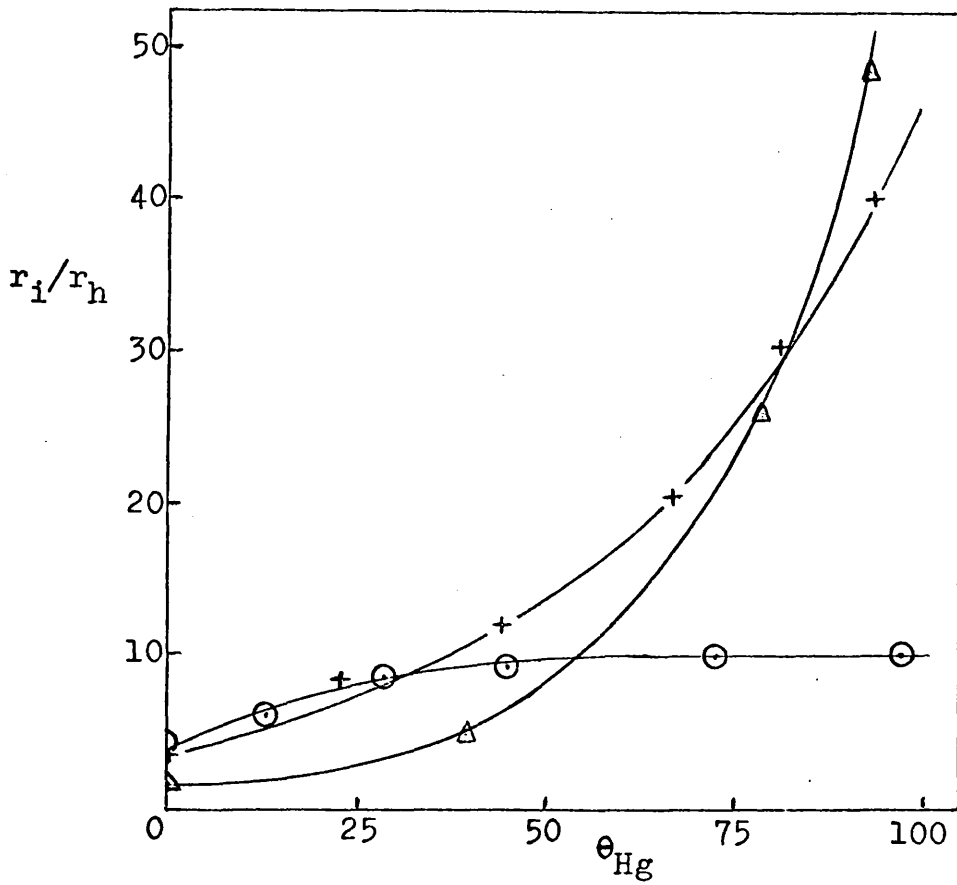


Fig. 11.1 Variation of  $r_i/r_h$  with  $\theta_{Hg}$ .

○ -  $0^\circ C$     Δ -  $21^\circ C$     + -  $69^\circ C$



this result is only a consequence of the increase in  $r_i/r_h$  with  $\theta_{Hg}$ : Comparison of the trans/cis ratio with the percentage 2-butenes, i.e. with the extent of isomerisation, for each value of  $\theta_{Hg}$  shows conclusively that the adsorbed mercury has little effect upon the ratio, and it is thus inferred that the main factor determining the proportions of the cis and trans 2-butene products is the extent of the isomerisation reaction. If it is assumed that the relative strength of adsorption decrease in the order

1-butene > cis 2-butene > trans 2-butene,

for which there is considerable indirect evidence,<sup>90,91</sup> it may be deduced that the trans/cis ratio is determined solely by the thermodynamics of the readsorption of the 2-butenes, and is not affected by the mercury.

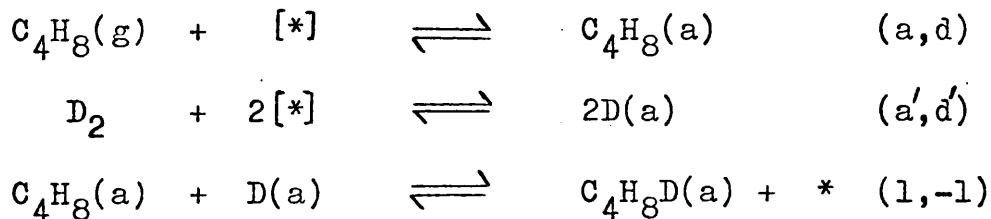
### 11.3 The Exchange Reactions.

#### 11.3.1 Butene Exchange on Unpoisoned Catalysts.

The discussion of the hydroisomerisation of 1-butene on poisoned and unpoisoned Rh/SiO<sub>2</sub> catalysts has enabled a number of postulates to be made concerning the mechanisms of the surface processes. The results of the exchange reactions will thus be considered with two aims in view; (i) to characterise the exchange of 1-butene on Rh/SiO<sub>2</sub>, and (ii) to determine if the results are consistent with the postulated reaction and poisoning mechanisms.

The principal features of the deuterio-butene distributions are that the 2-butenes initially have a considerably higher deuterium content than has the 1-butene, but as the conversion increases, the deuterium content of the reactant 1-butene increases more rapidly than that of the 2-butenes. The n-butane invariably contains a mean of less than two deuterium atoms per molecule, thus indicating considerable addition of exchanged hydrogen. It may be inferred from this that addition may at least partly occur by reaction of adsorbed 1-butene with molecular hydrogen; there is therefore no step giving direct recombination of hydrogen atoms, which accounts for a low rate of hydrogen exchange.

It was postulated in chapter 9 that butene exchange occurs by an alkyl reversal mechanism involving predominantly 1-butyl intermediates. The mechanism may be written as follows:



It is to be expected that the 2-butenes should initially contain more deuterium than the 1-butene, as all the isomerised molecules have been in contact with the surface at least once, and thus had the opportunity of exchanging,

whereas a large proportion of the reactant molecules have never been adsorbed. If the postulate that exchange occurs principally via a 1-butyl intermediate is valid, the resulting  $d_1$ -1-butene (the most abundant exchanged species) will contain the deuterium atom on the 2-position, unless multiple reactions occur. Isomerisation of this species, by loss of an  $\alpha$ -hydrogen atom, produces a  $d_1$ - $C_4H_7$  intermediate which may then gain a further deuterium atom, or another hydrogen atom. It is apparent, however, from the high percentage of  $d_0$ -2-butenes (60-90%) that isomerisation occurs mainly without incorporation of a deuterium atom; this evidence makes intra- or inter-molecular hydrogen transfer mechanisms (for isomerisation) seem more plausible, despite the results of the reactions in the absence of hydrogen. The gradual increase in the 2-butene deuterium content is therefore explained in terms of the exchange reaction of the 1-butene; as the reaction proceeds, the probability that adsorbed 1-butene contains at least one deuterium atom increases, and thus the total probability of such a molecule isomerising increases correspondingly. A feature of this mechanism for the incorporation of deuterium in 2-butenes is that one would expect the 2-butene deuterium content to reflect the change in that of the 1-butene, but at a slower rate;

this is in accord with the experimental observations.

It was stated in section 9.2 that Rh/SiO<sub>2</sub> behaved similarly to Rh/Al<sub>2</sub>O<sub>3</sub> with regard to the temperature dependence of the isomerisation and exchange reactions. The evidence for this may now be discussed in some detail. The partial pressure of the isomerisation products is readily obtained from a knowledge of the conversion and butene distribution for each reaction. The partial pressure of the exchanged 1-butenes may similarly be calculated from these factors and the percentage of total exchanged 1-butene. A comparison may therefore be made of the relative yields of isomerisation and exchange products; table 11.1 shows these results for reactions at 21° and 69°C.

It is evident from table 11.1 that Rh/SiO<sub>2</sub> is markedly more efficient for isomerisation than for exchange at 69° than at 21°C; the temperature dependences of the two reactions are thus very different, which would not be the case if the two reactions occurred by the same mechanism. It is thus shown that Rh/SiO<sub>2</sub> behaves in a manner similar to that reported for Rh/Al<sub>2</sub>O<sub>3</sub>, namely, that the activity for exchange falls less rapidly than for isomerisation, with decreasing temperature.

The n-butane is observed to contain a mean number of

deuterium atoms such that:  $D.N.(C_4H_{10}) = D.N.(C_4H_8) + 1 \pm 0.2$ .

TABLE 11.1

Relative Yields of Isomerisation & Exchange Products  
on Rh/SiO<sub>2</sub>.

<u>Reaction</u>	<u>Temperature</u> (°C)	<u>Conversion</u> (%)	<u>Partial Pressures</u>		
			<u>d-1-B</u> (mm.)	<u>2-B</u> (mm.)	<u>I/E</u>
5A/3	21	10.3	2.03	3.0	1.48
5A/1	"	26.5	2.18	7.0	3.21
5A/4	"	41.1	1.26	12.4	9.85
5A/2	"	57.9	0.57	10.6	18.60
8A/3	69	11.0	0.63	8.8	14.0
8A/2	"	51.3	0.38	13.3	35.0

[I/E = ratio of isomerisation yield : exchange yield]

This may indicate that addition is rarely the first process undergone by an adsorbed molecule; it is more certain, however, that a substantial amount of the atoms adding to the butene are exchanged hydrogen, not deuterium, atoms. The deuterium number rises slowly with conversion, and much of this increase is due to the increasing exchange of the butenes. The substantial addition of exchanged hydrogen is consistent with a relatively low initial rate of hydrogen exchange at 0°C.

### 11.3.2 Butene Exchange on Poisoned Catalysts.

The invariable effect of the adsorption of mercury on the catalyst is to increase the total deuterium content of each product. At 69°C, however, this increase is very much less than at lower temperatures, whereas the increase in 2-butene yield, relative to hydrogenation, has been shown to be substantial.

It is significant that the rate of 1-butene exchange generally falls by an amount intermediate between that of the hydrogenation and isomerisation rates, as  $\theta_{\text{Hg}}$  increases. If alkyl reversal is the rate-determining step, the rate expression is

$$\text{rate} = \frac{k_1 \theta_{\text{C}_4\text{H}_8} \theta_{\text{H}}}{k_{-1} + k_2 \theta_{\text{H}}}$$

and thus  $\text{rate} \propto p_{\text{H}_2}^{\frac{1}{2}}$ . It was postulated in section 11.2 that, while  $\theta_{\text{C}_4\text{H}_8}$  is necessarily reduced by the mercury,  $\theta_{\text{H}}$  is possibly reduced by a relatively greater extent; this offers a qualitative explanation of the decrease in the rate of exchange.

Concurrent with the increase in deuterium content of the butenes is a corresponding increase in the deuterio-n-butenes. It may be observed, however, that at 21°C this is partly accounted for by an increase in the  $d_2$ -maximum. As the hydrogen exchange reaction is increased

by the presence of the mercury at 69°C, although not at 0°C, this result is consistent with a greater probability of addition of two atoms of deuterium, at high temperatures. The increase in hydrogen exchange with  $\theta_{\text{Hg}}$  also provides further support for the postulate that  $\theta_{\text{H}}$  is substantially affected by the mercury.

#### 11.4 Conclusion.

Consideration of the hydrogenation and isomerisation reactions leads us to conclude that the former is inhibited to a very much greater extent than the latter by the adsorption of mercury on the catalyst. Whether or not the mercury has a poisoning role other than simple physical obstruction of surface sites cannot be determined by the techniques employed in this work. It appears, however, that the main effect of the mercury is to substantially reduce both  $\theta_{\text{C}_4\text{H}_8}$  and  $\theta_{\text{H}}$ , the latter probably to a greater relative extent than the former. Further evidence has been shown for the operation of a  $\pi$ -allyl isomerisation mechanism, and, further, there is a strong probability that some form of intermolecular hydrogen transfer occurs during this reaction. Irrespective of this, the relative yields of the 2-butene-isomers are unchanged by the mercury.

Reasonable evidence has been shown that exchange occurs predominantly via a 1-butyl intermediate, and that it is less temperature dependent than isomerisation.



CHAPTER 12DISCUSSION OF 1,3-BUTADIENE REACTIONS.12.1 The Hydrogenation Reaction.

The results presented in chapter 8 show that the butene product distribution in the Rh/SiO<sub>2</sub> catalysed hydrogenation of 1,3-butadiene is virtually independent of conversion until the point corresponding to the uptake of 1 mole of hydrogen per mole of butadiene is reached. The ratio 1-butene/2-butene is also independent of temperature, but the trans/cis ratio falls significantly with increasing temperature. Selectivity is high over the temperature range studied, and was initially unity at 83°C. The value decreased slightly with increasing conversion over the whole temperature range.

Two principal mechanisms have been advanced to explain the hydrogenation of 1,3-butadiene on metals; these are (i) direct formation of 1- and 2-butenes by separate 1,2- and 1,4-addition, and (ii) formation of 1-butene by 1,2-addition, and subsequent isomerisation of 1-butene to the 2-butenes. The reaction scheme suggested on the basis of the previous work is shown below. It is assumed the adsorbed structure contains two olefin  $\pi$ -complexes.



diminished. It may be assumed that the observed selectivity is a measure of the mechanistic factor, as the occurrence of the acceleration points in the rate of pressure fall at 25° and 48°C indicates that readsorption of butene occurred only after removal of virtually all the 1,3-butadiene. This is in agreement with the results of Bond, Dowden, and Mackenzie,<sup>87</sup> who showed that of a series of noble metals, rhodium had the highest thermodynamic selectivity factor. A 50 : 1 :: ethylene : acetylene ratio was required before hydrogenation of the ethylene took place to any significant extent.

The  $S_m$  values obtained on Rh/SiO<sub>2</sub>, (0.950 - 1.000) were considerably higher than those obtained by Bond et al. for Rh/Al<sub>2</sub>O<sub>3</sub> (0.743 - 0.906) over a similar temperature range.<sup>55</sup> It is interesting to consider whether the difference is the result of different mechanistic features on the two catalysts, or if thermodynamic factors are responsible. By interpolation in the selectivity vs. conversion curve for Rh-5, the selectivity at 110% conversion at 48°C may be estimated at 0.880. From this value the partial pressures of product butene and residual 1,3-butadiene are calculated to be 25.9mm. and 0.55mm. respectively; it is thus apparent that the acceleration point at 48°C corresponds to a butene/1,3-butadiene ratio of ~47. On Rh/Al<sub>2</sub>O<sub>3</sub>,<sup>55</sup> butane formation increased

significantly after  $\sim 80\%$  removal of butadiene; from the figures of Bond et al., partial pressures of 20mm. and 10mm. for butene and 1,3-butadiene respectively are calculated, leading to a corresponding ratio of  $\sim 2$  before butene readsorption occurs. On this evidence, it appears that the thermodynamic selectivity factors are very different on Rh/SiO<sub>2</sub> and Rh/Al<sub>2</sub>O<sub>3</sub> respectively. Two further points must be noted at this point, however. First, no acceleration in the pressure fall was obtained at 18°C using Rh/Al<sub>2</sub>O<sub>3</sub>; while this is at first sight surprising, it may be explained if the activation energies of hydrogenation of 1-butene and 1,3-butadiene are different, and at that particular temperature the respective reaction rates coincide. Second, the ratio of  $\sim 47$  on Rh/SiO<sub>2</sub>, corresponding to competitive readsorption of butene with 1,3-butadiene; is in striking agreement with the value ( $\sim 50$ ) obtained for ethylene and acetylene on Rh/Al<sub>2</sub>O<sub>3</sub>.<sup>87</sup>

One further feature of the acceleration points requires little explanation. At 25° and 48°C, the acceleration occurs at 120% and 110% conversion respectively. As the selectivity increases slightly with temperature, it follows that the 1,3-butadiene is consumed more rapidly, relative to the rate of pressure fall, at high temperatures, and thus the onset of butene readsorption must

occur at a lower total pressure fall. The absence of an acceleration at  $83^{\circ}\text{C}$  may be explained if the activation energy of hydrogenation is greater for 1,3-butadiene than for 1-butene.

The overall reaction kinetics on  $\text{Rh}/\text{SiO}_2$  were shown to be first order between  $25^{\circ}$  and  $83^{\circ}\text{C}$ . This is in agreement with the results of Bond et al. for the reaction on  $\text{Rh}/\text{Al}_2\text{O}_3$ .<sup>55</sup> The separate orders in initial hydrogen and 1,3-butadiene pressure were determined as 1.0 and 0.0 respectively,<sup>55</sup> and it will be assumed for the purpose of discussing reaction mechanisms that the orders on  $\text{Rh}/\text{SiO}_2$  are similarly unity and zero.

### 12.1.2 The Butene Distribution.

The main purpose in discussing the butene distribution will be to distinguish between the possible mechanisms. It is significant that the 1-butene/2-butene ratio is unchanged with temperature and conversion. Bond and Wells<sup>46</sup> have suggested there is good correlation between the isomerisation activity of a metal and the 2-butene yield from 1,3-butadiene, and have accordingly suggested that the 2-butenes are formed predominantly by isomerisation on Group VIII metals (except cobalt and palladium).  $\text{Rh}/\text{SiO}_2$  has been shown in this thesis to be an efficient catalyst for isomerisation, relative to hydrogenation, over the temperature range under

consideration, and, as the mean yield of 2-butene  $\approx 48\%$ , there is thus an argument for supporting the isomerisation mechanism on this catalyst. There are two mechanisms by which adsorbed 1-butene might isomerise. In the reaction scheme in this section, it may be seen that the reaction may proceed via (i) steps 6", 6 and 6' or (ii) steps -5 and 3. The alkyl reversal mechanism (i) may be discounted for two main reasons. First, as the selectivity is  $\sim 1.00$ , the concentration of adsorbed  $C_4H_9$  radicals must be almost negligibly small. Second, it has already been concluded (chapter 9) that 1-butene isomerisation proceeds via a  $\pi$ -allyl mechanism (i.e. (ii)) on Rh/SiO<sub>2</sub>. If  $k_4$  is the rate determining step in 1,2-addition, the reverse of this step must be considerably slower, and in particular,  $k_{-4} < k_7$ , in order to allow substantial amounts of 1-butene to appear in the gas-phase. It therefore is unlikely that adsorbed 1-butene is able to isomerise greatly via a  $\pi$ -allyl intermediate unless the step from adsorbed 1-butene to adsorbed 1-methyl- $\pi$ -allyl is favoured over the reverse to the half-hydrogenated intermediate, i.e.  $k_{-5} \gg k_{-4}$ .

The constancy of the 1-butene/2-butene ratio over the whole temperature range is further evidence against the operation of the isomerisation process. If  $k_{-5}$  is in

fact an important process, it is to be expected that the isomerisation reaction will follow similar trends to those found in the hydroisomerisation of 1-butene on the same catalyst. One might therefore expect a slight increase in 2-butene yield with increasing temperature, but, in fact, the yield remains constant at  $\sim 48\%$  from  $25^{\circ}$  to  $83^{\circ}\text{C}$ .

Further, there is no significant change in the butene distribution with increasing conversion, nor did the yield of cis 2-butene go through a maximum, at least until butene readsorption took place. It is possible, however, to conceive of a situation wherein the 1-butene might isomerise at a rate dependent on its surface concentration, and, by virtue of butene readsorption being prevented, continue to produce cis and trans isomers in the same proportion.

It may be noted that of the alumina-supported Group VIII metals, rhodium was the only one on which the butene distribution remained unchanged with varying conversion.<sup>55</sup> On account of other evidence, Bond and Wells<sup>46</sup> first advanced the 1,2-addition and isomerisation mechanism for rhodium, but Bond et al.<sup>55</sup> later concluded that 1,4-addition was more probable, although isomerisation may be occurring to a limited extent.

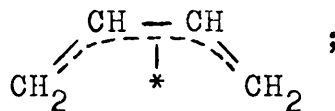
Further possible evidence for the operation of a  $\pi$ -allyl isomerisation mechanism may be found in further

comparison with the work on Rh/Al<sub>2</sub>O<sub>3</sub>. On both catalysts there was a gradual decrease in the selectivity during the initial stages of the reaction, which implies there was a corresponding increase in C<sub>4</sub>H<sub>9</sub> radicals. If isomerisation occurred via this intermediate, an increase in 2-butene yield or a change toward equilibrium proportions would be expected. This does not occur with either catalyst, and it may thus be inferred that any isomerisation must occur by the  $\pi$ -allyl process.

The trans/cis ratio was stated previously to be invariant with conversion. This is true at 25° and 83°C, but at 48°C there appears to be a general decrease with increasing conversion. It is unlikely that the behaviour at the intermediate temperature is quite different to that at the extremes, and if the result for reaction 5B/3 is considered to involve a relatively large experimental error, owing to the low yield of each of the butenes, it is not difficult to consider the mean value of the trans/cis ratio to be ~2.5, and to be independent of conversion. If this situation is accepted, the regular temperature dependence of the ratio becomes apparent; from 2.6 at 25°C it falls to 2.0 at 83°C. This trend is in broad agreement with results obtained elsewhere for both rhodium and other metals.<sup>55</sup>



Consideration of the trans/cis ratio with regard to the possible reaction mechanisms shows that its temperature dependence is in the direction opposite to that which would be expected if 1-butene isomerisation is occurring. It follows, therefore, that the ratio is tending in the same direction as the thermodynamic equilibrium ratio (3.45 and 2.62 at 25° and 83°C respectively). The relative yields of cis and trans 2-butene will be determined by (i) the proportions of the adsorbed anti and syn conformers respectively, and (ii) the rates  $k_3$  and  $k'_3$ . The corresponding gas-phase syn/anti ratio is  $\sim 15$ , but it has been suggested that the anti conformer may be particularly stabilised by adsorption as the structure



stabilisation is obtained by delocalisation of the  $\pi$ -orbitals, and the use of only one metal site reduces geometric restrictions. It is also possible, as a result of this geometric factor, that adsorbed hydrogen may be able to react more readily with this species than with di- $\pi$ -adsorbed syn-butadiene.

It may therefore be concluded, from consideration of both the 1-butene/2-butene and trans/cis ratios, that the butene distribution patterns may be best explained in terms of separate 1,2- and 1,4-addition, while if 1-butene isomerisation occurs to any extent, it must be via a

$\pi$ -allyl intermediate. It is worth noting, however, that, as the 1-butene may equally be formed via steps 1 and 5 or 2 and 4, the result of its isomerisation by steps -5 and 3 is indistinguishable from the product of true 1,4-addition. The constancy of the 1-butene/2-butene ratio with temperature implies further that activation energies of 1,2 and 1,4-addition are the same. If the possibility of reactant adsorption or product desorption as rate-determining steps is discounted, then either the same step is involved, or the energetics of the two steps must be the same. It may be suggested, therefore, that 1-butene is formed primarily by addition at the 2-position to adsorbed 1-methyl- $\pi$ -allyl. This would be expected to be similar to addition at the 4-position.

Further evidence in favour of separate 1,2- and 1,4-addition will be discussed when the effect of mercury poisoning of the catalyst is considered.

## 12.2 The Exchange Reactions.

In the preceding section it became apparent that the mechanism of separate 1,2- and 1,4-addition of hydrogen to the 1,3-butadiene offered the more satisfactory explanation of the butene distribution. Consideration will now be given to the deuterio-product distributions in the light of this, and an attempt made to determine the degree to

which they support the postulated mechanism.

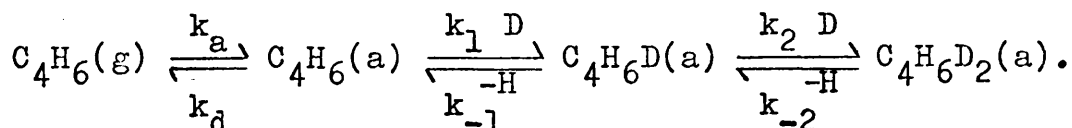
As the 1,3-butadiene is strongly adsorbed, the probability of its desorption is relatively low in the temperature range under consideration. The appearance of exchanged 1,3-butadiene in the gas-phase will therefore be governed more by the thermodynamics of adsorption and desorption than by the rate of the true surface exchange reactions. The distributions of deuterio-butadienes thus give no information regarding the surface concentrations of the various deuterio-butadienes. It follows, therefore, that in considering the exchange reactions, interest is focussed mainly on the deuterio-butenes.

The dominant features to emerge from the deuterium distributions in the products, and which require to be explained in a discussion of mechanisms are as follows.

- (i) The deuterium content of the gas-phase 1,3-butadiene increases uniformly with conversion at each temperature, although the total content is higher at 48°C than at 25° or 83°C.
- (ii) The deuterium number of each of the butenes rises slightly up to the point corresponding to the addition of one mole of deuterium per mole of 1,3-butadiene; this effect is greatest at 25°C (~1.4 to ~1.7) and is only just discernible

- (ii)/at 48°C, while at 83°C the deuterium numbers vary between 1.2 and 1.4, but exhibit no systematic trend.
- (iii) The deuterium content of the 1-butene is generally slightly greater than that of the 2-butenes.
- (iv) The hydrogen exchange process is slow, and increases only slightly with temperature; at 50% conversion, the hydrogen numbers of residual deuterium are 0.095 and 0.130 at 25° and 83°C respectively.

As each of the n-butenes has essentially the same deuterium distribution as the others at each temperature, they may provisionally be regarded as being formed by the same mechanism, which may be written as follows;



As desorption is a slow step, as discussed before, the equilibrium of  $k_1/k_{-1}$  will be reached rapidly compared with the rate of desorption. The exchange of adsorbed 1,3-butadiene is controlled by the relative forward and reverse rates of steps 1 and 2, and, as hydrogen exchange is very slow, it is apparent that when these equilibria are reached the hydrogen from the hydrocarbon must be in

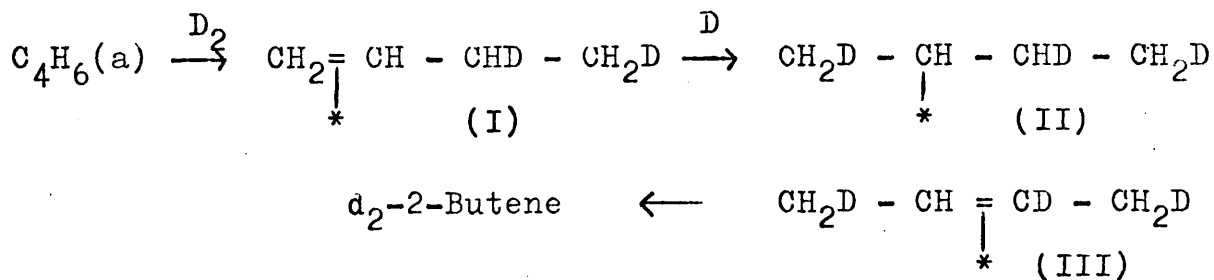
a "pool" of surface hydrogen. It was suggested in section 12.1.1 that the hydrogenation reaction is first order in hydrogen pressure. This implies that step 4 is rate-determining in the production of butene, and hence  $k_1 > k_4$  and  $k_1 > k_5$ . Also, in order that exchange of adsorbed 1,3-butadiene can occur,  $k_{-1} > k_4$  and  $k_{-1} > k_5$ ; it is also probable that  $k_{-2}$  is small. It thus follows that the  $k_1/k_{-1}$  equilibria is reached very rapidly, and that the butenes are formed by addition of a deuterium atom to adsorbed  $C_4H_xD_{7-x}$ , where the proportions of  $x$  and  $7-x$  ( $x=0$  to  $7$ ) are in equilibrium. As desorption of 1,3-butadiene occurs, there is a gradual build-up in the gas-phase of deuterobutadienes during the course of the reaction, and thus there is an increasing probability of readsorption of such species. The effect of this is to upset the equilibrium established when only the  $d_0$ -1,3-butadiene was adsorbed; the total deuterium content of the adsorbed 1,3-butadiene is therefore increased during the reaction, and thus the operation of steps 1 and 2 produces adsorbed butene of gradually increasing deuterium content.

It may be observed that the relative rates postulated for this mechanism implies that the deuterobutene distributions are essentially determined before the addition occurs, and hence that exchange of the adsorbed butene does

not play a major role. This is consistent with the earlier supposition that isomerisation of adsorbed 1-butene is unlikely.

It is apparent that the "pool" of surface hydrogen and deuterium reaches equilibrium rapidly, as is evidenced by the percentage abundances of  $d_0$ - and  $d_1$ -n-butene; these are  $10 \pm 5\%$  and  $25 \pm 5\%$  respectively at  $25^\circ$  and  $48^\circ\text{C}$ , and  $23 \pm 5\%$  and  $33 \pm 5\%$  respectively at  $83^\circ\text{C}$ , and are independent of conversion.

Consideration will now be given to the mechanisms for the formation of the 1- and 2-butenes in the light of their respective deuterium distributions. If the possibility is considered of the isomerisation of adsorbed 1-butene, formed by the addition of two deuterium atoms to  $d_0$ -1,3-butadiene, it is evident that, if isomerisation occurs



by an alkyl reversal mechanism, the most probable alkyl intermediate (structure (III)) will be the  $d_3$ -species; this has a probability of 1/2 of losing H or D from the 3-position, and hence the mean deuterium number of the adsorbed 2-butene (III) is greater than that of the 1-butene

whence it originated.

If, on the other hand, isomerisation occurs via a  $\pi$ -allylic intermediate, this is equivalent to  $k_{-2} > 0$  in the reaction scheme outlined earlier in this section. It follows that for the 2-butene to be so produced, the molecule must go through step 2 at least twice — addition at least once in the 2-position, and once in the 4-position, and the probability of gaining further deuterium atoms is exactly as in the alkyl reversal mechanism. The conclusion is that if isomerisation occurs, the products are more heavily deuterated. As the experimental observation is that the 2-butenes contain only the same or slightly less deuterium than the 1-butene, this must be ruled out as a mechanism for the production of 2-butenes.

Only at 25°C is the 1-butene deuterium content consistently greater than that of the 2-butenes, but the difference is not sufficient to justify suggesting that steps 2, 4, or 5 of the overall reaction scheme (section 12.1) are more readily reversible than steps 1 and 3. Comparison of the trans-cis deuterium distributions shows they are generally very similar, and it may be inferred that they are produced by identical mechanisms, i.e.

$$k_1 = k'_1 \text{ and } k_3 = k'_3.$$

### 12.3 The Effect of Mercury Poisoning.

#### 12.3.1 The Poisoning of the Catalyst for Hydrogenation.

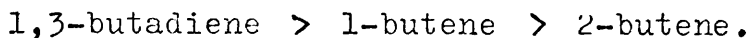
From the evidence presented in the preceding sections on the hydrogenation of 1,3-butadiene on "clean" Rh/SiO<sub>2</sub> catalysts, it has been concluded that the experimental observations are best explained by a mechanism in which 2-butene is formed predominantly by 1,4-addition. The results of the reactions on surfaces partially poisoned by the adsorption of mercury will now be considered.

The selectivity was observed to be high at each temperature studied; it was found to increase towards unity as the mercury coverage increased, the relative decrease in n-butane yield being greater at 83° than at 25°C. The significance of this may be shown by reference to the overall reaction scheme in section 12.1. Either (i) step 9 is inhibited, or (ii)  $k_6$ , the formation of the C<sub>4</sub>H<sub>9</sub> intermediate, is depressed, or (iii) both effects may occur. As the rate of addition to C<sub>4</sub>H<sub>9</sub> is proportional to the hydrogen coverage, and thus to the partial pressure of hydrogen, the hydrogen coverage,  $\theta_H$ , must be reduced by the adsorbed mercury if step 9 is responsible for the selectivity change.

The second possible cause, namely inhibition of step 6, may be considered from a thermodynamic standpoint. It has been shown that the sequence of adsorption strengths



decreases in the order



In view of the poisoning effect of mercury, one might suggest there is circumstantial evidence that mercury is more strongly adsorbed than 1,3-butadiene, despite the report by Campbell and Thomson that mercury did not displace propylene from a nickel film.<sup>72</sup> If this is so, the equilibrium 1,3-butadiene coverage is considerably reduced, and the surface fraction available to adsorbed butenes is therefore reduced correspondingly. Butene desorption must then be favoured over its remaining adsorbed, or its undergoing other steps; i.e.  $k_7/k_6$  and  $k_7/k_{-5}$  increase, with  $\theta_{\text{Hg}}$ . It is perhaps significant that the selectivity increase is greatest at high temperature; desorption, being an activated process, is favoured by increasing temperature, and hence this, also, tends to increase the ratios. It is therefore seen that formation of the  $\text{C}_4\text{H}_9$  intermediate may be inhibited on thermodynamic grounds, and this, together with the probability of  $\theta_{\text{H}}$  being reduced, is the main factor in raising the selectivity.

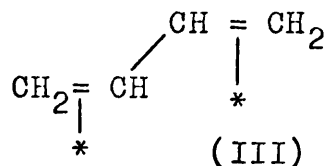
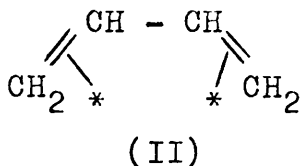
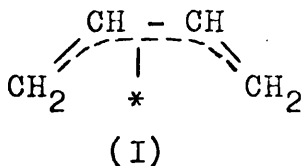
As the reactions were not generally studied beyond 50% conversion on the poisoned catalysts, the presence or absence of pressure fall acceleration points was not determined, and thus no correlation is possible with the

thermodynamic considerations surrounding these.

The salient features of the butene distributions are the constancy of the 1-butene/2-butene ratio, and the regular decrease in the trans/cis ratio at each temperature. It has been shown that a probable effect of adsorbed mercury is to increase the rate of butene desorption relative to the rates of the other processes which the adsorbed butene may undergo. It therefore follows that 1-butene isomerisation, if such occurs, must be considerably inhibited. That the 1-butene/2-butene ratio remains substantially the same over a range of  $\theta_{\text{Hg}}$  values between zero and  $\sim 95\%$  is strong evidence in support of separate 1,2- and 1-4 addition mechanisms.

Having shown that the 2-butenes are produced by direct 1,4-addition, consideration must now be given to the variation of the trans/cis ratio with  $\theta_{\text{Hg}}$ . It was suggested in section 12.1.2 that if 1,4-addition were responsible for the production of 2-butenes, the relative yields of the trans and cis isomers would be determined by the proportions of the adsorbed syn and anti conformers respectively. If this is the case it is apparent that increasing mercury coverage favours adsorption of the anti conformer, and in this context it is significant that two modes of adsorption have been proposed for it, namely

structures (I) and (II).



Structure (I) requires only one metal adsorption site, and must therefore be geometrically favourable compared with structure (II) for the same conformer; orbital delocalisation energy will also stabilise it further. The syn conformer, on the other hand, can adsorb only as structure (III), and therefore requires the availability of two adsorption sites. On this qualitative basis, it is apparent that increasing mercury coverage will induce a greater proportion of structure (I), by virtue of it having fewer geometrical restrictions, and thus, also, an increased yield of cis 2-butene. The statistical treatment of Herington and Rideal,<sup>88</sup> also, shows that the shape of the curve of the decrease of a reaction rate against the extent of poisoning is dependent upon the number of adsorption sites involved in the reaction. The observed curves for the poisoning of 1,3-butadiene hydrogenation (Fig. 8.3) are, on a quantitative basis, support for a mechanism requiring only two sites, i.e. one each for hydrogen 1,3-butadiene, as the curvature is only slight. A three-site process might be expected to produce a steeper curve.

It would be expected that the arrangement of the adsorbed mercury atoms would have an important bearing on the extent to which the 1,3-butadiene is preferentially adsorbed in this way. In particular, a random arrangement would be expected to have a substantially greater effect than one in which the mercury atoms were grouped in large clusters. It is therefore relevant to consider the variation of the trans/cis ratio with regard to two aspects of the mercury coverage. The decrease in the ratio vs. percentage monolayer coverage is shown in Fig. 12.1, and it may be seen that similar curves were obtained at each temperature. As was discussed in chapter 10, however, the mercury/rhodium ratio at  $\theta_{\text{Hg}} = 100\%$  varies with the temperature, and thus a different picture is presented by comparing the trans/cis ratio with the absolute mercury/rhodium ratio (Fig. 12.2). It is apparent that, after an initial rapid fall, the trans/cis ratio decreases linearly with increasing values of Hg/Rh. Further, the relative poisoning effects decrease with increasing temperature, and this is consistent with a more random adsorption of mercury at low temperatures and a greater degree of clustering at high temperatures. If the initial adsorption is a random process over the whole temperature range, clustering will only be achieved by surface migration of mercury; as this is an activated process, it will increase

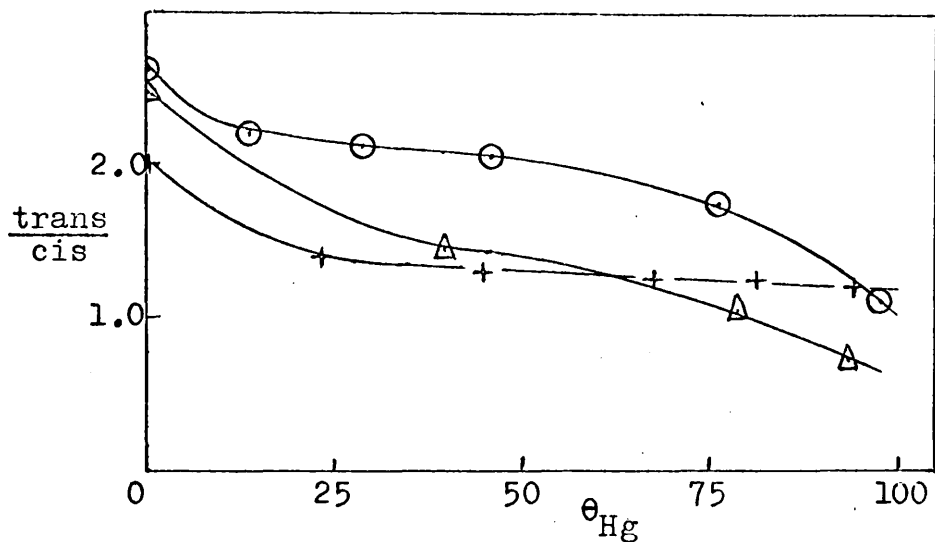


Fig. 12.1 Variation of trans/cis ratio with  $\theta_{\text{Hg}}$   
 $\odot$  - 25°C     $\Delta$  - 48°C    + - 83°C

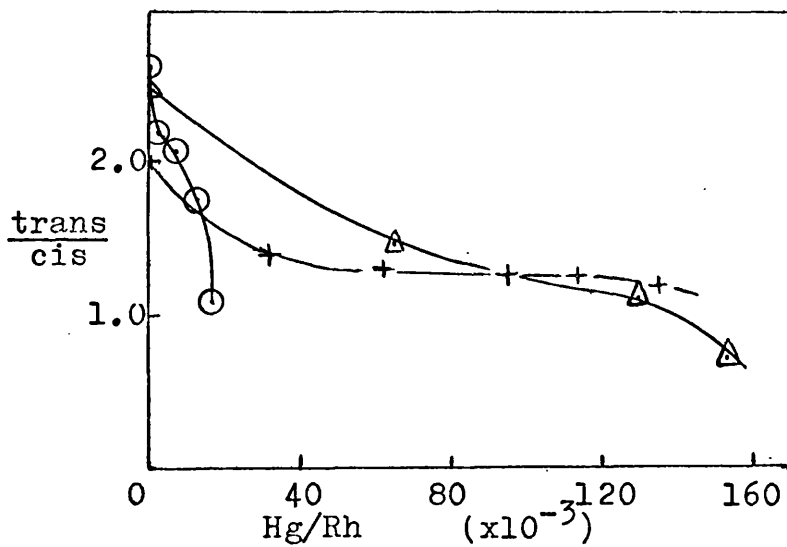


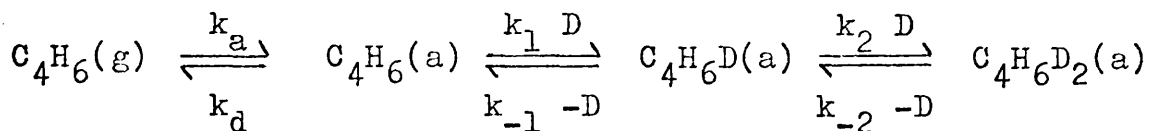
Fig. 12.2 Variation of trans/cis ratio with Hg/Rh atom ratio. (Symbols as in Fig. 12.1)

with temperature, and thus the energy considerations are consistent with the deductions made from Fig. 12.2, namely, that at a given mercury/rhodium ratio, the poisoning effect is greater at low temperatures. It is significant, also, that the poisoning of the hydrogenation reaction exhibits the same features.

It was shown in Fig. 8.3 that the rate of addition decreased uniformly to  $\sim$  zero at  $\theta_{\text{Hg}} \approx 100\%$ . This may be explained from two considerations. First, the surface area available for both 1,3-butadiene and hydrogen adsorption must be reduced by the mercury; it follows, therefore that the rate-determining step, addition to the  $\text{C}_4\text{H}_7$  intermediate, is inhibited, but it is not possible, at this stage, to deduce anything about the  $k_1/k_{-1}$  equilibria.

### 12.3.2 The Poisoning of the Catalyst for Exchange Reactions.

The deuterium content of each of the n-butenes rises with increasing  $\theta_{\text{Hg}}$ ; at  $25^\circ\text{C}$  the 2-butenes gain rather more deuterium than does the 1-butene, and at  $\theta_{\text{Hg}} \approx 75\%$  all the butenes are equally exchanged. All the deuterio-butene distributions, however, follow the same general trends with variation of  $\theta_{\text{Hg}}$  and temperature. The increase in total deuterium content may readily be explained in terms of the mechanism described in section 12.2. The rate-determining step in the n-butene formation is step 2, as there is



no change in the kinetic order; this step must therefore be inhibited by the mercury. The  $k_1/k_{-1}$  equilibrium therefore remains fast relative to  $k_2$ , despite  $k_1$  being dependent on  $\theta_H$  (or  $\theta_D$ ). As desorption will not be greatly affected by the mercury,  $k_d/k_{-2}$  will increase with  $\theta_{Hg}$ , and thus the gas-phase content of deuterio-butadiene will increase during the reaction rather more rapidly, relative to the rate of addition, than on the unpoisoned catalyst. It is therefore possible to have the apparently anomalous situation of the surface exchange reaction, that is, the rate at which  $k_1/k_{-1}$  equilibrium is attained, being inhibited, and yet there being a greater appearance of deuterio-butadiene in the gas-phase. Consideration of the results shows that this is consistent with the observations at 25° and 83°C, but, inexplicably, at 48°C the deuterium number of the 1,3-butadiene falls slightly with increasing  $\theta_{Hg}$ . This may possibly be due to statistical error on what are essentially very small measurements.

At 48° and 83°C the deuterio-butene distributions become rather narrower with increasing values of  $\theta_{Hg}$ ; the percentages of  $d_0$ - and  $d_1$ -species fall, while the  $d_2$ -butenes

become more abundant. Simultaneously the hydrogen exchange reaction at 83°C is inhibited by the mercury; this is consistent with a corresponding reduction in butene exchange, as was suggested when discussing the  $k_1/k_{-1}$  equilibrium. It therefore appears that the increase in the deuterium number of the butenes is caused, not by greater exchange, but by the greater probability of the addition of two deuterium atoms to an unexchanged 1,3-butadiene molecule.

#### 12.4 Conclusion.

Consideration of the features discussed in this chapter leads us to conclude that in the Rh/SiO<sub>2</sub> - catalysed hydrogenation of 1,3-butadiene the 1-butene is formed by direct 1,2-addition, and the 2-butenes by direct 1,4-addition. The ratio of the trans and cis 2-butenes is determined by the relative stability on the surface of the corresponding  $\pi$ -allylic intermediates. Exchange of adsorbed 1,3-butadiene is fast, but owing to the slow rate of desorption, this is not evident from the gas-phase 1,3-butadiene. There is therefore a considerable "pool" of exchanged hydrogen on the catalyst, resulting in considerable addition of hydrogen rather than deuterium, as the return of hydrogen atoms to the gas-phase by recombination is slow. The effect of adsorbed mercury is to inhibit the exchange reactions, and thus allow a greater addition of two deuterium atoms.



APPENDIX AEquations for calculation of parent ion concentrations  
in mass spectrometric analyses.

The reason for the need to correct the measured intensity of each mass for the fragmentation of higher masses has been described in section 4.5.1. The full equations are listed below.

$X$  = parent ion concentration ( $X = A, B, C, \dots$  etc.)

$x$  = measured positive ion current ( $x = a, b, c, \dots$  etc.)

$X'$  = parent ion concentration after correction for  $C^{13}$

( $X' = A', B', C', \dots$  etc.)

$f_1$  and  $f_2$  are the fractions of the first and second fragments respectively.

A. n-Butane.

m/e

$$68 \quad A = a$$

$$67 \quad B = b$$

$$66 \quad C = c - f_1(A + .10B)$$

$$65 \quad D = d - f_1(.90B + .20C)$$

$$64 \quad E = e - f_1(.80C + .30D) - f_2(A + .200B + .022C)$$

$$63 \quad G = g - f_1(.70D + .40E) - f_2(.80B + .356C + .067D)$$

$$62 \quad H = h - f_1(.60E + .50G) - f_2(.623C + .467D + .133E)$$

$$61 \quad I = i - f_1(.50G + .60H) - f_2(.467D + .534E + .222G)$$

$$60 \quad J = j - f_1(.40H + .70I) - f_2(.333E + .556G + .333H)$$

A. n-Butane./

m/e

$$59 \quad K = k - f_1(.30I + .80J) - f_2(.222G + .534H + .467I)$$

$$58 \quad L = l - f_1(.20J + .90K) - f_2(.133H + .467I + .623J)$$

$$57 \quad M = m - f_1(.10K + L) - f_2(.067I + .356J + .800K)$$

$$56 \quad N = n - f_2(.022J + .20K + L)$$

Correction for C<sup>13</sup>.

$$L' = L$$

$$K' = K - 0.044L'$$

$$J' = J - 0.044K'$$

etc.

B. n-Butenes.

m/e

$$64 \quad A = a$$

$$63 \quad B = b$$

$$62 \quad C = c - f_1(A + .125B)$$

$$61 \quad D = d - f_1(.875B + .25C)$$

$$60 \quad E = e - f_1(.375D + .750C) - f_2(.250B + .036C + A)$$

$$59 \quad G = g - f_1(.500E + .625D) - f_2(.107D + .429C + .750B)$$

$$58 \quad H = h - f_1(.625G + .500E) - f_2(.214E + .536D + .536C)$$

$$57 \quad I = i - f_1(.750H + .375G) - f_2(.357G + .572E + .357D)$$

$$56 \quad J = j - f_1(.875I + .250H) - f_2(.536H + .536G + .214E)$$

$$55 \quad (K = k - f_1(J + .125I) - f_2(.750I + .429H + .107G))$$

$$54 \quad (L = l - f_2(J + .250I + .036H) )$$

B. n-Butenes.Correction for C<sup>13</sup>.

$$J' = J$$

$$I' = I - 0.044J'$$

$$H' = H - 0.044I'$$

etc.

C. 1,3-Butadiene.

m/e

60 A = a

59 B = b

58 C = c - f<sub>1</sub>(A + .167B)

57 D = d - f<sub>1</sub>(.833B + .333C)

56 E = e - f<sub>1</sub>(.667C + .500D) - f<sub>2</sub>(A + .333B + .067C)

55 G = g - f<sub>1</sub>(.500D + .667E) - f<sub>2</sub>(.667B + .536C + .200D)

54 H = h - f<sub>1</sub>(.333E + .833G) - f<sub>2</sub>(.400C + .600D + .400E)

53 I = i - f<sub>1</sub>(.167G + H) - f<sub>2</sub>(.200D + .536E + .667G)

52 J = j - f<sub>2</sub>(.067E + .333G + H)

Correction for C<sup>13</sup>.

$$H' = H$$

$$G' = G - 0.044H'$$

$$E' = E - 0.044G'$$

etc.

REFERENCES.

1. J.E. Lennard-Jones, Trans. Faraday Soc. 28; 333 (1932).
2. H.S. Taylor, J. Amer. Chem. Soc. 53, 578 (1931).
3. e.g. J.K. Roberts, Proc. Roy. Soc. A152, 445, 464, & 477 (1935).
4. H.S. Taylor, Proc. Roy. Soc. A108, 105 (1925).
5. D. Cormack, S.J. Thomson, & G. Webb, J. Catalysis, 5, 224 (1966).
6. G.C. Bond in "Catalysis by Metals" (Academic Press, London, 1962), 85.
7. T.N. Rhodin, Jr., J. Amer. Chem. Soc. 72, 4343 & 5691 (1950).
8. M. Boudart, J. Amer. Chem. Soc. 74, 3556, (1952).
9. D.D. Eley, J. Phys. Chem. 55, 1017 (1951).
10. G.F. Taylor, S.J. Thomson, & G. Webb, J. Catalysis, in press; also G.F. Taylor, Ph.D. Thesis, Univ. of Glasgow, 1967.
11. O. Beeck, A.E. Smith, & A. Wheeler, Proc. Roy. Soc. A177, 62 (1941).
12. R.E. Cunningham & A.T. Gwathmey, Advan. Catalysis 9, 25 (1957); Advan. Catalysis 10, 57 (1958).
13. T.N. Rhodin, Jr., Advan. Catalysis 5, 39 (1953).
14. G.C. Bond & P.B. Wells, Proc. 2nd Intern. Congress on Catalysis, (Editions Technip Paris, 1961), 1 1159 (1961); Ref. 6, 283.
15. D.A. Dowden, J. Chem. Soc. p242 (1950).
16. L. Pauling, Proc. Roy. Soc. A196, 343 (1949).
17. D.A. Dowden, in "Chemisorption", ed. W.E. Garner (Butterworths, London, 1957); also D.A. Dowden & D. Wells, Proc. 2nd Intern. Congress Catalysis, (Edition Technip, Paris, 1961) 2, 1499.

18. B.M.W. Trapnell, in "Chemisorption" (Butterworths, London, 1955).
19. L. Pauling, J. Amer. Chem. Soc. 69, 592 (1947).
20. O. Beeck, Disc. Faraday Soc. 8, 118 (1950); also G.C.A. Schuit & L.L. van Reijën, Advanc. Catalysis 10, 242 (1958).
21. G. Schwab, Trans. Faraday Soc. 42, 689 (1946).
22. A. Couper & D.D. Eley, Disc. Faraday Soc. 8, 172 (1950).
23. G. Rienacker et al., Z. anorg. Chem. 251, 55 (1943).
24. A. Farkas, L. Farkas, & E.K. Rideal, Proc. Roy. Soc. A146, 630 (1934).
25. O. Beeck, Disc. Faraday Soc. 8, 118 (1950).
26. K. Morikawa, W.S. Benedict, & H.S. Taylor, J. Amer. Chem. Soc. 57, 592 (1935).
27. K. Morikawa, N.R. Trenner, & H.S. Taylor, J. Amer. Chem. Soc. 59, 1103 (1937).
28. D.D. Eley, Advan. Catalysis, 1, 157 (1948).
29. G.K.T. Conn & G.H. Twigg, Proc. Roy. Soc. A171, 55 (1939).
30. L.N. Kauder & T.I. Taylor, Science 113, 238 (1951).
31. C. Kemball, Proc. Roy. Soc. A223, 377 (1954).
32. J. Horiuti, G. Ogden, & M. Polanyi, Trans. Faraday Soc. 30, 663 (1934).
33. J. Horiuti & M. Polanyi, Trans. Faraday Soc. 30, 1164 (1934).
34. e.g. G.H. Twigg & E.K. Rideal, Proc. Roy. Soc. A171, 55 (1939).
35. R.K. Greenhalgh & M. Polanyi, Trans. Faraday Soc. 35, 520 (1939).
36. F.C. Gault, J.J. Rooney, & C. Kemball, J. Catalysis 1, 255 (1962).

37. J.J. Rooney & G. Webb, *J. Catalysis* 3, 488 (1964).
38. J.J. Rooney, *J. Catalysis* 2, 53 (1963).
39. G.H. Twigg & E.K. Rideal, *Trans. Faraday Soc.* 36, 533 (1940).
40. D.D. Eley, in "Catalysis" (Ed. P.H. Emmett) Vol III, (Reinhold, New York, 1955) Chap.2.
41. T.I. Taylor & V.H. Dibeler, *J. Phys. & Colloid. Chem.* 55, 1036 (1951).
42. G.H. Twigg, *Proc. Roy. Soc.* A178, 106 (1941).
43. G.H. Twigg, *Trans. Faraday Soc.* 35, 934 (1940).
44. G.C. Bond, *Ref.* 6, 255.
45. J. Turkevich & R.K. Smith, *J. Chem. Phys.* 16, 466 (1948).
46. G.C. Bond & P.B. Wells, *Advan. Catalysis* 15, 92 (1964).
47. J.M. Winterbottom, Ph.D. Thesis, Univ. of Hull, 1962.
48. G. Webb, Ph.D. Thesis, Univ. of Hull, 1963.
49. P.J. Lucchesi, D.L. Baeder, & J.P. Longwell, *J. Amer. Chem. Soc.* 81, 3235 (1959).
50. H.R. Gerberich & W.K. Hall, *J. Catalysis* 5, 99 (1966).
51. J.W. Hightower, H.R. Gerberich, & W.K. Hall, *J. Catalysis* 7, 57 (1967).
52. D.M. Brouwer, *J. Catalysis* 1, 22 (1962).
53. S.E. Tung & E. McIninch, *J. Catalysis* 3, 229 (1964).
54. S. Bielikoff, J. Fraissard, & B. Imelik, *Bull. Soc. Chem. France* p3271 (1967).
55. G.C. Bond, G. Webb, P.B. Wells, & J.M. Winterbottom, *J. Chem. Soc.* p3218 (1965).
56. G.C. Bond, G. Webb, P.B. Wells, & J.M. Winterbottom, *J. Catalysis* 1, 74 (1962).

57. E.F. Meyer & R.L. Burwell, J. Amer. Chem. Soc. 85, 2881 (1963).
58. W.G. Young et al. J. Amer. Chem. Soc. 69, 2046 (1947).
59. E.B. Maxted, Advanc. Catalysis 3, 129 (1951).
60. A. Couper & D.D. Eley, Nature 164, 578 (1949); also ref. 15.
61. M.H. Dilke, D.D. Eley & E.B. Maxted, Nature 161, 804 (1948).
62. E.B. Maxted & R.W.D. Morrish, J. Chem. Soc. p252 (1940).
63. E.B. Maxted & A.G. Walker, J. Chem. Soc. p1093 (1948).
64. E.B. Maxted & H.C. Evans, J. Chem. Soc. p603 (1937).
65. G.D. Luibarskii & L.B. Avdeyeva, Kinetica i Kataliz 4, 337 (1963).
66. E.B. Maxted & H.C. Evans, J. Chem. Soc. p1004 (1937).
67. W.G. Brown, G.E. Calf, & J.L. Garnett, Chem. Comm. p1066 (1967).
68. H.P. Leftin & E.W. Stern, J. Catalysis 6, 337 (1966).
69. H.P. Leftin & E. Hermana, Proc. 3rd Intern. Congress Catalysis 2, 1064 (1965).
70. E.B. Maxted, J. Chem. Soc. 117, 1501 (1920).
71. E.B. Maxted & A. Marsden, J. Chem. Soc. p469 (1940).
72. K.C. Campbell & S.J. Thomson, Trans. Faraday Soc. 55, 985 (1959).
73. K.C. Campbell & S.J. Thomson, Trans. Faraday Soc. 55, 306 (1959).
74. G. Jangg, H.R. Kirchmayr, & H.B. Mathis, Z. Metallkde. 58, 724 (1967).
75. T. Nicklin, R.J. Whitaker, & M. Dixon, Nature 212, 1357 (1966).

76. J.G. Firth & H.B. Holland, *Nature* 212, 1036 (1966).
77. D.V. Sokol'skii, O.A. Tyurenkova, & E.I. Seliverstova, *Russ. J. Phys. Chem.* 41, 744 (1967).
78. J.F. Harrod & A.J. Chalk, *J. Amer. Chem. Soc.* 86, 1776 (1964).
79. G.J.K. Acres, G.C. Bond, B.J. Cooper, & J.A. Dawson, *J. Catalysis* 6, 139 (1966).
80. R. Cramer & R.V. Lindsay, *J. Amer. Chem. Soc.* 88, 3534 (1966).
81. R.D. Gillard, J.A. Osborn, P.B. Stockwell, & G. Wilkinson, *Proc. Chem. Soc.* p284 (1964).
82. D.W. Moore, H.B. Jonassen, T. Joyner, & A.J. Bertrand, *Chem. Ind. (London)* p1304 (1960).
83. C. Kemball et al., private communication.
84. G.C. Bond, J.J. Phillipson, P.B. Wells, & J.M. Winterbottom, *Trans. Faraday Soc.* 60, 1874 (1964).
85. J.A. Altham & G. Webb, unpublished results.
86. J.S. Hislop, Ph.D. Thesis, Univ. of Glasgow, 1965.
87. G.C. Bond, D.A. Dowden, & N. Mackenzie, *Trans. Faraday Soc.* 54, 1537 (1958).
88. E.F.G. Herington & E.K. Rideal, *Trans. Faraday Soc.* 40, 505 (1944).
89. F.H. Field & J.L. Franklin, "Electron Impact Phenomena" (Academic Press, New York, 1957) p214.
90. F.R. Hepner, K.N. Trueblood, & H.J. Lucas, *J. Amer. Chem. Soc.* 74, 1333 (1952).
91. H.B. Jonassen & W.B. Kirsch, *J. Amer. Chem. Soc.* 79, 1279 (1957).